SYNTHESIS AND CHARACTERIZATION OF NEW DONOR-ACCEPTOR TYPE CONJUGATED POLYMERS FOR NLO APPLICATIONS

THESIS

Submitted in partial fulfilment of the requirements for the degree of
DOCTOR OF PHILOSOPHY

by

SUNITHA M. S.

(Registration No: 081021CY08F04)

DEPARTMENT OF CHEMISTRY

NATIONAL INSTITUTE OF TECHNOLOGY

KARNATAKA, SURATHKAL, MANGALORE – 575 025

July, 2012

SYNTHESIS AND CHARACTERIZATION OF NEW DONOR-ACCEPTOR TYPE CONJUGATED POLYMERS FOR NLO APPLICATIONS

THESIS

Submitted in partial fulfilment of the requirements for the degree of
DOCTOR OF PHILOSOPHY

by

SUNITHA M. S.

(Registration No: 081021CY08F04)

Research Supervisor

Prof. Airody Vasudeva Adhikari

DEPARTMENT OF CHEMISTRY

NATIONAL INSTITUTE OF TECHNOLOGY

KARNATAKA, SURATHKAL, MANGALORE – 575 025.

July, 2012

DECLARATION

by the Ph.D. Research Scholar

I hereby ***declare*** that the Research Thesis entitled **"Synthesis and characterization of new donor–acceptor type conjugated polymers for NLO applications"** which is being submitted to the ***National Institute of Technology Karnataka, Surathkal*** in partial fulfilment of the requirements for the award of the Degree of ***Doctor of Philosophy*** in ***Chemistry*** is a ***bonafide report of the research work carried out by me.*** The material contained in this Research Thesis has not been submitted to any University or Institution for the award of any degree.

Sunitha M. S.

(Reg. No: 081021CY08F04)

Department of Chemistry

Place: NITK, Surathkal

Date: 16/07/2012

CERTIFICATE

This is to *certify* that the Research Thesis entitled **"Synthesis and characterization of new donor–acceptor type conjugated polymers for NLO applications"** submitted by **Sunitha M. S.** (Register Number: **CY08F04**) as the record of the research work carried out by her, is *accepted as the Research Thesis submission* in partial fulfilment of the requirements for the award of degree of **Doctor of Philosophy.**

Prof. A. Vasudeva Adhikari
Research Guide
Date: 16/07/2012

Chairman-DRPC
Date: 16/07/2012

DEDICATED TO MY

Parents who laid the foundation…..

Teachers who paved the path…..

Friends who encouraged me…..

Husband who made it possible…..

ACKNOWLEDGEMENTS

ABSTRACT

Over the last two decades, conjugated polymers have received significant, scientific and technological interest due to their broad range of applications. Among various conjugated polymers, donor-acceptor (D-A) type conjugated polymers are in the forefront of research efforts because of their easy processability, stability, and readiness to functionalize.

The present research work was concentrated on design, synthesis and characterization of four new series (**P1-P16**) of D-A type conjugated polymers derived from 3,4-disubstituted thiophene. In the new polymers 3,4-dialkoxy/aryloxy thiophene and 1,3,4-oxadiazole were introduced as electron donor and electron acceptor segments respectively. Also, aromatic systems such as benzene, thiophene, pyridine, phenylenevinylene, EDOT, naphthalene and biphenyl groups were introduced as conjugated spacers in the polymer chain. It was expected that the new polymers would exhibit good electrochemical and optical properties.

The new intermediates, monomers and four series of polymers **P1-P16** were synthesized through multistep reactions. The structures of new intermediates and monomers were confirmed by FTIR, ^{1}H NMR, ^{13}C NMR spectral methods followed by elemental analyses. Further, the molecular structures of polymers were elucidated by FTIR, ^{1}H NMR spectroscopy, GPC and elemental analysis. Their thermal stability was determined using TGA. The linear optical properties of polymers were investigated by UV-visible absorption and fluorescence spectroscopic studies. The electrochemical properties were determined using cyclic voltammetry (CV). Their bandgap was found to be in the range of 1.8-2.5 eV. Further, their nonlinear optical (NLO) properties were investigated by Z-scan and degenerate four wave mixing (DFWM) methods using 532 nm, 7 ns laser pulses. The effect of different substitution was discussed in detail with regard to electrochemical and optical properties. Polymers of series 1, 2 and 4 showed two-photon absorption (2PA) while polymers of series 3 displayed three-photon absorption (3PA). A further insight on the NLO behavior was provided by employing suitable theories and equations.

Keywords: D-A conjugated polymers, electrochemical properties, optical properties, NLO

CONTENTS

CHAPTER-3

SYNTHESIS AND CHARACTERIZATION OF NEW MONOMERS AND POLYMERS

CHAPTERS- 4

ELECTROCHEMICAL, LINEAR AND NONLINEAR OPTICAL STUDIES OF POLYMERS

CHAPTER-5

SUMMARY AND CONCLUSIONS

LIST OF FIGURES   **Page No.**

xi

LIST OF DESIGNS

LIST OF SCHEMES

LIST OF TABLES

ABBREVIATIONS

$\overline{\text{M}}_w$	Weight average molecular weight
$\overline{\text{M}}n$	Number average molecular weight
^{13}C NMR	Carbon nuclear magnetic resonance
^{1}H NMR	Proton nuclear magnetic resonance
2PA	Two-photon Absorption
3PA	Three-photon Absorption
CV	Cyclic voltammetry
D-A	Donor-acceptor
DFWM	Degenerate four wave mixing
DMF	N,N-Dimethylformamide
DMSO-d^6	Deuterated dimethyl sulphoxide
EDOT	Ethylenedioxythiophene
E_g	Bandgap
EL	Electroluminiscence
ESA	Excited state absorption
FTIR	Fourier transform infrared
GPC	Gel permeation chromatography
HOMO	Highest occupied molecular orbital
ITO	Indium tin oxide
LEDs	Light emitting diodes
LUMO	Lowest unoccupied molecular orbital
NLO	Nonlinear optics
NMP	N-methyl pyrolidone
NMR	Nuclear magnetic resonance
OLEDs	Organic light emitting diodes
PA	Poly(acetylene)

PANI	Poly(aniline)
PBD	2-(4-tert-butylphenyl)-1,3,4-oxadiazole
PDI	Polydispersity index
PEDOT	Poly(ethylenedioxythiophene)
PL	Photoluminiscence
PLEDs	Polymer light emitting diodes
PPP	Poly(p-phenylene)
PPV	Poly(p-phenylenevinylene)
PPy	Poly(pyrrole)
PS	Poly(styrene)
PTh	Poly(thiophene)
SCE	Saturated calomel electrode
SOCl$_2$	Thionylchloride
TFTs	Thin film transistors
TGA	Thermogravimmetric analysis
THF	Tetrahydrofuran
UV	Ultra violet
β	Two-photon absorption coefficient
γ	Three-photon absorption coefficient
χ$^{(3)}$	Third order nonlinear optical susceptibility

Chapter 1

Abstract

 Chapter 1 *begins with a brief introduction on conjugated polymers followed by theory behind the conductivity in them. Also, it covers a brief account on D-A type concept in conjugated polymers and important methods for their synthesis. Further, it includes a concise description on their applications in various fields. Furthermore, it encompasses a brief introduction to NLO, its origin, different processes of NLO absorption and importance of conjugated polymers in NLO applications.*

1.1 INTRODUCTION

 Conjugated polymers are a class of conducting polymers and they opened the way to progress in understanding the fundamental chemistry and physics of bonded macromolecules. They are organic polymers with spatially extended π-conjugation system and they possess delocalized π-electron bonding along the polymer chain, which is the basis for origin of semiconducting properties in them. In such systems, the π-bonding and π*-antibonding orbitals form delocalized valence and conduction wave functions, respectively. They possess electrical, electronic, magnetic, and optical properties like metals. So, they are also called "synthetic metals". The electrical and optical properties of these polymers basically depend on the electronic structure as well as the chemical nature of the repeating moieties in the polymer backbone. Some common conjugated polymers include poly(acetylene) (PA), poly(pyrrole) (PPy), poly(aniline) (PANI), poly(p-phenylene) (PPP) and poly(thiophene) (PTh) and their structures are as shown in **S-1.1.** Their conductivity is mainly due to the extensive conjugation present in them. Majority of them possess rigid structures with aromatic ring systems in their backbone providing stability to the polymers.

Poly(acetylene) Poly(aniline) Poly(p-phenylene) Poly(pyrrole) Poly(thiophene)
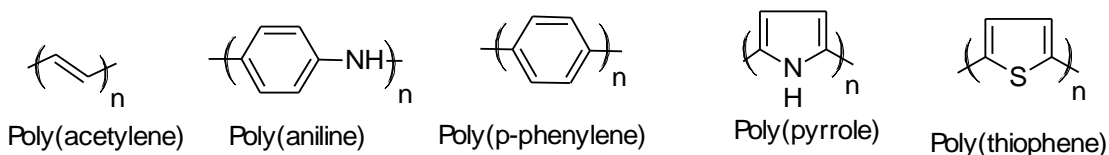
S-1.1

It is universally agreed that the doping process is an effective method to alter the conductivity in conjugated polymers. Doping allows electrons to flow forming conduction bands. In the doped conjugated polymers, the loosely bound electrons in the conjugated system are able to jump around the polymer chain, there by producing conductivity.

1.2 BRIEF HISTORY

The conducting polymer research began nearly a quarter of a century ago. Heeger, Shirakawa and MacDiramid synthesized and studied conductivity of PA when monomer of acetylene was doped with bromine and iodine vapor; the resulting electrical conductivity was 10 times higher than the undoped monomer and films of PA was found to exhibit profound increase in electrical conductivity when exposed to halogen vapor. For this achievement, they were awarded Nobel Prize in the year 2000. This breakthrough initiated fast progress in the scientific investigation of conducting polymer properties. The trend was to understand the chemical and physical aspects either in neutral (undoped) state or in charged (doped) states. Originally it was thought that the principal application for conjugated polymers would replace metals such as copper and aluminum in weight sensitive applications such as air and space travel. While heavily doped PA can be made more highly conducting than copper on conductivity per weight basis. But, its instability under ambient conditions has not permitted the practical use of PA.

Search for alternative conjugated polymers with superior stabilities led to the discoveries of conjugated polymers, viz. PANI (Huang et al. 1986), PPy (Diaz et al. 1979), PTh (Roncali et al. 1992, Della-Casa et al. 2005, Yasuda et al. 2007, Pal et al. 2007 and Faccinetto et al. 2008) and poly(3,4-ethylenedioxythiophene) (PEDOT) (Groenendaal et al. 2000) have been extensively studied and the field itself is the subject of many reviews. They are also blessed with improved stability in the doped conducting form; however they are still much less conductive than PA and have thus reduced research efforts into conjugated polymers as light-weight metal replacement conductors. Far from marking the termination of the field, the successors to PA have found use in a

wide range of applications including thin film transistors (TFTs) (Babel et al. 2002), flexible organic light emitting diodes (OLEDs) (Huang et al. 1999), photovoltaic cells (PV Cells) (Kim et al. 2011), sensors (Vidal et al. 2003), nonlinear optics (NLO) (Audebert et al. 2003, Caruso et al. 2005 and Li et al. 2010). The polymers like PA, PANI, PPy and PTh represent the first generation of conjugated polymers, and as such, are not the ideal materials for most applications.

PEDOT has been the most successful second generation conjugated polymer because of its reduced bandgap compared to PTh and increased environmental stability as a doped conductor. As such, it has been commercialized by Agfa and Bayer and found applications in transparent static protection of electronics during shipping, improved soldering processes for circuit boards, photographic film production and as a component OLEDs. Because of PEDOTs unique properties, research interest and related publications have increased exponentially over the last several years.

1.3 CONDUCTIVITY IN POLYMERS

Conductivity in conjugated polymers is mainly due to π-conjugation along the polymeric chain. In conjugated polymers, delocalization can be accomplished by forming a conjugated backbone of continuous overlapping orbitals. Alternating single and double bonds provide continuous path for overlapping of π-orbital. The continuous string of orbitals creates degeneracy in the highest occupied molecular orbital (HOMO) and lowest unoccupied molecular orbitals (LUMO). This leads to the filled (valence) and unfilled bands (conduction band) that describes a semiconductor. This movement of charge is responsible for electrical conductivity in conjugated polymers.

The simplest example of conjugated polymer is PA and its structure is shown in **Figure 1.1**.
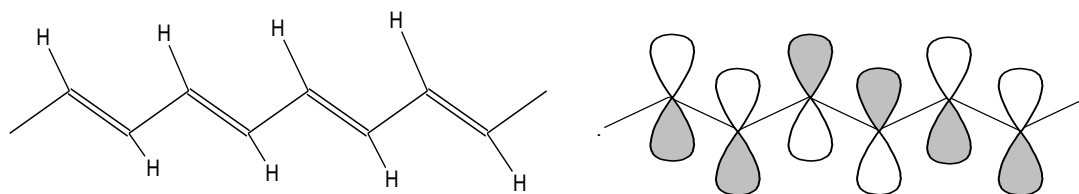
Figure 1.1 Structure of poly(acetylene)

Due to its structural and electronic simplicity, it is well suited to ab-initio and semi-empirical calculations and has therefore played a critical role in the elucidation of the theoretical aspects of any conjugated polymer. It possesses a spatially delocalized band-like electronic structure. These bands originate from the splitting of interacting molecular orbitals of the constituent monomer units, possessing band structure similar to the solid state semiconductors. Thus, because of the unique structure, it opens a gap between the HOMO level corresponding to fully occupied π-band (valence band) and the LUMO level corresponding to empty π^*-band (conducting band). In the simplest approach, PA can be treated as an intrinsic semiconductor with a bandgap of 1.5 eV. A schematic representation of energy level diagram showing conduction bands, bandgap and valence bands is given in **Figure 1.2**.

Figure 1.2 energy level diagrams

Conjugated homopolymers made up of heteroaromatic units such as pyrrole, indole, carbazole, imidazole, pyridine, and thiophene possess short π-conjugated electrons and low electrical conductivity. Whereas conjugated polymers formed with combination of aromatic, heteroaromatic and conjugated aliphatic units like vinylenes and substituted vinylenes possess enhanced chain length and coplanarity. Such polymers have higher conductivity than their corresponding homopolymers.

1.4 DONOR-ACCEPTOR (D-A) TYPE CONJUGATED POLYMERS

The practical usage of linear homopolymer PA is precluded due to its instability under ambient conditions (which comprise water and oxygen). As a result, the D-A

concept has been raised. The D‑A concept was proposed by Havinga and co‑workers (Havinga et al. 1993). The principle behind this strategy is that, alternate arrangement of donor and acceptor moieties in main chain of the polymer as shown in **Figure 1.3**. It is expected to have the lowest bandgap for such D‑A combination, if electronegativity difference between donor and acceptor moieties is the highest. In this approach, donor moieties are introduced in the polymer chain to increase the valence band edge of the polymer by donation of electron density to the conjugated backbone; acceptor moieties are introduced to lower the conduction band edge of the polymer by withdrawing electron density from the conjugated backbone.
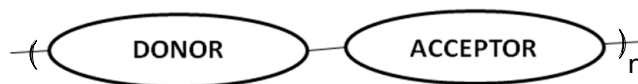
Figure 1.3 Alternate D‑A arrangement

Since both the electron acceptor and releasing segments are present alternatively in a single chain, high conductivity can be achieved in these polymers without doping. Also, incorporation of donor and acceptor moieties in conjugated chain causes reduction in its bandgap. Further, by proper selection of D‑A segments it is possible to create highly planar molecular systems which contribute further reduction in their band gap. Based on this, polymers with various combinations of donor and acceptor moieties were designed and synthesized.

Additionally, polymers must be functionalized with alkyl chains in order to have good solubility and fusibility. Such functionalization also influences on bandgap of the polymers. Although the attachment of such pendant groups does not lead directly to low bandgap materials with E_g, 1.5 eV, it represents the most direct and straightforward approach towards reducing the bandgap of such polymers. Due to electronic effects, the energy of absorption is found to decrease with alkyl substitution and it further diminishes with alkoxy functionalization. The presence of electron donating substituents (more prominent for the case of alkoxy pendants due to mesomeric effects) would lead to rise in the energy of the HOMO with a consequent narrowing of the energy bandgap. Further, upon functionalization with pendant groups, there would be reduction in coplanarity and

therefore the extent of conjugation in polymer is lowered. Because of this, bandgap of polymers may be increased. Electronic effects on lowering the bandgap are particularly prominent for the case of region-regular head-tail coupled 3-functionalised poly(thiophene)s where steric effects are minimal. A further lowering of the bandgap by electron-donating pendant groups is limited by the steric effects of the substituents on adjacent thiophene rings which force the rings out of coplanarity. The torsions introduced into the π-system of the PTh backbone result in the energy absorption maxima shifting to higher energies while the bandgap evaluated by extrapolation of the low-energy absorption edge, (Eckhardt et al. 1989) is also increased.

1.5 SYNTHETIC METHODS

Conjugated polymers can be synthesized using various methods which are mainly classified as chemical and electrochemical methods. Distinctly, there are a large number of available chemical methods which include Witting, Suzuki, Yamamoto, Knoevenagel, Grignard and polycondensation reactions. Some of the important methods reported in literature for the synthesis of conjugated polymers are outlined in the following section.

1.5.1 Chemical polymerization

Most of the chemical methods involve condensation polymerization, which generally proceeds via loss of small molecules resulting from the reaction of end groups on monomer unit. Generally, it involves loss or elimination of a chemical species resulting from the reaction of end groups of monomer chains.

Suzuki coupling is a blend reaction that takes place between the boronic acid functional groups and the bromo functional groups of different monomers (**S-1.2**) resulting in the formation of polyarylenes (**S-1.3**) in presence of palladium catalyst (Skothiem et al. 1998). The reaction is given in **Scheme 1.1.**

S-1.2 **S-1.3**
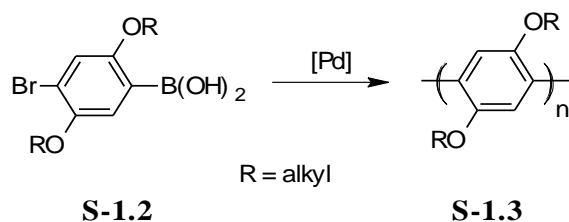
Scheme 1.1 Polymerization by Suzuki coupling method

Chapter 1

Polycondensation route is a well-known method generally used for synthesis of conjugated polymers. As described in the literautre, a polycondensation reaction (**Scheme 1.2**) between dicarbonyl chloride (**S-1.4**) and the aromatic dicarbohydrazide (**S-1.5**) yields polyhydrazide (**S-1.6**) with the loss of HCl molecule. This, on cyclodehydration with phosphorous oxychloride gives the final polymer (**S -1.7**).

S-1.4

S-1.5

S-1.6

S-1.7
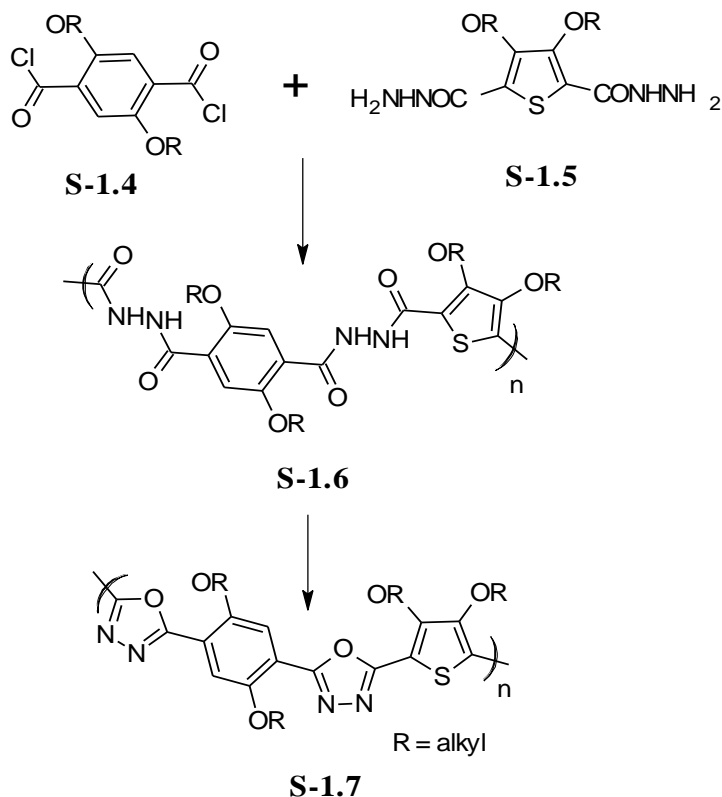
Scheme 1.2 Poycondensation route to synthesize poly(oxadiazole)s

Yamamoto method is another coupling reaction which involves coupling (Skothiem et al. 1998) between the bromo groups of different monomers (**S-1.8**) to yield polyarylenes (**S-1.9**) in presence of magnesium and nickel catalyst as given **Scheme 1.3**.

S-1.8

S-1.9
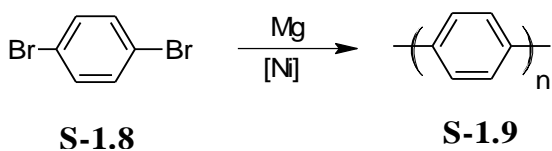
Scheme 1.3 Polymerization by Yamamoto coupling reaction

Knoevenagel reaction (Fink 2008) is a base catalyzed reaction that takes place between the active aldehyde and acetonitrile groups attached to different monomer units. This is an attractive route to synthesize cyanopolymers (**S-1.12**) from bis-dialdehydes (**S-1.10**) and the compounds substituted with bis-cyanomethylene groups (**S-1.11**), as explained in **Scheme 1.4**. This method allows the convenient synthesis of polymer backbone with a double bond.
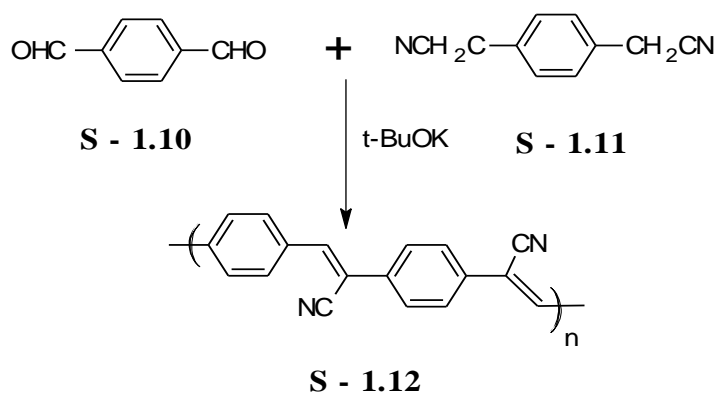
Scheme 1.4 Polymerization by Knoevenagel reaction

Wittig reaction is a commonly used synthetic method to introduce vinylic linkages in organic compounds (Skothiem et al. 1998). Using this reaction, poly(phenylvinylene)s (**S-1.15**) can be synthesized using dialdehyde (**S-1.13**) and triphenyl phosphonium salt (**S-1.14**) of an aromatic species, to produce polymers with vinylic linkages as shown in **Scheme 1.5**.
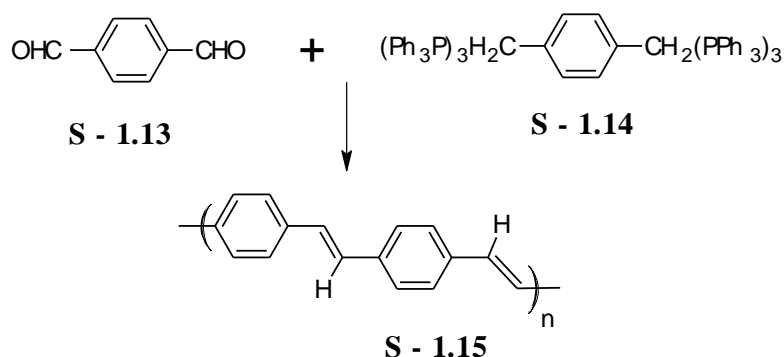
Scheme 1.5 Polymerization by Wittig reaction

Kumada coupling is a well-known polycondensation reaction, which is widely used for the synthesis of certain thiophene based conjugated polymers This method was

first used to synthesize soluble and processable poly(3-alkylthiophene)s by Elsenbaumer and co-workers (Elsenbaumer et al.1986). When 2,5-diiodo- 3-alkylthiophene (**S-1.16**) was treated with one mole equivalent of magnesium in presence of Ni(diphenylphosphinopropane)Br$_2$ as catalyst, poly(3-alkylthiophene) (**S-1.17**) was formed in good yield. **Scheme 1.6** depicts Kumuda coupling reaction.
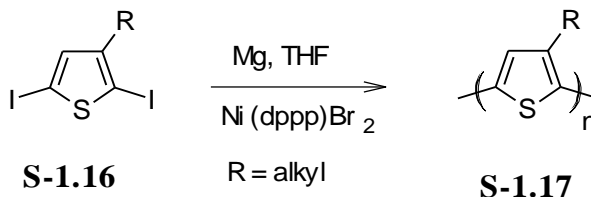
Scheme 1.6 Polymerization by Kumada coupling reaction

Some of the methods like, Reike method, Grignard polycondensation method, Stille coupling method etc. (Skothiem et al. 1998) are also being used for the synthesis of certain types of conjugated polymers.

Chemical polymerization not only provides many different possible routes to synthesize a variety of polymers, but also permits the scale-up for the production of these materials, which is currently not possible with electrochemical synthesis. Moreover, chemical polymerization has more options to modify conjugated polymer backbone.

1.5.2 Electrochemical polymerization

In practice, electrochemical synthesis is one of the techniques used for the synthesis of conjugated polymers. Generally, electrochemical polymerization is performed using a three-electrode system (working, counter, and reference electrodes) in a solution of the monomer, appropriate solvent, and electrolyte (dopant). When direct current is passed through the solution, electrodepositon occurs at the positively charged working electrode or anode. Monomers at the working electrode surface undergo oxidation to form radical cations, forming insoluble polymer chains on the electrode surface. It is a simple method to obtain doped polymers. Free standing as well as self-supporting conductive polymer films of desired thickness or geometry can be obtained. Using this novel technique a variety of conducting polymers like Ppy, PTh, PANI, Poly(pyrrole-aniline) have been generated.

Generally, electrochemical polymerization always takes place through oxidative polymerization. Its generic reaction pathway is given in **Scheme 1.7**, which includes: (i) the initiation step, radical generation, via electrochemical oxidation, (ii) propagation via radical-radical recombination. It involves loss of two protons from the radical-radical intermediate species generating the dimer, electrochemical oxidation of the dimer, combination of it with monomer radicals and repetition of steps 2 and 3. Termination via exhaustion of reactive radical species takes place accompanying oxidative or other chain termination process.
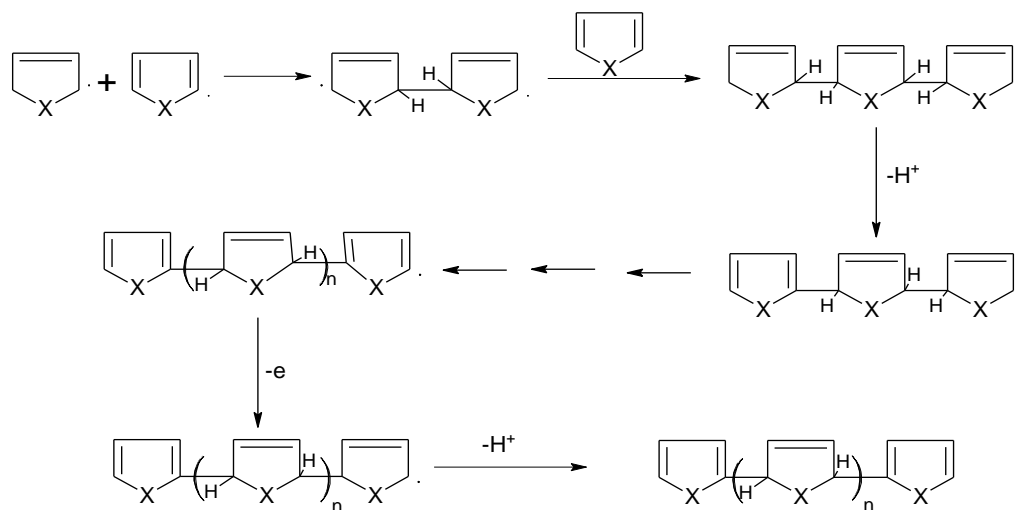
Scheme 1.7 Mechanism of electrochemical polymerization

1.6 APPLICATIONS

The discovery of conjugated polymers opened up many new possibilities for devices combining their unique optical, electrical and mechanical properties. The prospect of materials combining the properties of plastics and metals or semiconductors has led to the pursuit of varied applications in different fields. The strong interest in these polymeric materials arises from the curiosity about the transport mechanism plus the commercial possibilities of using these lightweight conductors whose properties could be potentially adjusted by modifying the polymer structure. In this regard, many reports describe prototypes or experiments demonstrating the feasibility of using these polymers in certain technologies. Based on their electrical conductivity, these materials have been

proposed for use in electrostatic materials, conducting adhesives, electromagnetic shielding, printed circuit boards, artificial nerves, antistatic clothing, piezoceramics, active electronics (LEDs, TFTs), aircraft structures, chemical, biochemical and thermal sensors, electrodes in rechargeable batteries, solid electrolytes, ion exchange membranes, electrochemical actuators, drug release systems and materials in electrical displays. On the other hand, based on their optical activity, they are useful as nonlinear optoelectronic materials which include optical limiters, optical communication and data storage devices, etc. Since polymeric materials possess distinct advantages like lightweight, bio-compatibility, high conductivity, good film forming property, easy tunability of desired properties through synthesis and relatively low manufacturing cost, they are potential candidates for the above mentioned applications.

Amongst the various applications reported for conjugated polymers, NLO is gaining more importance in recent years. A detailed account of their importance in NLO applications has been discussed in the following section.

1.7 INTRODUCTION TO NONLINEAR OPTICS

NLO deals with the interactions of applied electromagnetic fields in various materials to generate new electromagnetic field altered in phase, frequency, amplitude or other physical properties. Interestingly, the field of NLO and photonics are rapidly emerging as the technology for the 21st century (Prasad et al. 1990). Photonics is the technology in which a photon instead of an electron is used to acquire, store, process and transmit information. A photonic circuit is equivalent to electronic circuit, in which photons are conducted through channels. Light can be switched from one channel to another at certain junction points. For optical switching at these junctions, one needs to use a material that allows the manipulation of an electric field or laser pulse. The materials which manipulate the light at these junction points are known as NLO materials and these are gaining importance in technologies such as optical communication, optical computing and dynamic image processing (Boyd 1992). Photonics has many distinct merits over electronics. The most important advantage is the gain in speed due the fact that a photon travels much faster than an electron. Other advantages are that there is no electrical

and magnetic interference; thereby the photonic circuits are fully compatible with the existing fiber optics networks.

The quest for suitable materials to be used in devices for opto‑electronics and photonics has been of interdisciplinary interest in chemistry, physics and material science. Materials which exhibit high NLO responses are potential candidate for such devices, because they offer the possibility of high speed processing, transmission and storage of data. The nonlinear second and third order effects provide possibilities for optical frequency conversion, optical switching and optical memory operations. In particular, organic conjugated molecules and polymers have been unique candidates for solid-state devices due to their high second and third order responses. They have emerged as a dominant class of photonic materials because they exhibit large and ultra fast NLO responses, associated with their delocalized π‑electrons. In addition, they offer advantages to their inorganic counter parts such as chemical and thermal stability, and more possibilities for molecular engineering due to their versatility, either at the backbone or by suitable substitution of side groups.

Recently, conjugated polymers with extended conjugation attracted the interest of scientists to explore their NLO properties as they possess good optical and electronic response. One of the main reasons for their fast‑growing interest is that they possess good structural versatility that may be achieved for them by both high‑precision molecular design and an appropriate synthetic method. Additionally, their good processability and stability make them attractive for the development of optical components for industrial applications.

1.7.1 Origin of NLO

Before the advent of the lasers, optics assumed that optical parameters of the medium are independent of the intensity of the light propagating in these mediums. The reason is that, the electric field strength generated by the non-laser light sources is of the order of 10^3 V/cm, is very much smaller than the inter-atomic fields i.e. 10^7 to 10^{10} V/cm of the medium, which is unable to affect the atomic fields of the medium and there by the optical properties of the medium. Lasers have drastically changed the situation as they

generate electric field strength varying from 10^5 to 10^9 V/cm, which is able to commensurate to that of the atomic electric fields of the medium, and there by affect the optical properties of the medium and thus generate new electromagnetic fields altered in phase, frequency, and amplitude.

NLO processes can be viewed as dielectric phenomena. When an electric field such as an applied dc field or a propagating electromagnetic wave passes through the medium, it induces electron displacement. Electrons that are bound to the nearby nuclei in the medium gets slightly perturbed by the external applied electromagnetic field and begin oscillating at the applied frequency.

When an intense externally applied field interacts with the medium, the relation between the radiation field and the polarization is no longer linear. If the strength of the externally applied field is comparable with the atomic fields of the material ($\sim 10^8$ V/cm), the electric field created can disrupt the internal electric field of the atoms within the material. The result being that the laser radiation and the material modify one another. (Boyd 2002). The polarization response (including the permanent polarization) of the medium can now be expressed as a power series expansion of the form which is given in equation (1),

$$P = P_0 + \chi^{(1)} \cdot E + \chi^{(2)} \cdot EE + \chi^{(3)} \cdot EEE + \qquad \ldots\ldots\ldots\ldots\ldots\ldots (1)$$

where P is bulk polarization, P_0 is static dipole moment, E is applied electric field, $\chi^{(1)}$ is the previously mentioned linear susceptibility, $\chi^{(2)}$ is the second-order nonlinear susceptibility, and $\chi^{(3)}$ is the third-order nonlinear susceptibilities of the bulk material.

The magnitude of $\chi^{(2)}$ and $\chi^{(3)}$ respectively, describe the strength of the second order and third-order processes. Higher order terms are also possible, however; they are extremely difficult to observe and are of little consequence from a materials perspective. An analogous equation described by the field-dependent molecular dipole moment expansion can be generated for the individual molecules of the material to give the microscopic polarization as given in equation (2),

$$P = \mu_o + \alpha \cdot E + \beta \cdot EE + \gamma \cdot EEE + \qquad \ldots\ldots\ldots\ldots\ldots\ldots (2)$$

where μ_o is molecular dipole moment α, β and γ are respectively, the polarizability, the first hyperpolarizability, and the second hyperpolarizability. They are measure of the responsivity of the molecule to the applied field. An alternate way of viewing the bulk polarization is to view the electric field as a sinusoidal oscillation,

$$E(z,t) = E_0 \cos(\omega t - kz) \qquad \dots\dots\dots\dots\dots\dots (3)$$

where E is the applied electric field, z represents direction in space, t represents time, ω is the oscillation frequency, and k is the propagation vector in equation (3).

The combination of this equation with the proper trigonometric identities for $\cos2\theta$ and $\cos3\theta$ allows the polarization equation to become as

$$P = \chi^{(1)} E_0 \cos(\omega t - kz) + \chi^{(2)} E_0^2 [1 + \cos(2\omega t - 2kz)] + \chi^{(3)} E_0^3 [\cos(\omega t - kz) + \cos(3\omega t - 3k)] \ ..(4)$$

From this equation it can be seen that the second-order process produces a frequency contribution that is independent of the field, and a contribution at 2ω. The third-order process on the other hand gives contributions at ω and 3ω.

In general, NLO effects can be classified broadly into two types, viz. second-order effects that are dependent on the first hyperpolarizability tensor term $\chi^{(2)}$ and third-order effects that are dependent on the second hyperpolarizability tensor term $\chi^{(3)}$. Since other higher order effects are difficult to observe, they are not significant. For a medium to exhibit second-order nonlinear susceptibility it should not possess a center of symmetry, i.e. it should be non-centrosymmetric. In general almost all media and molecules exhibit third-order response. Basically all forms of matter exhibit nonlinear optical phenomena. The material must exhibit a high degree of nonlinearity at a reasonable power level to be useful in a device.

1.7.2 Conjugated polymers for NLO

In polymers, which contain asymmetric molecules, the polarization responds nonlinearly to an applied oscillating electric field and this asymmetric response can be modified by an external dc field. This distortion of the electron distribution gives rise to harmonic generation and the linear electro optic effect. For centrosymmetric media, displacement of electron distributions gives rise to third-order nonlinear effects. These

will be large in materials with a high density of polarizable electrons. Thus conjugated polymeric semiconductors and organic molecules with extended electron conjugation can exhibit large third-order nonlinearities.

There are two approaches to maximize the nonlinearities in polymers. Firstly, by synthetic design of molecules with large dipole moment and nonlinear coefficients, nonlinearity can be enhanced. In the second approach, by maximizing the applied poling field strength or by employing steric forces, it can be increased. The molecular parameters, which are open to synthetic modifications, are (i) the relative electron affinities of the donor and acceptor groups in the dipole. (ii) the length and nature of the connecting system. The maximum poling field, which can be applied to NLO polymers, is limited by the breakdown strength of the material. The best polymers can withstand fields up to 350 MVm^{-1} but the largest reported values of EO coefficients have reached up to about 200 MVm^{-1}. This might be regarded as an upper limit of all practical purposes and most research efforts are attempting to enhance nonlinear optical susceptibility through molecular properties.

According to the literature, the three basic requirements for organic materials to exhibit NLO activity are (i) polarizability (electrons need to be greatly perturbed from their equilibrium positions), (ii) asymmetric charge distribution (incorporation of D–A molecules) and (iii) acentric crystal packing. In the molecular level, the molecule must possess (a) excited states close in energy to the ground state, (b) large oscillator strength for electronic transitions from ground to excited state and (c) a large difference between ground and excited state dipole moments. Such requirements are best met by dipolar donor-π-acceptor (D-π-A) systems that allow charge transfer between electron donating and electron withdrawing moieties. As conjugated polymers satisfy all these necessities, many of them were studied for NLO properties and their device applications.

In literature, various polarizable D-A systems carrying different homo and hetero-aromatic rings, ethylene linkage, or a combination of both were reported. A significant enhancement of polarizability was demonstrated by extending the conjugation length between the donor and acceptor groups. According to literature reports, the systematic

Chapter 1

approach towards development of effective NLO materials involves the design, synthesis and characterization of highly active chromophore molecules that possess a large molecular hyperpolarizability β. While designing such molecules, the chromophore can be incorporated into polymer main chain or side chain through covalent linkages. It has been well-established that certain factors such as increased chain length, enhanced planarity, and overall improved conjugation, and the strength of donors and acceptor moieties play significant roles in the NLO activity. In recent years, interest in polymers has grown primarily because they are easy to tailor for specific properties through synthesis (Dalton 1998, Wise et al. 1998, Asselberghs et al. 2002 and Thackara et al. 1995). Generally, the properties like optical quality, transparency, refractive index, ability to form thin films and fibers, and high nonlinear susceptibility make them highly useful in optoelectronic devices.

Some of the nonlinear processes that are responsible for NLO behavior are discussed in the following sections.

1.7.3 Different nonlinear absorption processes

Generally, nonlinear absorption is the change in transmittance of material as a function of intensity or fluence. At very high intensities, the probability of absorbing more than one photon before relaxing to the ground state can be greatly enhanced. There are various phenomena responsible for the nonlinear absorption exhibited by the nonlinear materials. NLO involves various processes such as two-photon (2PA) and three-photon absorptions (3PA), excited state absorption, saturable absorption, and optical limiting.

1.7.3.1 Two-photon and three-photon absorption processes

Two-photon absorption (2PA) is the simultaneous absorption of two photons of identical or different frequencies in order to excite a molecule from one state (usually the ground state) to a higher energy electronic state. The energy difference between the involved lower and upper states of the molecule is equal to the sum of the energies of the two photons. The possible situation of two photon absorption is illustrated in **Figure 1.4(a)**. In the first step, a photon from the same optical field oscillating at frequency $h\omega$ is

absorbed to make the transition to reach a virtual state. In the next step, another photon of same energy is absorbed from the oscillating field to jump into the real exited state. In both cases, the intermediate (or virtual) state is not real (i.e. does not involve a real stationary state of the system). Hence the system must absorb the two photons simultaneously. This makes the process sensitive to the instantaneous optical intensity.

Although the transition does not involve a real intermediate state, often there are impurities present that will produce a small amount of linear absorption. It should be understood that this absorption does not contribute to the transition to the final state of the process but only serves as an additional loss mechanism. Two-step absorption involving a single photon pumped intermediate state is described as excited state absorption. It may be a second-order process, several orders of magnitude weaker than linear absorption and is therefore not an everyday phenomenon.

The 3PA involves a transition from the ground state of a system to a higher-lying state by the simultaneous absorption of three photons (of energy, $3h\omega$) from an incident radiation field. The schematic representation of this process is given in **Figure 1.4(b)**. When the input intensity increases, multi photon absorption processes, characterized by the simultaneous absorption of three or more photons, can occur in the system.
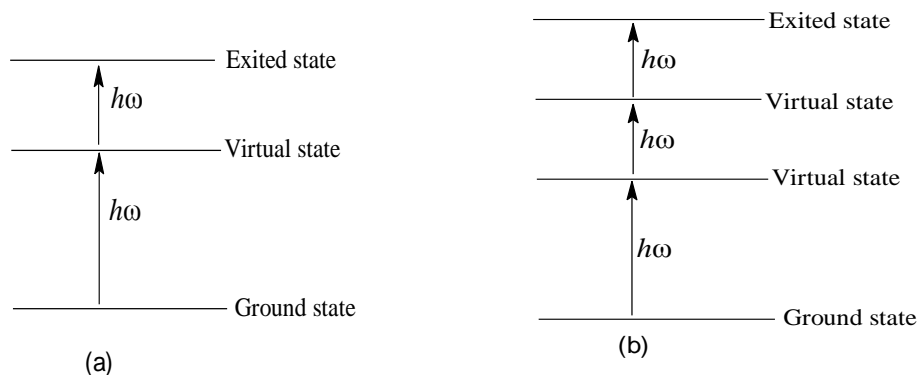
Figure 1.4 Two (a) and three-photon (b) absorption processes

1.7.3.2 Excited state absorption

When the incident intensity is well above the saturation intensity, then the exited state becomes significantly populated. In systems, such as polyatomic molecules and

semiconductors, there is a high density of states near the state involved in the excitation. The exited electrons can rapidly make a transition to one of these states before it eventually transits back to the ground state. There are also a number of higher lying states that may be radiatively coupled to these intermediate states and for which the energy difference are in near resonance with the incident photon energy. Therefore, before the electron completely relaxes to the ground state, it may experience absorption that promotes it to a higher-lying state. This process is called exited state absorption (ESA). It is apparent when the incident intensity is sufficient to deplete the ground state significantly.

The mechanism of various types of absorption processes is given in an energy level diagram as shown in **Figure 1.5**. The diagram shows different energy levels of a molecule, the singlet ground state S_0, the exited singlet states S_1 and S_2, as well as triplet exited states T_1 and T_2. It also displays the different transitions between the energy levels.

The transition from the ground S_0 to a higher singlet state by the absorption of a single photon gives rise to linear absorption. When the photons of the same or the different energy are simultaneously absorbed from the ground to higher exited state (S_0 to S_1), it is denoted as 2PA, which occurs at high light intensities.
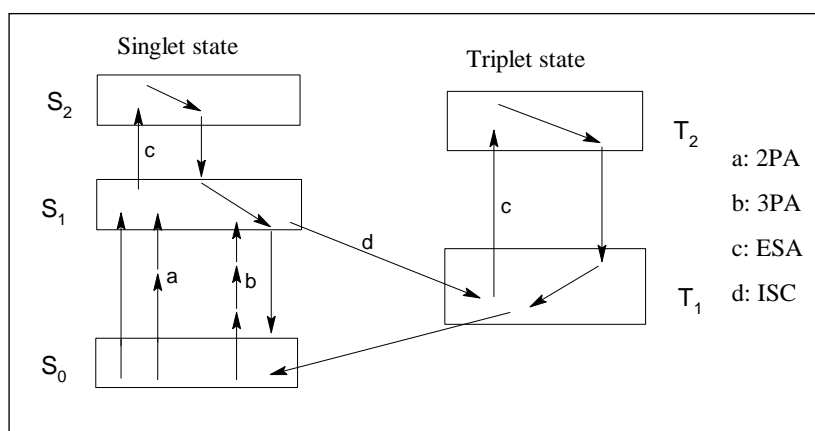
Figure 1.5 Energy level diagram showing 2PA, 3PA, ESA and ISC

When the exited state absorption (ESA) occurs, molecules are exited from an already exited state to a higher exited state (S_1 to S_2 and/or T_1 to T_2). For this to happen

the population of the exited states (S_1 and/or T_1) needs to be high so that the probability of photon absorption from that state is high. Therefore high intensity light is needed to pump up the molecules to the exited states before a substantial amount of ESA starts to take place. Also, it is important that life times of exited states are long enough so that a population of exited states can be obtained. The life times of the triplet states are longer than the singlet states and therefore ESA could be enhanced if the molecules could undergo intersystem crossing (ISC) to the triplet states. More ISC could be achieved by including heavy atoms which introduces a strong spin orbit coupling between the states. If more absorption occurs from the excited state than from the ground state, it is usually referred to as reverse saturable absorption (RSA).

1.7.3.3 Saturable absorption

Many material systems have the property that their absorption coefficient decreases when measured using high laser intensity. Often the dependence of the measured absorption coefficient α on the intensity I of the incident laser radiation is given by the expression (5) (Robert 2007),

$$\alpha = \frac{\alpha_0}{1 + I / I_s} \qquad \dots\dots\dots\dots\dots\dots (3)$$

where α_0 is the low-intensity absorption coefficient, and I_s is a parameter known as the saturation intensity. When the absorption cross section of the exited state is smaller than that of ground state, the transmission of the system will be increased once the system is highly exited. This process is called as saturable absorption. One consequence of saturable absorption is optical bistability. Certain nonlinear optical systems can possess more than one output state for a given input state. The term optical bistability refers to the situation in which two different output intensities are possible for a given input intensity, and the more general term optical multistability is used to describe the circumstance in which two or more stable output states are possible. Interest in saturable absorption originates from its potential usefulness as a switch, for its use in optical communication and in optical computing.

All of the nonlinear phenomena discussed above can be used for optical limiting (Tutt and Bogass, 1998) configurations. The optical limiting devices that have been

reported in the literature are many and varied, but they all rely on a material (or materials) that exhibit at least one nonlinear optical mechanism. The origins of such nonlinearities vary widely. Often materials may exhibit multiple nonlinear properties.

1.7.3.4 Optical limiting property

Optical limiters display a decreasing transmittance as a function of intensity or fluence of the laser. The greatest amount of attention in optical limiters in recent years has been for optical sensor protection from intense laser light. Several physical mechanisms have been exploited for optical limiting, including the nonlinear refractive index. Primarily these are based on the various nonlinear absorption processes in the limiting materials.

The operation of an ideal optical limiter is illustrated in **Figure 1.6**. For low incident intensity or fluence, the device has a linear transmittance. For some materials, e.g. two-photon absorbers, this transmittance may be near 100%, and the input-output curve would have a slope of 45°. On the other hand, RSA materials require a certain amount of linear absorption, and thus the input-output slope in the linear regime would be <45°. At some critical intensity or threshold in an ideal limiter, the transmittance changes suddenly and exhibits an inverse intensity or fluence dependence. Thus the output is clamped at some value that would actually be less than the amount required to damage the sensor. This critical point is called the threshold of the device, while the clamped output is called the limiting value of intensity or fluence.
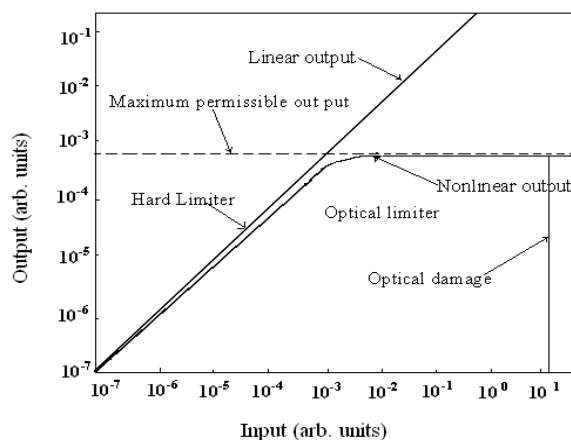
Figure 1.6 Operation of an ideal optical limiter

An optical limiter must provide protection over a wide range of incident intensity or fluence. Thus if the input-output slope is nonzero, at some input above the threshold the device will fail to provide protection. In some cases, the material itself may be damaged if its damage threshold is below this point, or the intensity/fluence dependent transmittance may approach a constant asymptote so that the input-output slope again increases. Any one of these situations will define a maximum input for which the device will provide effective limiting. The ratio of this input value to the threshold is called the dynamic range of the limiter.

Therefore, two desirable attributes of an optical limiter are low threshold and wide dynamic range. In addition, since the device is usually passive and must respond to pulses of arbitrary duration, a fast optical response is required. Also, as optical sensors usually have wide spectral pass bands, the device should have a broadband response. Other requirements may include high linear transmittance, optical clarity, color neutrality, and robustness (i.e., resistance to damage and degradation due to humidity, temperature swings, etc.). These necessities place severe restrictions on materials. Consequently, development of good optical limiter materials is an active research area in recent years.

1.7.4 Measurement methods

A number of techniques have been used for the measurement of NLO properties of molecules, the most popular of which are second harmonic generation, third harmonic generation, hyper-rayleigh scattering , Z-scan, degenerate four wave mixing (DFWM), optical kerr-gate and pump-probe measurements (Sutherland,1996). Among various measurement methods, we have used Z-scan and DFWM methods.

1.7.4.1 Z-scan technique

The Z-scan technique is a very simple and convenient way of investigating nonlinear absorption in a nonlinear material (Sheik-Bahae et al. 1990). **Figure 1.7** provides a schematic diagram of a Z-scan experiment. The "open aperture" Z-scan gives information about the nonlinear absorption coefficient. Here a Gaussian laser beam is used for molecular excitation, and its propagation direction is taken as the z-axis. The

beam is focused using a convex lens, and the focal point is taken as z=0. Obviously, the beam will have maximum energy density at the focus, which will symmetrically reduce towards either side of it, for the positive and negative values of z.
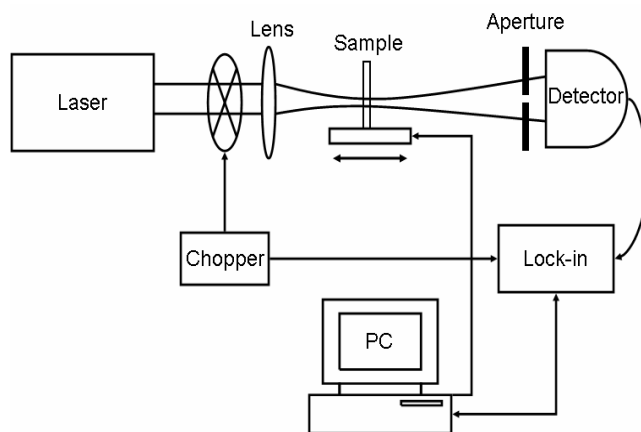
Figure 1.7 The open aperture Z-Scan experimental set-up

The experiment is done by placing the sample in the beam at different positions with respect to the focus (different values of z), and measuring the corresponding transmission. For a focused Gaussian beam, each z position corresponds to an input laser energy density of F(z) = $4\sqrt{\ln 2}E_{in}\left/ \pi^{3/2}\omega(z)^2\right.$, and intensity of I(z) = F (z)/τ, where E_{in} is the input laser pulse energy, ω(z) is the beam radius, and τ is the laser pulse width. Thus the sample experiences different laser intensity at each position, and hence, the measured position-dependent transmission gives information about its intensity-dependent transmission. From the open aperture Z-scan data, the nonlinear absorption coefficient of the material can be calculated.

1.7.4.2 Degenerate four wave mixing (DFWM) method

DFWM is one more important technique for investigating third order nonlinearities in various materials. The principle of DFWM is the interaction of three laser beams of same frequency to generate a fourth beam of same frequency. When all the waves have the same frequency, it is called DFWM. We used the forward folded BOXCARS geometry for the experiment, where a laser beam is split into three and the beams are aligned such that they form three corners of a square (**Figure 1.8**). The

diametrically opposite beams are the pump beams, and they have the same intensity. The third beam is the probe, which has an intensity of about 20% of the pump beam. When the beams are focused onto the sample the fourth beam (signal beam) is generated due to nonlinear interaction, which will appear on the fourth corner of the square. It can be measured using a photo detector. The beam waist used for the measurement is 20 μm, estimated by knife edge method. The diameter of the lens used is 2.54 cm of 1 inch. Focal length is 10 cm with F number 3.93
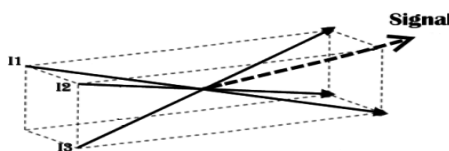
Figure 1.8 Four wave mixing in the BOXCARS geometry

The present research work involving design, synthesis, characterization and NLO investigation of new thiophene based D-A type conjugated polymers, is divided into five chapters. **Chapter 1** covers a brief introduction on conjugated polymers and nonlinear optics. It also enlists the various methods which are used to synthesize conjugated polymers and to measure their NLO property.

Chapter 2 presents a literature overview to highlight the significance of different conjugated polymers reported in the literature together with their various applications. It also outlines the scope and objectives of the present research work, based on literature survey.

Chapters 3 describe the synthesis and characterization of intermediates, monomers and four new series comprising sixteen conjugated polymers consisting of substituted thiophene unit as electron donating moiety and 1,3,4-oxadiazole as electron acceptor group with/without different spacer groups.

Chapter 4 includes electrochemical, linear optical and NLO studies of newly synthesized conjugated D-A type polymers.

Finally, **Chapter 5** outlines the summary and conclusions of the entire research work along with the scope for future work.

Chapter 2

Abstract

  This chapter covers a review of literature reported on design and synthesis of various types of conjugated polymers consisting of different aromatics/heteroaromatics for diverse applications. Also, it includes scope and objectives of the present research work, arrived at on the basis of detailed literature survey. Further, it covers the design of four new series of D-A type conjugated polymers centered on thiophen-yloxadiazoles.

2.1 INTRODUCTION

  In the last few decades there is tremendous increase in the usage of conjugated polymers in various applications like, LEDs (Burroughes et al. 1990), solar cells (Sariciftci et al. 1993, Gunes et al. 2007 and Kim et al. 2011), thin-film transistors (Halls et al. 1995 and Babel et al. 2004), batteries (Kerr et al. 1996), sensors (Albert et al. 2000 and Vidal et al. 2003) and electrochromic devices (Ohsedo et al. 2000). Also, conjugated polymers with their extended delocalization of π-electrons along the molecular backbone are interesting materials for NLO applications (Samoc et al. 2000, Ak et al. 2005, Li et al. 2008, Li et al. 2008, Cho et al. 2008 and Ramos-Ortíz et al. 2010). Among conjugated polymers D-A type conjugated polymers have attracted increasing attention since they can serve as efficient NLO and electrochromic materials as well as low-band-gap polymers with high intrinsic conductivity (Thomas et al. 2004, Koynov et al. 2005, Colladet et al. 2007, Beaujuge et al. 2010, Yuen et al. 2011 and Zhang et al. 2012).

  For any application, it is the capability of conjugated polymers to tailor the electronic and material properties via their molecular structure that makes this class of polymers useful in different applications. In fact, properties of these materials can be varied over a wide range of conductivity, processability, and stability depending on the type of substituents, rings, and ring fusions in the polymer chain. The development of novel polymers that are soluble in common organic solvents and processable by industrially relevant techniques, such as spin coating, screen printing, inkjet printing, or roller coating, is necessary for the practical applications of conjugated polymers. Such polymers with tailored electronic structures also possess the ability to be multifunctional materials that can find applications in numerous device architectures. Recently, the

alteration of polymer chain with suitable donor and acceptor type groups is one of the promising approaches for designing new conjugated polymers with improved optoelectronic properties.

2.2 LITERATURE REVIEW

In the last few decades, several D-A type conjugated polymers were designed and synthesized for various applications. Several reports are available on investigation of their opto-electronic properties (Karikomi et al. 1995, Lee et al. 1999, Jenekhe et al. 2001, Zhu et al. 2005 and Sonmez et al. 2005). These polymers mainly consist of electron-donors such as substituted benzenes, carbazoles, thiophenes and 3,4-disubstituted thiophenes etc. and strong electron acceptors like 1,3,4-oxadiazole, cyano, pyridine etc. as active units in their chains. A brief account on literature reports available on the important D-A type conjugated polymers carrying different types of electron releasing and electron withdrawing segments has been given in the following section. Further, their synthetic methodologies and effect of various substitutional groups on optical and electrochemical properties of the polymers have been described.

With regard to NLO properties, a strong delocalization of π-electrons in the polymer backbone is highly significant as it determines a very high molecular polarizability and thus giving rise to remarkable optical nonlinearity. Large molecular hyperpolarizabilities and low optical losses within the spectral region of interest are the basic requirements for NLO applications. A general approach for obtaining materials with significant NLO properties consists in synthesizing polymer framework involving electron-donor and electron-acceptor groups linked through a π-conjugated bridge (Kanis et al. 1994, Shi et al. 2000 and Kaloian et al. 2005). Such D-π-A systems exhibit a prominent intramolecular charge transfer (ICT) along the π-conjugated bridges, which is crucial in promoting large optical nonlinearities and ultra-fast responses due to instantaneous electronic polarization. Thus, an optimal combination of various factors such as π-delocalization length, D-A nature, dimensionality, conformation and orientation of molecular structure results in a large hyperpolarizability in the polymeric systems and hence it leads to achieve good nonlinearities in them (Cheng et al. 1991, Dalton et al.

Chapter 2

1995, Verbiest et al. 1997 and Audebert et al. 2003). Moreover, theoretical calculations further suggest that the electronic nature and location of heterocyclic rings in the system play a subtle role in the development of NLO properties of D‑A compounds (Varanasi et al. 1996 and Breitung et al. 2000).

The polymer bandgap and HOMO/LUMO energy levels are easily controlled by adjusting the molecular orbital overlapping effect and also by intra‑chain charge transfer from the donor to the acceptor (Zhang et al. 2010). This interest is driven by the need for devices for optical signal processing, all-optical switching, optical computing, logic devices and sensor protection (Zyss et al. 1994, Zhan et al. 2001, Koynov et al. 2005 and Beaujuge et al. 2010). NLO materials are currently the focus of intensive research efforts because of their potential civilian and military applications in signal processing, ultrafast optical communication, data storage, optical limiting, logic devices, optical switching, image transmission, and optical computing (Torre et al. 2004 and Pomerantz et al. 2002). Research advances in this field depend critically on the development of new materials with strong NLO capabilities (Samoc et al. 2006 and Borbone et al. 2011). In this context, conjugated polymers are the alternative candidates for NLO applications.

It has been shown that optical nonlinearity of polymers can be enhanced by introducing proper electron donating and withdrawing entities as well as by optimizing steric repulsion between donor and acceptor groups (Groenendaal et al. 1998, Babudri et al. 2001, Caruso et al. 2005, Li et al.2010 and Li et al. 2011). This generates a highly polarizable charge transfer system with an asymmetric electron distribution. Further, the strength of D‑A interactions is determined by the nature of donor and acceptor groups with π-conjugated spacers. Strong electron accepting groups and short spacers generally enhance D‑A interactions, whereas weak electron-accepting groups and long spacers lower the D‑A strength (Delgado et al. 2008, Grazulevicius et al. 2003, Zhu et al. 2006 Li et al. 2008 and Ramos‑Ortíz et al. 2010). Among various D‑A type conjugated polymers, thiophene based polymers and oligomers are of special interest mainly due to their high thermal stability, readiness to accommodate functional groups and solubility in common organic solvents. The introduction of side‑chain can also ameliorate the film‑

forming ability of polymers, which offer great promise for practical device applications. It is observed that enhancement in their optical nonlinearity can be achieved by introducing proper electron donating and electron withdrawing groups as well as by optimizing steric repulsion between these groups through structural modification. Earlier studies reveal that the incorporation of a 3,4-dialkoxythiophene moiety along the backbone of a polymer enhances the polymer's dopability and decreases its band gap. In addition, the incorporation of a highly electron-withdrawing oxadiazole ring along the conjugation path increases the charge carrying properties of the polymer (Li et al. 1996, Lima et al. 1998, Peng et al. 1999, Paik et al. 2002, Udayakumar et al. 2007 and Li et al. 2012).

2.2.1 Thiophene based polymers

Thiophene is the simplest aromatic heterocyclic compound containing sulfur atom in its ring and it shares some analogous chemical properties with benzene. The lone pair of electrons on sulfur in the delocalized π-electron system does not exhibit the properties of thioethers but aromaticity. Its derivatives are widely used as monomers to make condensation polymers. PTh and its derivatives have been the most studied materials and are important representative class of organic semiconducting materials that can be used in many electro-optical applications. Because of their good electrical properties, lightness, flexibility, processability, environmental and thermal stability they can be used as electrical conductors, nonlinear optical devices, PLEDs, electrochromic or smart windows, photoresists, antistatic coatings, sensors, batteries, electromagnetic shielding materials, artificial noses and muscles, solar cells, electrodes, microwave absorbing materials, new types of memory devices, optical modulators and valves, imaging materials, polymer electronic interconnects, optical devices and transistors. Among the electrochromic polymers, especially PTh derivatives, gained special interest owing to their facile switching properties, processibility and ease of tuneability (Pinar et al. 2008).

In recent years, chemical modifications of PThs have been widely carried out to satisfy different application requirements. Introduction of pendant alkyl chains of suitable lengths on thiophene ring improves the solvent processibility and hole carrying property

(Skotheim et al. 1998, ojha, et al. 2003 and Uday Kumar et al. 2006). In addition, incorporation of electron-accepting units like 1,3,4-oxadiazole, pyridine into the polymer chain enhances the electron-carrying property of the corresponding polymer. Consequently, it leads to a D-A type of arrangement along the polymer chain and provides the polymer chain a good charge-carrying property which is one of the major requirements for the development of efficient optoelectronic devices. Based on this, several D-A type polymers carrying substituted thiophenes have been reported in the literature.

A new series of poly-dialkoxythiophenes containing 1,3,4-oxadiazole (Brown 1992, Meng and Huang 2000) moiety along the main chain was shown to be efficient electron transport or emission transfer materials. They were synthesized through the dehydrocyclization of corresponding polyhydrazide using polyphosphoric acid (PPA) as cyclizing agent. The resulting polymers **S-2.1** were found to be stable up to 480 °C. Also, they were shown to exhibit blue fluorescence and possess relatively a high quantum yield (7-46%). Here the stability is mainly attributed to the presence of 1,3,4-oxadiazole ring in the polymer chain.

$R = H, OCH_3, OC_4H_9, OC_{12}H_{25}$
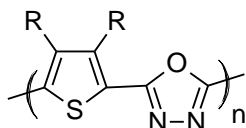
S-2.1

In pioneering studies by Yu et al. (1998), it was reported synthesis and evaluation of optical properties of a new D-A type light-emitting polymer (**S-2.2)** composed of 3,3'-didecyl-2,2'-bithiophene and 2,6-bis(1,3,4-oxadiazolyl)toluene. It is highly soluble and it emits green light under the irradiation of UV photons. The comparison of their electrochemical properties with other light-emitting polymers indicates the possibility of developing highly electroluminescent polymeric materials with balanced transporting ability for electrons and holes.
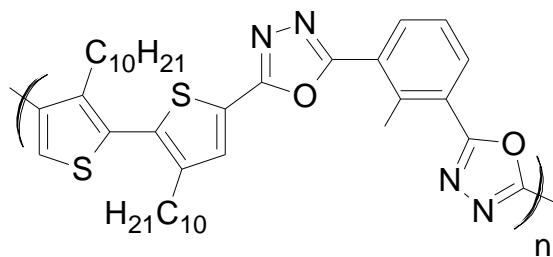
S-2.2

A new series of D-A type conjugated polymers (**S-2.3a-d**), composed of oligothiophenes and 1,4-bis(oxadiazolyl)-2,5-dialkoxybenzenes was synthesized and studied their optical properties by Huang et al. (1999). According to the studies, the insertion of 1,4-bis(1,3,4-oxadiazole)-benzene serves as a conjugation extending block in the polymers. This provides the promising approach to balance the barrier between the LUMO of an electroluminescent material and the work function of ITO and the barrier between the HOMO of the electroluminescent material and the work function of the metal electrodes. The reduction potential of the polymers did not change remarkably with variation of thiophene ring number in the oligothiophene blocks, which indicated that the reduction properties of the polymers were dominated by the 1,3,4-oxadiazole segments (Faid et al. 1993).
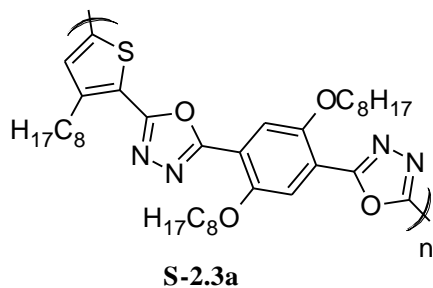
S-2.3a
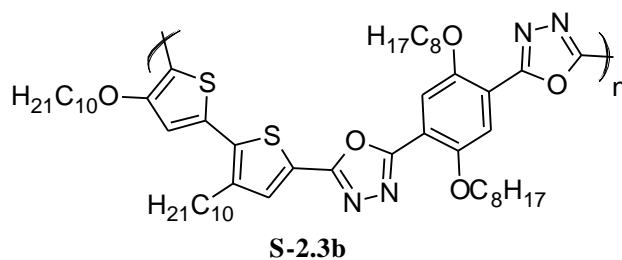
S-2.3b
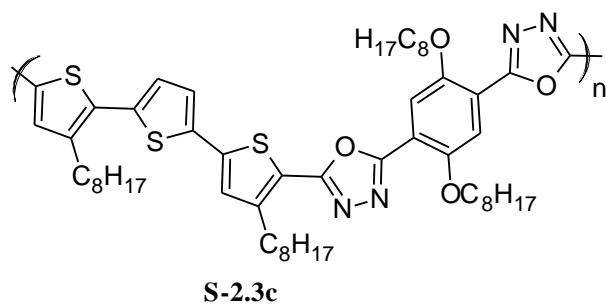
S-2.3c
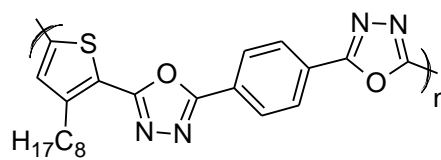
S-2.3d

S -2.3a-d

Chapter 2

The initial role of side chains on the PTh backbone was to improve solubility; later it was established that the introduction of various substituents along the backbone not only enhances the processibility of these polymers, but also alters their material properties, including their electrical properties and optical properties. PThs are known to exhibit a variety of sensory properties upon exposure to external stimuli such as affinity chromism, photochromism, piezochromism, solvatochromism, and thermochromism. These chromic effects are due to a planar and non-planar transition of the conjugated chain (Levesque and Leclerc 1995).

Pei et al. synthesized new series of poly[1,4-bis(4-alkyl-2-thienyl)-2,5-disubstituted phenylene]s (**S-2.4**) with different substituents on the phenylene and thiophene ring. It was observed that, the electronic spectra of the polymers can be tuned by changing the substitution on both the phenylene and thiophene rings, emitting blue to green light. The electronic structures of the polymers can also be tuned by different substitutions, as demonstrated by electrochemical measurements. The absolute PL efficiencies of the polymers in films can be remarkably effected by the substitution on both the phenylene ring and the thiophene, much higher than the PL efficiencies in other poly(thiophene) based light-emitting materials. It was demonstrated that inserting substituted phenylene rings into the backbone of poly(thiophene) is a useful approach to improve the PL efficiency of thiophene-based conjugated polymers (Pei et al. 2000).
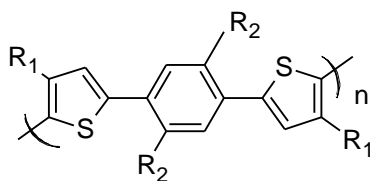
R$_1$ = Cyclohexyl, hexyl
R$_2$ = H, methyl, decyloxy

S -2.4

Ojha and coworkers reported the synthesis and characterization of certain polyoxadiazoles (**S-2.5a-c**) containing 3,4-dialkylenedioxythiophenes as electron donor segment and 1,3,4-oxadiazole as electron withdrawing segment. The polymers were obtained using precursor polyhydrazide route. The authors observed that the presence of

alternating electron donor and acceptor units resulted in lowering of their bandgap. They also reported that these polymers possess good hole-blocking properties (Ojha et al. 2003).

S-2.5a   **S-2.5b**

S-2.5c   n

S-2.5a-c
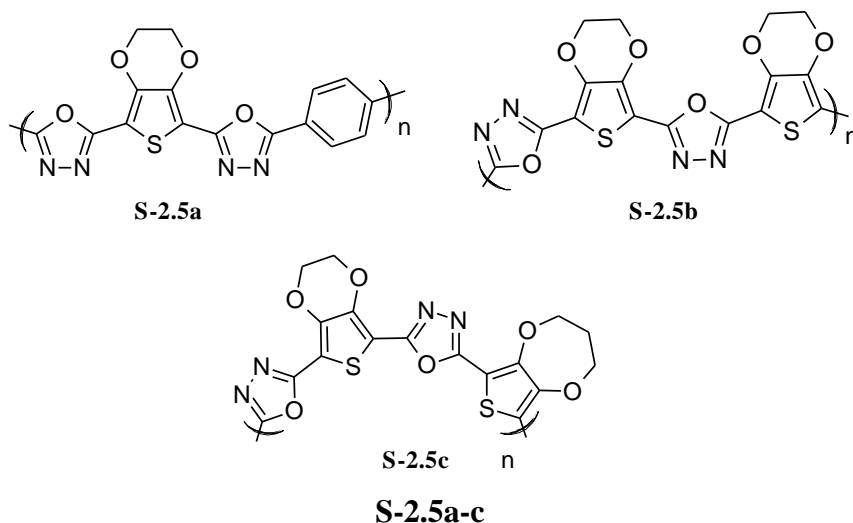
Udayakumar et al. (2006) synthesized a new series of D-A type polymers (**S-2.6**) carrying 1,3,4-oxadiazole and 3,4-dialkoxythiophene units via precursor polyhydrazide route. These polymers were shown to exhibit good hole blocking and electron carrying properties. Also, they were shown to possess good NLO properties with reverse saturable absorption and good optical limiting behavior. According to the authors, introduction of strong electron donors and acceptors along the polymer backbone could be a promising molecular design to enhance the NLO property of the conjugated polymer.

$R = C_6H_{13}, C_8H_{17}, C_{10}H_{21}$
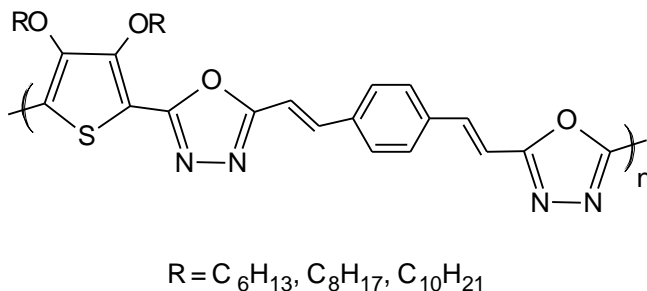
S-2.6

Henckens and co-workers showed that poly(thienylene vinylene) (PTV) type, low band gap polymers carrying 3,4-diphenylthiophene unit in its chain, synthesized by them,

via dithiocarbamate precursor route possess very good optical properties. The researchers investigated the detailed optical properties of newly synthesized polymers **S-2.7a-b**. These polymers were shown to exhibit enhanced stability and low bandgap (1.7-1.8 eV). This may be attributed to the presence of phenyl rings on 3- and 4- positions of the thiophene moiety. They also observed that introduction of butyl chain to the polymer **S-2.7b** resulted in improved solvent processibility (Henckens, et al. 2005).

S - 2.7a   **S - 2.7b**
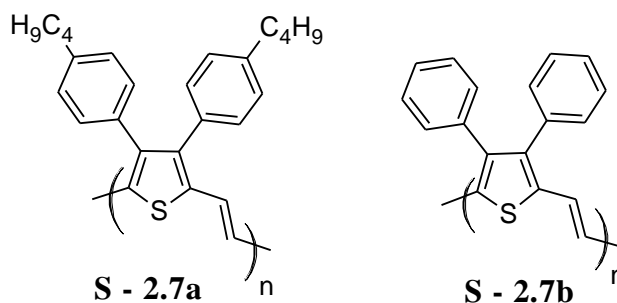
From the forgoing account, it is clear that 3,4-dialkoxy substituted PThs show facile dopability and lower bandgap ascribe to the electron donating nature of the alkoxy moiety. Further, introduction of long alkoxy pendants at 3- and 4- positions of the thiophene ring improves the solvent processibility and hole carrying ability of the corresponding polymer. Against this background, it can be concluded that 3,4-dialkoxythiophenes acts as an interesting moiety for exhibiting stability, good charge carrying and optical properties of the polymer. In view of this, it has been planned to design some new D-A type conjugated polymers carrying 3,4-dialkoxythiophene units as electron rich segments and to synthesize them. It is hoped that the resulting polymers would show improved charge carrying and optical properties.

2.2.2 1,3,4-Oxadiazole based polymers

The 1,3,4-oxadiazole is a five membered heterocycle containing nitrogen atoms at positions 3 and 4, and oxygen atom at position 1 of the ring. It is a promising template due to its luminescent, electron-deficient property and thermal stability. As a result, polymers carrying 1,3,4-oxadiazoles are chemically and thermally stable, with high glass transition temperatures, making them one of new choices of polymers to be used in extreme condition (Bottino et al. 1999). The optical and electronic properties of 1,3,4-

oxadizole (Chihaya et al. 1990, Zhu et al. 2003 and Emi et al. 2006) and thiophene (Huang et al. 1998 and Blumstengel et al. 1999) derivatives have been paid great attention in the field of electroluminescence. Later years, many investigations have proven that modifying of side chains or inserting of other heterocyclic in 1,3,4-oxadiazole based polymeric systems could lead to good organic electroluminescent molecules (OELM) (Zhu et al. 2002, Peng et al. 2006 and Bugatti et al. 2006). The structural investigation of OELM molecules in solid state is one of the promising research fields because luminescent and electron-transporting behaviors are believed to be dependent on the conformation of OELM molecule and also on molecular level interactions between the OELM molecule and substrate (Domenico et al. 2002, Acierno et al. 2003, Neitzert et al. 2006, and Guan et al. 2006). Thus, it was well-established that the introduction of an oxadiazole ring into molecular structures is one of the promising approaches to the attainment of high charge-carrier mobility.

Peng and his coworkers (1998) synthesized a polymer **S-2.8** containing alkoxy substituted PPV and 1,3,4-oxadiazole units, as good EL material. Also, the presence of alkoxy groups increased the solubility of the resulting polymer. Several new PPV derivatives containing 1,3,4-oxadiazole units either in the main chain or as pendants to the main chain were reported in the literature as effective EL materials (Mikroyannidis et al. 2004).
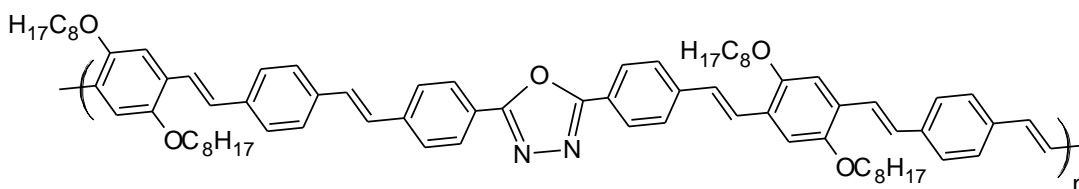
S-2.8

A novel PPV based D-A type conjugated polymer containing electron-affinitive bis-1,3,4-oxadiazole and hole-transporting distyrylbenzene (**S-2.9)** was reported by Wu and his coworkers (Wu et al. 2003). A new route was designed by them for the synthesis. The polymer showed good thermal stability and its photoluminescence (PL) maxima was found to be in the range of 515-550 nm. It was observed that there is a gradual transition

of its maxima from 515 to 544 nm, as its concentration in tetrachloroethylene increases. The authors showed that single-layer LED with a structure of ITO/**S-2.19**/Al displayed a bright yellow emission.
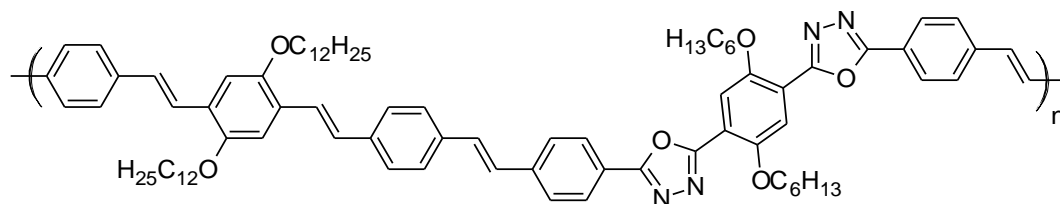
S-2.9

Chung and his group members reported the synthesis and luminescent properties of an attractive polymer (**S-2.10**) carrying 2-(4-tert-butylphenyl)-5-phenyl-**1,3,4-**oxadiazole (PBD) pendants directly attached to the PPV back bone (Chung et al. 1998). A simple modification in structure resulted in six times higher EL efficiency than that of simple PPV. Further, introduction of 2-ethylhexyloxy pendant afforded increase in EL performance of the corresponding polymer **S- 2.11**.
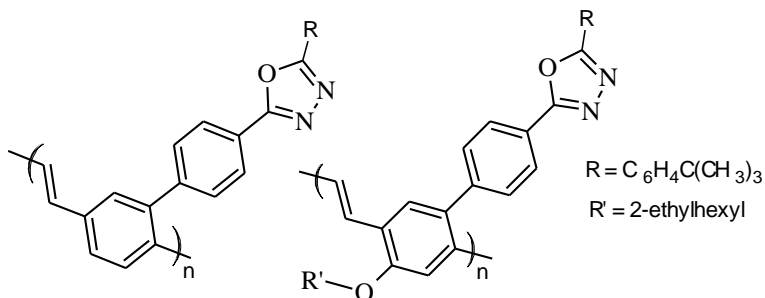
S-2.10   **S-2.11**

An interesting D-A type conjugated polymer (**S-2.12**) consisting of *m*-(butyl phenyl)-**1,3,4-**oxadiazole and *p*-phenyl-**1,3,4-**oxadiazole in its structure was synthesized by Li and his research team. This polymer on irradiation with UV light emits purple light with a quantum yield of 11%. Further, its electrochemical studies revealed that it possesses very good electron transporting and hole blocking properties. Under redox 1996).
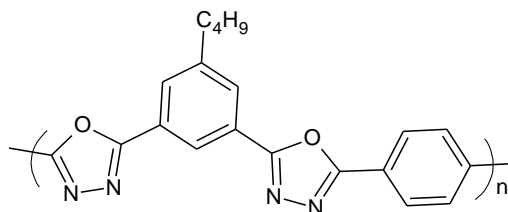
S-2.12

Hoon and Soon (2008) designed and synthesized a series of novel poly(dialkoxyphenylene-1,3,4-oxadiazole)s (**S-2.13** to **S-2.14**) carrying three different alkyl substituents and three regio-isomeric structures. The polymers were shown to possess well defined structures, excellent thermal stability and good solubility in co-solvents of chloroform and trifluoroacetic acid. Their relative solubility was found to depend on alkyl chain length.   Meta-polymers were found to be more soluble than para-polymers. Their wide-angle X-ray diffractograms indicated that polymers adopted a stacked planar conformation.   Further, layer-to-layer thickness was 3.4A° for all polymers, but within a layer side chain-to-side chain and main chain-to-main chain distances increased with alkyl chain length. The authors also reported that the chain-to-chain distances of meta-polymers were greater than those of equivalent para-polymers.

$R = C_2H_5, C_4H_9, C_8H_{17}$
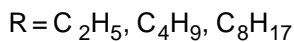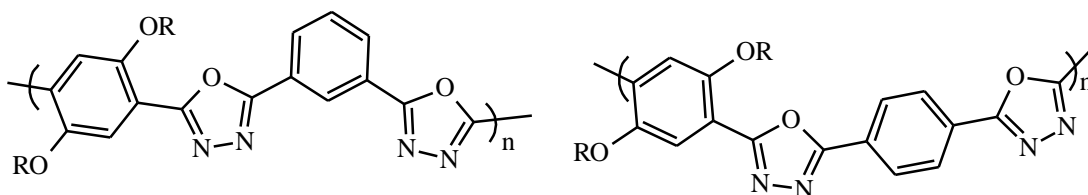
S-2.13

S-2.14

Three new D-A type poly(3,4-dialkoxythiophene)s (**S-2.15**) carrying 1,3,4-oxadiazole units were synthesized by Udayakumar et al. (2006) through precursor polyhydrazide route. The optical and electrochemical properties were studied in detail. These polymers were shown to display good hole blocking and electron carrying properties. Besides these characteristics, they were also shown to possess good NLO properties. The polymers exhibited reverse saturable absorption and good optical limiting behavior for the laser pulses of wavelength 532 nm. As concluded by the authors,

introduction of strong electron donors and acceptors along the polymer backbone is a promising molecular design to enhance the NLO property of the conjugated polymer.


$R = C_6H_{13}, C_8H_{17}, C_{10}H_{21}$
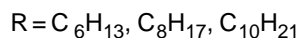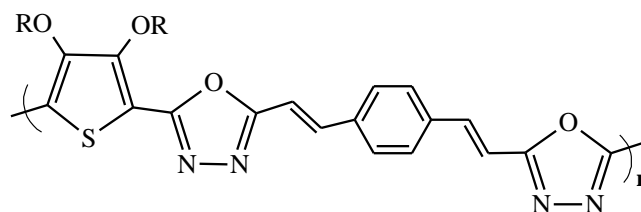
S-2.15

John et al. (2006) evaluated the third order NLO properties of conjugated polymers containing electron rich 3,4-dialkoxy thiophene and electron affinitive 1,3,4-oxadiazoles in their structure, by Z-scan and DFWM techniques. The compounds were shown to possess good nonlinear optical susceptibility of the order of 10^{-12} esu owing to the presence of 1,3,4-oxadiazole group.

With relevance to the literature reports, it is clear that the 1,3,4-oxadiazole is a strong electron acceptor and has remarkable influence on the charge-carrying ability and NLO property when it is present in the polymer chain. Consequently, polymers carrying 1,3,4-oxadiazole display enhanced optical and electrochemical response. Also, polymers derived from 1,3,4-oxadiazole have good thermal stability. Owing to the importance and established properties of various conjugated polymers based on 1,3,4-oxadiazoles, it has been planned to introduce 1,3,4-oxadiazole ring as an electron accepting moiety in our new molecular design with the expectation that new polymers would show superior optical and electrochemical properties.

2.2.3 Pyridine based polymers

Pyridine is an electron deficient heterocyclic compound, structurally related to benzene with one C-H group replaced by a nitrogen atom. Interestingly, one of the most important features of pyridine-based polymers is the high electronic affinity. Generally, pyridine is incorporated to conjugated polymer structures because of the fact that they show strong electron accepting character and good thermal stability. As a consequence, the resulting polymer is more resistant to oxidation and shows better electron transport

properties. Also many literature reports are available on D-A type conjugative polymers carrying pyridine as electron acceptor units in the main chain of the polymer. It is well-established that pyridine ring being an electron affinitive unit enhances the electron accepting nature when it is present in the polymer chain along with electron releasing thiophene ring. Some of the literature reports on synthesis and properties of certain D-A type conjugated polymers carrying pyridine ring are presented below.

In a review reported by Akcelrud, it was described that conjugated polymers **S-2.16** containing pyridine and phenylenevinylene are highly luminescent and their internal quantum efficiencies are in the range of 75-90% in solution and 18-30% in film form. These polymers possess good solubility in common organic solvents when compared to PPV. Time resolved studies showed that the presence of n and π^* states leads to enhanced intersystem crossing to triplet excitons in the powder form, while aggregate formation plays a key role in the optical and electronic properties of the films (Akcelrud et al. 2003).

$$R = C_{12}H_{25} \text{ or } COOC_{12}H_{25}$$
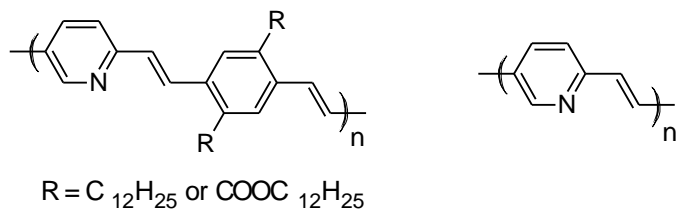
S-2.16

Following Suzuki coupling approach, Ng et al. (2001) synthesized successfully four new blue fluorescent alternating D-A type conjugated polymers (**S-2.17**) with high photo- and electro-luminescence property. Also, these polymers were shown to possess good solubility and processability due to the presence of alkoxy substitution on benzene ring.

$$R = C_4H_9, C_8H_{17}, C_{12}H_{25}, C_{16}H_{33}$$
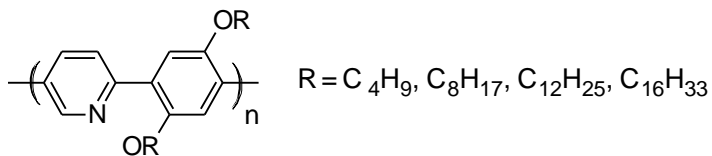
S-2.17

Wang et al. (1997) presented new light-emitting devices based on several pyridine-containing conjugated polymers and copolymers (**S-2.18**) in various device configurations. The high electron affinity of pyridine-based polymers improves stability as well as electron transport properties of the polymers and hence enables the use of relatively stable metals such as Al as electron injecting contacts when used in PLEDs.
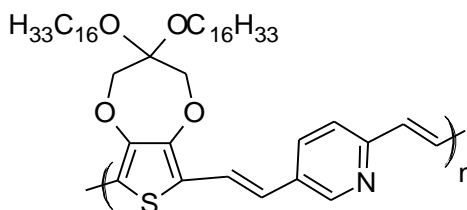
S -2.18

Recently, Hegde et al. reported the synthesis and NLO properties of a new series of D-A type of polymers containing 3,4-dialkoxythiophene as electron rich segment, and 1,3,4-oxadiazole and pyridine moieties as electron deficient units (**S -2.19**). The polymers were shown to possess good optical limiting properties (Hegde et al. 2009).
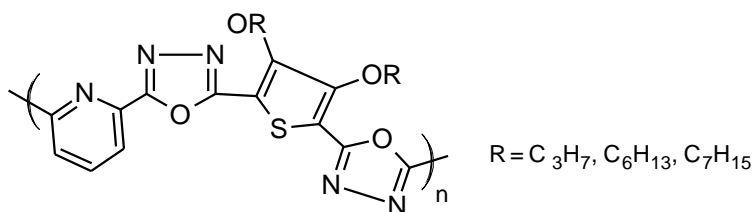
S-2.19

Wu and co-workers (2005) described the synthesis and properties of pyridine based polymers **S-2.20** and **S-2.21**. The polymers were obtained starting from 2,6-bis-(3-octylthiophen-2yl)-pyridine using nickel-mediated Stille coupling or by palladium catalyzed Yamamoto coupling. The polymers were shown to exhibit good solubility in common organic solvents. They were found to be amorphous in nature and thermally stable up to 400 °C. Further, they were shown to possess strong luminescence property both in chloroform solution and film state. The polymers emit blue light in solution with emission maxima at 420-484 nm and green light with PL emission maxima at 500-514 nm in thin films. Interestingly, the polymer **S-2.20** shows very high quantum efficiency in

the film form and it is 60 times higher than its thiophene analogs. EL was achieved from a single-layer PLED with the configuration of ITO/Polymer /Al. The turn-on voltage of the device is 10 V and the λ_{max} (550 nm) of the EL is voltage independent. The authors established that the presence of pyridine moiety in the polymer backbone brought about increased photoluminescence quantum efficiency as well the solvent processability.
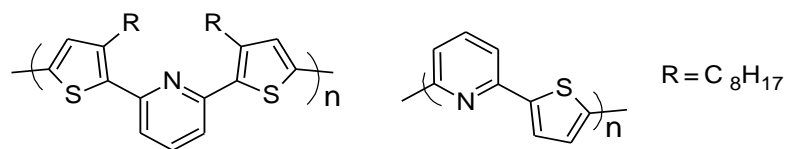
S-2.20   **S-2.21**

From the foregoing account, it is clear that incorporation of electron withdrawing pyridine ring along with thiophene in the main chain has brought about enhancement in luminescent and NLO properties of resulting polymers. In view of this, it has been planned to introduce pyridine unit in the structural design of new polymers carrying 3,4-disubstituted thiophene and 1,3,4-oxadaizole moieties, with the hope that new structural entities would offer improved optical and electrochemical properties. Further, it is expected that incorporation of pyridine unit into the polymer main chain would increase thermal stability of the polymer. Also, there is a good scope for functionalization of pyridine ring with appropriate substituent for tailoring the desired properties of the polymers.

2.2.4 Phenyl/biphenyl based polymers

Phenyl and biphenyl groups are aromatic conjugated systems. The introduction of these groups into the polymeric systems imparts good extent of conjugation to the polymer and also improves stability. Poly(p-phenylenevinylene) (PPV) is the first reported conjugated electroluminescent polymer and is the only polymer of this type that has so far been successfully processed into a highly ordered crystalline thin film. PPV and its derivatives are conducting polymers with rigid-rod like structure. They can be easily synthesized in good purity and with high molecular weight. The physical and electronic properties of PPV can be easily altered by the inclusion of functional side

groups. The interesting properties like low optical band gap, bright yellow fluorescence make PPV a potential candidate in many electronic applications in PLED and photovoltaic devices. Some of the literatures showing the importance of phenyl and biphenyl moieties in conjugated polymers are highlighted as follows.

Samoc et al. (2000) studied nonlinear optical property of PPV derivatives using Z-scan and DFWM measurement methods. The authors observed that all the studied polymers are NLO active and their two photon absorption coefficient is in the order of 10^{-8} cm/W. Different derivatives of PPV (**S-2.22a-f**) displayed good optical limiting properties with varied absorption coefficient values.

S-2.22a-f
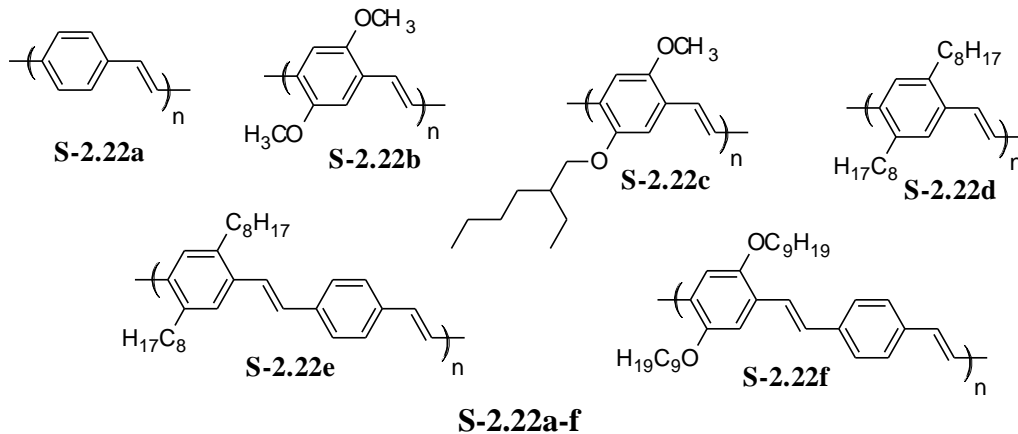
A study by Krishnamoorthy and coworkers (Krishnamoorthy et al. 2001) claimed that polymer having cyanobiphenyl and EDOT (**S-2.23**) imparted improved contrast and better switching. The substitution of bulky biphenyl ring with cyano group to EDOT showed a contrast of 67% at 660 nm which is the best reported contrast for an EDOT derivative. They also explained that compared to simple EDOT derivative the substitution of cyanobiphenyl on EDOT ring would further enhance the contrast and might result in polymer with improved electrochromic properties.
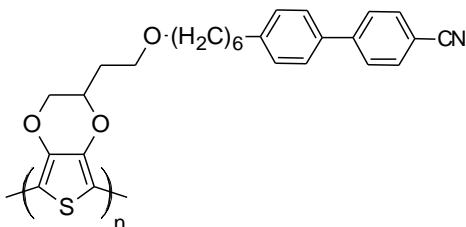
S-2.23

Agarwal and co-workers reported the synthesis of a biphenyl carrying polymer (**S-2.24**) and studied its electrochemical and optical properties. The polymer was shown to possess good mechanical and thermal stability. The bandgap of the polymer was found to be 2.81 eV. The polymer possesses good electronic, photoelectronic, and NLO properties (Agarwal et al. 1993).
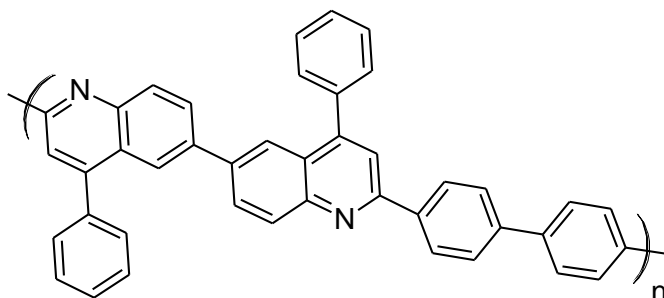
S-2.24

In an another research publication, Norio and Akira described the synthesis of two new poly(2′,5′-dioctyloxy-4,4′,4″terphenylenevinylene)s   (**S-2.25** and **S-2.26**) with different *cis*/*trans* vinylene ratios. These polymers were synthesized through palladium catalysed Suzuki cross coupling reaction of organo-boron compounds (Miyaura and Suzuki 1995). Later, Ronchi and coworkers (Ronchi et al. 2005) investigated the third-order nonlinear NLO properties of these polymers. The nonlinear measurements were performed at $\lambda = 532$ nm in chloroform solutions using single-beam Z-scan technique with pico second laser pulses. The polymers were shown to exhibit two-photon absorption characteristics at this wavelength. The magnitude of the nonlinear refractive index is high and it shows a considerable dependence on the *cis*/*trans* polymers. The polymer with monomers having vinylene unit in *trans*-configuration shows the largest third-order nonlinear optical susceptibility in the order of 10^{-10} esu. According to the authors, the *cis*-configuration of vinylene unit causes steric effects that reduce the effective conjugation length of the molecule. These results suggest an effective route to modulate third-order nonlinear optical properties of a molecule through structural modification.
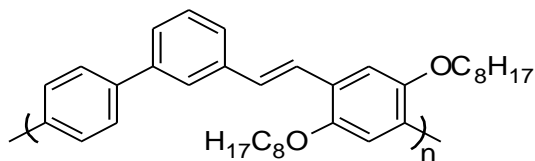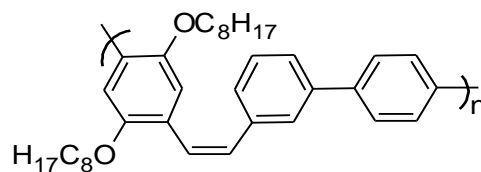
S-2.25   **S-2.26**

The above literature reports clearly indicate that the introduction of phenyl and biphenyl molecules enhances the optical properties and also reduces the band gap of the resulting polymers due to increased conjugation path length. In this context, it has been planned to incorporate phenyl and biphenyl units in our new polymer design. It is expected that inclusion of these groups along with 3,4-disubstituted thiophene and 1,3,4-oxadiazole units would further enhance the optical properties and impart good thermal stability to the new polymer.

2.2.5 Naphthalene based polymers

Naphthalene is a bicyclic aromatic ring consisting of a pair of fused benzene rings. When it is introduced into a polymeric system, it gives thermal stability to the resulting polymer. Also, its presence in polymer main chain increases the glass transition temperature because of its rigid structure. Further, its incorporation in polymer backbone results in a hypsochromic shift in the spectra. This is mainly attributed to the fact that introduction of the heavier electrophilic naphthalene units disrupts and hinders the formation of the conjugation along the backbone.

Liou et al. reported the synthesis of a new phenyl and naphthalene-substituted conjugated poly(1,3,4-oxadiazole) (**S -2.27**) from the rigid rod like monomers, viz. 2,2'-diphenyl-biphenyl-4,4'-dicarboxylic   acid   and   2,2'-di(1-naphthyl)biphenyl-4,4'-dicarboxylic acid through thermal cyclodehydration reaction. They observed that introduction of bulky phenyl or naphthalene substituted groups into the polymer side chain disrupts the coplanarity of aromatic units in chain packing, which increases the space between the chains or free volume and thus enhancing the solubility of the formed poly(1,3,4-oxadiazole) in common organic solvents (Liou et al. 2006).
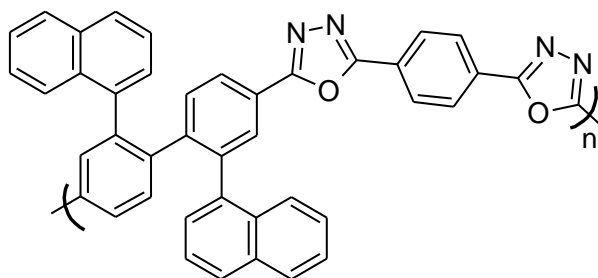
S -2.27

Ahn and his coworkers synthesized a new series of naphthalene and fluorene containing conjugated polymers **S-2.28**, **S-2.29**, and **S-2.30** and studied their opto-electronic properties. These polymers were synthesized using well known Wittig polycondensation method wherein the dialdehyde of fluorine derivative was condensed with triphenyl phosphene salt of the corresponding naphthalene monomer in DMF. The conjugation lengths of the polymers were varied by differently linked naphthalenes in the polymer main chain. The resulting polymers were found to be completely soluble in common organic solvents. Further, they exhibit good thermal stability up to 400°C. They were shown to possess UV-visible absorbance and PL in the ranges 352-379 and 465-512 nm, respectively (Ahn et al. 2002).

S-2.28

S-2.29

S-2.30
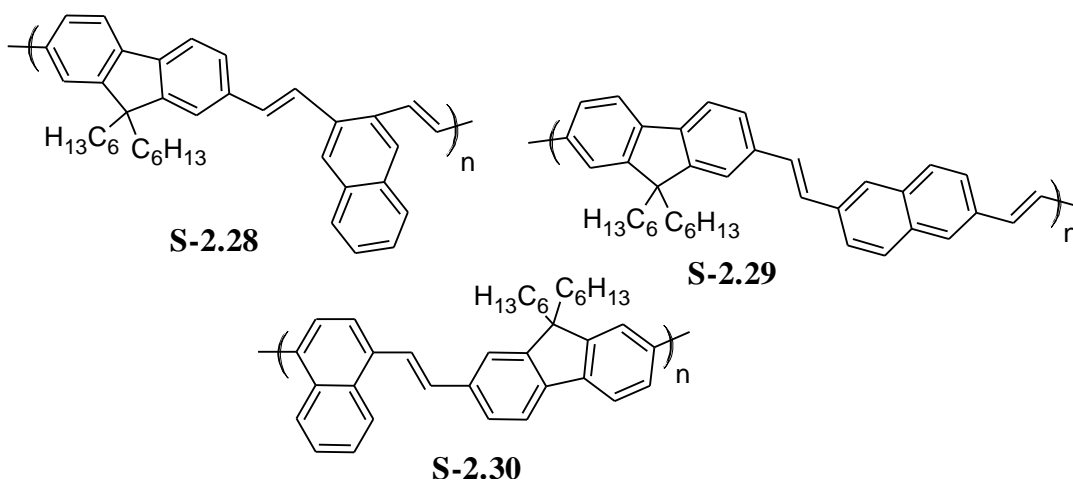
Feng et al. (2008) reported the synthesis and optical properties of a new polymer **S- 2.31** containing 1,3,4-oxadiazole and carbazole units in its main chain and naphthalene moieties as side groups through Wittig reaction. The results of UV- absorption and fluorescence emission spectra showed that the luminescence quantum yield of polymer

was 0.673 in chloroform, and it emitted bluish-green light with a band gap of 3.49 eV. Thermogravimetric analysis and differential scanning calorimetry showed that the polymer exhibited good thermal stability up to 354 °C with a glass-transition temperature higher than 110 °C. Further, the fluorescent quenching technique was used to determine the interactions between the polymer and the electron donor and electron acceptors, which in turn reveals the electron donating and accepting capabilities of the polymers. The results showed that the light emission could be quenched by both the electron donor (N,N-dimethylaniline) and electron acceptor (dimethyl terephthalate) systems.

S-2.31
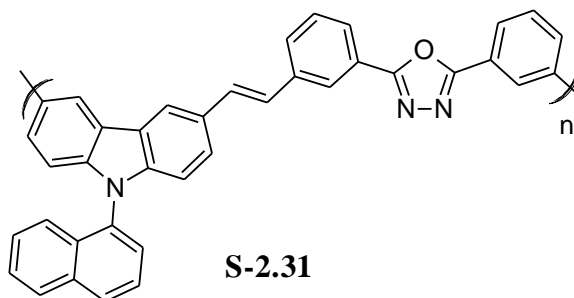
Sung et al. (2004) reported the photophysical and electrochemical properties of polymers carrying naphthalene, alkylated flourene and 1,3,4-oxadiazole units (**S-2.32**). The polymers were shown to possess photoluminescence emissions in both solution and solid states. The authors found that the presence of 1,3,4-oxadiazole pendants along with naphthalene moiety in the polymer chain provided the polymer films with lower HOMO and LUMO energy levels and better electron injection property.
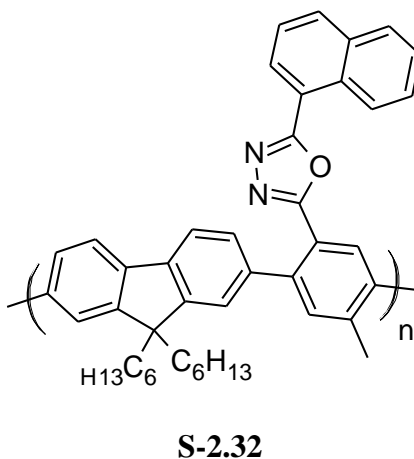
S-2.32

Recently, synthesis and investigation of optical properties of a new series of naphthalene based polymers **S-3.32a-b**, **S-3.33a-b and S-3.34a-b** were reported by Takeshi Mori and Masashi Kijima (Takeshi Mori and Masashi Kijima 2007). Polymers **S-2.32a-b**, **S-2.33a-b** were obtained by Ni-catalyzed polycondensation method while **S-2.34a-b** were synthesized by Suzuki coupling reactions. In PL spectra, all polymers emitted bluish purple in solution state with good quantum yield. Particularly, 2,6-poly(naphthalene) derivatives showed very high quantum efficiencies ($\Phi_{fl} = 0.60$–0.96). Authors also reported that among these polymers, 2,6-poly(naphthalene)s exhibited most planar conformation and hence it showed the highest luminescent properties in the solution and thin film state.

S-3.32a   **S-3.32b**   **S-3.33a**

S-3.33b   **S-3.34a-b**
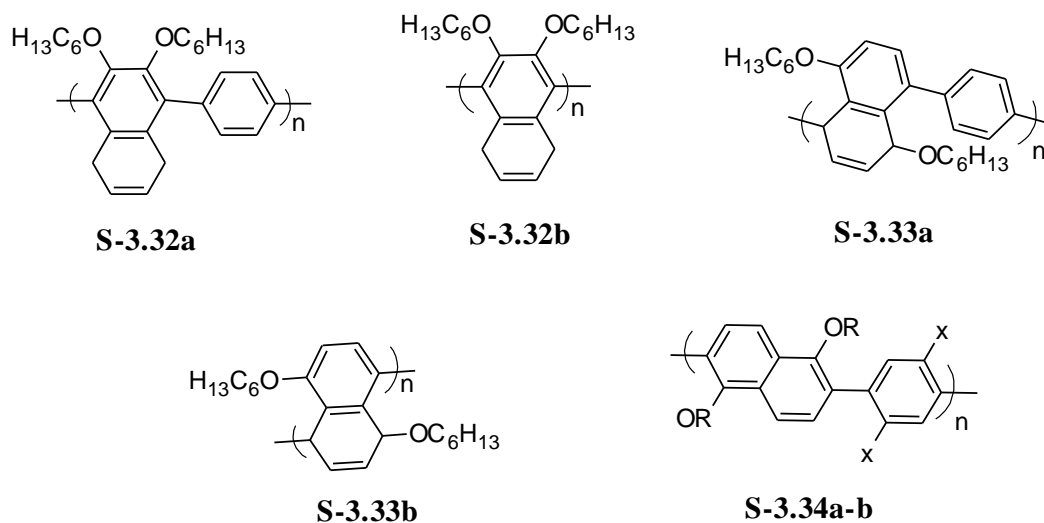
S-2.44a: R=hexyl, X=H; S-2.44b: R=2-ethylhexyl, X=H; S-2.44c: R=2-ethylhexyl, X=hexyl

In an interesting study by Gubler et al. (2002), the effect of different spacer groups on nonlinear optical properties of conjugated poly(triacetylene) (PTA) was investigated. In their studies, they used different moieties like pyridine, pyrazine, benzene, biphenyl, naphthalene, anthracene as spacer groups, as shown in the structure **S-2.35**. It was observed that the largest second-order hyperpolarizability (γ) was measured for the naphthalene-PTA combination.
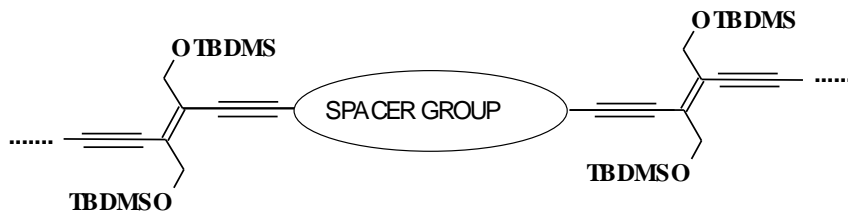
SPACER GROUP = Benzene, naphthalene, thiophene, tetramethylbenzene
anthracene, pyridine, pyrazine, biphenyl

OTBDMS = [(tertbutyl)dimethylsilyloxy

S-2.35

Owing to the importance and established properties of the various naphthalene based polymers, it has been contemplated to prepare new D-A type polymers carrying a rigid naphthalene unit along with electron releasing 3,4-disubstituted thiophenes and electron accepting 1,3,4-oxadiazole rings. It is hoped that new polymers would exhibit good thermal stability and optoelectronic properties.

2.3 SCOPE AND OBJECTIVES

Amongst many classes of materials, oligomeric and polymeric structures containing π-electron conjugated chains showed continuing interest in various fields. They are potential candidates for their applications in important areas like LEDs, photovoltaic cells, thin film transistors, frequency doublers, optical limiters, optical storage devices, and electro-optic switches and modulators. The key advantage of organic conjugated polymers over their inorganic counterparts is their ease of processing by dip coating or spin casting techniques. They combine the optical and electronic properties of semiconductors with the processing advantages and mechanical properties of polymers. Also, these polymers offer added advantages like good environmental stability and low cost of manufacturing. In addition, polymeric systems with delocalized π-electrons have been shown to possess very high molecular polarizability and optical nonlinearities.

At the earlier stages the devices fabricated using primitive conjugated polymers showed very low efficiency due to the imbalanced charge carrying property, lack of environmental stability, and poor film forming ability etc. So, now researchers concentrating their efforts in structural modifications of polymer chains in order to

improve their properties and hence their device efficiencies. This approach led to the investigation of many new conjugated polymers with different types of moieties in the polymeric network. Among various conjugated polymers, D-A type conjugated polymers with alternating donor and acceptor groups have attained vast significance in recent years. Generally in such polymers, it is easy to manipulate desired optical, thermal, electronic and mechanical properties through their structural modification. Further, it is possible to introduce dipole moment along the polymer chain bringing asymmetric electron distribution, which is a required criterion for a molecule to exhibit good NLO properties. In the literature, several D-A types of polymers were reported with the possible applications in optoelectronic and photonic devices.

Owing to the facts stated above, researchers are now focusing, attention on developing new D-A type conjugated polymers with required properties. Still, there are adequate possibilities to investigate new D-A type polymers with improved properties such as stability, processability, optical and electrochemical properties. Development of new D-A type conjugated polymers has become quite energetic and also affording many promising research opportunities. Presently, the design and development of new polymers with high efficacy has become a challenge for polymer researchers.

Keeping all these in view, the present work has been focused on design and synthesis of new series of D-A type conjugated polymers carrying 3,4-disubstituted thiophene as donor group and 1,3,4-oxadiazole as electron acceptor unit with different conjugated spacer groups in between them. Further, it has been aimed at investigation of their electrochemical and optical properties. It is expected that the new polymers would be promising materials for photonics and opto-electronic applications, as the polymers have been designed to possess good charge carrying property and optical response.

Based on the literature studies, the following objectives have been proposed for the present research work.

➢ To design and synthesize four new series of D-A type conjugated polymers consisting of 3,4-disubstituted thiophene as electron donor and 1,3,4-oxadiazole as electron

    acceptor units with pyridine, thiophene, phenyl, biphenyl, EDOT and naphthalene moieties as conjugated spacers in between them.

➢ To characterize new intermediates and monomers by FTIR, ^{1}H NMR, ^{13}C NMR, Mass spectral and elemental analyses.

➢ To characterize new polymers by FTIR spectroscopy, ^{1}H NMR spectroscopy, CHNS analysis, gel permeation chromatography (GPC) and thermogravimetric analysis (TGA).

➢ To evaluate the electrochemical and optical properties of the newly synthesized conjugated polymers.

➢ To investigate NLO properties of newly synthesized polymers using Z‑scan and DFWM techniques.

    Conclusively, the present work involves design, synthesis, characterization of thiophene and 1,3,4‑oxadiazole based D‑A type conjugated polymers carrying different conjugated spacers. Their electrochemical and optical properties are expected to contribute significantly to the development of new polymeric materials for PLEDs and NLO applications. Further, there is a scope for modifications of molecular structures of polymers through functionalization of their respective monomers that may lead to achieve desired properties in resulting polymers. In addition, the study also would add some additional information to the chemistry of thiophene‑oxadiazole based D‑A conjugated polymers. Further, study of effect of structure on their electrochemical and optical properties would throw some light upon the concept for new designs in future.

2.4 DESIGN OF NEW D‑A TYPE CONJUGATED POLYMERS

    The extensive literature survey on D‑A type polymers reveals that still there is a scope for the design and synthesis of new D‑A type conjugated polymers for photonic applications. It has been established that to have good optical and electrochemical properties in the polymers, the molecular/structural design should possess good conjugation length, planarity, polarizable double bonds and balanced arrangement of donor and acceptor moieties in the polymer backbone. Also, presence of conjugated spacers between donor and acceptor moieties is necessary in order to avoid steric

repulsion and to increase the extent of conjugation in the main chain. Based on these design strategies, four new series of D-A type polymers having 3,4-disubstituted thiophene as electron donor and 1,3,4-oxadiazole as electron acceptor units have been designed. In the new design it has been planned to incorporate different conjugated spacer groups in combination with D-A arrangement. The newly designed polymers are expected to show good electrochemical and optical properties. Further, the presence of long alkoxy side chain in the polymer scaffold would endow with improved solubility in the common organic solvents and hence to have good solvent processability.

As described in chapter 2, thiophene is a vital electron donating heteroaromatic system which can be easily functionalized with different active groups. Further, 1,3,4-oxadiazole is well studied heterocyclic moiety as electron acceptor unit in conducting polymers for their applications in opto-electronics and photonics. Taking into consideration of these facts regarding substituted thiophene and 1,3,4-oxadiazole, , it has been intended to choose these moieties as electron donor and acceptor, respectively in all the newly designed polymers to obtain D-A type arrangement which would furnish better electrochemical and optical properties. The design of four new series of polymers has been discussed below.

2.4.1 Polymers carrying 3,4-dialkoxythiophene, 1,3,4-oxadiazole and 3,4-dibenzyloxythiophene units (P1-P3), Series-1

As explained earlier, our new design has centered on thiophen-yloxadiazole system wherein 3,4-disubstituted thiophene and 1,3,4-oxadiazole arise alternatively to lead D-A type structure as shown in **S-2.36**. We have designed the new polymer **P1** carrying electron donors, viz. 3,4-dibenzyloxy substituted thiophene and 3,4-ditetradecyloxythiophene in between electron accepting 1,3,4-oxadiazole systems. In polymer **P2,** we have included 3,4-dibenzyloxythiophene and 3,4-didodecyloxythiophene as electron donors alternatively between strong electron acceptor, i.e. 1,3,4-oxadiazole. Similarly in polymer **P3,** 3,4-dibenzyloxythiophene and 3,4-dihexyloxythiophene have been introduced as electron donors alternating with 1,3,4-oxadiazole as electron acceptor group. Thus, the structures of new polymers are varied with different alkyl substitution,

keeping benzyloxy substitution invariable to study their effect on electrochemical and optical properties of the final polymers. These polymers are believed to possess high molecular hyperpolarizability due to effective delocalization of π-electron cloud along the polymer main chain. Moreover, charge transfer would take place over nonconjugated bonds between benzyl and thiophene units owing to the presence of -OCH$_2$ linkage. Further, this linkage may also decrease the torsional angle between the benzyl groups. Therefore, we expect better NLO properties in polymers **P1-P3.**

$$R = C_{14}H_{29}, C_{12}H_{25}, C_6H_{13}$$
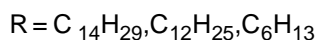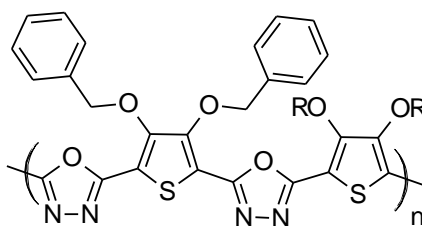
S-2.36 Design of **P1-P3,** Series-1

2.4.2 Polymers containing 3,4-dialkoxythiophene, 1,3,4-oxadiazole and bis 3,4[2-(naphthalene-2-ylmethoxy)] thiophene units (P4-P6), Series-2

In Series-2, three polymers **P4-P6** carrying electron donating 3,4-dinaphthalene-2-ylmethoxy and 3,4-dialkoxy substituted thiophene systems positioned in alternative combination with electron accepting 1,3,4-oxadiazole, have been designed. In polymer **P4**, 3,4-ditertadecyloxythiophene and 3,4-dinaphthalene-2-ylmethoxy have been introduced as electron donating moieties in alternative combination with 1,3,4-oxadiazole as electron acceptor. Whereas in polymer **P5**, we have 3,4-didodecyloxythiophene and 3,4-dinaphthalene-2-ylmethoxy as electron donating moieties alternatively with 1,3,4-oxadiazole as electron acceptor. Similarly in polymer **P6**, 3,4-dinaphthalene-2-ylmethoxy and 3,4-dihexyloxythiophene have been introduced as electron donors alternating with 1,3,4-oxadiazole as electron acceptor group. In our design, the electron donating 3,4-dinaphthalene-2-ylmethoxy has been incorporated to enhance the stability and optical properties of the polymer. So, these polymers are anticipated to exhibit better electrochemical and optical properties with good thermal stability. Also, the long alkoxy

chains in the new polymers are expected to furnish good solubility to the polymers. Accordingly, hitherto unknown polymers with above mentioned combinations in the polymer chain have been designed as shown in **S-2.37**.

$R = C_{14}H_{29}, C_{12}H_{25}, C_6H_{13}$
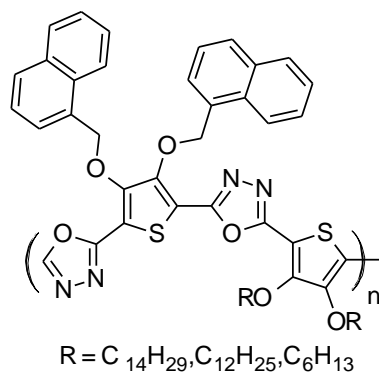
S-2.37 Design of **P4-P6**, Series-2

2.4.3 Polymers carrying 3,4 bis(methoxy/methyl/nitrobenzyloxy)thiophene, 1,3,4-oxadiazole and 3,4-didodecyloxythiophene units (P7-P9), Series-3

In Series-3, three new D-A type conjugated polymers have been designed. The new designs carry electron donating 3,4-didodecyloxythiophene and thiophene with substituted benzyl oxy groups attached to its 3rd and 4th positions, alternatively with 1,3,4-oxadiazole as electron acceptor unit. In polymer **P7**, 3,4 bis(4-methoxybenzyloxy) thiophene and 3,4-didodecyloxythiophene have been introduced as electron donating rings alternatively with 1,3,4-oxadiazole unit as electron acceptor. Whereas design of polymer **P8** includes introduction of 3,4 bis(4-methylbenzyloxy)thiophene and 3,4-didodecyloxythiophene as electron donor segments in combination with electron accepting 1,3,4-oxadiazole moiety alternatively. Similarly in polymer **P9**, we have the arrangement of 3,4-bis(4-nitrobenzyloxy)thiophene and 3,4-didodecyloxythiophene as electron releasing units alternatively with electron accepting 1,3,4-oxadiazole unit. Different substituents have been introduced at positions 3 and 4 of thiophene ring in order to study their influence on electrochemical and optical properties of the polymers. In all the polymers of this series, 3,4-didodecyloxythiophene has been kept as invariable group. Further, presence of dodecyloxy chains at positions 3 and 4 of one of the thiophene rings

is expected to enhance the solubility of the new polymers. Thus, unknown polymers (**P7-P9**) with the above mentioned arrangement of electron donors and electron acceptors have been designed as given in **S-2.38**.

$R = C_{12}H_{25}$; $R' = CH_3$, OCH_3, NO_2

S-2.38. Design of **P7-P9,** Series-3

2.4.4 Polymers carrying 3,4-bis[(4-decyloxy-3-methoxybenzyl)oxy]thiophene, 1,3,4-oxadiazole and different aromatic spacers (P10-16), Series-4

In the design of polymers of Series-4, viz. **P10-P16**, strongly electron donating 3, 4-bis[4-decyloxy-3-methoxybenzyl)oxy]thiophene ring has been placed alternatively with 1,3,4-oxadiazole in the polymer chain. These donor and acceptor moieties are connected through different conjugated spacer groups. The newly designed polymers **P10-P16 (S-2.39)** contain benzene, thiophene, pyridine, phenylenevinylene, EDOT, naphthalene and biphenyl as conjugated spacer groups, respectively. In all the polymers of this series, we have kept 3,4-bis[(4-decyloxy3-methoxybenzyl)oxy]thiophene ring as invariable. The different spacer groups have been introduced in order to study their influence on electrochemical, linear and nonlinear optical properties of polymers.
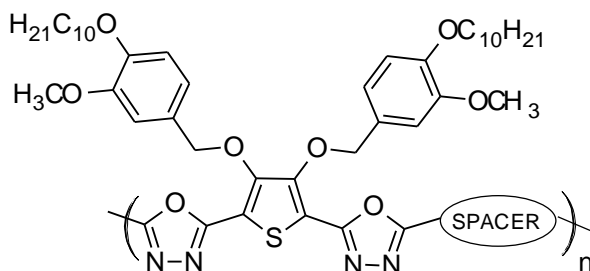
SPACER = Thiophene, phenyl, phenylenevinylene, biphenyl, pyridine, EDOT, naphthalene

S-2.39 Design of **P10-P16,** Series-4

The newly designed polymers have been synthesized from simple thiophene derivatives through multi-step reactions according to **Schemes 2.1** and **2.2**. As described in **Scheme 2.1**, the polymers of Series 1 to 3 have been obtained from their precursor polyhydrazides **6a-i** through cyclodehydration. These polyhydrazides have been synthesized by condensing 3,4-disubstituted thiophene diacid chlorides **4a-e** with substituted thiophene dihydrazides **5a-c**, which are obtained from different 3,4-disubstituted thiophene derivatives **2a-e** and **3a-e**. Further, we have synthesized seven polymers of Series 4 starting from their monomers (**14a-g** and **12**) through precursor polyhydrazide route as mentioned in **Scheme 2.2**. The details of synthesis are given in the next chapter.

The synthetic procedures for intermediates, monomers and polymers have been well established. Their purification methods have been established. The structures of newly synthesized intermediates and monomers have been characterized by FTIR, ^{1}H NMR, ^{13}C NMR spectral followed by elemental analyses. Further, the new polymers have been characterized by FTIR spectroscopy, ^{1}H NMR spectroscopy, gel permeation chromatography (GPC) and thermogravimetric analysis (TGA). Their electrochemical properties have been investigated by cyclic voltammetry studies and their optical properties have been evaluated by UV-visible absorption and fluorescence emission spectral methods. Finally, the NLO properties of new polymers have been investigated by Z-scan and DWFM methods.

The details of the experimental work leading to synthesis of various intermediates, monomers and their polymers along with their structural characterization data have been presented in chapter 3. Further, a detailed investigation of electrochemical, linear and nonlinear optical properties of the new polymers has been discussed in chapter 4.

Scheme 2.1 Synthesis of polymers **P1-P9** of Series**-**1 to 3
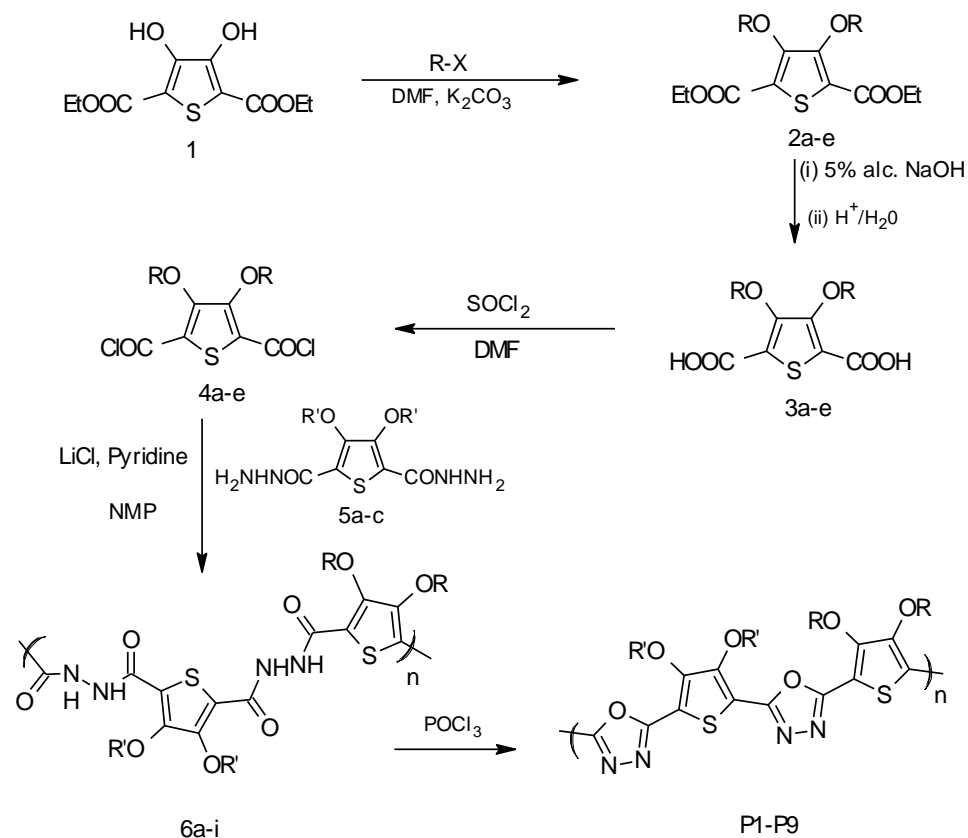
Series	Compound	R	R'
1	2a,3a,4a,5a,6a, P1	n-CH$_3$(CH$_2$)$_{13}$-	(benzyl CH$_2$)
	5b,6b,P2	n-CH$_3$(CH$_2$)$_{11}$-	
	5c,6c,P3	n-CH$_3$(CH$_2$)$_5$-	
2	2b,3b,3c,4c,6d,P4	n-CH$_3$(CH$_2$)$_{13}$-	(naphthylmethyl CH$_2$)
	6e,P5	n-CH$_3$(CH$_2$)$_{11}$-	
	6f,P6	n-CH$_3$(CH$_2$)$_5$-	
3	2b,3c,4c,6g,P7		(4-OCH$_3$ benzyl) CH$_2$
	2c,3c,4c,6h,P8	n-CH$_3$(CH$_2$)$_{11}$-	(3-CH$_3$ benzyl) CH$_2$
	2d,3d,4d,6i,P9		(4-NO$_2$ benzyl) CH$_2$
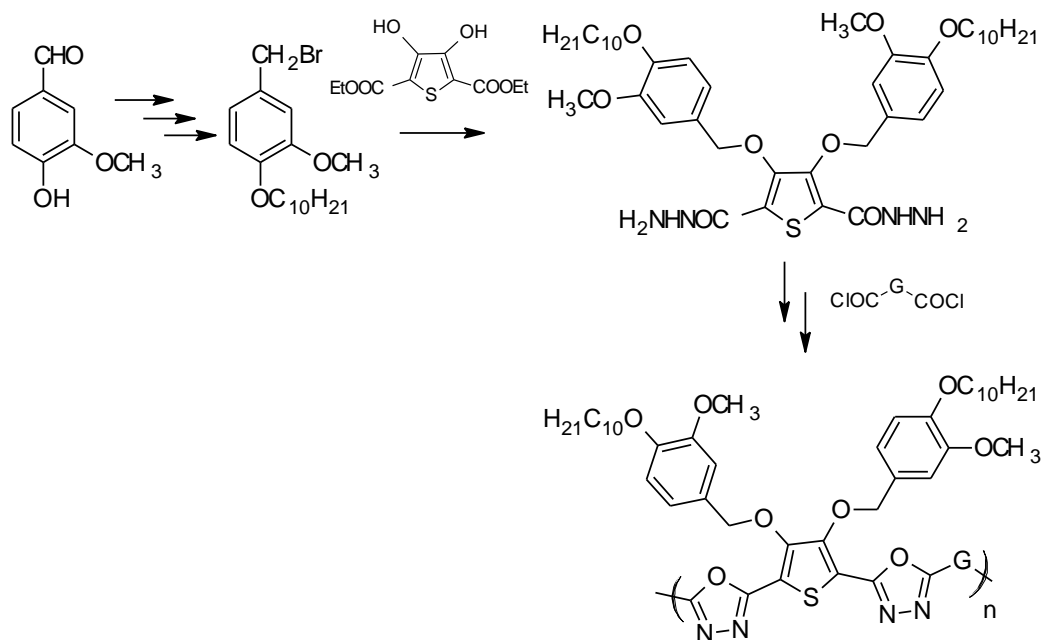
Series	Compdound	G
4	P10	
	P11	
	P12	
	P13	
	P14	
	P15	
	P16	

Scheme 2.2 Synthesis of polymers **P10-P16** of Series**-**4

Chapter 3

Abstract

This chapter includes experimental procedures followed for the synthesis of intermediates and monomers required for the preparation of newly designed polymers. Also, it covers the synthetic methods for target polymers. Further, it encompasses the structural characterization of all the newly synthesized molecules by spectral and elemental analyses.

3.1 INTRODUCTION

In the previous chapter 2, it has been discussed design of four new series of D-A type conjugated polymers on the basis of literature review. Chapter 3 encompasses details of synthesis of newly designed polymers starting from diethyl 3,4-dihydroxythiophene-2,5-dicarboxylate through multistep reactions. These conjugated polymers include:

a. Polymers carrying 3,4-ditetradecyloxy/didodecyloxy/dihexyloxythiophene, 1,3,4-oxadiazole and 3,4-bis(benzyloxy)thiophene/ (**P1–P3, Series–1, Scheme 3.1**)

b. Polymers containing 3,4-ditetradecyloxy/didodecyloxy/dihexyloxythiophene, 1,3,4-oxadiazole and bis 3,4[2-(naphthalene-2-ylmethoxy)] thiophene (**P4–P6, Series–2, Scheme 3.2**)
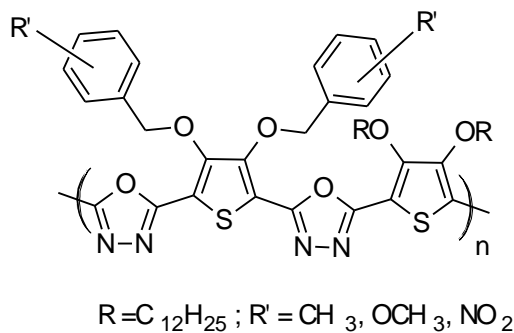
c. Polymers carrying 3,4-bis(methoxy/methyl/nitrobenzyloxy)thiophene, 1,3,4-oxadiazole and 3,4-didodecyloxythiophene (**P7–P9, Series–3, Scheme 3.3**)

d. Polymers carrying 3,4-bis[(4-decyloxy-3-methoxybenzyl)oxy]thiophene, 1,3,4-oxadiazole and different aromatic spacers, viz. benzene, thiophene, pyridine, phenylenevinylene, EDOT, naphthalene and biphenyl (**P10–16, Series–4, Scheme 3.4**)

The synthesis and characterization of new intermediates, monomers and target polymers are discussed in the following section in detail.

3.2 MATERIALS AND INSTRUMENTATION

The required starting materials, diethyl 3,4-dihydroxythiophene-2,5-dicarboxylate, 3,4-dialkyloxythiophene-2,5-dicarbohydrazides were synthesized according to the reported procedures (Lima et al. 1998, Udayakumar et al. 2006).

Dimethylformamide (DMF), N-methyl pyrolidone (NMP), Tetrahydrofuran (THF), acetonitrile (ACN) and other solvents were dried over CaH_2 were used. Thiodiglycolic acid, diethyl oxalate and tetrabutylammonium perchlorate (TBAPC) were purchased from Lanchaster (UK). (Chloromethyl)benzene, 2-(chloromethyl)naphthalene, 1-(chloromethyl)-4-methoxybenzene, 1-(chloromethyl)-3-methylbenzene, 1-(bromomethyl)-4-nitrobenzene, thiophehe-2,5-dicarboxylic acid, biphenyl-4,4'-dicarboxylic acid, pyridine-2,6-dicarboxylic acid, benzene-1,4-dicarboxylic acid and lithium chloride were purchased from Sigma-Aldrich and were used as received. All the solvents and reagents were of analytical grade, purchased commercially and used without further purification.

Infrared spectra of all intermediate compounds and polymers were recorded on a Nicolet Avatar 5700 FTIR (Thermo Electron Corporation). ^{1}H and ^{13}C NMR spectra were obtained with 300 and 400MHz on Bruker NMR spectrometer using TMS/solvent signal as internal reference. Elemental analyses were performed on a Flash EA1112 CHNS analyzer (Thermo Electron Corporation). Molecular weights of the polymers were determined with a WATERs make Gel Permeation Chromatograph (GPC) against poly(styrene) (PS) standards with teterhydrofuran (THF) as an eluent. The thermal stability of polymers was studied by SII–EXSTAR6000–TG/DTA6300 thermogravimetric analyzer.

3.3 SYNTHESIS AND CHARACTERIZATION OF POLYMERS CARRYING 3,4-DIALKOXYTHIOPHENE, 1,3,4-OXADIAZOLE AND 3,4-DIBENZYLOXYTHIOPHENE (P1–P3), SERIES–1

We synthesized three new polymers **P1–P3** in this series with 3,4-benzyloxy/alkoxy segments as electron donor moieties and 1,3,4-oxadiazole as electron withdrawing segment along the polymer chain. The synthetic route towards the preparation of new intermediates, monomers and polymers is outlined in **Scheme 3.1**.

3.3.1 Chemistry

The required intermediate 3,4-bis(benzyloxy)thiophene-2,5-dicarboxylic acid (**3a**) was synthesized by alkali hydrolysis of the diethyl 3,4-bis(benzyloxy)thiophene-2,5-dicarboxylate (**2a**), which was obtained by condensation of 3,4-dihydroxy-thiophene-2,5-

diester (**1**) with (chloromethyl)benzene in presence of potassium carbonate and DMF. The diacid (**3a**) was refluxed with excess thionyl chloride to obtain 3,4-bis (benzyloxy)thiophene-2,5-dicarbonyl dichloride (**4a**), which on treatment with the dihydrazides **5a–c** in presence of lithium chloride and pyridine underwent polycondensation to give required polyhydrazides **6a–c**. The compounds **6a–c** obtained were converted into corresponding target polymers **P1–P3** through cyclodehydration reaction using phosphorus oxychloride as dehydrating agent.
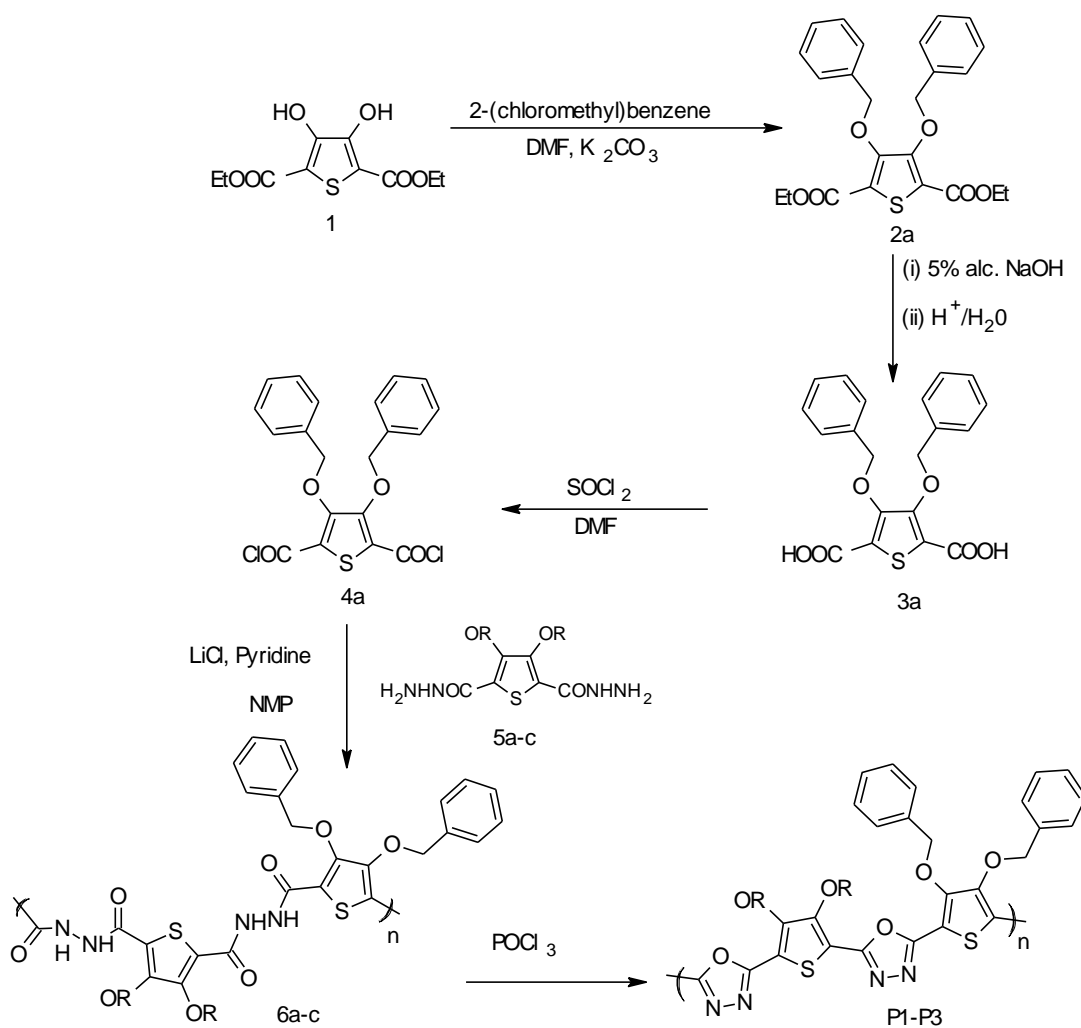
where 5a,6a,P1: R= n-$C_{14}H_{29}$; 5b,6b,P2: R= n-$C_{12}H_{25}$; 5c,6c,P3: R= n-C_6H_{13}

Scheme 3.1 Synthesis of polymers **P1–P3** of Series-1

3.3.2 Experimental procedure

The experimental protocols for the synthesis of intermediates, new monomers and polymers are given in the following section.

3.3.2.1 Synthesis of intermediates and monomers

The required intermediate **2a** was synthesized from 3,4-dihydroxythiophene-2,5-dicarboxylate (**1**) and ester **2a** was converted to monomer **3a** according to the following procedures.

3.3.2.1.1 Synthesis of diethyl 3,4-bis(benzyloxy)thiophene-2,5-dicarboxylate (2a)

To a mixture of diethyl 3,4-dihydroxythiophene-2,5-dicarboxylate (**1**) (3.0 g, 12 mmol) and K_2CO_3 (4.77 g, 36 mmol) in 30 mL of DMF, (chloromethyl)benzene (4.0 g, 23 mmol) was added drop-wise. The reaction mixture was refluxed for 20 h. After the completion of reaction, it was cooled to room temperature and poured into cold water. The yellow precipitate formed was filtered, dried and recrystalized using ethanol. Mp: 71–73 ^{o}C. Yield: 83%. FTIR (KBr, υ, cm^{-1}): 2974 (–CH), 1696 (–C=O). ^{1}H NMR (CDCl$_3$, δ ppm): 7.45–7.27 (m, 10H, aromatic), 5.19 (s, 4H, –OCH$_2$–Ar), 4.40 (q, 4H, –OCH$_2$, J=7.2 Hz), 1.41 (t, 6H, –CH$_3$, J=6.8 Hz). Element. Anal. Calcd. For $C_{24}H_{24}O_6S$: C, 65.44%; H, 5.49%; S, 7.28%. Found: C, 65.03%; H, 5.39%; S, 7.17%.

3.3.2.1.2 Synthesis of 3,4-bis(benzyloxy)thiophene-2,5-dicarboxylic acid (3a)

A mixture of diethyl 3,4-bis(benzyloxy)thiophene-2,5-dicarboxylate (**2a,** 2.0 g, 4.5 mmol) and 20 mL of 5% alcoholic sodium hydroxide was refluxed for 6 h. The resulting clear solution was concentrated and cooled. Further, it was washed with ethyl acetate to remove trace of organic impurities and then was acidified with concentrated HCl, to get white precipitate. The precipitate was filtered, washed with water and recrystalized from ethanol. Mp: 213–215 ^{o}C. Yield: 76%. FTIR (KBr, υ, cm^{-1}): 3041 (–OH), 2628 (–CH), 1674 (–C=O). ^{1}H NMR (DMSO–d^{6}, δ ppm): 13.2 (s, 2H, carboxylic acid), 7.93–7.49 (m, 10H, benzyl), 5.15 (s, 4H, –OCH$_2$–Ar). Element. Anal. Calcd. for $C_{20}H_{16}O_6S$: C, 62.49%; H, 4.20%; S, 8.34%. Found: C, 62.12%; H, 4.12%; S, 8.21%.

3.3.2.2 Synthesis of polymers

The monomers were then polymerized to the precursor polyhydrazides **6a–c** and finally they were cyclized to get corresponding poly(oxadiazole)s **P1–P3** for which the following procedures were followed.

3.3.2.2.1 General procedure for the synthesis of precursor polyhydrazides (6a–c)

To a mixture of 1 equivalent of dihydrazide (**5**), 2 equivalents of lithium chloride and 0.1 mL of pyridine, 1 equivalent of appropriate diacid chloride **4a** was added slowly at room temperature with stirring and stirring was continued for 3 h. Further, it was heated at 60 $^{\circ}$C for 12 h. After cooling to room temperature the reaction mixture was poured into ice cold water and the precipitate separated was collected by filtration. The polymer was purified by soxhlet extraction technique using ethyl acetate as solvent and finally it was dried in vacuum oven at 40 $^{\circ}$C. Their characterization data are as follows.

6a: Yield: 81%, FTIR (KBr, υ, cm^{-1}): 3286 (–NH), 2847 (–CH), 1631 (–C=O). ^{1}H NMR (DMSO–d^{6,} δ ppm): 10.13 (s, 2H,–NH), 9.98 (s, 2H,–NH), 7.32–6.61 (m, 10H, aromatic), 5.03 (s, 4H, –OCH$_2$), 4.24 (t, 4H, –OCH$_2$, tetradecyl, J=6.4 Hz), 1.78–1.19 (m, 48H, –C$_{24}$H$_{48}$), 0.84 (t, 6H, –CH$_3$, alkyl, J=6.8 Hz). Element. Anal. Calcd. for C$_{54}$H$_{76}$N$_4$O$_8$S$_2$: C, 66.63%; H, 7.87%; N, 5.75%; S, 6.59%. Found: C, 66.34%; H, 7.53%; N, 5.21%; S, 5.98%.

6b: Yield: 73%, FTIR (KBr, υ, cm^{-1}): 3215 (–NH), 2849 (–CH), 1611 (–C=O). ^{1}H NMR (DMSO–d^{6,} δ ppm): 11.14 (s, 2H,–NH), 10.12 (s, 2H,–NH), 7.34–6.58 (m, 10H, aromatic), 4.27 (s, 4H, –OCH$_2$), 4.19 (t, 4H, –OCH$_2$–, dodecyl, J=6.4 Hz) 1.99–1.23 (m, 40H, –C$_{20}$H$_{40}$), 0.83 (t, 6H, –CH$_3$, J=6.8 Hz). Element. Anal. Calcd. for C$_{50}$H$_{68}$N$_4$O$_8$S$_2$: C, 65.47%; H, 7.47%; N, 6.11%; S, 6.99%. Found: C, 65.33%; H, 7.25%; N, 6.04%; S, 6.95%.

6c: Yield: 78%, FTIR (KBr, υ, cm^{-1}): 3220 (–NH), 2846 (–CH), 1615 (>C=O). ^{1}H NMR (DMSO–d^{6,} δ ppm): 11.38 (s, 2H,–NH), 10.16 (s, 2H,–NH), 7.56–7.02 (m, 10H, aromatic), 4.29 (s, 4H, –OCH$_2$–Ar) 4.21 (t, 4H, –OCH$_2$–, hexyl, J=6.4 Hz), 1.86–1.24 (m, 16H, –C$_8$H$_{16}$), 0.84 (t, 6H, –CH$_3$, J=6.8 Hz). Element. Anal. Calcd. for

$C_{38}H_{44}N_4O_8S_2$: C, 60.94%; H, 5.92%; N, 7.48%; S, 8.56%. Found: C, 59.91%; H, 5.81%; N, 7.35%; S, 8.41%.

3.3.2.2.2 General procedure for the synthesis of polymers P1–P3

A mixture of polyhydrazide (**6a–c**, 0.5 g) and 20 mL of phosphorus oxychloride was heated at 90 ^{o}C for 8 h with stirring. The reaction mixture was then cooled to room temperature and poured to excess of ice cold water. The resulting orange-red precipitate was collected by filtration, washed with water followed by ethyl acetate thoroughly and finally dried in vacuum oven at 40 ^{o}C. Their characterization data are summarized below.

P1: Yield: 73%, FTIR (KBr, υ, cm^{-1}): 2919, 2852 (–CH), 1580 (C=N), 1035 (Aromatic –CH=CH–). ^{1}H NMR (DMSO–d^{6,} δ ppm): 7.45–7.09 (m, 10H, Ar), 4.99 (s, 4H, –OCH$_2$–Ar), 4.26 (t, 4H, –OCH$_2$–, tetradecyl, J=6.4 Hz), 3.76 (s, 6H, –OCH$_3$) 1.69–1.19 (m, 48H, –C$_{24}$H$_{48}$), 0.86 (t, 6H, –CH$_3$, J=6.8 Hz). Element. Anal. Calcd. for $C_{54}H_{72}N_4O_6S_2$: C, 69.20%; H, 7.74%; N, 5.98%; S, 6.84%. Found: C, 68.92%; H, 7.21%; N, 5.45%; S, 7.15%. GPC (THF, PS standard): $\overline{M}_w$: 6286 g/mol, PDI = 2.11.

P2: Yield: 69%, FTIR (KBr, υ, cm^{-1}): 2902, 2851 (C–H), 1591 (C=N), 1476, 1150 (–CH, Ar). ^{1}H NMR (DMSO–d^{6,} δ ppm): 7.35–6.99 (m, 10H, Ar), 4.46 (s, –OCH$_2$–Ar), 4.27 (t, 4H, –OCH$_2$–, dodecyl, J=6.4 Hz), 1.81–1.21 (m, 40H, –C$_{20}$H$_{40}$), 0.85 (t, 6H, –CH$_3$, J=6.8 Hz). Element. Anal. Calcd. for $C_{50}H_{64}N_4O_6S_2$: C, 68.15%; H, 7.32%; N, 6.36; S, 7.28%. Found: C, 67.92%; H, 7.21%; N, 6.25%; S, 7.17%. GPC (THF, PS standard): $\overline{M}_w$ =13380, PDI = 1.30.

P3: Yield: 63%, FTIR (KBr, υ, cm^{-1}): 2934, 2862 (–CH), 1590 (C=N), 1479, 1156 (–CH, Ar). ^{1}H NMR (DMSO–d^{6,} δ ppm): 7.32–6.95 (m, 10H, Ar), 4.43 (s, 4H, –OCH$_2$), 4.24 (t, 4H, –OCH$_2$–, hexyl, J=6.4 Hz) 1.59–1.22 (m, 16H, –C$_8$H$_{16}$), 0.83 (t, 6H, –CH$_3$, J=6.8 Hz). Element. Anal. Calcd. for $C_{38}H_{40}N_4O_6S_2$: C, 64.02%; H, 5.66%; N, 7.86%; S, 9.00%. Found: C, 63.92%; H, 7.36%; N, 7.01%; S, 8.65%. GPC (THF, PS standard): $\overline{M}_w$ = 8600, PDI = 1.4.

3.3.3 Results and discussion

The structures of diethyl 3,4-bis(benzyloxy)thiophene-2,5-dicarboxylate (**2a**) and 3,4-bis(benzyloxy)thiophene-2,5-dicarboxylic acid (**3a**) were confirmed by its ^{1}H NMR, FTIR spectral and elemental analyses. FTIR spectra of ester **2a** showed a broad peak at 2974 cm^{-1} for alkyl group and a sharp peak at 1696 cm^{-1} for carbonyl group of ester as shown in **Figure 3.1**.
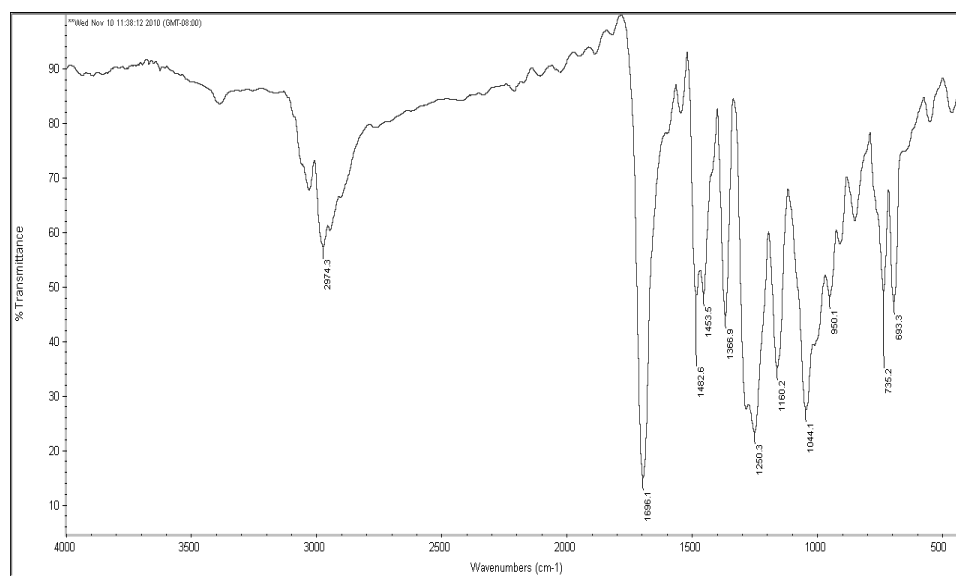
Figure 3.1 FTIR spectrum of diethyl 3,4-bis(benzyloxy)thiophene-2,5-dicarboxylate **(2a)**

Further, ^{1}H NMR spectrum of ester **2a** (**Figure 3.2**) showed multiplet between 7.45–7.27 ppm that corresponds to benzyl group, singlet at 5.19 ppm for aralkyloxy (–OCH$_2$–Ar) substituent at 3,4 positions of the thiophene ring, quartet at 4.40 ppm for three protons of ester and triplet at 1.41 ppm for two protons of ester.
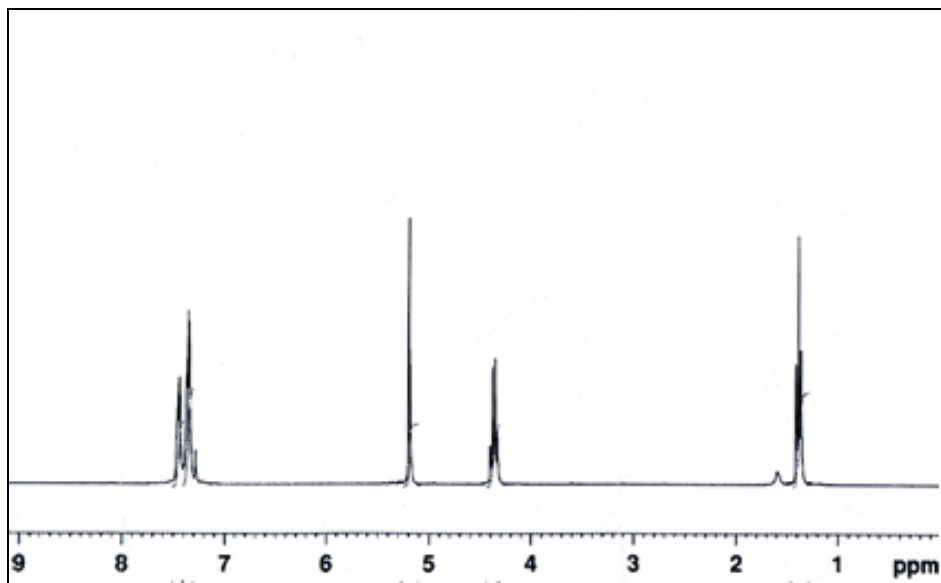
Figure 3.2 ^{1}H NMR spectrum of diethyl 3,4-bis(benzyloxy)thiophene-2,5-dicarboxylate **(2a)**

FTIR spectrum of the diacid **3a** showed a broad peak at around 3000 cm^{-1} which corresponds to –OH group of acid and a peak at 1674 cm^{-1} for carbonyl group of diacid **3a** was observed as shown in **Figure 3.3**.
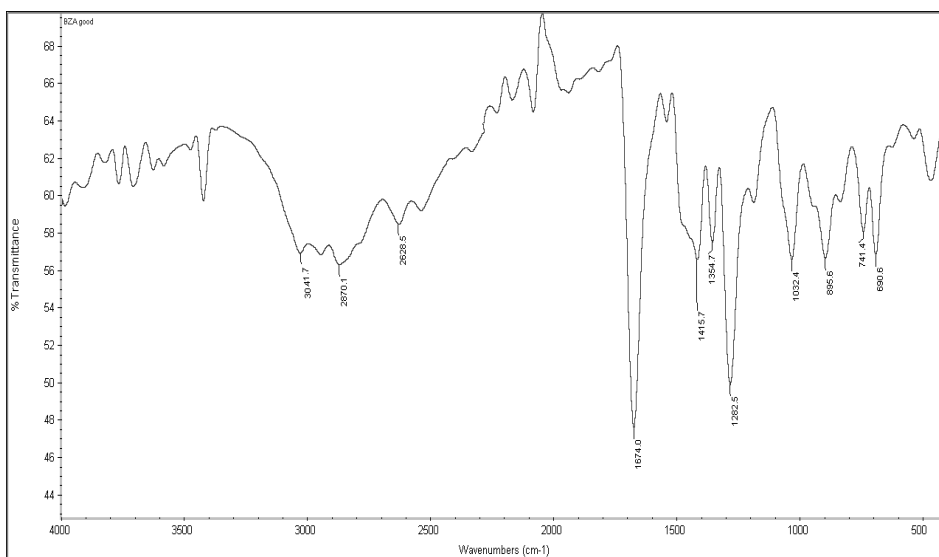
Figure 3.3 FTIR spectrum of 3,4-bis(benzyloxy)thiophene-2,5-dicarboxylic acid

(3a)

^{1}H NMR of the diacid **3a** (**Figure 3.4**) showed singlet peak at δ, 13.2 ppm that corresponds to the protons of the carboxylic acid. A set of multiplet peaks between δ values 7.93–7.49 ppm was observed for the aromatic protons corresponding to the benzyl segment, while the methylene oxy protons resonated at δ, 5.15 ppm.
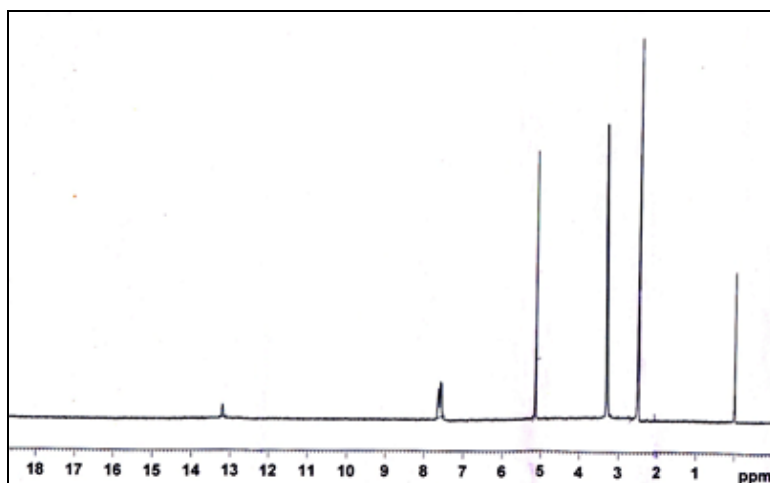
Figure 3.4 ^{1}H NMR spectrum 3,4-bis(benzyloxy)thiophene-2,5-dicarboxylic acid **(3a)**

The structures of the polymers were established by FTIR and ^{1}H NMR spectral methods. Formation of precursor polyhydrazide **6b** from monomers **4a** and **5b** was evidenced by its FTIR spectrum, wherein sharp peaks were observed at 3215 and 1611 cm^{-1} accounting for amide and carbonyl groups respectively as shown in **Figure 3.5**.
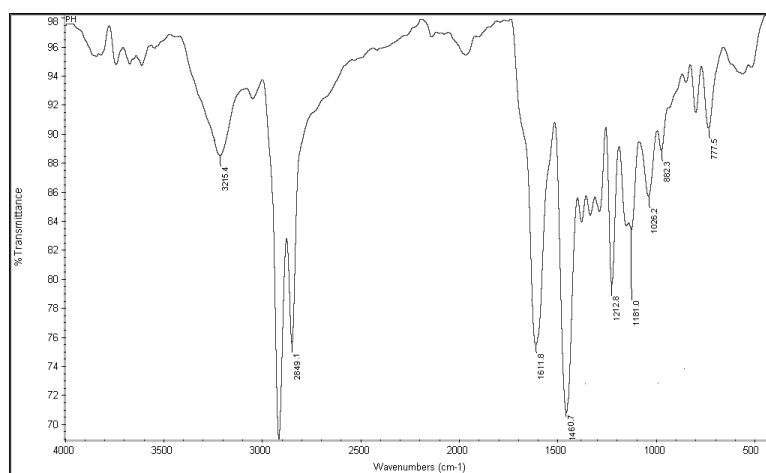
Figure 3.5 FTIR spectrum of polyhydrazide **6b**

FTIR spectrum of polymer **P2** showed characteristic absorption peaks at 2902 and 2851 cm^{-1} accounting for C–H stretching of aliphatic segments. The appearance of peak at 1591 cm^{-1} corresponds to C=N of 1,3,4-oxadiazole group, this indicates the conversion of polyhydrazide **6b** to polyoxadiazole **P2** as shown in **Figure 3.6**.
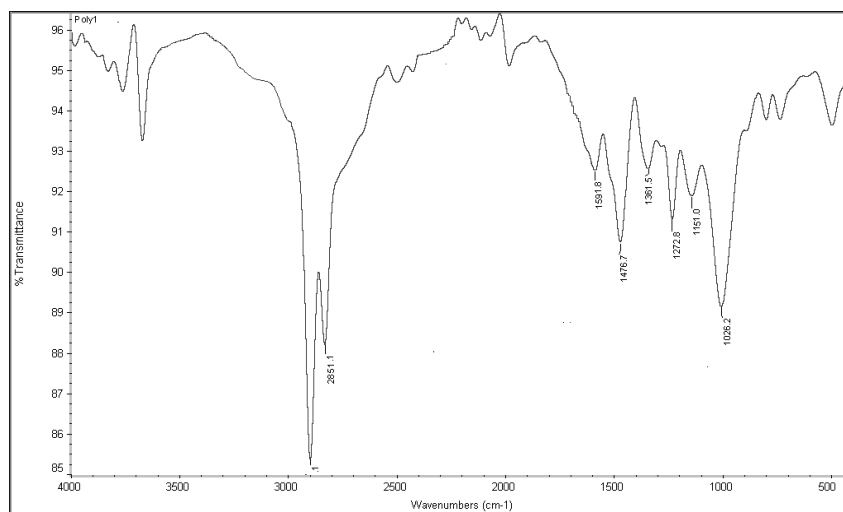
Figure 3.6 FTIR spectrum of poly(oxadiazole) **P2**

The ^{1}H NMR spectrum (**Figure 3.7**) of polyhydrazide **6b** displayed two sharp peaks at 11.14 and 10.12 ppm due to hydrazide protons (–NH). Benzyl protons were resonated at 7.34–6.58 ppm as multiplet and –OCH$_2$ protons of alkoxy group appeared at 4.27 and 4.19 ppm as singlet. Further, alkyl protons resonated at δ 1.99–1.23 ppm as multiplet.
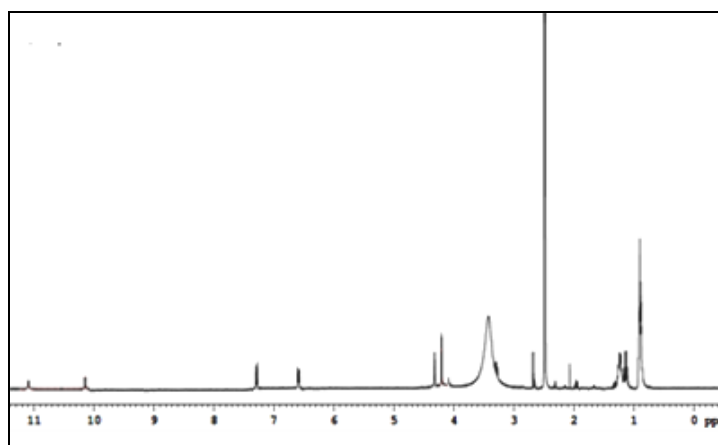
Figure 3.7 ^{1}H NMR spectrum of polyhydrazide **6b**

^{1}H NMR spectra (**Figure 3.8**) of polymer **P2** showed disappearance of amine (–NH) peak at 11.14 and 10.12 ppm confirming the formation of 1,3,4-oxadiazole in the polymer backbone. ^{1}H NMR spectrum of **P2** displayed a set of multiplet peaks at δ 7.35–6.99 ppm due to protons of the two benzyl rings attached to 3,4-positions of the thiophene ring. The observed peaks at δ values 4.27 and 4.19 ppm, correspond to methylene oxy (–OCH$_2$) group of alkyl and benzyl moieties respectively. The protons of dodecyl chain substituted at 3,4 positions of the thiophene ring was resonated at δ values in the region of 1.81 to 1.21 ppm as multiplet peaks.
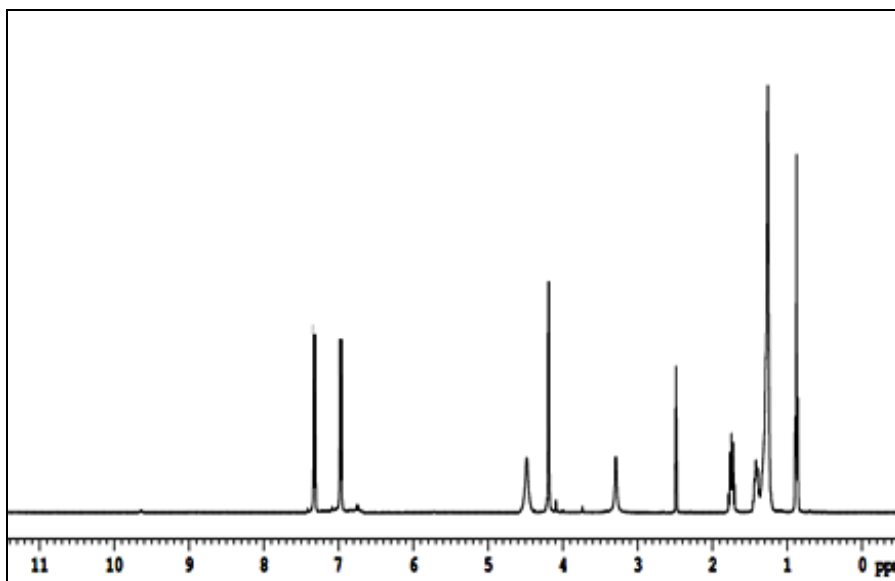
Figure 3.8 ^{1}H NMR spectrum of polymer **P2**

The newly synthesized D-A polymers were soluble in organic solvents such as chloroform, toluene, and chlorobenzene at room temperature. But, it is moderately soluble in THF. The weight average molecular weight of the polymer was determined by GPC against polystyrene standards in THF. The weight average molecular weight ($\overline{\text{M}}_\text{w}$) of polymers **P1**–**P3** was determined to be 6286 g/mol, 13380 g/mol and 8600 g/mol with PDI 2.11, 1.30 and 1.4, respectively.

TGA scan of polymer **P2** is shown in **Figure 3.9**. The TGA thermogram revealed that the onset decomposition temperature of the polymer under nitrogen was 290 °C.
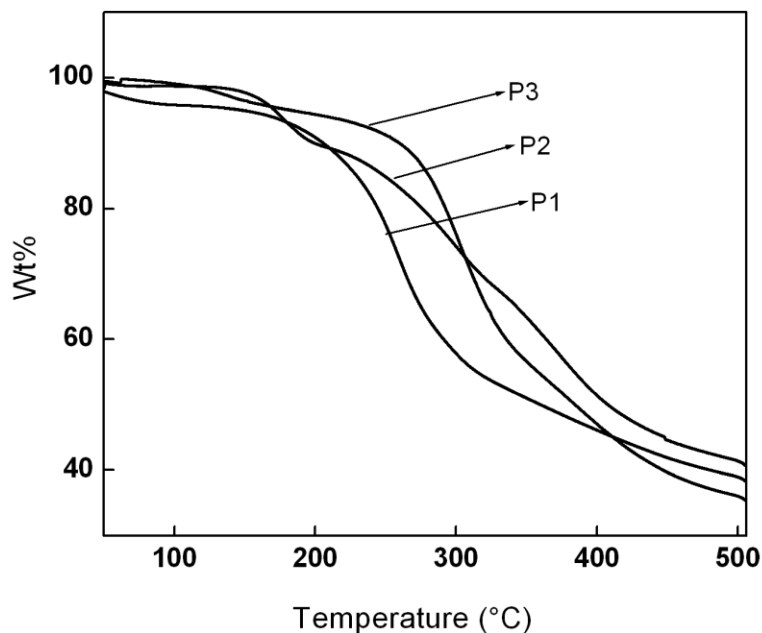
Figure 3.9 Thermogravimetric traces of polymer**s P1–P3.**

From the trace it is clear that the polymer is thermally stable up to about 300 °C. Similarly, polymers **P1** and **P3** showed thermal stability up to 250–300 °C

3.4 SYNTHESIS AND CHARACTERIZATION OF POLYMERS CONTAINING 3,4-DIALKOXYTHIOPHENE, 1,3,4-OXADIAZOLE AND 3,4-BIS [2-(NAPHTHALENE-2-YLMETHOXY)] THIOPHENE (P4–P6), SERIES – 2

In this series, three new polymers **P4–P6** containing 3,4-bis [2-(naphthalene-2-ylmethoxy)] thiophene, 3,4-dialkoxy thiophene and 1,3,4-oxadiazole units, were synthesized from their monomers through multistep reactions. The synthetic route for their preparation from diethyl 3,4-dihydroxythiophene 2,5-carboxylate (**1**) is shown in **Scheme 3.2**.

3.4.1 Chemistry

The required intermediate 3,4-bis(naphthalene-2-ylmethoxy)thiophene-2,5-dicarboxylate (**2**) was obtained by condensation of diethyl 3,4-dihydroxy-thiophene-2,5-diester (**1**) with 2-(chloromethyl)naphthalene in presence of potassium carbonate and DMF. Further, hydrolysis of compound **3** yielded 3,4-bis(naphthalene-2-ylmethoxy)thiophene-2,5-dicarboxylic acid (**3**). The essential monomer 3,4-

Chapter 3

bis(naphthalene-2-ylmethoxy)thiophene-2,5-dicarbonyl dichloride (**4**) was obtained by refluxing with thionyl chloride and a drop of DMF, which on further reaction with dihydrazides **5a–c**, in presence of lithium chloride and a trace of pyridine readily underwent polycondensation to give corresponding polyhydrazides **6d–f**. The compounds **6a–c** obtained were converted into corresponding target polymers (**P4–P6**) through cyclodehydration reaction using phosphorus oxychloride as dehydrating agent.

3.4.2 Experimental procedure

The detailed experimental protocol followed for the synthesis of required monomers and target polymers is given in the following section.

3.4.2.1 Synthesis of intermediates and monomers

The required intermediate **2b** was synthesized from 3,4-dihydroxythiophene-2,5-dicarboxylate (**1**) and ester **2b** was converted to monomer **3b** according to the following procedures.

3.4.2.1.1 Synthesis of diethyl 3,4-bis(naphthalene-2-ylmethoxy)thiophene-2,5-dicarboxylate (2b)

The diester **2b** was synthesized as per the procedure described for compound **2a** (section **3.3.2.1.1**). It was recrystalized from ethanol.

FTIR (KBr, υ, cm^{-1}), 2977 (–CH), 1693 (–C=O). ^{1}H NMR (CDCl$_3$, δ ppm): 7.61–7.42 (m, 14H, aromatic), 5.20 (s, 4H, –OCH$_2$–Ar), 4.41 (q, 4H, –OCH$_2$, J=7.2 Hz), 1.44 (t, 6H, –CH$_3$, J= 6.8 Hz). Element. Anal. Calcd. For C$_{32}$H$_{28}$O$_6$S: C, 71.09%, H, 5.22%, S, 5.93%. Found:C, 70.93%, H, 5.16%, S, 5.56%.

3.4.2.1.2 Synthesis of 3,4-bis(naphthalene-2-ylmethoxy)thiophene-2,5-dicarboxylic acid (3b)

A mixture of diethyl 3,4-bis(naphthalene-2-ylmethoxy)thiophene-2,5-dicarboxylate (**2b,** 2.0 g, 4.5 mmol), 30 mL of 5% alcoholic sodium hydroxide and 5 mL THF was refluxed for 8 h to get a clear solution. The resulting solution was concentrated and cooled. Further, it was washed with ethyl acetate to remove trace of organic impurities and then was acidified with concentrated HCl, to get white precipitate. The precipitate was filtered, washed with water and recrystalized from ethyl acetate.

Mp: 216–218 °C, yield: 85%, FTIR (KBr, υ, cm⁻¹): 3024 (–OH), 2627 (–CH), 1687 (>C=O). ¹H NMR (DMSO–d⁶, δ ppm): 13.6 (s, broad), 8.16–7.27 (m, 14H, naphthalene), 5.59 (s, 4H, –OCH₂–). Element. Anal. Calcd. for $C_{28}H_{20}O_6S$: C, 69.41%; H, 4.16%; S, 6.62%. Found: C, 69.37%, H, 4.02%, S, 6.23%.
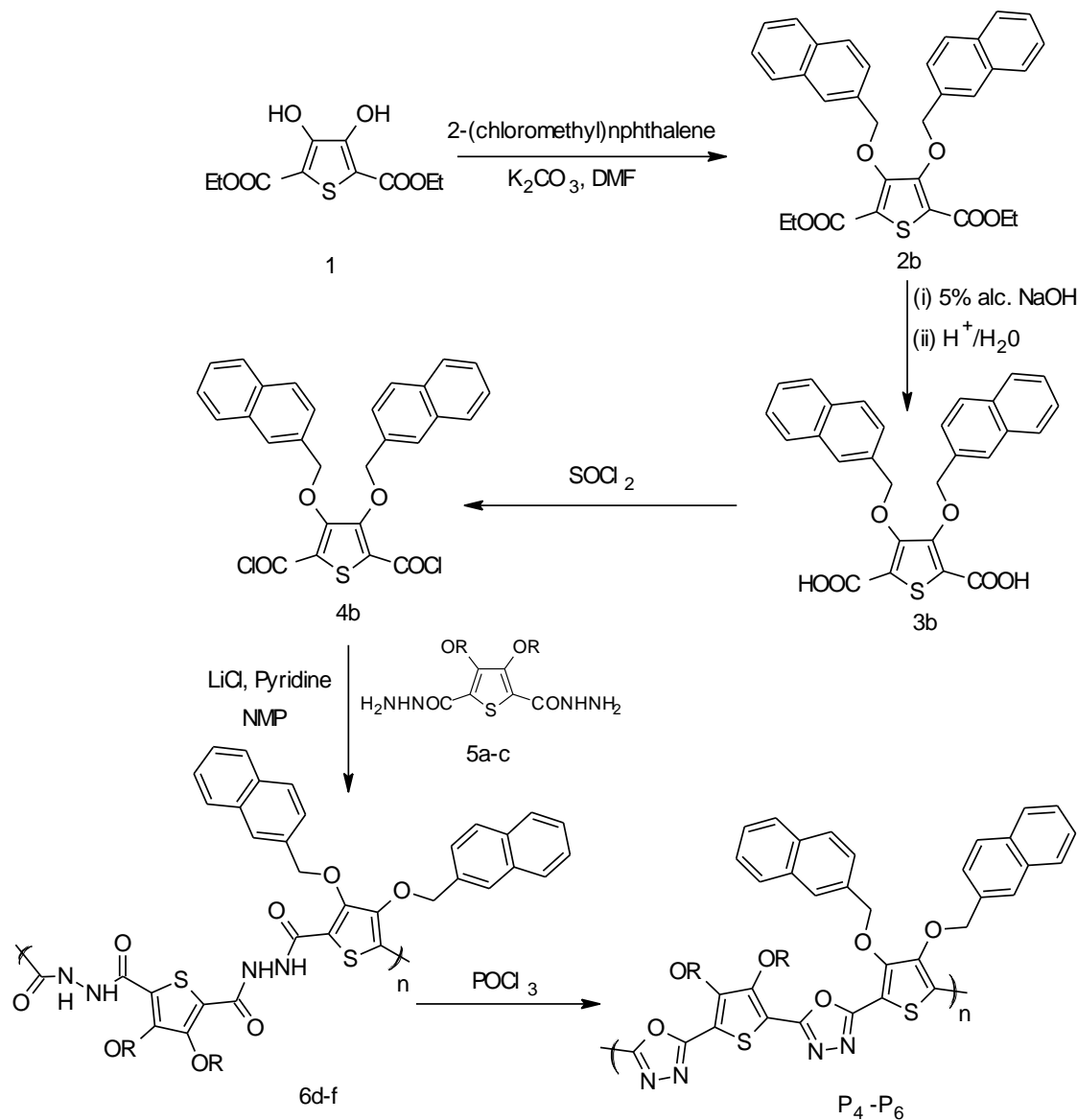
where 5a,6a,P4: R= n-$C_{14}H_{29}$; 5b,6b,P5: R= n-$C_{12}H_{25}$; 5c,6c,P6: R= n-C_6H_{13}

Scheme 3.2 Synthesis polymers **P4–P6** of Series-2

3.4.2.1.3   Synthesis   of   3,4-bis(naphthalen-2-ylmethoxy)thiophene-2,5-dicarbonyldichloride (4b)

The diacid chloride **4b** was synthesized by following the procedure used for the synthesis of diacid chloride **4a** (section–**3.4.2.1.3).** IR (KBr, υ, cm^{-1}): 1670 (C=O).

3.4.2.2 Synthesis of polymers

The precursor polyhydrazides **6d–f** and their corresponding polymers **P4–P6** were synthesized as follows.

3.4.2.2.1 Synthesis of polyhydrazides 6d–f

The synthesis of polyhydrazides **6d–f** was carried out using the similar procedure followed for the synthesis of polyhydrazides **6a–c** (section–**3.3.2.2.1**). Their characterization data are given below.

6d: Yield: 79%, FTIR (KBr, υ, cm^{-1}): 3342 (–NH), 1635 (–C=O), ^{1}H NMR (DMSO–d^6, δ ppm): 10.81 (s, 1H,–NH), 9.73 (s, 1H,–NH), 8.09–7.32 (m, 14H, naphthalene), 5.26 (s, 4H, –OCH$_2$– naphthalene), 4.32 (t, 4H, –OCH$_2$–, tetradecyl, J=6.8 Hz), 1.27–1.69 (m, 48H, –C$_{24}$H$_{48}$). Element. Anal. Calcd. for C$_{62}$H$_{80}$N$_4$O$_8$S$_2$: C, 69.37%; H, 7.51%; N, 5.22%; S, 5.97%. Found: C, 68.98%; H, 7.35%; N, 5.10%; S, 5.85%.

6e: Yield: 79%, FTIR (KBr, υ, cm^{-1}): 3349 (–NH), 1630 (–C=O), ^{1}H NMR (DMSO–d^6, δ ppm): 10.84 (s, 1H,–NH), 9.91 (s, 1H,–NH), 8.19–7.45 (m, 14H, naphthalene), 5.27 (s, 4H, –OCH$_2$– naphthalene), 4.30 (t, 4H, –OCH$_2$– dodecyl, J=6.8 Hz), 1.61–1.31 (m, 40H, –C$_{20}$H$_{40}$). Element. Anal. Calcd. for C$_{58}$H$_{72}$N$_4$O$_8$S$_2$: C, 68.47%; H, 7.13%; N, 5.51%; S, 6.30%. Found: C, 68.21%; H,6.99%; N, 5.09%; S, 6.17%.

6f: Yield: 84%, FTIR (KBr, υ, cm^{-1}): 3340 (–NH), 1642 (–C=O), ^{1}H NMR (DMSO–d^6, δ ppm): 10.92 (s, 1H,–NH), 9.97 (s, 1H,–NH), 8.0–7.41 (m, 14H, naphthalene), 5.25 (s, 4H, –OCH$_2$– naphthalene), 4.29 (t, 4H, –OCH$_2$–, hexyl, J=6.8Hz), 1.63–1.36 (m, 16H, –C$_8$H$_{16}$). Element. Anal. Calcd. for C$_{46}$H$_{48}$N$_4$O$_8$S$_2$: C, 65.07%; H, 5.70%; N, 6.60%; S, 7.55%. Found: C, 64.99%; H, 5.59%; N, 6.45%; S, 7.41%.

3.4.2.2.2 Synthesis of polymers P4–P6

To synthesize polymers **P4–P6**, procedure described for the synthesis of polymers **P1–P3** of Series–1 was followed (section–**3.3.2.2.2**). Their characterization data are as follows.

P4: Yield: 78%, FTIR (KBr, υ, cm^{-1}): 2869, 2713 (–CH), 1587 (–C=N), 1448, 1062 (Aromatic –CH=CH–). ^{1}H NMR (DMSO–d^6, δ ppm): 7.89–7.12 (m, 14H, naphthalene), 5.23 (s, 4H, –OCH$_2$– naphthalene), 4.91 (t, 4H, –OCH$_2$–, tetradecyl, *J*=6.8 Hz), 1.66–1.23 (m, 48H, –C$_{24}$H$_{48}$), 0.86 (t, 6H, –CH$_3$, *J*=7 Hz). Element. Anal. Calcd. for C$_{62}$H$_{76}$N$_4$O$_6$S$_2$: C, 71.78%; H, 7.38%; N, 5.40%; S, 6.18%. Found: C, 71.03%; H, 7.19%; N, 5.25%; S, 6.06%. GPC (THF, PS standard): Weight average molecular weight ($\overline{\mathrm{M}}_w$) =13235 g/mol, PDI = 1.56.

P5: Yield: 78%, FTIR (KBr, υ, cm^{-1}): 2906, 2850 (–CH), 1580 (–C=N), 1450, 1064 (Aromatic –CH=CH). ^{1}H NMR (DMSO–d^6, δ ppm): 7.98–6.87 (m, 14H, naphthalene), 5.27 (s, 4H, –OCH$_2$– naphthalene), 4.93 (t, 4H, –OCH$_2$–, dodecyl, *J*=6.8 Hz), 1.36–1.18 (m, 40H, –C$_{20}$H$_{40}$), 0.87 (t, 6H, –CH$_3$, *J*=7 Hz). Element. Anal. Calcd. for C$_{58}$H$_{68}$N$_4$O$_6$S$_2$: C, 70.99%; H, 6.98%; N, 5.71%; S, 6.54%. Found: C, 70.12%; H, 6.74%; N, 5.61%; S, 6.43%. GPC (THF, PS standard): Weight average molecular weight ($\overline{\mathrm{M}}_w$) =14517 g/mol, PDI= 1.38.

P6: Yield: 73%, FTIR (KBr, υ, cm^{-1}): 2845, 2774 (–CH), 1583 (–C=N), 1458, 1061 (Aromatic –CH=CH). ^{1}H NMR (DMSO–d^6, δ ppm): 8.18–7.09 (m, 14H, naphthalene), 5.31 (s, 4H, –OCH$_2$– naphthalene), 4.97 (t, 4H, –OCH$_2$–, hexyl, *J*=6.8 Hz), 1.36– 1.22 (m, 16H, –C$_8$H$_{16}$), 0.90 (t, 6H, –CH$_3$, *J*=7 Hz). Element. Anal. Calcd. for C$_{46}$H$_{44}$N$_4$O$_6$S$_2$: C, 67.96%; H, 5.46%; N, 6.89%; S, 7.89%. Found: C, 67.10%; H, 5.31%; N, 6.73%; S, 7.71%. GPC (THF, PS standard): Weight average molecular weight ($\overline{\mathrm{M}}_w$) = 8655 g/mol, PDI = 1.40.

3.4.3 Results and discussion

The molecular structures of newly synthesized intermediates, monomers, precursors and the final polymers were confirmed by their FTIR, ^{1}H NMR and elemental analyses. FTIR spectrum (**Figure 3.10**) of diethyl 3,4-bis(naphthalene-2-

ylmethoxy)thiophene-2,5-dicarboxylate (**2b**) showed a sharp peak at 1693 cm^{-1} that corresponds to carbonyl group of ester.
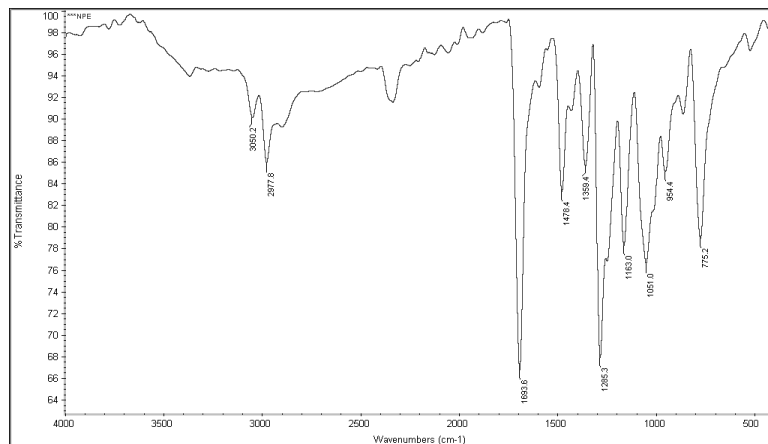
Figure 3.10 FTIR spectrum of diethyl 3,4-bis(naphthalene-2-ylmethoxy)thiophene-2,5-dicarboxylate **(2b)**

Further, its ^{1}H NMR spectrum (**Figure 3.11**) showed multiplet between 7.61–7.42 ppm that corresponds to naphthalene protons, singlet at 5.20 ppm for –OCH$_2$ protons of naphthalene-2-ylmethoxy substituent at 3,4 positions of the thiophene ring, quartet at 4.41 ppm for three protons of ester and triplet at 1.44 ppm for two protons of ester
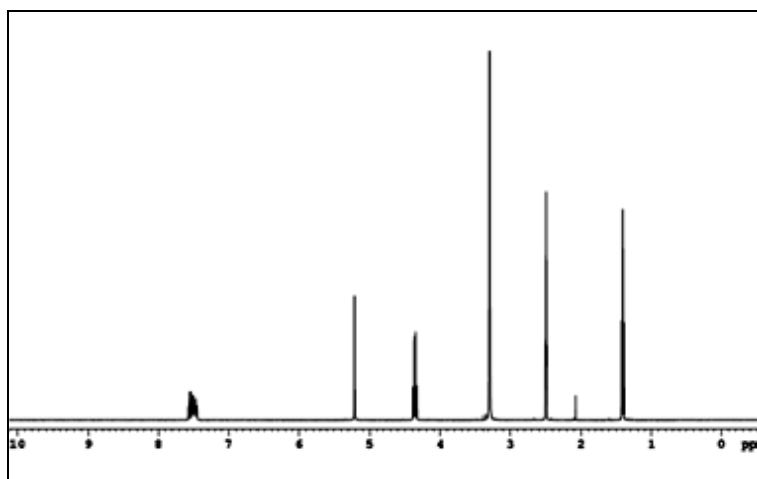
Figure 3.11 ^{1}H NMR spectrum of diethyl 3,4-bis(naphthalene-2-ylmethoxy)thiophene-2,5-dicarboxylate **(2b)**

The structure of 3,4-bis(naphthalene-2-ylmethoxy)thiophene-2,5-dicarboxylic acid (**3b**) was confirmed by its FTIR, ^{1}H NMR spectral and elemental analyses. Its FTIR

(**Figure 3.12**) spectrum showed a broad peak at around 3024 cm^{-1} indicating the presence of –OH group of acid. Also, it exhibited a sharp peak at 1687 cm^{-1} for carbonyl group of acid.
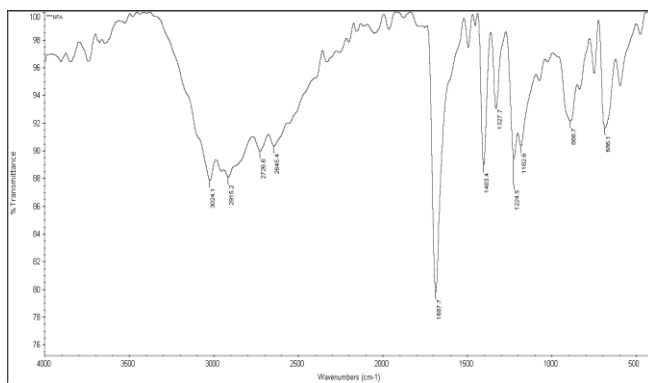
Figure 3.12 FTIR spectrum of 3,4-bis(naphthalene-2-ylmethoxy)thiophene-2,5-dicarboxylic acid **(3b)**

Further, ^{1}H NMR spectrum (**Figure 3.13**) of diacid **3b** showed singlet peak at 13.6 ppm that corresponds to the protons of the carboxylic acid. A set of multiplet between 8.16–7.27 ppm was observed for the protons corresponding to the naphthalene segment, while the methoxy protons of naphthalene-2-ylmethoxy attached at 3,4-postions of thiophene resonated at 5.59 ppm.
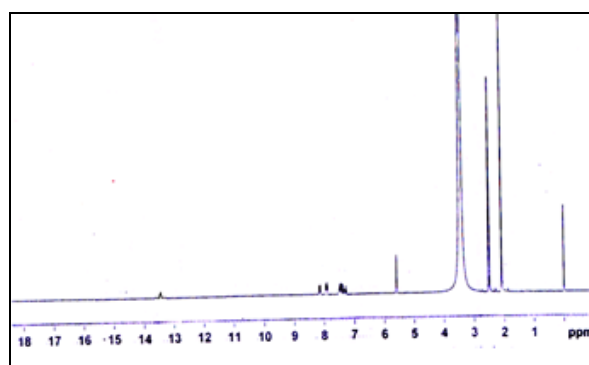
Figure 3.13 ^{1}H NMR spectrum of 3,4-bis(naphthalene-2-ylmethoxy)thiophene-2,5-dicarboxylic acid**(3b)**

The structures of the polymers were confirmed by FTIR and ^{1}H NMR spectral and elemental analyses. Formation of precursor polyhydrazide **6e** was evidenced by

FTIR (**Figure 3.14**) spectrum, wherein it exhibited sharp peaks at 3349 and 1630 cm^{-1} accounting for amide and carbonyl groups, respectively.
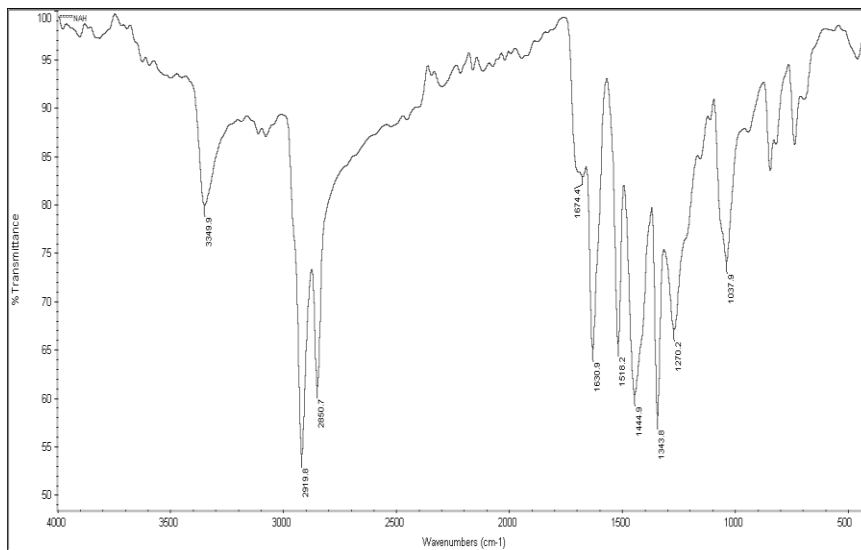
Figure 3.14 FTIR spectrum of polyhydrazide **6e**

The successful conversion of polyhydrazide **6e** to poly(oxadiazole) **P5** was confirmed by its FTIR spectrum (**Figure 3.15**). Disappearance of amine and carbonyl stretching absorption bands and appearance of sharp peak at around 1580 cm^{-1} due to the formation of C=N of the 1,3,4-oxadiazole ring, clearly indicate the cyclization of **6e** to **P5**.
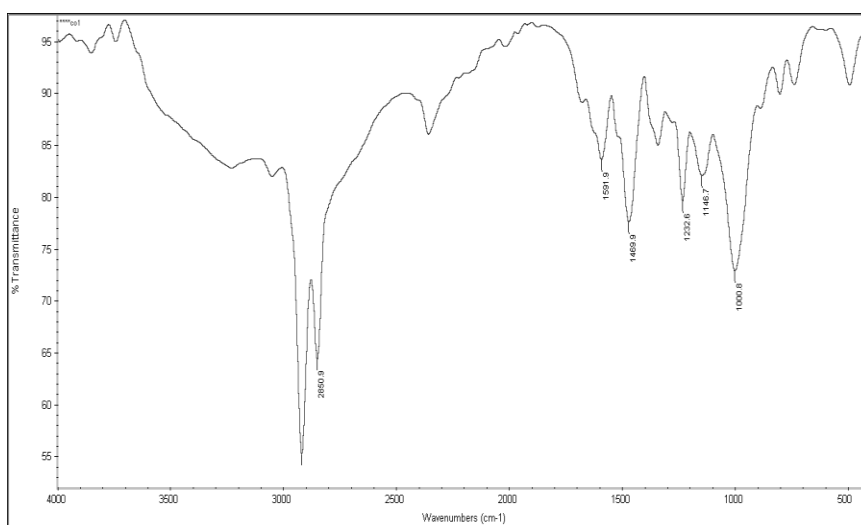
Figure 3.15 FTIR spectrum of polymer **P5**

The ^{1}H NMR spectrum of polyhydrazide **6e** displayed two sharp peaks at 9.91 to 10.84 ppm due to amide protons as shown in **Figure 3.16**. Naphthalene protons resonated at 8.19–7.45 ppm as multiplet and –OCH$_2$ protons of naphthalene-2-ylmethoxy group appeared at 5.27 ppm as singlet, whereas –OCH$_2$ protons of dodecyl chain appeared as triplet at 4.30–4.27. Further, alkyl protons resonated at 1.61–1.31 ppm as multiplet. ^{1}H NMR spectrum of polymer **P5** showed disappearance of peaks due to amide protons at 9.91 to 10.84 ppm, confirming the formation of 1,3,4-oxadiazole in the final polymer. It also displayed a set of multiplet peaks at δ 7.98–6.87 ppm (**Figure 3.17**) due to the protons of two naphthalene rings on 3,4-positions of the thiophene ring. Appearance of a triplet at 4.93–4.90 and a singlet at 5.26 ppm correspond to oxymethylene (–OCH$_2$) group of dodecyloxy chain and 2-(naphthalene-2-ylmethoxy) moiety, respectively. The protons of dodecyl chain substituted at 3,4 positions of the thiophene ring resonated at in the region of 0.87 to 1.36 ppm as multiplet. The results of elemental analysis of polymers were in agreement with its expected empirical formula.
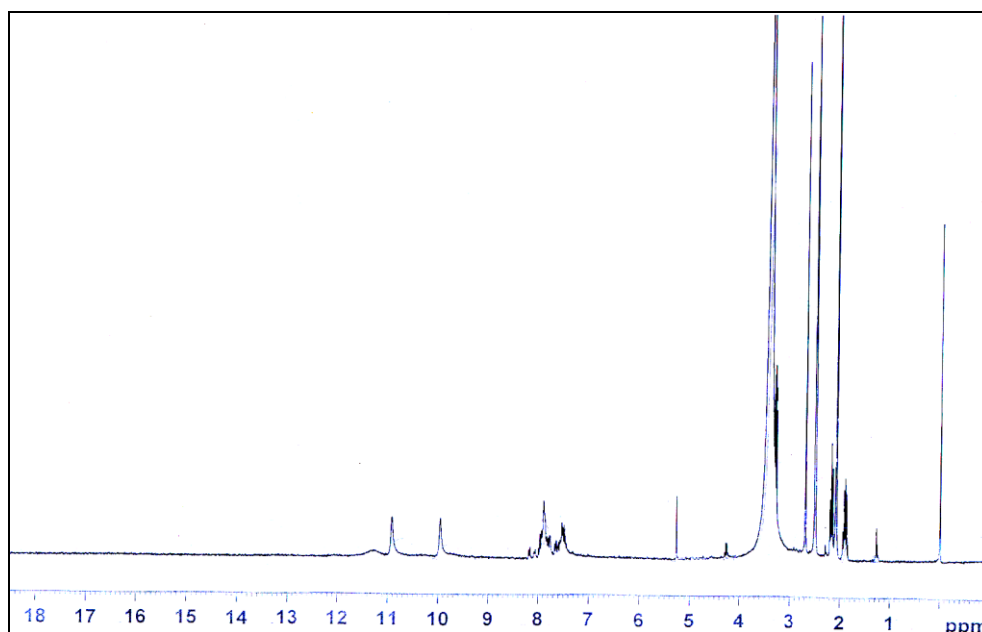
Figure 3.16 ^{1}H NMR spectrum of polyhydrazide **6e**
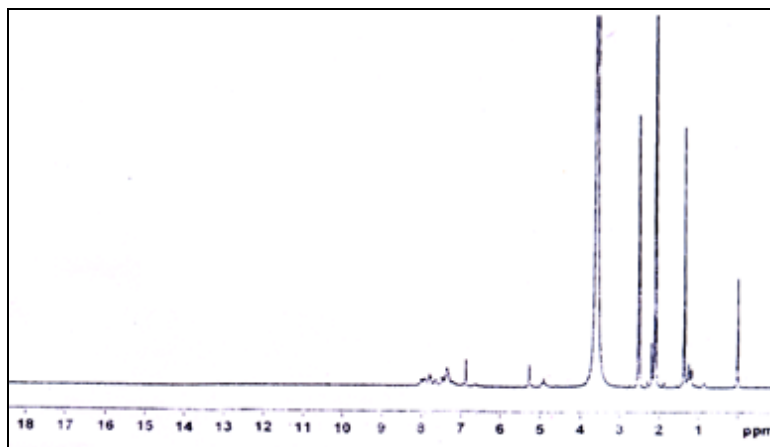
Figure 3.17 ^{1}H NMR spectrum of polymer **P5**

The polymers were soluble in common organic solvents such as chloroform, toluene, and chlorobenzene at room temperature. The weight average molecular weight ($\overline{\mathrm{M}}_w$) of polymers **P4–P6** was determined to be 13235 g/mol, 14517 g/mol and 8655 g/mol and its PDI was found to be 1.56, 1.38 and 1.40, respectively. The thermogravimetric trace of polymers **P4–P6** is shown in **Figure 3.18**. From the trace it is clear that the polymer is thermally stable up to about 300 °C.
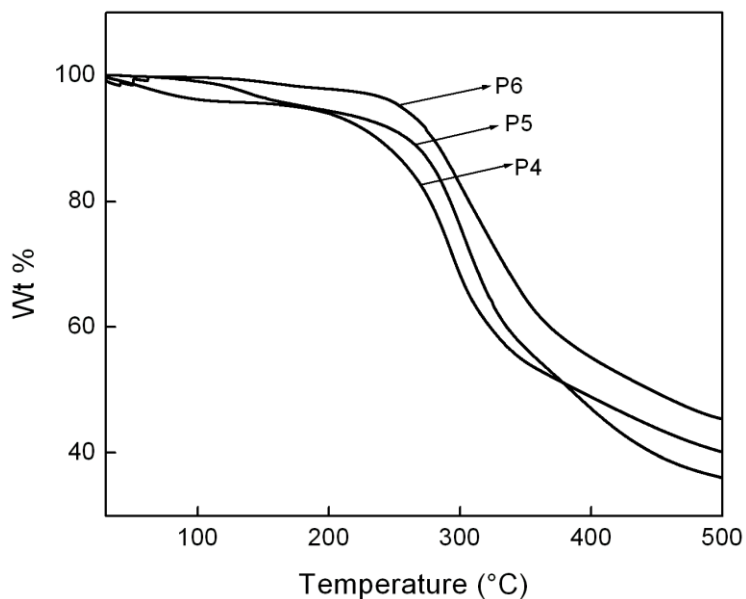
Figure 3.18 Thermogravimetric traces of polymers **P4–P6**

3.5 SYNTHESIS AND CHARACTERIZATION OF POLYMERS CARRYING 3,4-BIS(METHOXY/METHYL/NITROBENZYLOXY)THIOPHENE, 1,3,4-OXADIAZOLE AND 3,4-DIALKYLOXYTHIOPHENE (P7–P9), SERIES–3

We synthesized three new D-A type conjugated polymers consisting of 3,4-bis(methoxy/methyl/nitrobenzyloxy)thiophene as electron donor and 1,3,4-oxadiazole as electron acceptor group in this series. Further, it includes the characterization of new monomers and polymers. The synthetic routes towards the preparation of new intermediates and monomers and finally polymerization of monomers to **P7–P9** are outlined in **Scheme 3.3**.

3.5.1 Chemistry

Required intermediates, viz. 3,4-bis[(3-methylbenzyl)oxy}thiophene-2,5-dicarboxylicacid (**3c**), 3,4-bis[(4-methoxybenzyl)oxy}thiophene-2,5-dicarboxylic acid (**3d**) and 3,4-bis[(4-nitrobenzyl)oxy}thiophene-2,5-dicarboxylic acid (**3e**), were synthesized by alkali hydrolysis of their corresponding esters **2c–e**. These esters **2c–e** were obtained by condensation of 3,4-dihydroxy-thiophene-2,5-diester (**1**) with 1-(chloromethyl)-4-methoxybenzene, 1-(chloromethyl)-3-methylbenzene, 1-(bromomethyl)-4-nitrobenzene, respectively in presence of potassium carbonate and DMF. The diacids **3c–e** were refluxed with excess thionyl chloride to obtain diacid chlorides **4c–e**, which on treatment with dihydrazide **5b**, in presence of lithium chloride and pyridine underwent polycondensation to give required polyhydrazides **6g–i**. The polyhydrazides on cyclodehydration with phosphorous oxychloride yielded target polymers **P7–P9**.

3.5.2 Experimental procedure

The detailed experimental procedures for the synthesis of monomers **4c–e** and their intermediates and finally polymers **P7–P9** are given in the following section.

3.5.2.1 Synthesis of new intermediates and monomers

Synthetic procedures of new intermediates and monomers along with their characterization data are given below.

3.5.2.1.1 Synthesis of 3,4-bis[(4-methoxybenzyl)oxy] thiophene-2,5-dicarboxylate (2c)

To a mixture of diethyl 3,4-dihydroxythiophene-2,5-dicarboxylate (**1**) (1 g, 3.8 mmol) and K_2CO_3 (1.6 g, 11.5 mmol) in 30 ml of DMF was added drop-wise 1-(chloromethyl)-4-methoxybenzene (1.2 g, 7.6 mmol). The reaction mixture was refluxed for 24 h at 60 °C. When the reaction was completed, it was cooled to room temperature and poured into water. The white precipitate formed was filtered, dried and recrystalized using ethanol. Its characterization data is as follows.

2c: Mp: 106–108 °C. Yield: 78%. FTIR (KBr, υ, cm^{-1}): 2978 (–CH), 1697 (>C=O). ^{1}H NMR (DMSO–d^6, δ ppm): 7.29– 6.86 (m, 8H,–C$_6$H$_4$), 5.04 (s, 4H, –OCH$_2$), 4.27 (q, 4H, –CH$_2$, *J*=7.2 Hz), 3.71 (s, 6H, –OCH$_3$), 1.26–1.22 (t, 6H, –CH$_3$, *J*=7.2 Hz). ^{13}C NMR (DMSO–d^6, δ ppm):159.89, 159.30, 152.59, 130.13, 128.24, 119.42, 113.63, 75.52, 61.30, 55.06, 13.97. Element. Anal. Calcd. For $C_{26}H_{28}O_8S$: C, 62.39%, H, 5.64%, S, 6.41%. Found: C, 62.41%, H, 5.51%, S, 6.54%.

3.5.2.1.2 Synthesis of diethyl 3,4-bis[(3-methylbenzyl)oxy] thiophene-2,5-dicarboxylate (2d)

Compound **2d** was synthesized according to the procedure described for **2a** by the reaction of compound **1** with 1-(chloromethyl)-3-methylbenzene (1 g, 7.6 mmol). Its characterization data is given below.

2d: Mp: 63–65 °C. Yield: 73%. FTIR (KBr, υ, cm^{-1}): 2972 (–CH), 1695 (–C=O). ^{1}H NMR (DMSO–d^6, δ ppm): 7.25–7.13 (m, 8H, –C$_6$H$_4$), 5.10 (s, 4H, –OCH$_2$), 4.26 (q, 4H, –CH$_2$, *J*=7.2 Hz), 2.26 (s, 6H, –CH$_3$), 1.29 (t, 6H, –CH$_3$, *J*=7.2 Hz). ^{13}C NMR (DMSO–d^6, δ ppm): 159.87, 152.53, 137.39, 136.21, 128.80, 128.75, 128.14, 125.23, 119.59, 75.86, 61.36, 20.82, 13.94. Element. Anal. Calcd. For $C_{26}H_{28}O_6S$: C, 66.65%, H, 6.02%, S, 6.84%. Found: C, 66.46%, H, 6.19%, S, 6.68%.
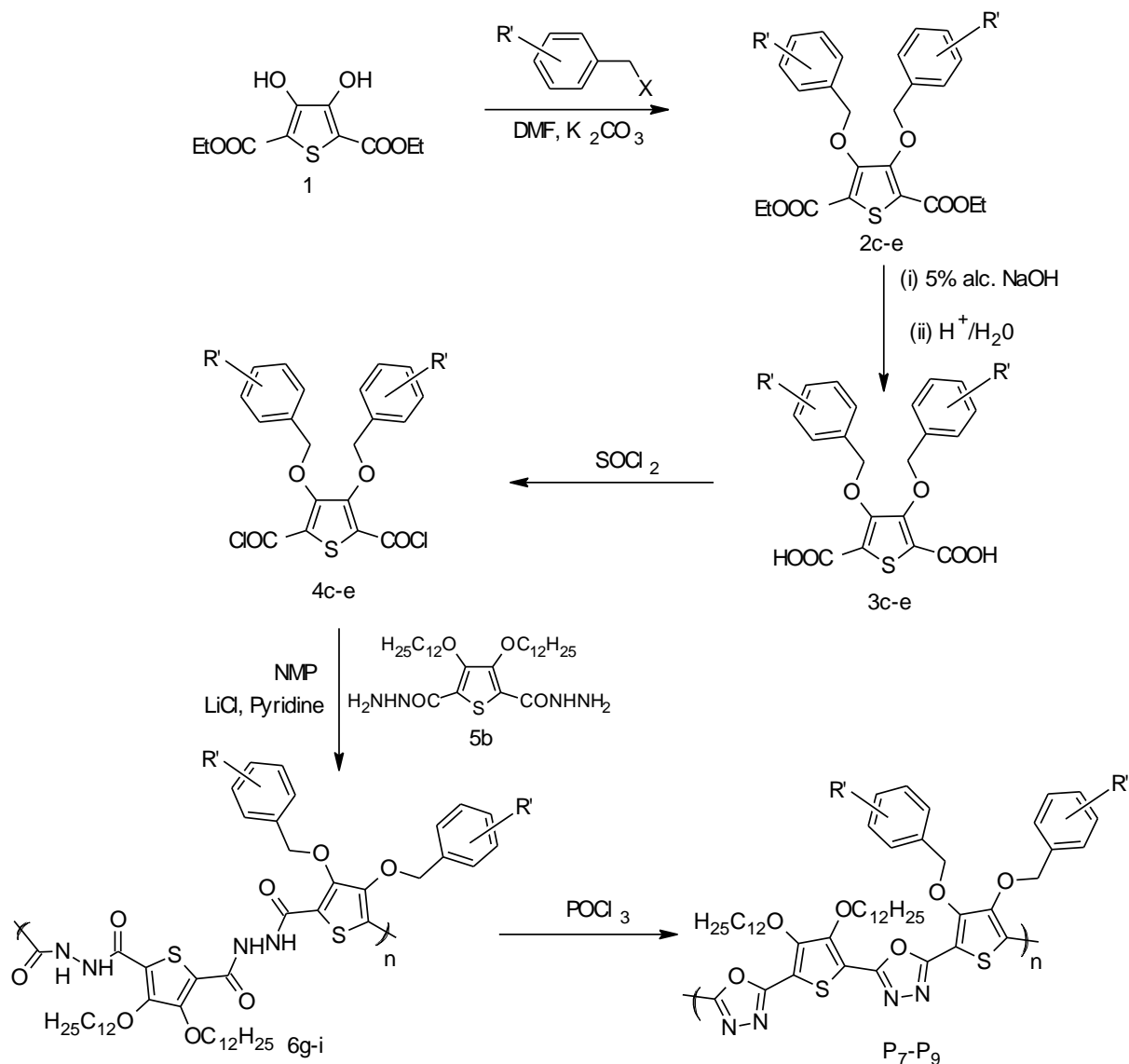
where 2c, 3c, 4c, 6g, P7: R'= 4-methoxy, X=Cl; 2d, 3d, 4d, 6h, P8: R' = 3-methyl, X=Cl;
2e, 3e, 4e, 6i, P9: R' = 4-nitro, X=Br

Scheme 3.3 Synthesis polymers **P7–P9** of Series-3

3.5.2.1.3 Synthesis of diethyl 3,4-bis[(4-nitrobenzyl)oxy] thiophene-2,5-dicarboxylate (2e)

To get 3,4-bis[(4-nitrobenzyl)oxy] thiophene-2,5-dicarboxylate (**2e**) similar procedure was followed as explained for **2c**, by the reaction of ester **1** with 1-

(bromomethyl)-4-nitrobenzene (1.66 g, 7.6 mmol). Its characterization data is given below.

2e: MP: 158–160 ^{o}C, yield: 79%, FTIR (KBr, υ, cm^{-1}): 2977 (–CH), 1693 (–C=O). ^{1}H NMR (DMSO–d^{6,} δ ppm): 8.18–7.64 (m, 8H, –C$_6$H$_4$), 5.30 (s, 4H, –OCH$_2$), 4.26 (q, 4H, –CH$_2$, *J*=7.2 Hz), 1.26 (t, 6H, –CH$_3$, , *J*=7.2 Hz). ^{13}C NMR (DMSO–d^{6,} δ ppm): 159.73, 151.97, 147.13, 144.03, 128.57, 123.37, 119.80, 74.66, 61.56, 13.93. Element. Anal. Calcd. For C$_{24}$H$_{22}$N$_2$O$_{10}$S: C, 54.34%, H, 4.18%, N, 5.28%, S, 6.04%. Found: C, 54.56%, H, 4.13%, N, 5.31%, S, 6.13%.

General procedure for the synthesis of diacids (3c–e)

A mixture of diester **2c–e** (1.0 g), 30 mL of 5% alcoholic sodium hydroxide was refluxed for 8 h to get a clear solution. The resulting solution was concentrated and cooled. Further, it was washed with ethyl acetate to remove trace of organic impurities and then was acidified with concentrated HCl, to get white precipitate of diacids **3c–e**. The precipitate was filtered, washed with water and recrystalized from ethyl acetate. Similarly diacids **3b** and **3c** were synthesized. Their characterization data are given below.

Diethyl 3,4-Bis[(4-methoxybenzyl)oxy] thiophene-2,5-dicarboxylic acid (3c): Mp: 107–109 ^{o}C. Yield: 69%, FTIR (KBr, υ, cm^{-1}): 3002 (–OH), 2628 (–CH), 1671 (>C=O). ^{1}H NMR (DMSO–d^{6,} δ ppm): 13.54 (s, 2H, -carboxylic acid), 7.19–7.01 (m, 8H, aromatic), 5.02 (s, 4H, –OCH$_2$–Ar), 3.80 (s, 6H, –OCH$_3$). Element. Anal. Calcd. for C$_{22}$H$_{20}$O$_8$S: C, 59.45%; H, 4.45%; S, 7.21%. Found: C, 59.49%; H, 4.56%; S, 7.19%.

Diethyl 3,4-Bis[(3-methylbenzyl)oxy] thiophene-2,5-dicarboxylic acid (3d): Mp: 203–205 ^{o}C. Yield: 65%. FTIR (KBr, υ, cm^{-1}): 3019 (–OH), 2634 (–CH), 1635 (>C=O). ^{1}H NMR (DMSO–d^{6,} δ ppm): 13.49 (s, 2H, –carboxylic acid), 7.24–7.12 (m, 8H, aromatic), 5.08 (s, 4H, –OCH$_2$) 2.25 (s, 6H, –CH$_3$). Element. Anal. Calcd. for C$_{22}$H$_{20}$O$_6$S: C, 64.06%; H, 4.89%; S, 7.77%. Found: : C, 64.13%; H, 4.81%; S, 7.65%.

Diethyl 3,4-Bis[(4-nitrobenzyl)oxy] thiophene-2,5-dicarboxylic acid (3e): Mp: 253–255 ^{o}C. Yield: 78%. FTIR (KBr, υ, cm^{-1}): 3024 (–OH), 2726 (–CH), 1687 (>C=O). ^{1}H NMR (DMSO–d^{6,} δ ppm): 13.57 (s, 2H, –carboxylic acid), 7.63–8.16 (m, 8H,

aromatic), 5.29 (s, 4H, –OCH$_2$). Element. Anal. Calcd. for C$_{20}$H$_{14}$N$_2$O$_{10}$S: C, 50.64%, H, 2.97%, N, 5.90%, S, 6.76%. Found: C, 50.76%, H, 2.86%, N, 5.79%, S, 6.81%.

3.5.2.1.8 Synthesis of diacid chlorides (4c–e)

The diacids chlorides **4c–e** were synthesized using the procedure followed for the synthesis of diacids chloride **4** (section–**3.4.2.1.3**). A pale yellow (**4c,d** as liquid and **4e** as semi–solid) product was obtained in good yield.

3.5.2 Synthesis of polymers

The synthesis of new polyhydrazides **6g–i** and their conversion to polymers **P7– P9** are as follows.

3.5.2.1 Synthesis of precursor polyhydrazides (6g–i)

The polyhydrazides 6g–i were synthesized according to the procedure used for the synthesis of polyhydrazides **6a–c** (section–**3.3.2.2.1**). Their characterization data are as follows.

6g: Yield: 73%. FTIR (KBr, υ, cm^{-1}): 3218 (–NH), 1630 (–C=O). ^{1}H NMR (DMSO–d^6, δ ppm): 10.18 (s, 1H, –NH), 10.07 (s, 1H, –NH), 7.25–7.13 (m, 10H, aromatic), 5.04 (s, 4H, –OCH$_2$), 3.82 (s, 6H, –OCH$_3$–Ar), 4.35 (t, 4H, –OCH$_2$–, alkyl, J=6.8 Hz), 3.82 (s, –OCH3), 1.77–1.21– (m, 40H), 0.83 (t, 6H, –CH$_3$, alkyl, J=6.8 Hz). Element. Anal. Calcd. for C$_{52}$H$_{72}$N$_4$O$_8$S$_2$: C, 66.07%; H, 7.68%; N, 5.93%; S, 6.78%. Found: C, 65.92%; H, 7.56 %; N, 5.87%; S, 6.34%.

6h: Yield: 76%. FTIR (KBr, υ, cm^{-1}): 3345 (–NH), 1633 (–C=O). ^{1}H NMR (DMSO–d^6, δ ppm): 10.27 (s, 1H,–NH), 10.17 (s, 1H, –NH), 7.25–7.13 (m, 10H,aromatic), 5.18 (s, 4H, –OCH$_2$), 4.34 (t, 4H, –OCH$_2$–, alkyl, J=6.8 Hz), 2.07 (s, 6H, CH$_3$–Ar), 1.19–1.78 (m, 40H), 0.83 (t, 6H, –CH$_3$ alkyl, J=6.8 Hz). Element. Anal. Calcd. for C$_{52}$H$_{72}$N$_4$O$_{10}$S$_2$: C, 63.91%; H, 7.43%; N, 5.73%; S, 6.56%. Found: C, 63.07%; H, 7.18%; N, 5.13%; S, 6.08%.

6i: Yield: 81%. FTIR (KBr, υ, cm^{-1}): 3286 (–NH), 1631 (–C=O). ^{1}H NMR (DMSO–d^6, δ ppm): 10.17 (s, 1H,–NH), 9.90 (s, 1H,–NH), 8.66–7.62 (m, 10H, aromatic), 5.33 (s, 4H, –OCH$_2$), 4.24 (t, 4H, –OCH$_2$–, alkyl, J=7 Hz), 1.78–1.19 (m, 40H), 0.83 (t, 6H, –CH$_3$ alkyl, J=7 Hz). Element. Anal. Calcd. for C$_{50}$H$_{66}$N$_6$O$_{12}$S$_2$: C, 59.62%; H, 6.60%; N, 8.34%; S, 6.37%. Found: C, 59.56%; H, 6.69%; N, 8.41%; S, 6.28%.

3.5.2.2.2 Synthesis of polymers P7–P9

Polymers **P7–P9** were obtained using the procedure described for the synthesis of polymers **P1–P3** (section–**3.3.2.2.2**). Their characterization data are as follows.

P7: Yield: 73%. FTIR (KBr, υ, cm^{-1}): 2913, 2852 (–CH), 1580 (–C=N), 1035 (Aromatic –CH=CH). ^{1}H NMR (DMSO–d^{6,} δ ppm): 7.45–7.29 (m, 10H, aromatic), 4.99 (s, 4H, –OCH$_2$–Ar), 4.29 (t, 4H, –OCH$_2$–, alkyl, J=7 Hz), 3.76 (s, –OCH$_3$) 1.89–1.19 (m, 40H, –C$_{20}$H$_{40}$), 0.91 (t, 6H, –CH$_3$, J=6.8 Hz). Element. Anal. Calcd. for C$_{52}$H$_{68}$N$_4$O$_8$S$_2$: C, 66.35%; H, 7.28%; N, 5.95%; S, 6.81%. Found: C, 66.46%; H, 7.31%; N, 5.82%; S, 6.93%. GPC (THF, PS standard): Weight average molecular weight ($\overline{\text{M}}_\text{w}$) = 6286 g/mol, PDI =1.87.

P8: Yield: 76%. FTIR (KBr, υ, cm^{-1}): 2916, 2851 (–CH), 1573 (–C=N), 1452, 1022 (Aromatic –CH=CH). ^{1}H NMR (DMSO–d^{6,} δ ppm): 7.26–7.14 (m,10H, aromatic), 5.20 (s, 4H, –OCH$_2$–Ar), 4.23 (t, 4H, –OCH$_2$–, alkyl, J=7 Hz), 2.02 (s, 6H, –CH$_3$–Ar) 1.88–1.22 (m, 16H, –C$_8$H$_{16}$), 0.84 (t, 6H, –CH$_3$, J=6.8 Hz). Element. Anal. Calcd. for C$_{52}$H$_{68}$N$_4$O$_6$S$_2$: C, 68.69%; H, 7.54%; N, 6.16%; S, 7.05%. Found: C, 68.73%; H, 7.61%; N, 6.23%; S, 7.09%. Weight average molecular weight ($\overline{\text{M}}_\text{w}$) = 7146 g/mol, PDI = 1.58.

P9: Yield:76%. FTIR (KBr, υ, cm^{-1}): 2920, 2855 (–CH), 1581 (–C=N), 1458, 1035 (Aromatic –CH=CH). ^{1}H NMR (DMSO–d^{6,} δ ppm): 8.19–7.82 (m, 10H, aromatic), 5.35 (s, 4H, –OCH$_2$–Ar), 4.33 (t, 4H, –OCH$_2$–, alkyl, J=7 Hz), 1.99 –1.78 (m, 16H, –C$_8$H$_{16}$), 0.85 (t, 6H, –CH$_3$, J=6.8 Hz). Element. Anal. Calcd. for C$_{50}$H$_{62}$N$_6$O$_{10}$S$_2$: C, 61.83%; H, 6.43%; N, 8.65%; S, 6.60%. Found: C, 61.71%; H, 6.54%; N, 8.79%; S, 6.81%. Weight average molecular weight ($\overline{\text{M}}_\text{w}$) = 3781 g/mol, PDI = 1.65.

3.5.3 Results and discussion

Structures of newly synthesized intermediates, monomers and final polymers were confirmed by their FTIR, ^{1}H NMR and ^{13}C NMR spectral data, followed by elemental analysis. Formation of diester **2c** from dihydroxy compound **1** was confirmed by its FTIR, ^{1}H NMR and ^{13}C NMR spectral study. Its FTIR (**Figure 3.19**) spectrum showed sharp peaks at 1697 cm^{-1} and 2978 cm^{-1} indicating the presence of carbonyl and alkoxy groups, respectively.
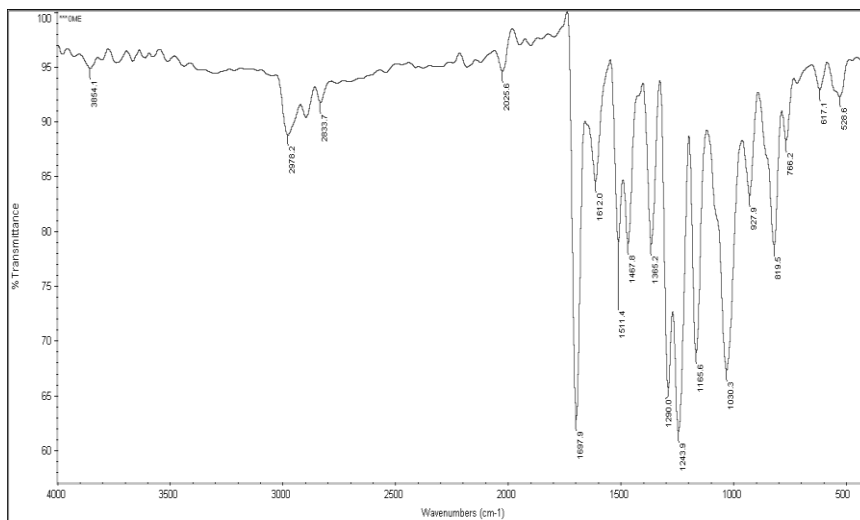
Figure 3.19 FTIR spectrum of 3,4-bis[(4-methoxybenzyl)oxy] thiophene -2,5-
dicarboxylate **(2c)**

The FTIR spectra of esters **2d** and **2e** also showed sharp peaks at around 1690 cm^{-1} confirming the presence of carbonyl group of ester. The **Figures 3.20** and **3.21** represent FTIR spectra of **2d** and **2e**, respectively.
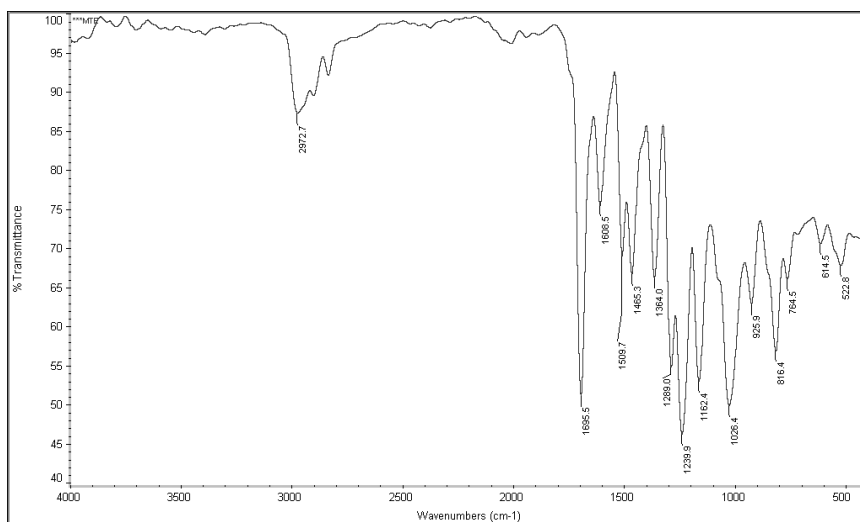
Figure 3.20 FTIR spectrum of 3,4-bis[(3-methylbenzyl)oxy] thiophene-2,5-dicarboxylate

(2d)
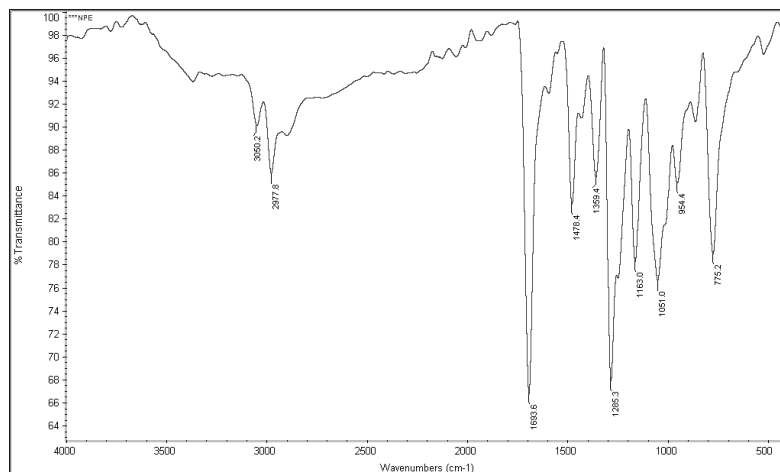
Figure 3.21 FTIR spectrum of 3,4-bis[(4-nitrobenzyl)oxy] thiophene -2,5-dicarboxylate

(2e)

Further, ^{1}H NMR spectrum of ester **2c** (**Figure 3.22**) showed a multiplet at 7.29–6.86 ppm due to aromatic protons and a singlet at 5.04 ppm that corresponds to –OCH_2 of benzyl group. Furthermore, the peaks at 4.27–4.22 ppm as quartet and 1.26–1.22 ppm as triplet indicated the presence of –CH_2 and –CH_3 of ester group, respectively. Also, the appearance of singlet at 3.71 ppm confirmed the presence of –OCH_3 attached to benzyl group. The **Figures 3.23** and **3.24** represent ^{1}H NMR spectra of **2d** and **2e**, respectively.
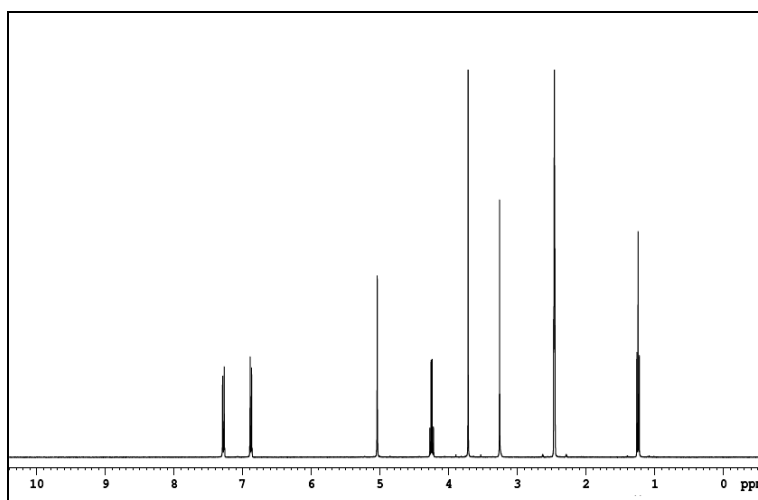
Figure 3.22 ^{1}H NMR spectrum of 3,4-bis[(4-methoxybenzyl)oxy] thiophene -2,5-dicarboxylate **(2c)**
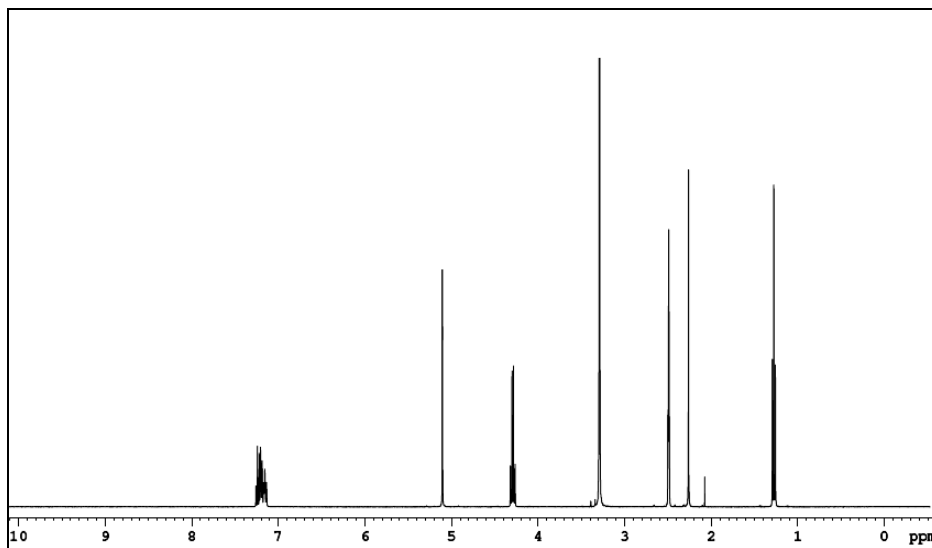
Figure 3.23 ^{1}H NMR spectrum of 3,4-bis[(3-methylbenzyl)oxy] thiophene-2,5-dicarboxylate **(2d)**
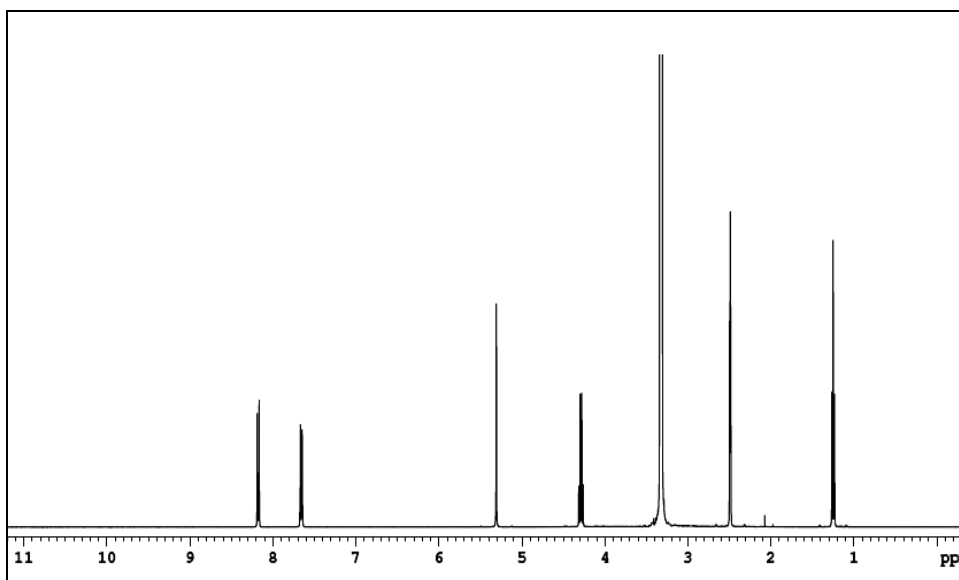
Figure 3.24 ^{1}H NMR spectrum of 3,4-bis[(4-nitrobenzyl)oxy] thiophene-2,5-dicarboxylate **(2e)**

Further, ^{13}C NMR spectrum (**Figure 3.25**) of **2c** showed a series of peaks at 159.89, 159.30, 152.59, 130.13, 128.24, 119.42, 113.63, 75.52, 61.30, 55.06 ppm confirming the presence of carbons of carbonyl, thiophene, benzyl, alkoxy and ester groups.

The **Figures 3.26** and **3.27** show ^{13}C NMR spectra of esters **2d** and **2e**, respectively.
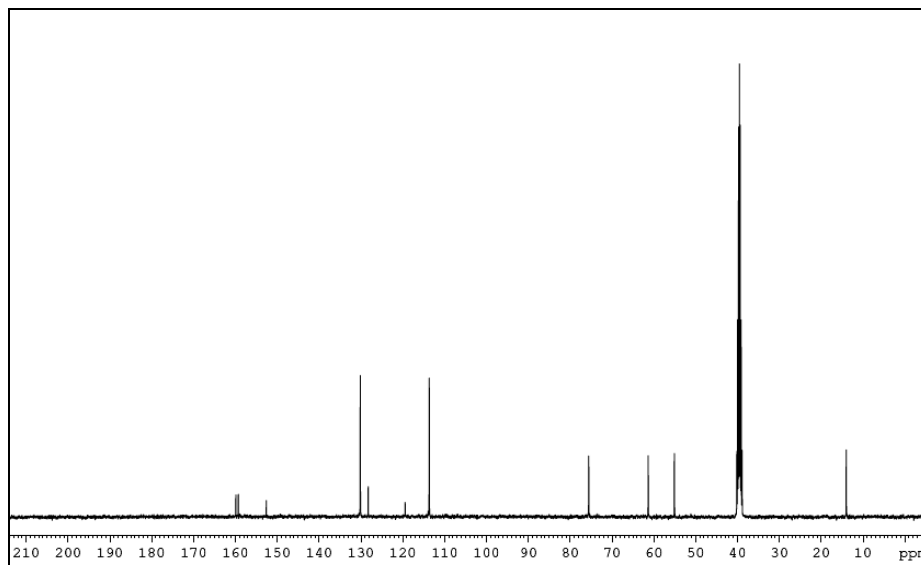
Figure 3.25 ^{13}C NMR spectrum of diethyl3,4-bis[(4-methoxybenzyl)oxy] thiophene -2,5-dicarboxylate (**2c**)
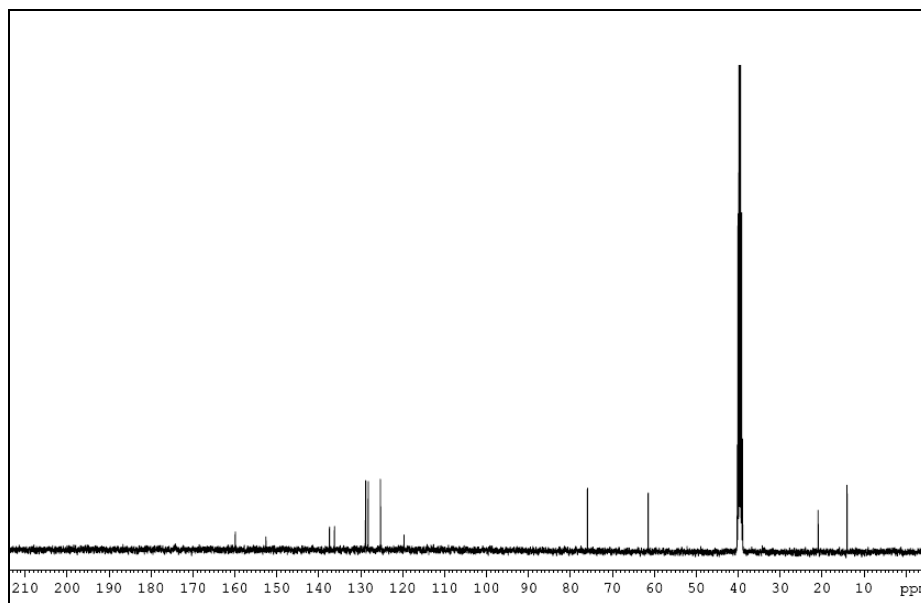
Figure 3.26 ^{13} C NMR spectrum of 3,4-bis[(3-methylbenzyl)oxy] thiophene-2,5-dicarboxylate **(2d)**
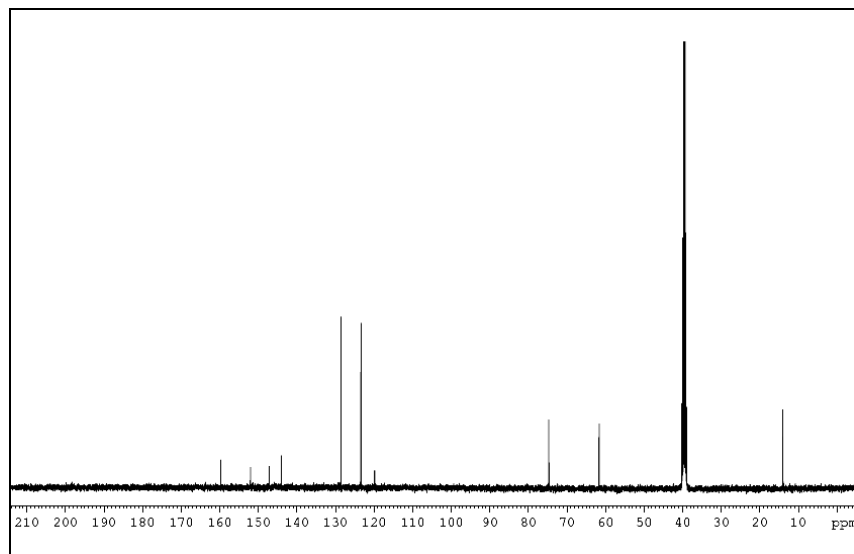
Figure 3.27 ^{13}C NMR spectrum of 3,4-bis[(4-nitrobenzyl)oxy] thiophene –2,5–dicarboxylate **(2e)**

The conversion of diester **2c** to diacid **3c** was established by its FTIR, ^{1}H NMR spectral data. The FTIR spectrum (**Figure 3.28**) of **3c** displayed a broad peak at around 3000 cm^{-1} signifying the presence of acid group and a strong peak at 1671 cm^{-1} indicating the presence of carbonyl group. The **Figures 3.29** and **3.30** represent FTIR spectra of **3d** and **3e**, respectively.
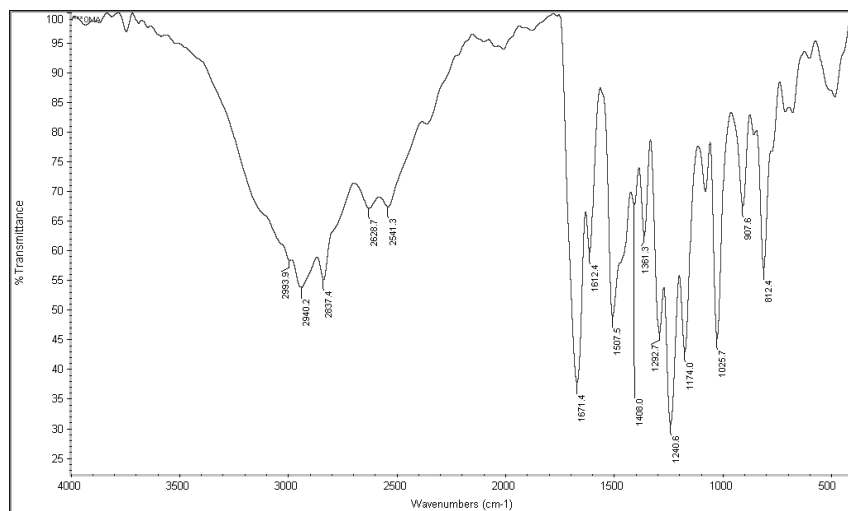
Figure 3.28 FTIR spectrum of 3,4-bis[(4-methoxybenzyl)oxy] thiophene-2,5-dicarboxylic acid (**3c**)
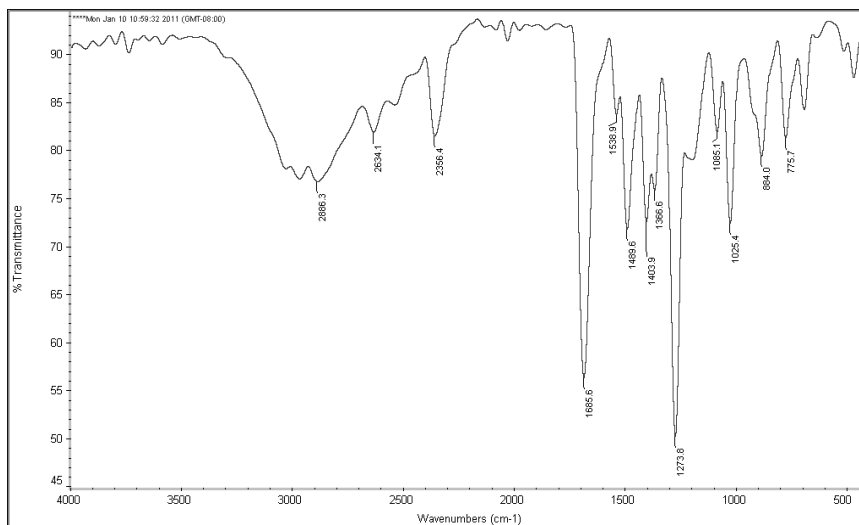
Figure 3.29 FTIR spectrum of 3,4-bis[(3-methylbenzyl)oxy]thiophene-2,5-dicarboxylic
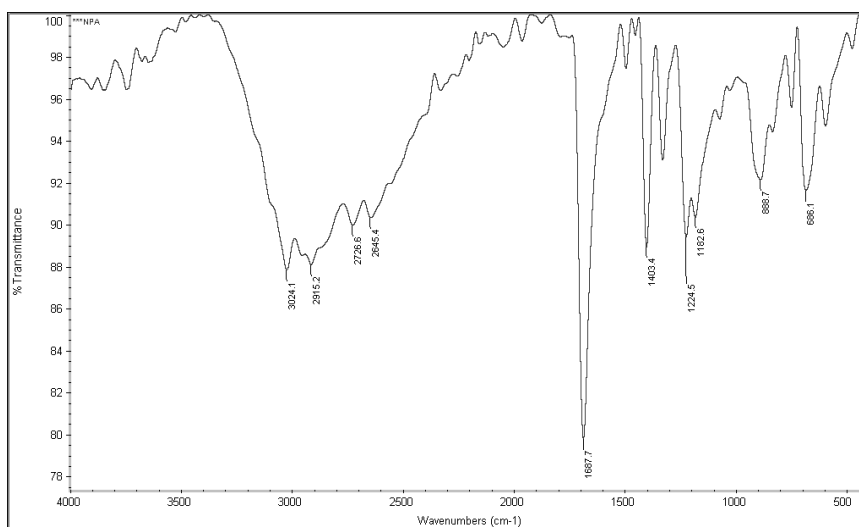
acid **(3d)**

Figure 3.30 FTIR spectrum of 3,4-bis[(4-nitrobenzyl)oxy]thiophene-2,5-dicarboxylic

acid **(3e)**

The ^{1}H NMR spectrum (**Figure 3.31**) of diester **3c** displayed a broad singlet at 13.54 ppm which entails the presence of carboxylic acid proton and a multiplet at 7.19–7.01ppm because of aromatic protons. The appearance of a singlet at 5.02 ppm indicated the presence of –OCH$_2$ linked to phenyl group while presence of another singlet at 3.80

ppm was attributed to –OCH$_3$ attached to benzyl group. The **Figures 3.32** and **3.33** represents ^{1}H NMR spectra of diacids **3d** and **3e**, respectively.
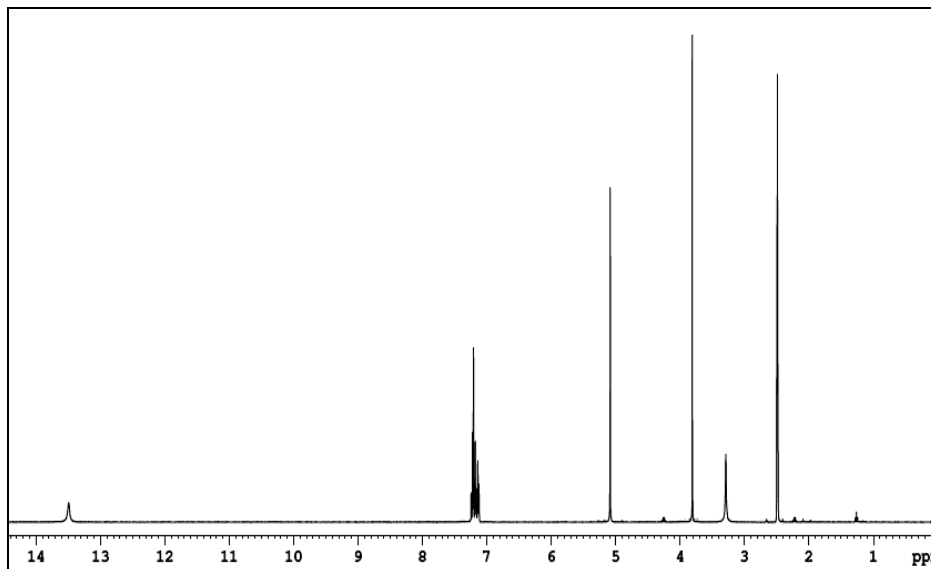
Figure 3.31 ^{1}H NMR spectrum of 3,4-bis[(4-methoxybenzyl)oxy] thiophene-2,5-dicarboxylic acid (**3c**)
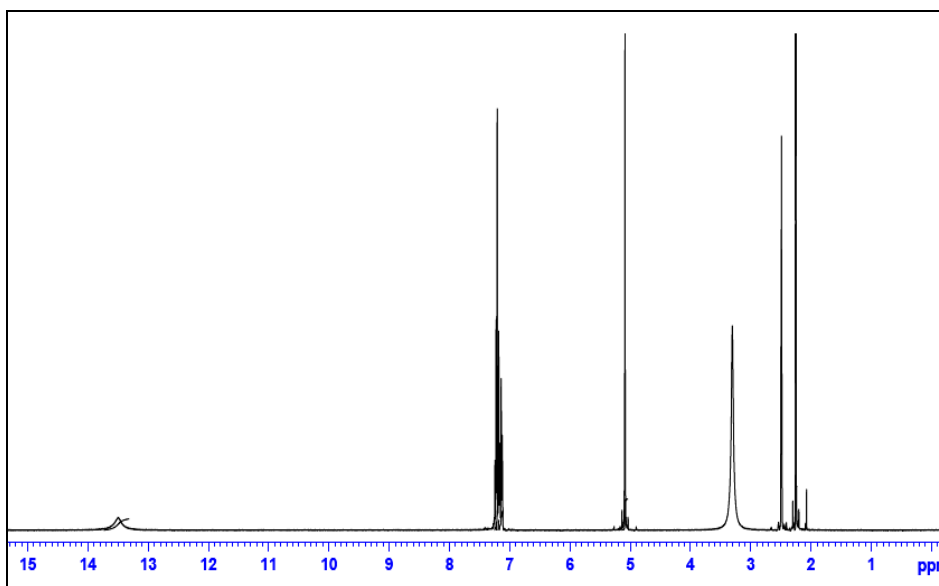
Figure 3.32 ^{1}H NMR spectrum of 3,4-bis[(3-methylbenzyl)oxy] thiophene-2,5-dicarboxylic acid (**3d**)
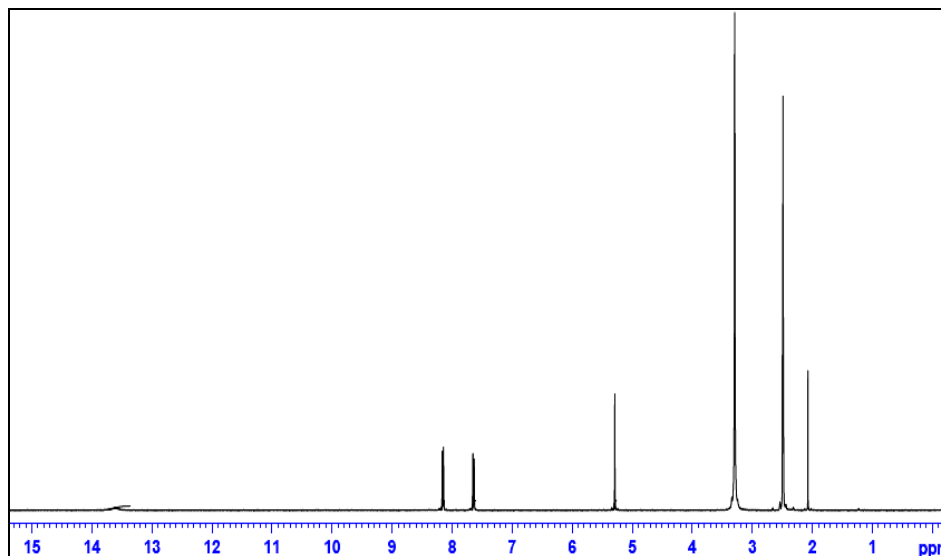
Figure 3.33 ^{1}H NMR spectrum of 3,4-bis[(4-nitrobenzyl)oxy] thiophene-2,5-dicarboxylic acid **(3e)**

Further, FTIR spectrum (**Figure 3.34**) of precursor polymer, i.e. polyhydrazide **6g,** showed a peak at 3218 cm^{-1} that corresponds to –NH of amide and also a sharp peak appeared at 1630 cm^{-1} that shows the presence of carbonyl group.
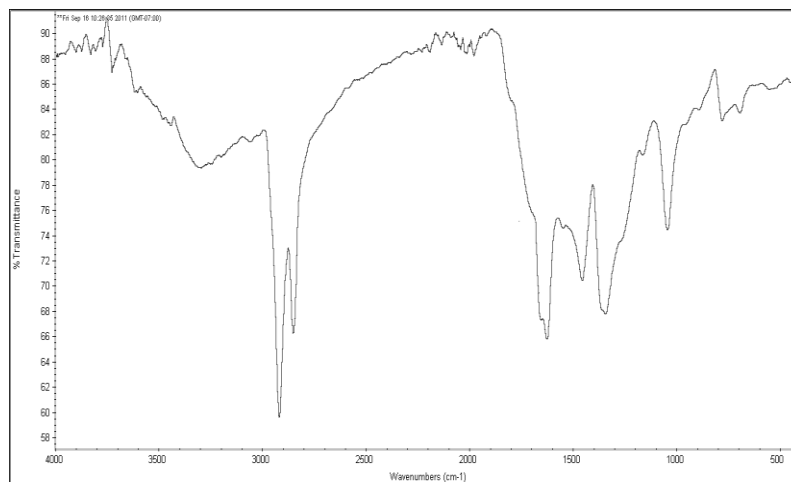
Figure 3.34 FTIR spectrum of polyhydrazide **6g**

The cyclization of polyhydrazide **6g** to get target polymer **P7** was established by FTIR and ^{1}H NMR spectral data. The disappearance of peaks due to amide and carbonyl stretching frequencies and appearance of a new peak at 1580 cm^{-1} due to C=N group in

FTIR spectrum (**Figure 3.35**) of **P7** clearly indicated the formation of 1,3,4-oxadiazole ring.
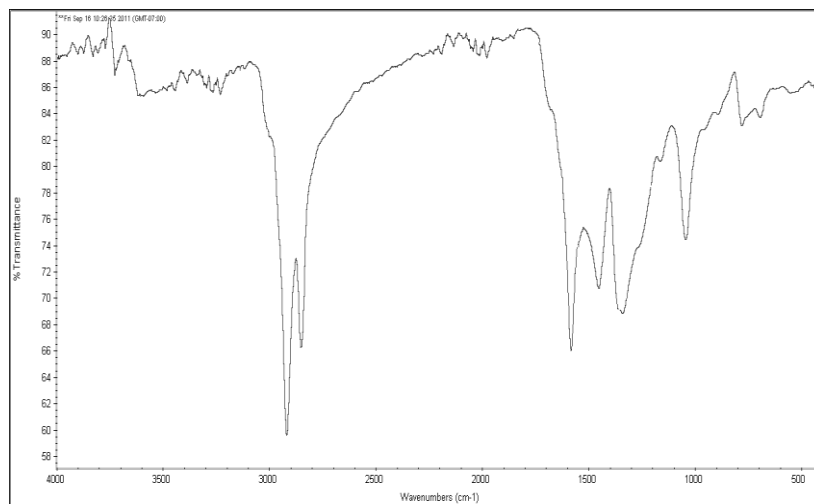
Figure 3.35 FTIR spectrum of polymer **P7**

Further, ^{1}H NMR spectrum (**Figure 3.36**) of precursor polyhydrazide **6g** displayed peaks of amide protons at 10.18 ppm and 10.07 ppm and aromatic protons resonated as multiplets at 7.25–7.13 ppm. It also showed a singlet at 5.04 ppm due to presence of –OCH$_2$ attached to phenyl moiety. As expected, a singlet for –OCH$_2$ of compound **6i** appeared at downfield due to the desheilding effect of nitro group on benzyl ring. Further, ^{1}H NMR spectrum (**Figure 3.37**) of **P7** showed no peaks due to amide group in the region of 10 ppm confirming the cyclization.
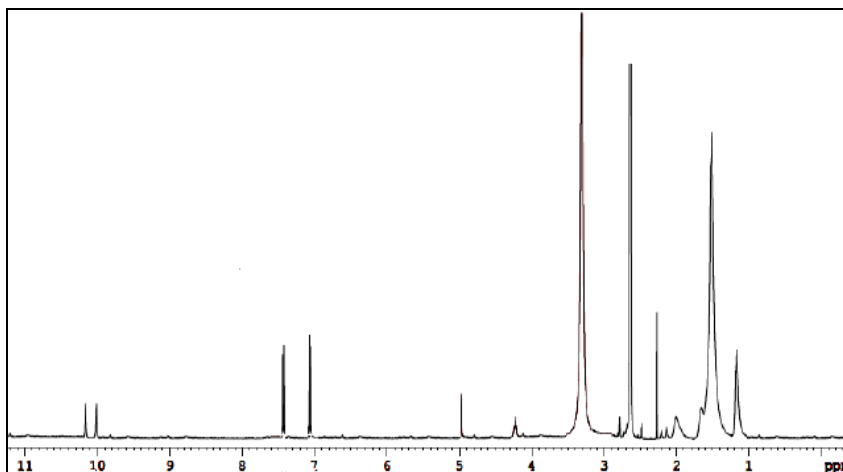
Figure 3.36 ^{1}H NMR spectrum of polyhydrazide **P6g**
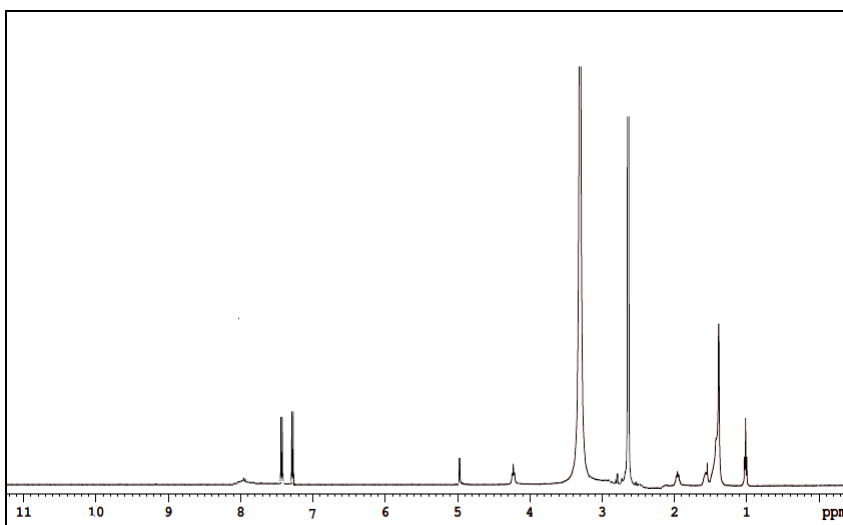
Figure 3.37 ^{1}H NMR spectrum of polymer **P7**

The average molecular weight of polymers was determined to be to be 6286 g/mol, 7146 g/mol and 3781 g/mol, with PDI 1,89, 1.27 and 2.1, respectively. The solubility of polymers is good in organic solvents such as chloroform, toluene and chlorobenzene at room temperature. The results of TGA of the polymers **P7–P9** revealed that the onset decomposition temperature of the polymer under nitrogen was about 300 °C as shown in **Figure 3.38**. From the trace it is clear that the polymer is thermally stable up to about 300 °C. The decrease in the mass of polymers from 50 $^{\circ}$C to 300 $^{\circ}$C continuously is attributed to the loss of the alkoxy side chain and the amount of this

weight loss was found to increase with pendant chain length further. The second weight loss step, which took place in the temperature range of 300–500 ^{o}C corresponds to the degradation of polymer backbone leaving behind a residue.
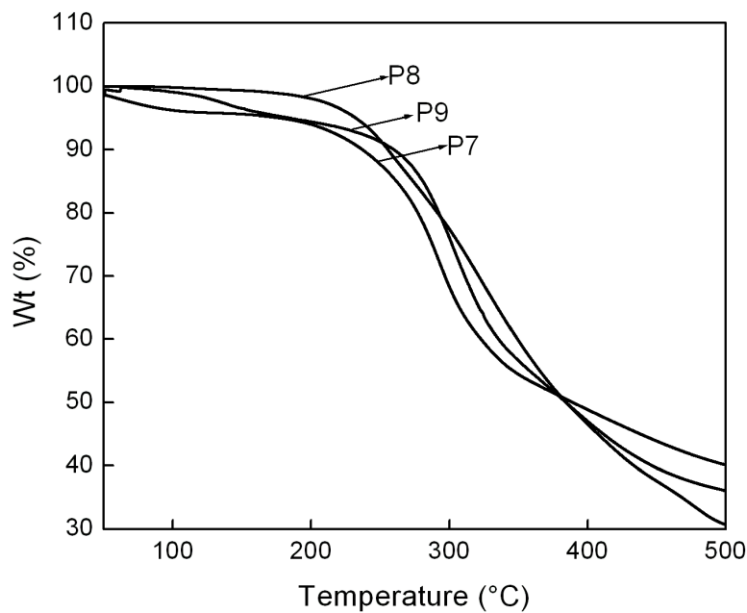
Figure 3.38 Thermogravimetric traces of polymers **P7–P9**

3.6 POLYMERS CARRYING 3,4-BIS [(4-DECYLOXY-3-METHOXYBENZYL)OXY] THIOPHENE, 1,3,4-OXADIAZOLE AND DIFFERENT AROMATIC SPACERS (P10–16), SERIES–4

We prepared seven new D-A type conjugated polymers of Series–4 carrying 3,4-disubstituted thiophene and 1,3,4-oxadiazole moiety with different spacer groups through multistep reactions. Further, the structure of new intermediates, monomers and polymers were characterized using different spectroscopic techniques. The synthetic route towards the preparation of new intermediates and monomers is given in **Scheme 3.4** and finally polymerization of monomers to **P10–P16** is outlined in **Scheme 3.5**.

3.6.1 Chemistry

The alkylated vanillin **8**, obtained from vanillin was reduced to corresponding alcohol **9** using sodium borohydride. The resulting alcohol was then bromomethylated using phosphorous tribromide. The compound **10** was then condensed with diethyl 3,4-dihydroxythiophene-2,5-dicarboxylate (**1**) to yield diethyl 3,4-bis[4-(decyloxy)-3-

methoxybenzyloxy]thiophene-2,5-dicarboxylate (**11**), which was then converted to corresponding bishydrazide **7** using hydrazine hydrate. Further, the bishydrazide **12** was condensed with different substituted diacid chlorides, viz. benezene-1,4-dicarbonyl dichloride (**14a**), thiophene-2,5-dicarbonyl dichloride (**14b**), pyridine-2,6-dicarbonyl dichloride (**14c**), phenylenevinylene-1,4-dicarbonyl dichloride (**14d**), 2,3-dihydrothieno [3,4-b][1,4]dioxine-5,7-dicarbonyl dichloride (**14e**), naphthalene-2,6-dicarbonyl dichloride (**14f**) and biphenyl-4,4'-dicarbonyl dichloride (**14g**), in presence of lithium chloride and pyridine to get corresponding polyhydrazides **15a–g** in good yield. Finally these precursors were subjected to cyclodehydration with phosphorous oxychloride to obtain the target polymers **P10–P16** of Series-4.

3.6.2 Experimental procedure

The experimental protocol for the synthesis of monomers bishydrazide 7, diacid chlorides **14a–f** including their intermediates and polymer precursors **14a–g** and final polymers **P10–P16** is described as follows.

3.6.2.1 Synthesis of intermediates and monomers

The procedure for the synthesis of required intermediates and monomers are given in the following section.

3.6.2.1.1 Synthesis of 4-decyloxy-3-methoxybenzaldehyde (8)

To a mixture of 4-hydroxy-3-methoxybenzaldehyde (1 g, 6 mmol) and potassium carbonate (0.9 g, 1 mmol) in 25 mL of DMF 1-bromodecane (1.3 g, 1 mmol) was added drop-wise. The reaction mixture was stirred at 60 °C. After completion of the reaction, the reaction mixture was poured into water and the product was extracted twice using 20 ml of diethyl ether. The organic layer was dried over sodium sulphate and solvent was removed under reduced pressure to yield the white semi-solid crystalline product.
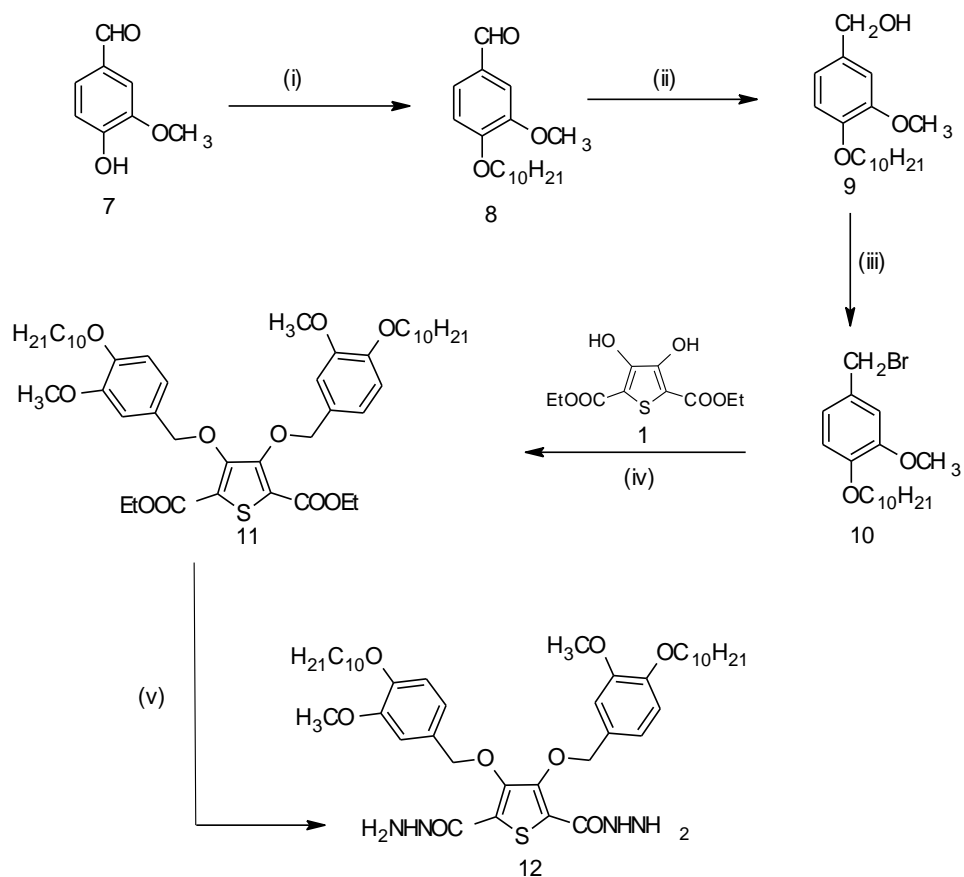
(i) $C_{10}H_{21}Br$, DMF, K_2CO_3 (ii) $NaBH_4$, MeOH (iii) PBr_3, DEE (iv) DMF, K_2CO_3 (v) C_2H_5OH, $NH_2NH_2 \cdot 2H_2O$

Scheme 3.4 (a) Synthesis of monomer of Series-4
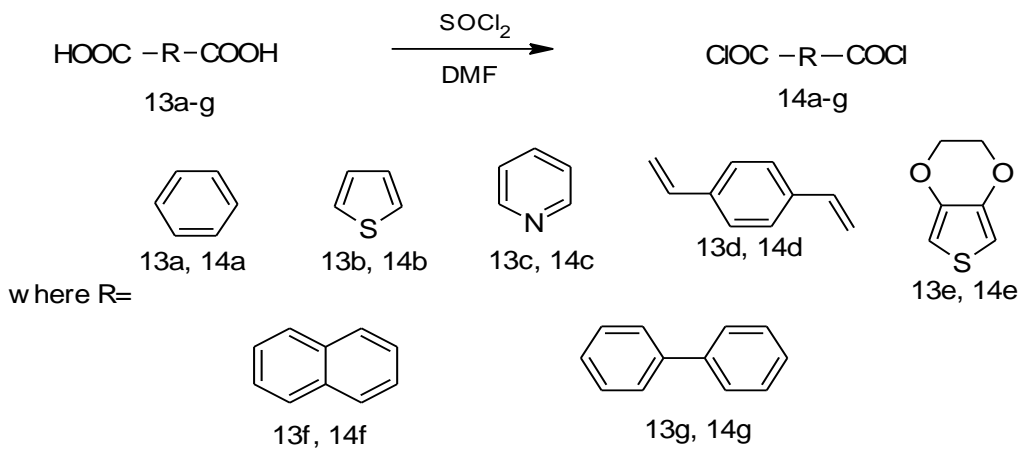
Scheme 3.4 (b) Synthesis of monomers of Series-4
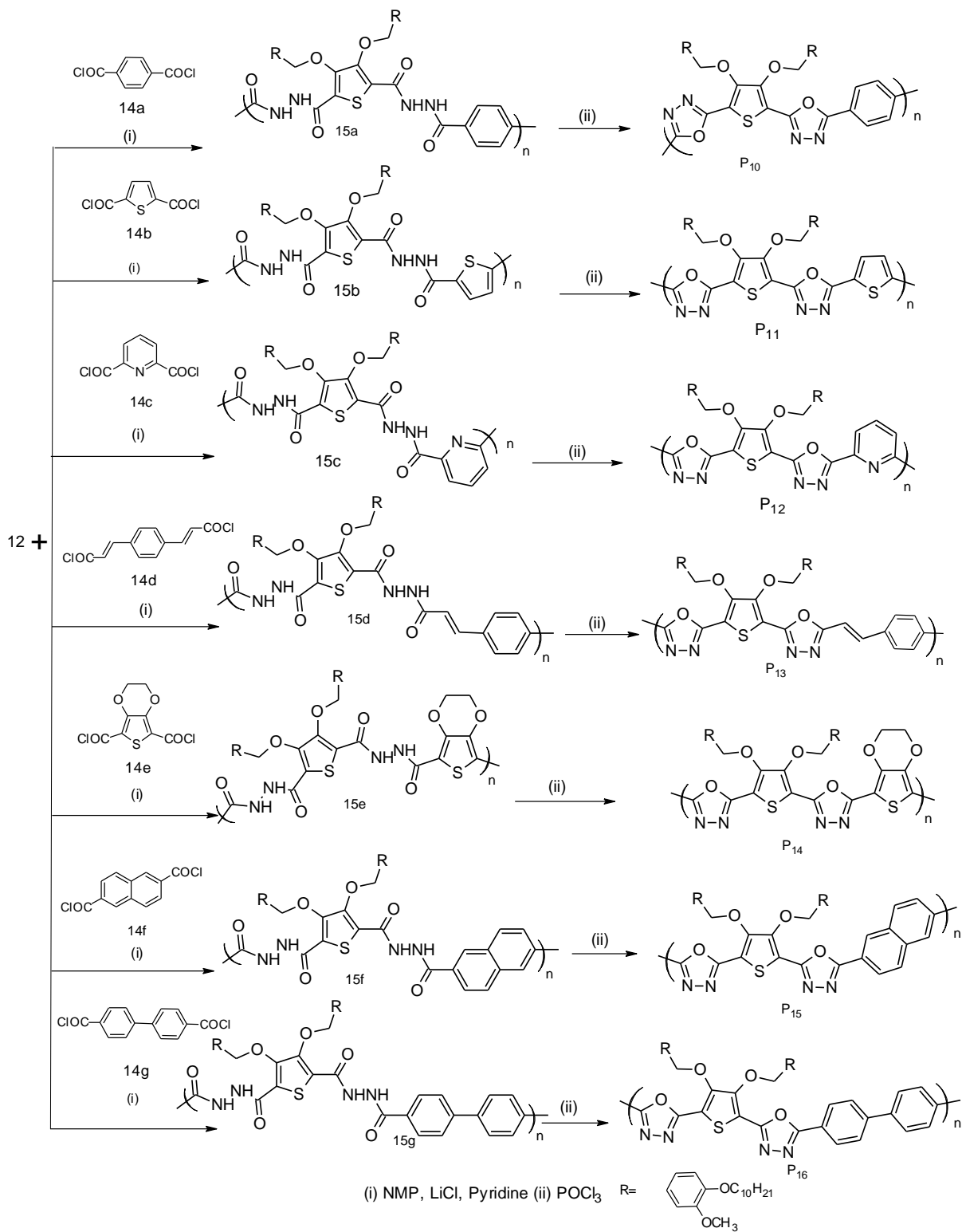
Scheme 3.5 Synthesis of polymers **P10–P16** of Series-4

The characterization data of 4-decyloxy-3-methoxybenzaldehyde (**8**) is as follows.

Mp: 60–61 °C. Yield: 91 %. FTIR (KBr, υ, cm^{-1}): 2916, 2849(–CH), 1679(–C=O), 1583, 1458, 1128. ^{1}H NMR (DMSO–d^6, δ ppm): 9.79 (s, 2H, –CHO), 7.50–7.11 (m, 3H, Ar), 4. 04 (t, 2H, –OCH$_2$–alkyl, J=6.8 Hz), 3.79 (s, 3H, –OCH$_3$), 1.73–1.21 (m, 16H, aliphatic), 0.83 (t, 3H, –CH$_3$, J=6.4 Hz). Element. Anal. Calcd. for C$_{18}$H$_{28}$O$_3$: C, 73.93%; H, 9.65%; Found: C, 73.90%; H, 9.59%.

3.6.2.1.2 Synthesis of (4-decyloxy-3-methoxyphenyl)methanol (9)

To a solution of 3.42 mmol (1 g) of 4-decyloxy-3-methoxybenzaldehyde (**2**) in 15 mL methanol, sodium borohydride (0.03 g, 0.85 mmol) was added pinch-wise during 15 min with stirring. After the complete addition of sodium borohydride, the reaction mixture was stirred at room temperature for 2 h. Then, the solvent was removed under reduced pressure; to this 20 mL of cold water was added and the product was extracted using 15 mL of diethyl ether twice. The organic layer was dried over sodium sulphate and then distilled under pressure to get white solid product, which was recrystalized using ethyl acetate.

Mp: 53–55 °C. Yield: 86 %. FTIR (KBr, υ, cm^{-1}): 3349, 2915, 2850, 1512, 1458, 1236, 1133, 1024. ^{1}H NMR (DMSO–d^6, δ ppm): 6.87–6.73 (m, 3H, Ar), 4.99 (t, 1H, –OH, J=5.6 Hz), 4.37 (d, 2H, Ar–CH$_2$, J=5.6 Hz), 3.7 (s, 3H, OCH$_3$), 1.67–1.21 (m, 16H, aliphatic), 0.83 (t, 3H, –CH$_3$, J=6.8 Hz). Element. Anal. Calcd. for C$_{18}$H$_{30}$O$_3$: C, 73.43%; H, 10.27%; Found: C, 73.38%; H, 10.12%.

3.6.2.1.3 Synthesis of 4-(bromomethyl)-1-ethoxy-2-methoxybenzene (10)

The compound **9** (1 g, 3.40 mmol) was dissolved in diethyl ether (25 mL); to this 0.3 mL of phosphorous tribromide (1 mmol) was added drop-wise and kept for stirring at 20 °C for 5 h. After completion of the reaction, the reaction mixture was poured into water and the ether layer was separated, dried over sodium sulphate and solvent was evaporated under reduced pressure to obtain white puffy solid. The product obtained was recrystalized using ethyl acetate. FTIR (KBr, υ, cm^{-1}): 2915, 2850, 1511, 1458, 1254, 1087.

3.6.2.1.4 Synthesis of diethyl 3,4-bis(4-(decyloxy)-3-methoxybenzyloxy)thiophene-2,5-dicarboxylate (11)

To a mixture of diethyl 3,4-dihydroxythiophene diester **1** (1 g, 3.84 mmol) and potassium carbonate (1.16 g, 8.46 mmol) in DMF, solution of bromomethyl derivative **10** in DMF (10 mL) was added drop-wise with stirring. The reaction mixture was refluxed for 8 h at 60 °C. After completion of the reaction, it was poured into water to get creamish white solid. The product was recrystalized from ethyl acetate to get white crystalline solid.

Mp: 70–73 °C. Yield: 73 %. FTIR (KBr, υ, cm^{-1}): 2914, 2848, 1711, 1467, 1234, 1143, 1040. ^{1}H NMR (DMSO–d^{6,} δ ppm): 6.97–6.83 (m, 6H, Ar), 5.06 (s, 2H, –OCH$_2$), 4.30 (q, 2H, –CH$_2$, J=7.2 Hz), 3.92 (t, 3H, –CH$_3$, J=6.4 Hz), 3.65 (s, 3H, –OCH$_3$), 1.70–1.23 (m, 32H, aliphatic), 0.86 (t, 3H, –CH$_3$, J=6.8 Hz). Element. Anal. Calcd. for C$_{46}$H$_{68}$O$_{10}$S: C, 67.95%; H, 8.43%; S, 3.94%; Found: C, 67.91%; H, 8.33%; S, 3.78%.

3.6.2.1.5 Synthesis of 3,4-bis(4-(decyloxy)-3-methoxybenzyloxy)thiophene-2,5-dicarbohydrazide (12)

One gram (1.23 mmol) of diester (**11**) was added to a solution of 0.30 mL (6.15 mmol) of hydrazine hydrate in 25 mL of ethanol. The reaction mixture was refluxed for 5 h. Upon cooling, white precipitate was obtained. The product was then filtered, washed with alcohol and dried to get white solid. The product was recrystalized using chloroform.

MP: 133–135 °C. Yield: 76 %. FTIR (KBr, υ, cm^{-1}): 3386, 3325, 2919, 2857, 1664, 1513, 1466, 1306, 1247, 1137, 1025. ^{1}H NMR (DMSO–d^{6,} δ ppm): 8.80 (s, 2H, –NH$_2$), 7.01–6.77 (m, 6H, Ar), 5.14 (s, 4H, –OCH$_2$), 4.54 (s, 1H,–NH–), 3.93 (t, 3H, –CH$_3$, J=6.4 Hz) , 3.68 (s, 3H, –OCH$_3$), 1.69–1.24 (m, 32H, aliphatic), 0.86 (t, 3H, –CH$_3$, J=6.8 Hz). Element. Anal. Calcd. for C$_{42}$H$_{64}$N$_4$O$_8$S: C, 64.26%; H, 8.22%; N, 7.14%; S, 4.08%; Found: C, 64.12%; H, 8.02%; N, 6.98%, S, 3.89%.

3.6.2.1.6 General procedure for the synthesis of diacid chlorides 14a–g

A mixture of 3 mmol of diacid **13a–g** (**13a:** benezene-1,4-dicarboxylic acid, **13b:**thiophene-2,5-dicarboxylic acid, **13c:** pyridine-2,6-dicarbonyl dichloride, **13d:**

phenylenevinylene-1,4-dicarboxylic acid, **13e:** 2,3-dihydrothieno [3,4-b][1,4]dioxine-5,7-dicarboxylic acid, **13f:** naphthalene-2,6-dicarboxylic acid, **13g:** biphenyl-4,4'-dicarboxylic acid), excess of thionyl chloride (5 mL) and a drop DMF was refluxed for 5 h. The excess thionyl chloride was removed by distillation under reduced pressure. The residue was washed with methylene dichloride to remove trace amount of thionyl chloride. The acid choride (**14a–g**) was directly used for the next step.

3.6.3 Synthesis of polymers

The synthetic procedures for the preparation of polyhydrazides **14a–g** and their conversion to polymers **P10–P16** are given below.

3.6.3.1 General procedures for the synthesis of polyhydrazides 15a–g

To a stirred solution of 0.5 g of monomer dihydrazide (**7**) in 20 mL N-methylpyrrolidinone (NMP) containing LiCl (1 g) and 1-2 drops of pyridine, another monomer diacid chloride **13a** was added drop-wise. The reaction mixture was then heated to 80 °C and stirred for 6 h. After cooling to room temperature, it was plunged into cold water and the separated precipitate was filtered and washed with ethanol to give corresponding polyhydrazide **15a**. Further polymer was purified by soxhlet extraction technique using ethyl acetate and finally it was dried in vacuum oven at 40 °C. Following similar procedure polyhydrazides **15b–g** were obtained. Characterization data of **15a–g** are given below.

15a: Yield: 61 %. FTIR (KBr, υ, cm^{-1}): 3298 (–NH), 2918, 2851 (–CH), 1621 (–C=O), 1453, 1274, 1021. ^{1}H NMR (DMSO–d^6, δ ppm): 10.94 (s, 1H, –NH), 9.16 (s, 1H, –NH), 7.22–6.98 (m, 6H, Aromatic), 5.71 (s, 4H, –OCH$_2$–Ar), 3.91 (s, 6H, –OCH$_3$), 3.73 (t, 6H, –OCH$_2$–alkyl, J=6.8 Hz), 1.66–1.22 (m, 34H, aliphatic), 0.83 (t, 6H, –CH$_3$, 3H, –CH$_3$, J=6.8 Hz). Element. Anal. Calcd. for C$_{48}$H$_{60}$N$_4$O$_8$S: C, 67.58%; H, 7.09%; N, 6.57%; S, 3.76%. Found: C, 67.73%; H, 7.13%; N, 6.23%; S, 3.29%.

15b: Yield: 60 %. FTIR (KBr, υ, cm^{-1}): 3225 (–NH), 2921, 2852 (–CH), 1622 (–C=O), 1481, 1261, 1024. ^{1}H NMR (DMSO–d^6, δ ppm): 10.65 (s, 1H, –NH), 9.17 (s, 1H, –NH), 8.59–7.66 (m, 6H, Ar), 7.22–6.83 (m, 2H, Th), 5.72 (s, 4H, –OCH$_2$–Ar), 3.93 (t, 4H, –OCH$_2$–alkyl, J=6.4 Hz), 3.75 (s, 6H, –OCH$_3$), 1.68–1.23 (m, 34H, aliphatic), 0.85

(t, 6H, –CH$_3$, 3H, –CH$_3$, *J*=6.8 Hz). Element. Anal. Calcd. for C$_{48}$H$_{64}$N$_4$O$_8$S$_2$: C, 64.84%; H, 7.25%; N, 6.30%; S, 7.21%. Found: C, 64.73%; H, 7.29%; N, 6.25%; S, 7.19%.

15c: Yield: 63 %. FTIR (KBr, υ, cm^{-1}): 3199, 2917, 2850, 1612 (–C=O), 1452, 1250, 1016. ^{1}H NMR (DMSO–d^{6,} δ ppm): 10.78 (s, 1H, –NH), 9.29 (s, 1H, –NH), 8.33– 8.10 (m, 3H, pyridine), 8.01–7.79 (m, 6H, Ar), 5.76 (s, 4H, –OCH$_2$–Ar), 4.04 (t, 4H, – OCH$_2$–alkyl, *J*=6.4 Hz), 3.78 (s, 6H, –OCH$_3$), 1.69–1.26 (m, 34H, aliphatic), 0.86 (t, 6H, –CH$_3$, 3H, –CH$_3$, *J*=6.8 Hz). Element. Anal. Calcd. for C$_{47}$H$_{59}$N$_5$O$_8$S: C, 66.10%; H, 6.96%; N, 8.20%; S, 3.75%. Found: C, 65.93%; H, 6.44%; N, 8.11%; S, 3.29%.

15d: Yield: 69 %. FTIR (KBr, υ, cm^{-1}): 3199 (–NH), 2917, 2850, 1629 (–C=O), 1452, 1250, 1016. ^{1}H NMR (DMSO–d^{6,} δ ppm): 10.62 (s, 1H, –NH), 9.15 (s, 1H, –NH), 7.72–6.78 (m, Ar), 5.71 (s, 4H, –OCH$_2$–Ar), 3.93 (t, 4H, –OCH$_2$–alkyl, *J*=6.8 Hz), 3.75 (s, 6H, –OCH$_3$), 1.68–1.22 (m, 34H, aliphatic), 0.84 (t, 6H, –CH$_3$, y*J*=6.8 Hz). Element. Anal. Calcd. for C$_{50}$H$_{62}$N$_4$O$_8$S: C, 68.31%; H, 7.11%; N, 6.37%; S,3.65%. Found: C, 68.73%; H, 7.19%; N, 6.23%; S, 3.19%.

15e: Yield: 63 %. FTIR (KBr, υ, cm^{-1}): 3298 (–NH), 2918, 2851, 1621 (–C=O), 1453, 1274, 1021. Element. Anal. Calcd. for C$_{49}$H$_{63}$N$_4$O$_{10}$S$_2$: C, 63.13%; H, 6.81%; N, 6.01%; S, 6.88%. Found: C, 62.81%; H, 6.66%; N, 5.98%; S, 6.13%.

15f: Yield: 71 %. FTIR (KBr, υ, cm^{-1}): 3225 (–NH), 2921, 2852, 1632 (–C=O), 1481, 1261, 1024. Element. Anal. Calcd. for C$_{53}$H$_{65}$N$_4$O$_8$S: C, 69.33%; H, 7.14%; N, 6.10%; S, 3.49%. Found: C, 68.13%; H, 7.17%; N, 5.95%; S, 3.08%.

15g: Yield: 67 %. FTIR (KBr, υ, cm^{-1}): 3199 (–NH), 2917, 2850, 1612 (–C=O), 1452, 1250, 1016. Element. Anal. Calcd. for C$_{55}$H$_{67}$N$_4$O$_8$S: C, 69.96%; H, 7.15%; N, 5.93%; S, 3.04%. Found: C, 69.15%; H, 08.%; N, 8.79%; S, 2.81%.

3.6.3.2 General procedure for the synthesis of polymers P10–P16

Polyhydrazide (**15a–g**, 0.3 g) was dispersed in 20 mL of phosphorus oxychloride. The reaction mixture was refluxed for 12 h. After cooling to room temperature, the reaction mixture was poured into ice cold water. The precipitate was collected by filtration and was washed with water, ethanol, followed by ethyl acetate and finally dried under vacuum at 40 °C.

P10: Yield: 86 %. FTIR (KBr, υ, cm⁻¹): 2917, 2850 (–CH), 1581 (–C=N), 1450, 1271, 1031. ^{1}H NMR (DMSO–d^6, δ ppm): 7.69–6.89 (m, 6H, Aromatic), 5.70 (s, 4H, –OCH$_2$–Ar), 3.96 (t, 6H, –OCH$_2$,–alkyl, J=6.4 Hz), 3.86 (s, 6H, –OCH$_3$), 1.66–1.21 (m, 34H, aliphatic), 0.84 (t, 6H, –CH$_3$, J=6.8 Hz). Element. Anal. Calcd. for C$_{49}$H$_{59}$N$_4$O$_6$S: C, 70.73%; H, 7.15%; N, 6.73%; S,3.85%. Found: C, 70.21%; H, 7.21%; N, 6.56%; S,3.61%. Weight average molecular weight ($\overline{\text{M}}_w$): 8121 g/mol, PDI =2.13.

P11: Yield: 86 %. FTIR (KBr, υ, cm⁻¹): 2924, 2854 (–CH), 1597 (–C=N), 1469, 1248, 1021. ^{1}H NMR (DMSO–d^6, δ ppm): 8.15–7.69 (m, 6H, Ar), 7.25–6.99 (m, 2H, Th), 5.72 (s, 4H, –OCH$_2$–Ar), 3.94 (t, 6H, –OCH$_2$,–alkyl, J=6.4 Hz), 3.82 (s, 6H, –OCH$_3$), 1.66–1.22 (m, 34H, aliphatic), 0.85 (t, 6H, –CH$_3$, J=6.8 Hz).). Element. Anal. Calcd. for C$_{47}$H$_{57}$N$_4$O$_6$S$_2$: C, 67.35%; H, 6.86%; N, 6.68%; S, 7.65%. Found: C, 67.73%; H, 6.43%; N, 6.29%; S, 7.07%. Weight average molecular weight ($\overline{\text{M}}_w$) = 8198 g/mol, PDI =2. 32.

P12: Yield: 86 %. FTIR (KBr, υ, cm⁻¹): 2916, 2852 (C–H), 1580 (–C=N), 1449, 1264, 1023. ^{1}H NMR (DMSO–d^6, δ ppm): ^{1}H NMR (DMSO–d^6, δ ppm): 8.21–7.78 (m, 3H, pyridine), 8.13–7.67 (m, 6H, Ar), 5.74 (s, 4H, –OCH$_2$–Ar), 4.05 (t, 4H, –OCH$_2$–alkyl, J=6.4 Hz), 3.79 (s, 6H, –OCH$_3$), 1.68–1.26 (m, 34H, aliphatic), 0.87 (t, 6H, –CH$_3$, 3H, –CH$_3$, J=6.8 Hz). Element. Anal. Calcd. for C$_{49}$H$_{61}$N$_5$O$_8$S: C, 66.87%; H, 6.99%; N,7.96%; S,3.64%. Found: C, 66.61%; H, 6.46%; N, 7.23%; S, 3.09%. Weight average molecular weight ($\overline{\text{M}}_w$) = 6560 g/mol, PDI =1.97.

P13: Yield: 86 %. FTIR (KBr, υ, cm⁻¹): 2917, 2878 (–CH), 1582 (–C=N), 1443, 1264, 1027. ^{1}H NMR (DMSO–d^6, δ ppm): 6.97–7.87 (m, 10H, Ar), 5.71 (s, 4H, –OCH$_2$–Ar), 3.93 (t, 4H, –OCH$_2$–alkyl, 3H, –CH$_3$, J=6.4 Hz), 3.75 (s, 6H, –OCH$_3$), 1.68–1.23 (m, 34H, aliphatic), 0.85 (t, 6H, –CH$_3$, 3H, –CH$_3$, J=6.8 Hz). Element. Anal. Calcd. for C$_{52}$H$_{64}$N$_6$O$_8$S: C, 69.00%; H,7.13%; N,6.19%; S, 3.54%. Found: C, 68.71%; H, 7.18%; N, 5.94%; S, 3.18%. Weight average molecular weight ($\overline{\text{M}}_w$): 8570g/mol, PDI =2.71.

P14: Yield: 86 %. FTIR (KBr, υ, cm⁻¹): 2924, 2854 (–CH), 1597(–C=N), 1469, 1248, 1021. ^{1}H NMR (DMSO–d^6, δ ppm): 7.12–6.98 (m, 6H, Aromatic), 5.70 (s, 4H, –OCH$_2$–Ar), 3.90 (t, 6H, –OCH$_2$–alkyl, 3H, –CH$_3$, J=6.4 Hz), 3.73 (s, 6H, –OCH$_3$), 1.66–1.21 (m, 34H, aliphatic), 0.83 (t, 6H, –CH$_3$, 3H, –CH$_3$, J=6.8 Hz). Element. Anal. Calcd.

for $C_{50}H_{62}N_4O_{10}S_2$: C, 63.67%; H, 6.63%; N, 5.94%; S, 6.80%. Found: C, 63.73%; H, 6.43%; N, 5.23%; S, 6.29%. Weight average molecular weight ($\overline{M}_w$) = 3698 g/mol, PDI =1.26.

P15: Yield: 86 %. FTIR (KBr, υ, cm^{-1}): 2913, 2882 (C–H), 1589 (C=N), 1451, 1271, 1033. ^{1}H NMR (DMSO–d^{6,} δ ppm): 7.64–6.98 (m, 12H, Ar), 5.74 (s, 4H, –OCH$_2$–Ar), 3.92 (t, 4H, –OCH$_2$–alkyl, 3H, –CH$_3$, J=6.4 Hz), 3.76 (s, 6H, –OCH$_3$), 1.67–1.23 (m, 34H, aliphatic), 0.85 (t, 6H, –CH$_3$, 3H, –CH$_3$, J=6.8 Hz). Element. Anal. Calcd. for $C_{54}H_{64}N_4O_8S$: C, 69.80%; H, 6.94%; N, 6.03%; S, 3.45%. Found: C, 69.15%; H, 6.43%; N, 5.83%; S, 3.08%. Weight average molecular weight ($\overline{M}_w$) = 27731 g/mol, PDI =2.33.

P16: Yield: 86 %. FTIR (KBr, υ, cm^{-1}): 2914, 2854 (C–H), 1584 (C=N), 1465, 1269, 1031. ^{1}H NMR (DMSO–d^{6,} δ ppm): 6.99–7.31 (m, 13H, Aromatic), 5.71 (s, 4H, –OCH$_2$–Ar), 3.36 (t, 6H, –OCH$_2$,–alkyl, 3H, –CH$_3$, J=6.4 Hz), 3.88 (s, 6H, –OCH$_3$), 1.66–1.22 (m, 34H, aliphatic), 0.84 (t, 6H, –CH$_3$, 3H, –CH$_3$, J=6.8 Hz). Element. Anal. Calcd. for $C_{56}H_{66}N_4O_8S$: C, 70.41%; H, 6.96%; N, 5.87%; S, 3.36%. Found: C,70.31%; H, 6.54%; N, 5.59%; S, 3.01%. Weight average molecular weight ($\overline{M}_w$) = 15127g/mol, PDI =1.74.

3.6.4 Results and discussion

Structures of newly synthesized intermediates, monomers and final polymers were confirmed by their FTIR, NMR and spectral data, followed by elemental analysis. Formation of compound **8** from 4-hydroxy-3-methoxybenzaldehyde (**7**) was confirmed by its FTIR spectrum (**Figure 3.39**) wherein it showed sharp peaks at 2916 cm^{-1} and 2849 cm^{-1} indicating the presence of alkyl chain, and another sharp peak at 1679 cm^{-1} that corresponds to aldehydic carbonyl group.
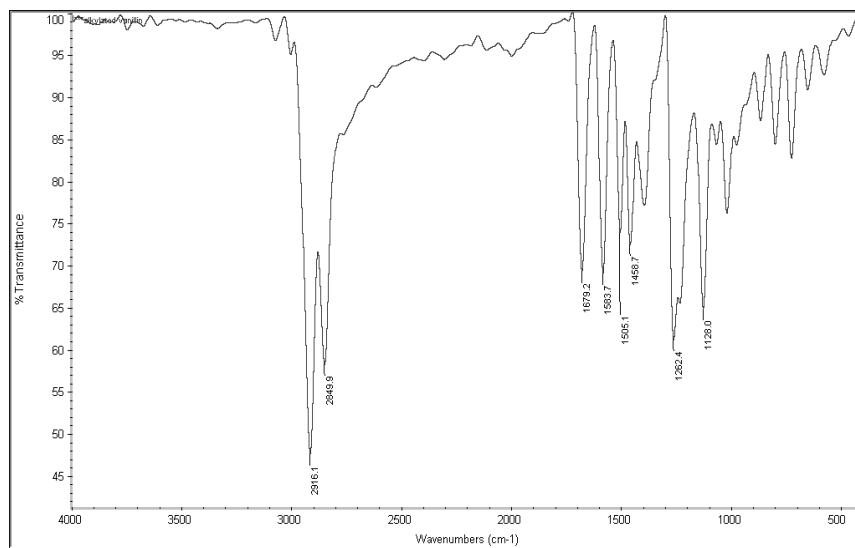
Figure 3.39 FTIR spectrum 4-decyloxy-3-methoxybenzaldehyde **(8)**

Further, its ^{1}H NMR (**Figure 3.40**) spectrum displayed a singlet at 9.79 ppm due to aldehyde proton, multiplet at 7.50–7.11 ppm for aromatic protons, and a triplet at 4.03–4.01 ppm for alkoxy –OCH_2 group. Furhermore, a singlet appeared at 3.79 ppm corresponds to methoxy group attached to benzene ring and peaks at 1.73–1.21 as multiplet and 0.83–0.80 as triplet correspond to alkyl chains and –CH_3 group, respectively.
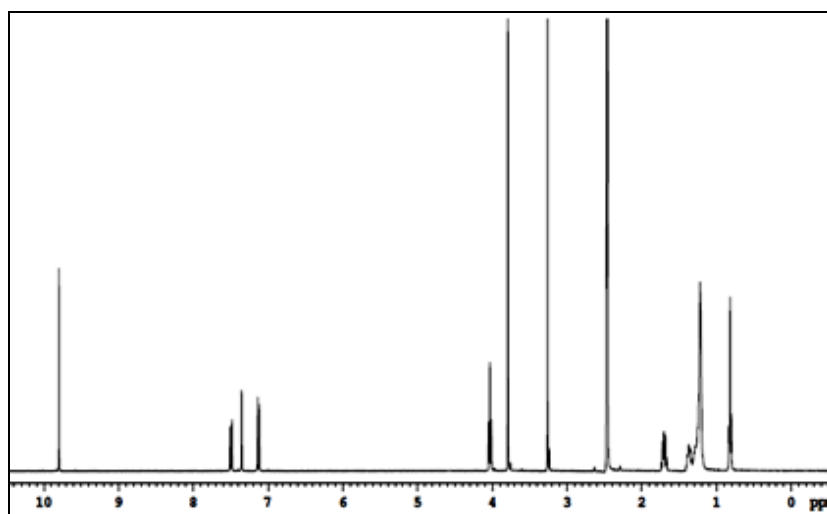
Figure 3.40 ^{1}H NMR spectrum of 4-decyloxy-3-methoxybenzaldehyde **(8)**

The FTIR spectrum (**Figure 3.41**) of compound **9** showed a broad peak at 3349 cm^{-1} and sharp peaks at 2915 and 2860 cm^{-1} correspond to alkyl chain.
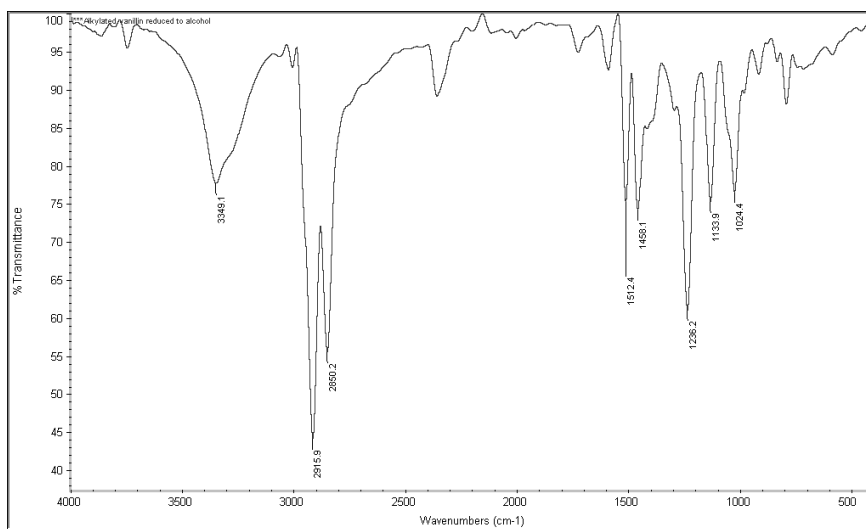
Figure 3.41 FTIR spectrum of (4-decyloxy-3-methoxyphenyl) methanol (**9**)

The **Figure 3.42** show ^{1}H NMR spectrum of (4-decyloxy-3-methoxyphenyl)methanol (**9**) showed multiplet for aromatic protons at 6.87–6.73 ppm, and triplet at 4.99–4.96 ppm that corresponds to –OH group. Further, it displayed peaks at 4.37–4.35 ppm appeared as doublet for –CH$_2$ of benzyl group , a singlet at 3.7 ppm for methoxy attached at meta position, multip1et at 1.67–1.21 ppm for alkyl protons and triplet at 0.80–0.83 ppm that corresponds to methyl group present at the end of alkyl chain. Formation of compound 4-(bromomethyl)-1-ethoxy-2-methoxybenzene (**10**) was confirmed by its FTIR spectrum (**Figure 3.43**), which showed the disappearance of –OH peak at 3349 cm^{-1}.
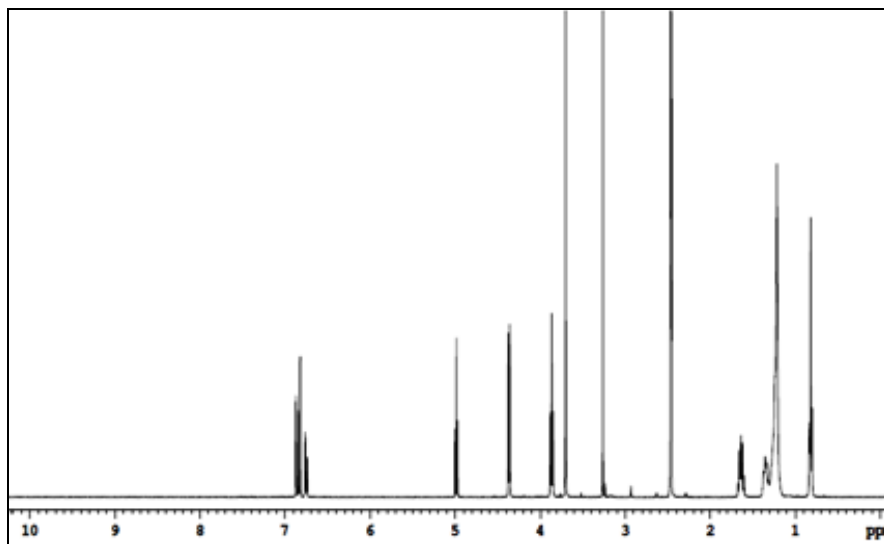
Figure 3.42 ^{1}H NMR spectrum of (4-decyloxy-3-methoxyphenyl)methanol **(9)**
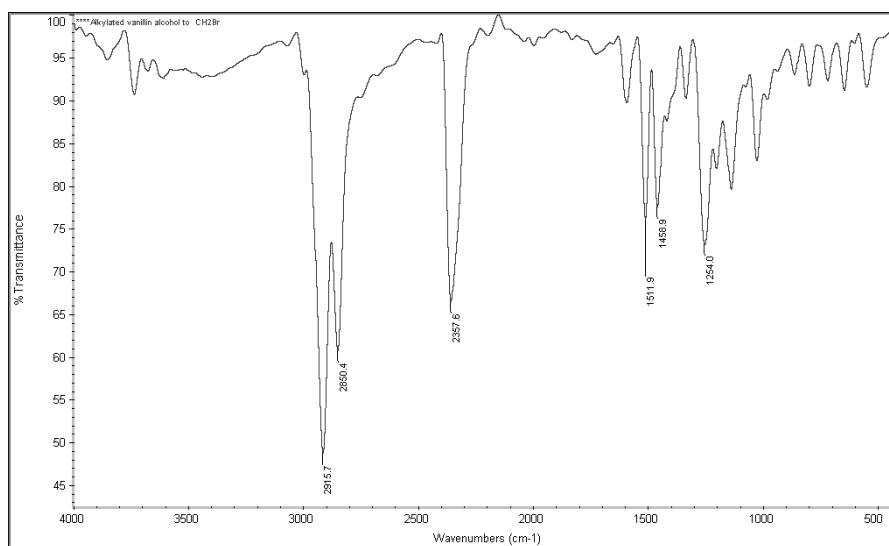
Figure 3.43 FTIR spectrum of 4-(bromomethyl)-1-ethoxy-2-methoxybenzene **(10)**

Further, formation of ester **11** was confirmed by its IR, ^{1}H NMR, ^{13}C NMR spectral data and elemental analysis. Its FTIR spectrum (**Figure 3.44**) showed sharp peaks at 2914 and 2848 cm^{-1} due to –CH stretching and a sharp peak at 1711 cm^{-1} which corresponds to carbonyl group of ester.
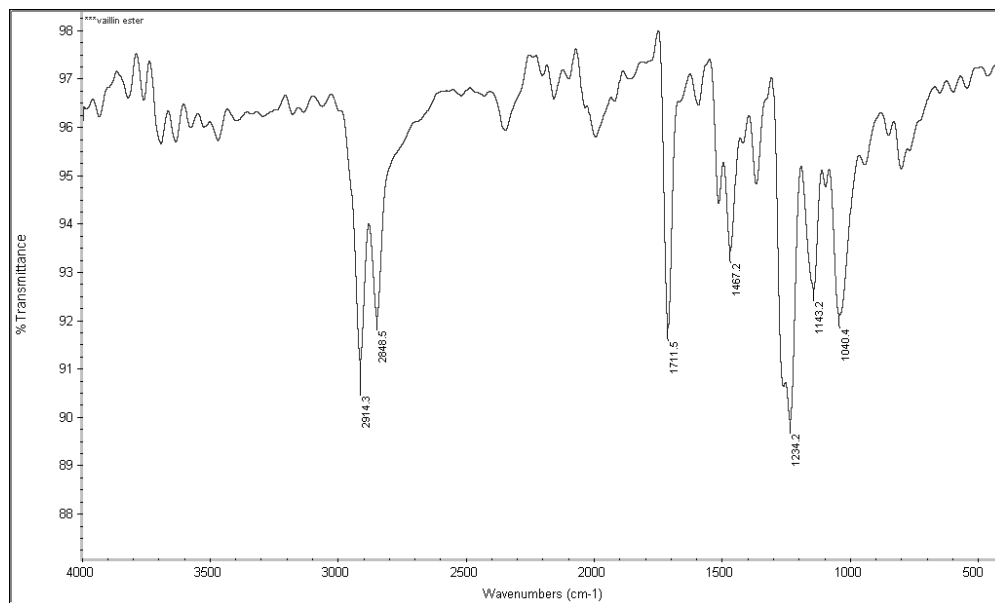
Figure 3.44 FTIR spectrum of diethyl 3,4-bis(4-(decyloxy)-3-methoxybenzyloxy)thiophene-2,5-dicarboxylate **(11)**

Its ^{1}H NMR spectrum (**Figure 3.45**) displayed a multiplet for aromatic protons at 6.97–6.83 ppm, a singlet at 5.06 for –OCH$_2$ of substituted benzyl group, a quatert at 4.30–4.25 ppm for –CH$_2$ and triplet at 3.92–3.89 for –CH$_3$ of ester.   A singlet appeared at 3.65 ppm is attributed to methoxy group attached to benzene. The peaks at 1.70–1.23 ppm as multiplet and 0.86–0.82 ppm as triplet correspond to aliphatic and end methyl group protons, respectively.

Further, ^{13}C NMR spectrum (**Figure 3.46**) of ester **11** showed a series of peaks at 159.85, 152.63, 148.73, 148.26, 128.62, 121.05, 119.20, 112.65, 112.53, 75.84, 68.17, 61.28, 55.33, 31.22, 30.61, 28.93, 28.88, 28.68, 28.61, 25.44, 22.01, 13.94, and 13.86 ppm confirming the presence of carbons of carbonyl, thiophene, benzyl, alkoxy and ester groups.
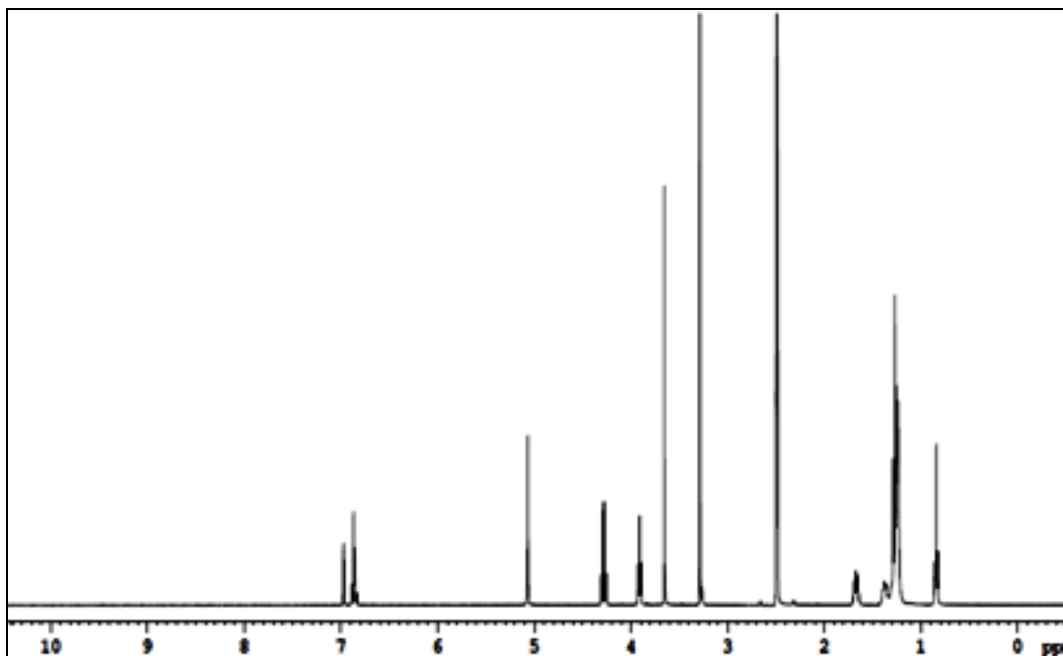
Figure 3.45 ¹H NMR spectrum of diethyl 3,4-bis(4-(decyloxy)-3-methoxybenzyloxy)thiophene-2,5-dicarboxylate **(11)**
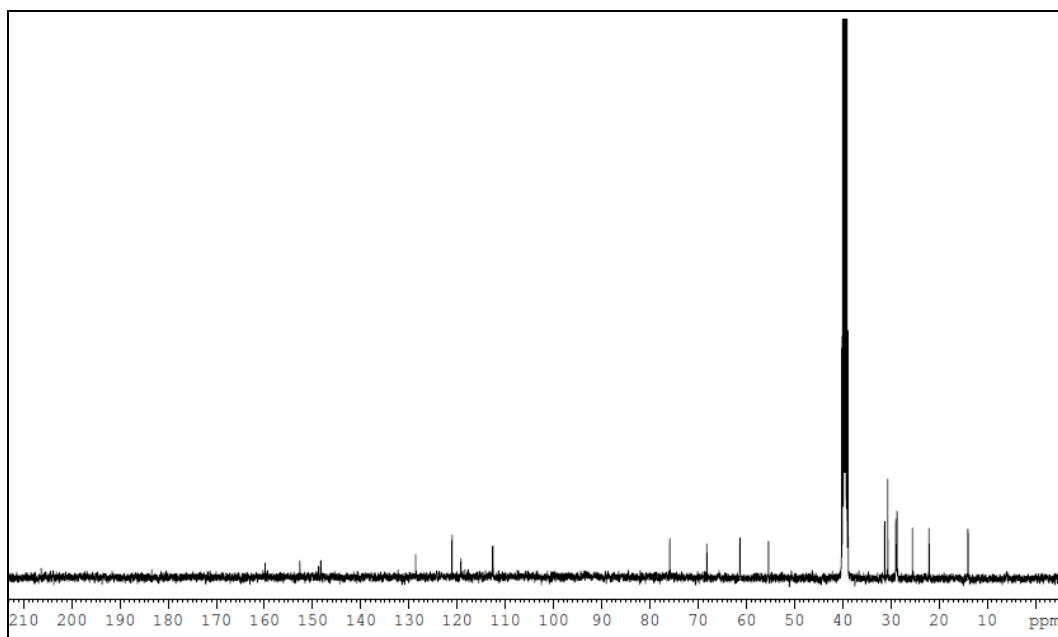
Figure 3.46 ¹³C NMR spectrum of diethyl 3,4-bis(4-(decyloxy)-3-methoxybenzyloxy)thiophene-2,5-dicarboxylate **(11)**

The structure of dihydrazide **12** was confirmed by its FTIR, ^{1}H NMR and elemental analyses. The FTIR spectrum (**Figure 3.47**) showed sharp peaks at 3386 and 3325 cm^{-1} that correspond to –NH and –NH$_2$, and peaks at 2919 and 2857 cm^{-1} due to alkyl –CH stretching. A strong peak appeared at 1664 cm^{-1} implied the presence of carbonyl group of carbonyl hydrazide.
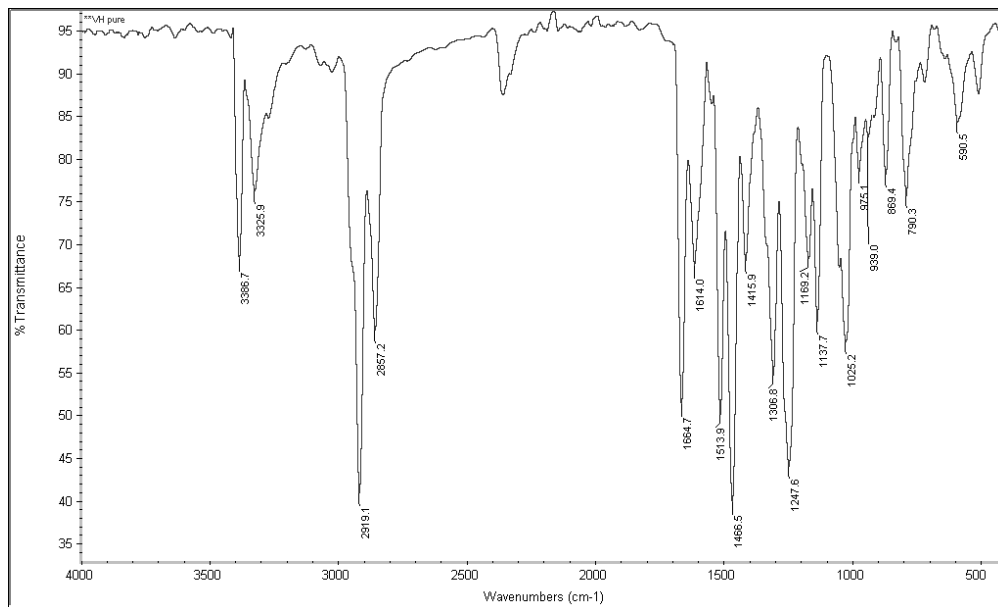
Figure 3.47 FTIR spectrum of 3,4-bis(4-(decyloxy)-3-methoxybenzyloxy)thiophene-2,5-dicarbohydrazide **(12)**

Further, ^{1}H NMR spectrum (**Figure 3.48**) showed broad singlet at 8.80 ppm for – amine protons and multiplet at 7.01–6.77 ppm for aromatic protons. Oxymethylene protons of benzyloxy group appeared at 5.14 ppm as singlet and another proton –NH– resonated as singlet at 4.54 ppm. Alkoxy –OCH$_2$ protons appeared as triplet at 4.30–4.24 ppm while protons of methoxy group attached to benzyl group appeared as a signlet at 4.54 ppm; the peaks at 1.69–1.24 ppm appeared as multiplet for alkyl protons and 0.86–0.82 ppm as triplet for end methyl protons.
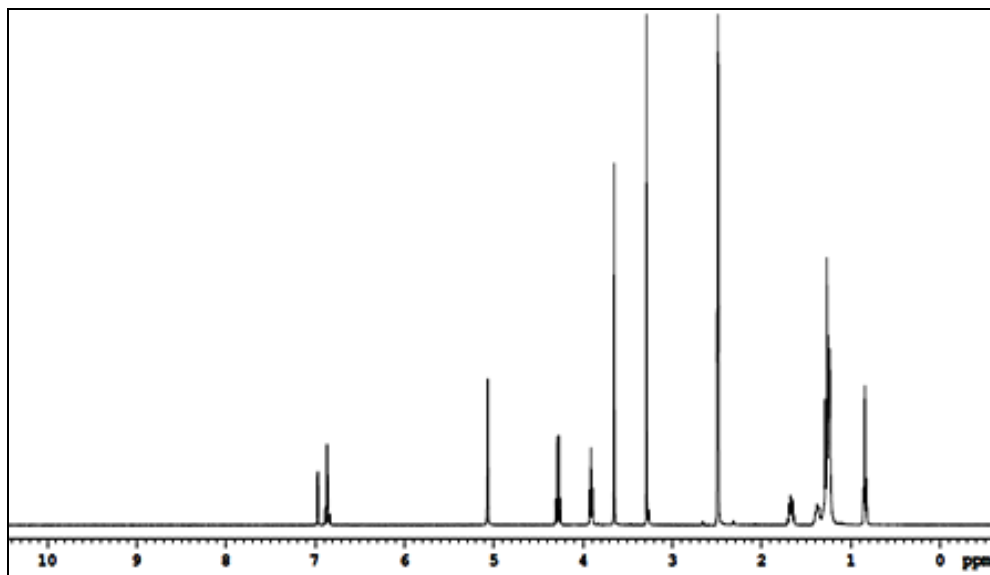
Figure 3.48 ^{1}H NMR spectrum of 3,4-bis(4-(decyloxy)-3-methoxybenzyloxy)thiophene-2,5-dicarbohydrazide **(12)**

The precursor polymer, i.e. polyhydrazide **15a** showed a absorption peak at 3298 cm^{-1} that corresponds to –NH of amide and also a sharp peak appeared at 1621 cm^{-1} that shows the presence of carbonyl group as shown in **Figure 3.49**.
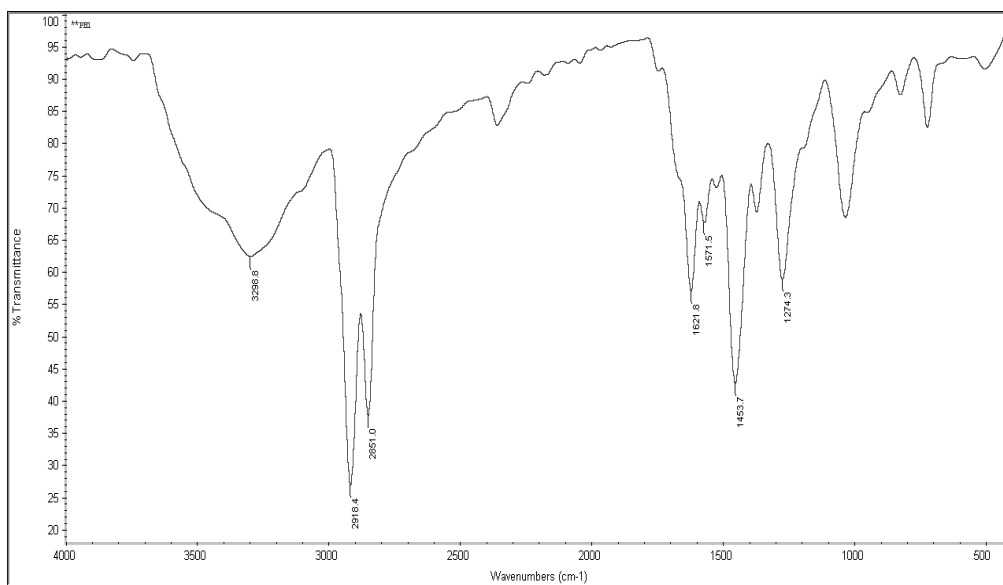
Figure 3.49 FTIR spectrum of polyhydrazide **15a**

The disappearance of peaks in polymer **P10** due to amide and carbonyl stretching frequencies and appearance of a new peak at 1581 cm^{-1} due to –C=N group in FTIR spectrum (**Figure 3.50**) of **P10** clearly indicated the formation of 1,3,4-oxadiazole ring in **P10**.
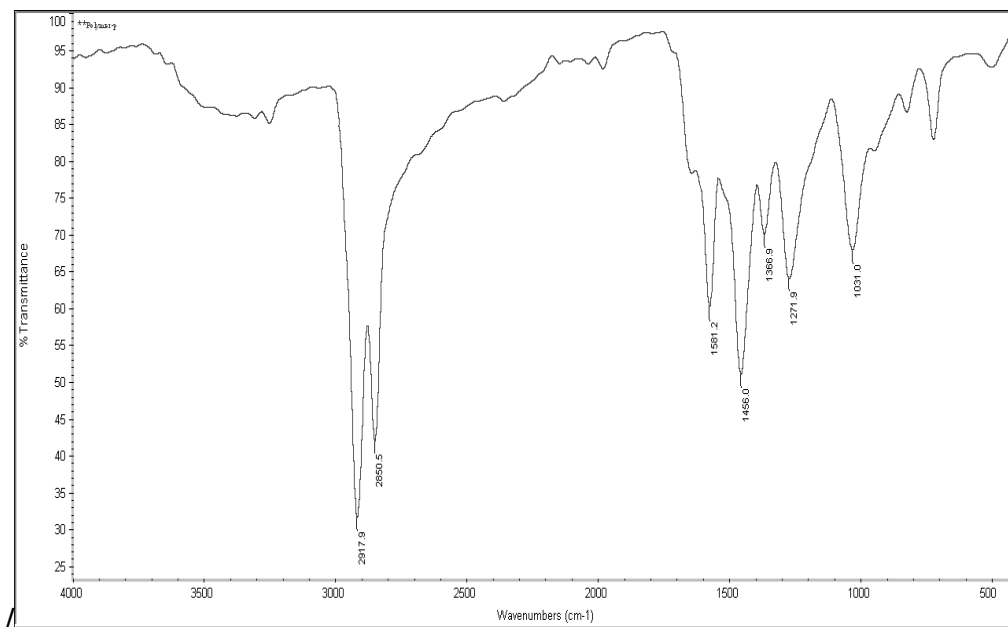
Figure 3.50 FTIR spectrum of polymer **P10**

Further, ^{1}H NMR spectrum (**Figure 3.51**) of polyhydrazide **15a** displayed peaks of amide protons at 10.94 ppm and 9.16 ppm and aromatic protons resonated as multiplets at 7.22–6.98 ppm. It also showed a singlet at 5.71 ppm due to presence of –OCH$_2$ attached to thiophene moiety. A singlet at 3.86 ppm appeared for –OCH$_3$ attached to benzyl ring, and a triplet appeared at 3.73 ppm for –OCH$_2$ of alkyl chain. Furhter, multiplet at 1.66–1.21 ppm and triplet at 0.84 ppm indicated the presence of aliphatic protons of benzyl group attached to 3,4 positions of the thiophene.
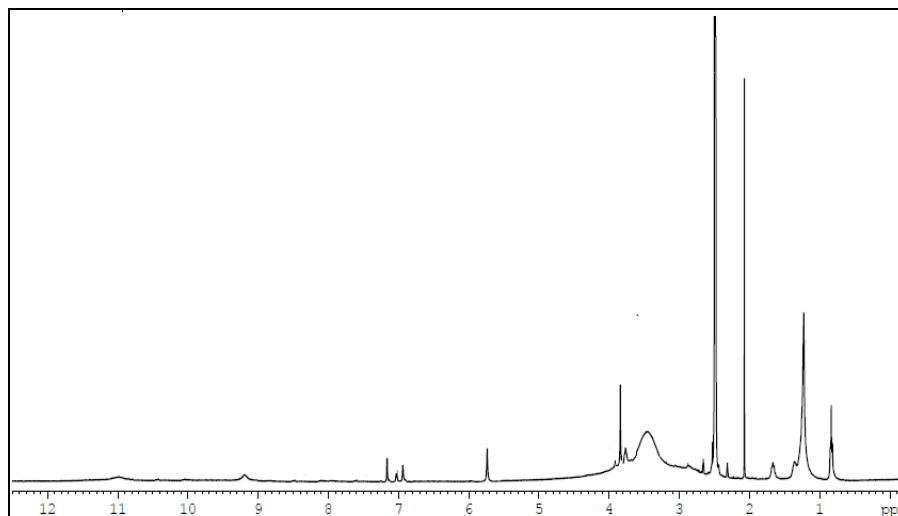
Figure 3.51 ^{1}H NMR spectrum of polyhydrazide **15a**
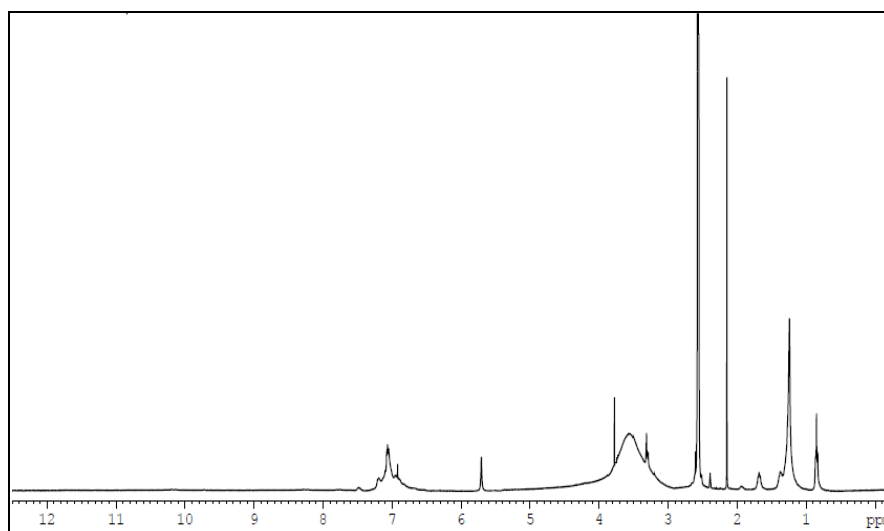
Figure 3.52 ^{1}H NMR spectrum of polymer **P10**

The cyclization of polyhydrazide **15a** to target polymer **P10** was established by its FTIR and ^{1}H NMR spectral data. Further, ^{1}H NMR spectrum (**Figure 3.52**) of **P10** showed no peaks due to amide group in the region of 9–10 ppm confirming the cyclization.

The newly synthesized polymers are soluble in common organic solvents such as chloroform, toluene, and chlorobenzene at room temperature. The $\overline{M}_w$ of the polymers was determined by gel permeation chromatography (GPC) against polystyrene standards

in THF. Their $\overline{M}_w$ values were determined to be 8121 g/mol, 8198 g/mol, and 6560 g/mol, 8570 g/mol, 3698 g/mol, 27731 g/mol and 15127 g/mol, respectively.

The thermogravimetric traces of the polymers **P10–P16** are shown in **Figure 3.52**. It revealed that the onset decomposition temperature of the polymers under nitrogen was 250–300 °C. The initial decrease in the mass of polymers continuously was attributed to the loss of the alkoxy side chain and the amount of this weight loss was found to increase with pendant chain length further. The second weight loss step took place that corresponds to the degradation of polymer backbone leaving behind a residue.
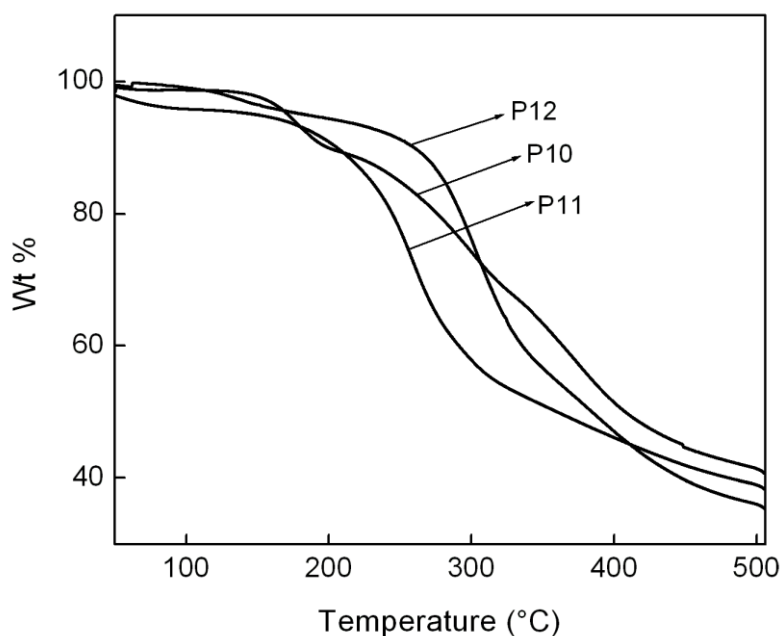
Figure 3.53 Thermogravimetric traces of polymers **P10–P12**

3.7 CONCLUSIONS

In conclusion, we synthesized new monomers, viz. 3,4-bis(benzyloxy)thiophene-2,5-dicarbonyl dichloride (**4a**), 3,4-bis(naphthalene-2-ylmethoxy)thiophene-2,5-dicarbonyl dichloride (**4b**), 3,4-bis[(4-methoxybenzyl)oxy] thiophene-2,5-dicarbonyl dichloride (**4c**), 3,4-bis[(3-methylbenzyl)oxy] thiophene-2,5-dicarbonyl dichloride (**4d**), 3,4-bis[(4-nitrobenzyl)oxy] thiophene-2,5-dicarbonyl dichloride (**4e**) and 3,4-bis(4-(decyloxy)-3-methoxybenzyloxy)thiophene-2,5-dicarbohydrazide (**12**) starting from

diethyl 3,4-dihydroxythiophene-2,5-dicarboxylate and their synthetic procedures were established. Newly synthesized intermediates and monomers were well characterized by different spectral methods and elemental analysis. They were conveniently polymerized to get four new series of polymers **P1–P16**. Their polymerization methods were established. Their structures were confirmed using different spectral techniques and elemental analysis. We successfully introduced different donors, acceptors and various spacer groups in the main chain of polymer to obtain new D-A type conjugated polymers **P1–P16**. The presence of alkoxy chain in all the polymers favored for their solubility. They possess well defined structure and good thermal stability at around 300°C.

Chapter 4

Abstract

This chapter covers the electrochemical studies of newly synthesized D-A type polymers using cyclic voltammetry. It also includes linear optical characterization of polymers using UV-visible and fluorescence spectroscopic methods. Further, it deals with NLO studies of new polymers using Z-scan and DFWM measurement techniques.

4.1 INTRODUCTION

The newly synthesized polymers were subjected to electrochemical and optical studies in order to determine their electrochemical and optical properties. These properties would furnish valuable information regarding the usage of polymers in opto-electronic and photonic devices. In the present work, the electrochemical properties were studied using CV and optical properties were elucidated using UV-visible and fluorescence spectroscopy. Further, their NLO properties were investigated following Z-scan and DFWM techniques. Experiments leading to determination of electrochemical and optical properties of new polymers are given in the following section.

4.2 ELECTROCHEMICAL STUDIES

Investigation of electrochemical properties of new polymers helps in understanding their basic electronic structures, onset redox potentials, HOMO, LUMO energy levels and bandgap. In addition to this, electrochemical data are useful in deciding the polymers for further applications. In order to study these properties CV was used in the present research. This tool is also being used as one of the methods in polymerization to synthesize polymers in thin film form from their monomers.

4.2.1 Cyclic voltammetry (CV)

CV is a very useful electroanalytical technique employed to determine the electrochemical properties of electroactive species. The electrochemical properties include redox potentials, HOMO and LUMO energy levels which are of importance to estimate the bandgap of the material.

The CV instrument consists of a potentiostat with scan capability and a display of current versus potential (voltage). The apparatus consists of three electrode system. The electrodes include a working electrode (glassy carbon), a platinum auxiliary electrode,

and Ag/AgCl reference electrode. The Ag/AgCl reference electrode requires initial calibration using the previously prepared ferrocene internal standard (Pommerche et al. 1995). The electrochemical cell-top contains four holes. One for each of the electrodes and one for introducing atmosphere gas (typically used for deoxygenation by bubbling a stream of nitrogen prior to measurement). Nitrogen should be passed through the solution 10 minutes before any measurement is made. After bubbling nitrogen through the solution the tip of the deoxygenation tube should be raised above the surface of the liquid and a flow of nitrogen continued throughout the experiment to maintain inert atmosphere above the solution level. During the course of the CV the solution should remain quiescent and be oxygen free.
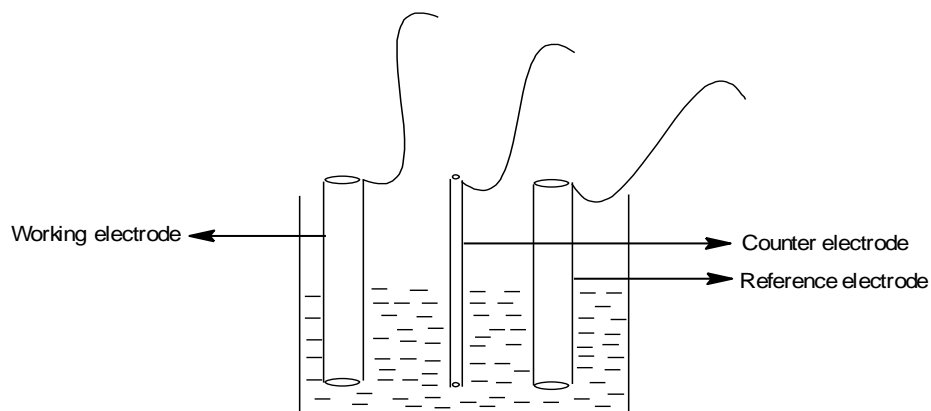
Figure 4.1 Schematic representation of an electrochemical cell

During the experiments, the potential is scanned between two extreme potentials linearly with respect to time. When a negative potential is applied to the electrode, the electrons go from the electrode to the solution and the analyte present in solution is reduced. Similarly, on the return scan, as the working electrode potential becomes more positive and the reverse reaction occurs (electrons goes from solution to the electrode and the analyte is oxidized). By convention, the cathodic currents are positive and anodic currents are negative.

4.2.2 Materials, instrumentation and measurement methods

Dimethylformamide (DMF), chloroform, acetonitrile and tertiary butyl ammonium perclorate (TBAP) were purchased commercially from Lanchaster (UK) and

used as received. The electrochemical studies of the polymers were carried out using AUTOLAB PGSTAT30 electrochemical analyzer. Cyclic voltammograms were recorded using a three electrode cell system, with glassy carbon button as working electrode, a platinum wire as counter electrode and an Ag/AgCl electrode as the reference electrode. Thin films of polymers were prepared on dissolving the polymer in a suitable solvent and dried over the glassy carbon button. The ferrocene/ferrocenium oxidation couple was used as an internal calibration with all potentials adjusted to the Ag/AgCl scale.

Experiments were conducted in nitrogen purged, oxygen and water free environment. The nitrogen is purged due to the instability of the polymers in reduced form. During the cyclic scan over full potential range, polymers undergo rapid degradation; so the oxidation and reduction processes were carried out separately. The electrochemical reduction behavior of the polymers was studied in the potential range 0 to -2.5 eV, whereas the oxidation cyclic voltammograms were recorded by sweeping the potential in the range 0 to +2.5 eV. The onset oxidation and reduction potentials were used for the determination of HOMO and LUMO energy levels of the polymers.

4.2.3 Results and discussion

The results of electrochemical properties of newly synthesized polymers **P1-P16** are tabulated in **Table 4.1** (Series-1), **Table 4.2** (Series-2), **Table 4.3** (Series-3) and **Table 4.4** (Series-4). Their results are discussed as follows.

Polymers P1-P3 (Series-1)

The cyclic voltammograms of polymers **P1-P3** displayed distinct oxidation and reduction processes as shown in **Figures 4.2 (a) and 4.2 (b)**. In the reduction sweep, the polymers **P1-P3** showed reduction peak at -1.18, -1.27 and -1.26 eV, respectively. These reduction potentials are lower than that of 2-(4-tert-butylphenyl)-1,3,4-oxadiazole (PBD) (Strukelj et al. 1995 and Janietz et al. 1997), one of the most widely used electron transporting materials. In the anodic sweep, polymers **P1-P3** showed small oxidation peak at 1.32, 1.10 and 1.12 eV, respectively. The observed bandgap is more in case of polymer **P1**, due to the presence of long alkoxy chain (tetradecyloxy) when compared to polymers **P2** and **P3**. This is attributed to the steric hindrance caused by lengthy alkoxy

chain, which in turn disrupts the extent of conjugation and influences the HOMO and LUMO energy levels. As a result the increased bad gap was observed for polymer **P1** when compared to **P2** which showed higher bandgap than **P3**. The observed redox values are comparable with those of reported D‑A type polymers containing thiophene and 1,3,4‑oxadiazole moieties (Udayakumar et al. 2006). The onset oxidation and reduction potentials are used to estimate HOMO and LUMO energy levels. The equations,

$E_{LUMO} = -[E_{Onset}^{Red} - 4.4eV]$ and $E_{HOMO} = -[E_{Onset}^{Oxd} + 4.4eV]$ where E_{Onset}^{Red} and E_{Onset}^{Oxd} were used

for the calculations. Here E_{Onset}^{Red} and E_{Onset}^{Oxd} are the onset potentials versus SCE for the oxidation and reduction processes, respectively (de Leeuw et al. 1997). The calculated HOMO, LUMO energy levels and band gap ($^{a}E_g$) of the polymers are tabulated in **Table 4.1.**

Table 4.1 Electrochemical potentials, energy levels and band gap ($^{a}E_g$) of **P1-P3**

Polymer	E_{oxd} (V)	E_{red} (V)	E_{oxd} (onset)	E_{red} (onset)	E_{HOMO} (eV)	E_{LUMO} (eV)	$^{a}E_g$ (eV)
P1	1.32	-1.18	1.12	-1.09	-5.52	-3.31	2.21
P2	1.10	-1.27	1.01	-1.19	-5.41	-3.21	2.20
P3	1.12	-1.26	1.04	-1.14	-5.44	-3.26	2.18
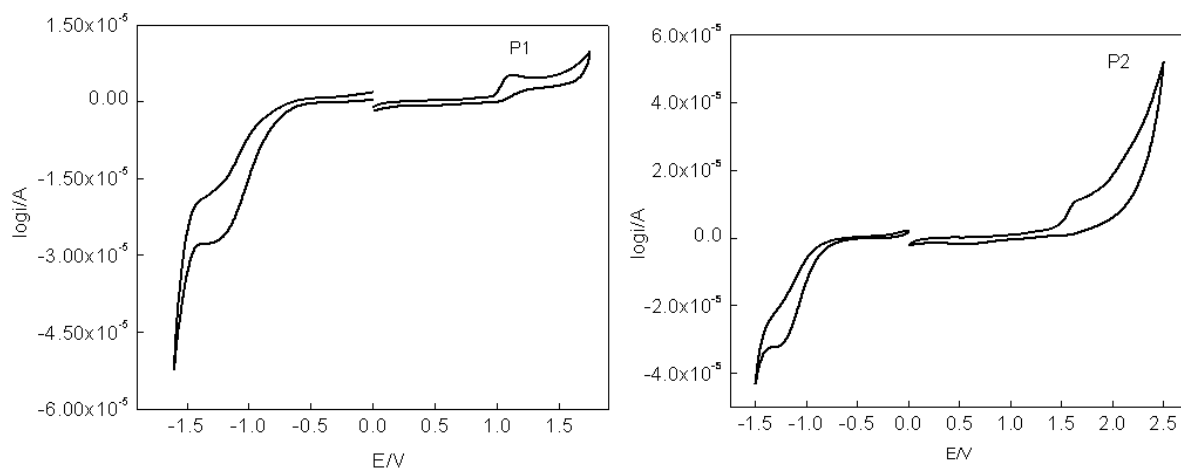
Figure 4.2(a) Cyclic voltammetric waves of **P1** and **P2**
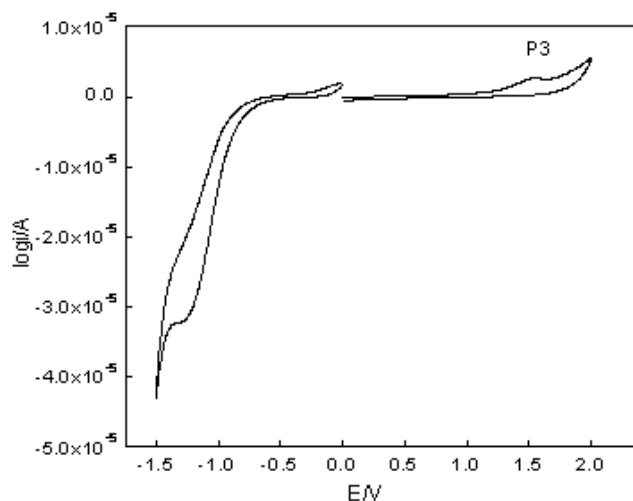
Figure 4.2(b) Cyclic voltammetric waves of **P3**

Polymers P4-P6 (Series-2)

The cyclic voltammetric traces of polymers **P4-P6** are given **Figure 4.3**. These polymers showed similar redox behavior when they are compared with polymers **P1-P3** of Series**-**1. Their electrochemical potentials, energy levels and electrochemical bandgap are listed in **Table 4.2**. In cathodic sweep, polymers **P4-P6** displayed reduction peaks at **-**1.30, **-**1.57 and **-**0.99 eV, respectively. Since these reduction potentials are lower than PBD, they are expected to show good charge carrying ability when they are used in photonic devices. In the anodic sweep, polymers **P4-P6** showed small oxidation peak at 1.23, 1.44 and 1.63 eV, respectively. The variation in alkoxy chain has little effect on bandgap and increased bandgap was observed for polymer **P4** due to the presence of bulky tetradecyloxy group. The bulky alkoxy side chains in polymer would bring about twisting the units out of plane and cause increase in bandgap. However, the higher oxidation potentials compared to PBD indicate that the polymers possess good hole blocking properties within a solid state device.

Table 4.2 Electrochemical potentials, energy levels and band gap of (^aE_g) **P4-P6**

Polymer	E_{oxd} (V)	E_{red} (V)	E_{oxd} (onset)	E_{red} (onset)	E_{HOMO} (eV)	E_{LUMO} (eV)	^aE_g (eV)
P4	1.23	-1.30	1.12	-0.98	-5.52	-3.13	2.39
P5	1.44	-1.57	1.05	-1.32	-5.45	-3.08	2.37
P6	1.63	-0.99	1.49	-0.74	-5.89	-3.66	2.23
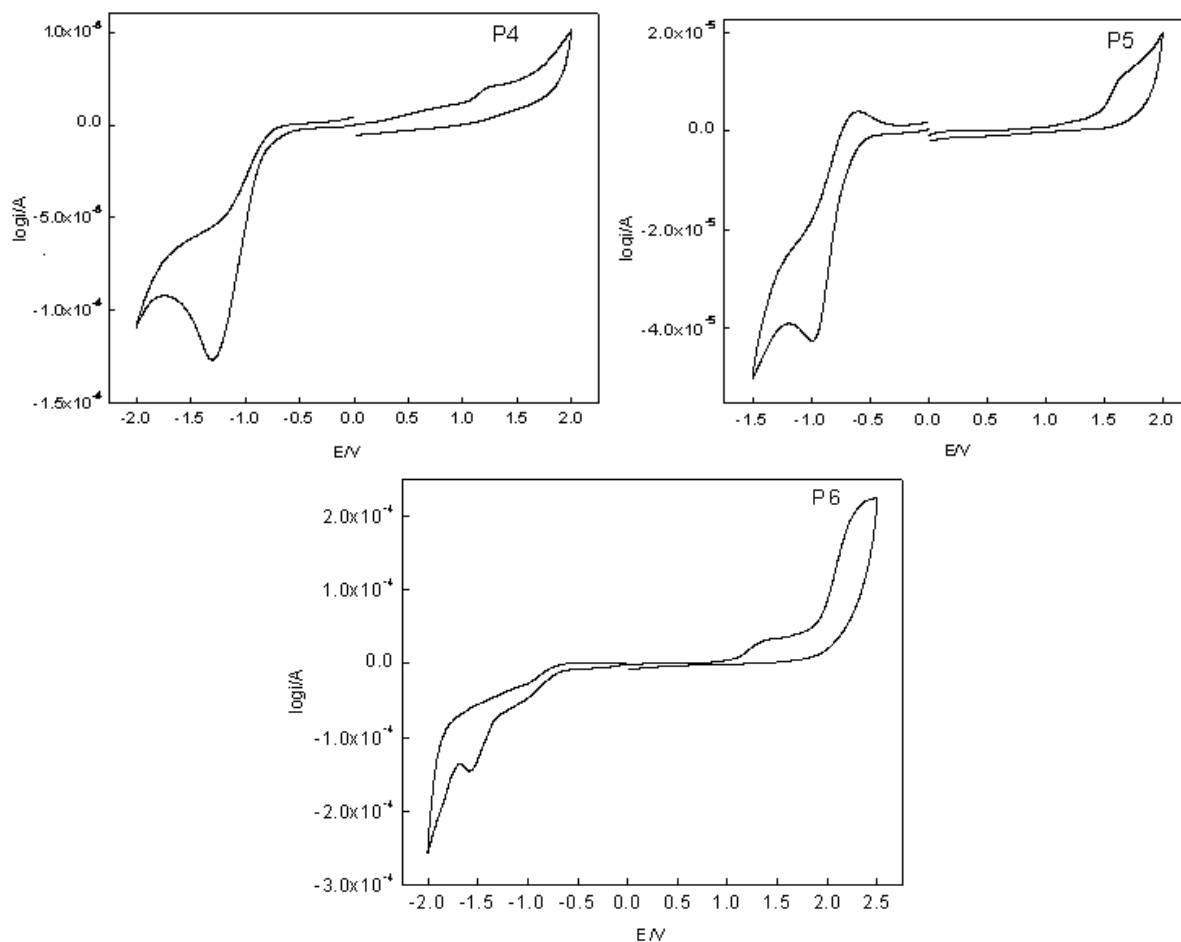
Figure 4.3 Cyclic voltammetric waves of **P4-P6**

Polymers P7-P9 (Series-3)

The cyclic voltammograms of polymers **P7-P9** displayed distinct oxidation and reduction processes as shown in **Figure 4.4**. In the negative bias, they showed reduction

peaks at **-**1.15, **-**1.13 and **-**1.01 eV, respectively. In the anodic sweep, they displayed small oxidation peaks at 1.18, 1.27 and 1.52 eV, respectively. These values are comparable with those of reported D**-**A type polymers containing thiophene and 1,3,4**-**oxadiazole moieties (Udayakumar et al. 2006). The onset oxidation and reduction potentials were used to estimate energy levels of HOMO and LUMO. Their electrochemical potentials, energy levels and bandgap are listed in **Table 4.3.**

Usually band gap of any conjugated polymer is influenced by the extent of its conjugation, solid**-**state ordering, the existence of electron**-**withdrawing and electron donating moieties in the polymer backbone. Also, many other factors such as the nature of (solubilizing) side**-**chains, the conformation of the main chain and its chemical constituents normally influence their bandgap. Consequently, one can tune the electrochemical behavior of any conjugated polymer by varying the above properties. As a rule, presence of electron donating and withdrawing groups causes a partial charge separation along the polymer back bone and hence it lowers the bandgap. It is evident that the effective conjugation length in a polymer can be easily controlled by incorporating proper electron releasing and withdrawing conjugated moieties. The central concept of this route is that the interaction between alternating electron rich donors and electron deficient acceptors will result in a compressed bandgap. Furthermore, by changing the substituents of the polymer, the band gap can be fine tuned. Generally, presence of nitro substituted monomer unit causes decrease in the dispersion of the LUMO level and this phenomenon may well account for the increase in bandgap of such polymers (Van Mullekom et al. 2001). Accordingly, our polymers **P7-P9** carrying 1,3,4**-**oxadiazole as an electron acceptor moiety and 3,4**-**bis[(4-methyl/3methoxybenzyl)oxy] thiophene and 3,4**-**bis(dodecyloxy)thiophene as electron donor units showed reduced band gap, while the polymer **P9** containing 3,4**-**bis[(4-nitrobenzyl)oxy]thiophene as electron donor unit displayed slightly increased band gap. This is due to the little interruption in electron donating tendency of alternating units by the substitution of electron withdrawing **-**NO$_2$ group in polymer **P9**.

Table 4.3 Electrochemical potentials, energy levels and band gap (^aE_g) of **P7-P9**

Polymer	E_{oxd} (V)	E_{red} (V)	E_{oxd} (onset)	E_{red} (onset)	E_{HOMO} (eV)	E_{LUMO} (eV)	^aE_g (eV)
P7	1.18	-1.15	1.12	-0.86	-5.52	-3.54	1.98
P8	1.27	-1.13	1.13	-1.01	-5.53	-3.39	2.14
P9	1.52	-1.01	1.33	-0.85	-5.73	-3.55	2.18
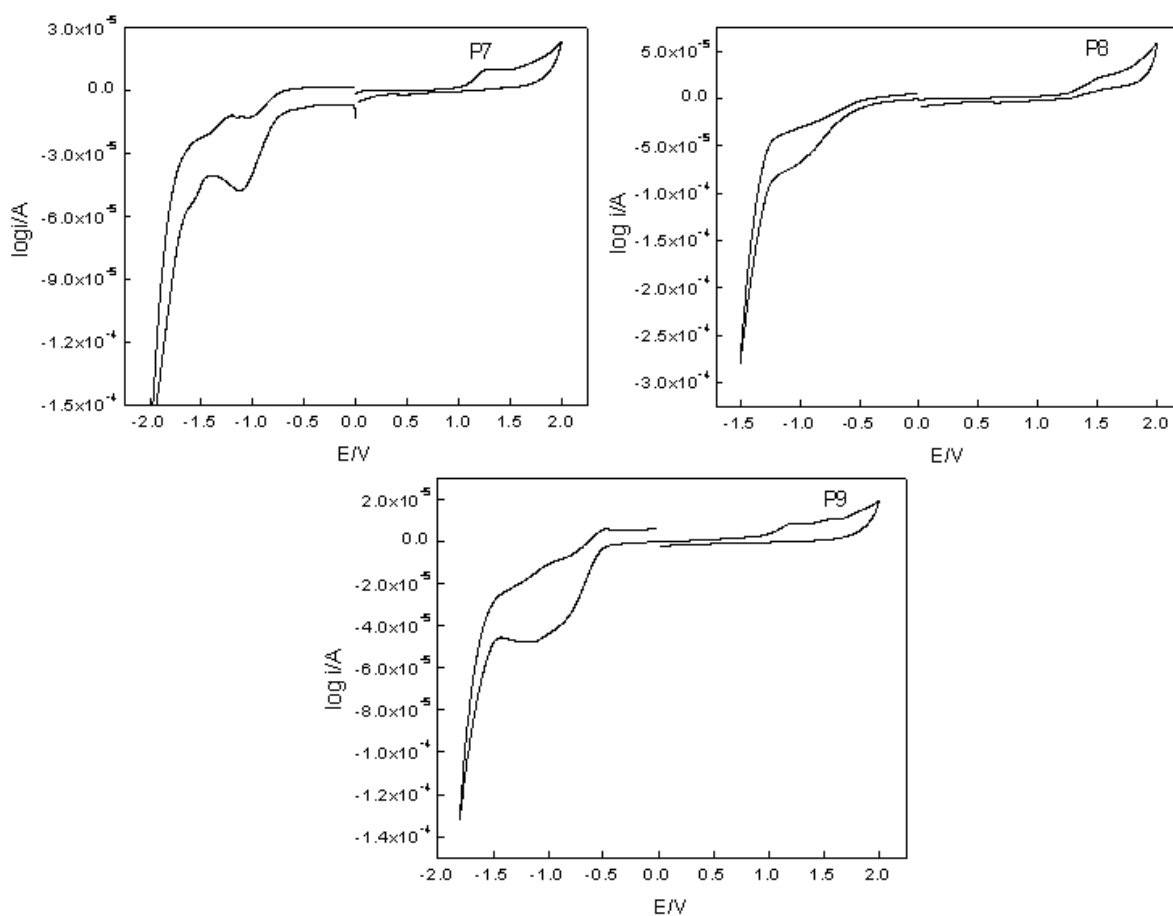
Figure 4.4 Cyclic voltammetric waves of **P7-P9**

Polymers P10-P16 (Series -4)

The cyclic voltammograms of polymers **P10-P16** displayed clear oxidation and reduction processes as shown in **Figures 4.5 (a) and 4.5 (b)**. As explained earlier, polymers **P10-P16** consists of different structures with electron donating and electron acceptor units along with various spacer groups. Their reduction potentials were found to

be lower than that of PBD.   In the anodic and cathodic sweeps, polymers **P10-P16** showed distinct oxidation and reduction peaks.   The electrochemical data of polymers **P10-P16** are given in **Table 4.4**.   Among all the polymers in this series, the maximum bandgap was observed for **P15** containing naphthalene as a spacer group. This is mainly attributed to the fact that introduction of the heavier naphthalene units disrupts and hinders the conjugation along the backbone. Polymer **P13** containing phenylvinylene group spacer exhibited little decreased in bandgap compared to polymer **P10, P15** and **P16**.   This is due to increase in extent of conjugation along the polymer chain, which would have reduced the bandgap by decreasing the HOMO level.   The reduced band gap was observed for polymers **P11** and **P14** containing thiophene and EDOT as spacers, respectively.   The tendency of thiophene and their alkoxy substituted derivatives acts as good electron donors, the presence of these as spacer units in these polymers (**P11** and **P14**) alternatively with 1,3,4-oxadiazole electron acceptor unit causes reduction in bandgap.   In polymer **P12,** the observed bandgap was little more when compared to polymers containing thiophene and EDOT as spacers. This is ascribed to the electron acceptor nature of pyridine ring as a spacer in polymer **P12**.

Table 4.4 Electrochemical potentials, energy levels and band gap (^{a}E$_g$) of **P10-P16**

Polymer	E_{oxd} (eV)	E_{red} (eV)	E_{oxd} (onset)	E_{red} (onset)	E_{HOMO} (eV)	E_{LUMO} (eV)	^aE_g (eV)
P10	1.56	-0.95	1.41	-0.68	-5.81	-3.74	2.07
P11	1.37	-0.80	1.27	-0.64	-5.67	-3.76	1.91
P12	1.50	-0.94	1.22	-0.83	-5.62	-3.57	2.06
P13	1.51	-1.23	1.24	-0.80	-5.64	-3.60	2.04
P14	1.52	-1.18	1.10	-0.76	-5.50	-3.64	1.86
P15	1.79	-1.29	1.49	-0.99	-5.89	-3.41	2.48
P16	1.89	-0.82	1.63	-0.75	-6.03	-3.65	2.38
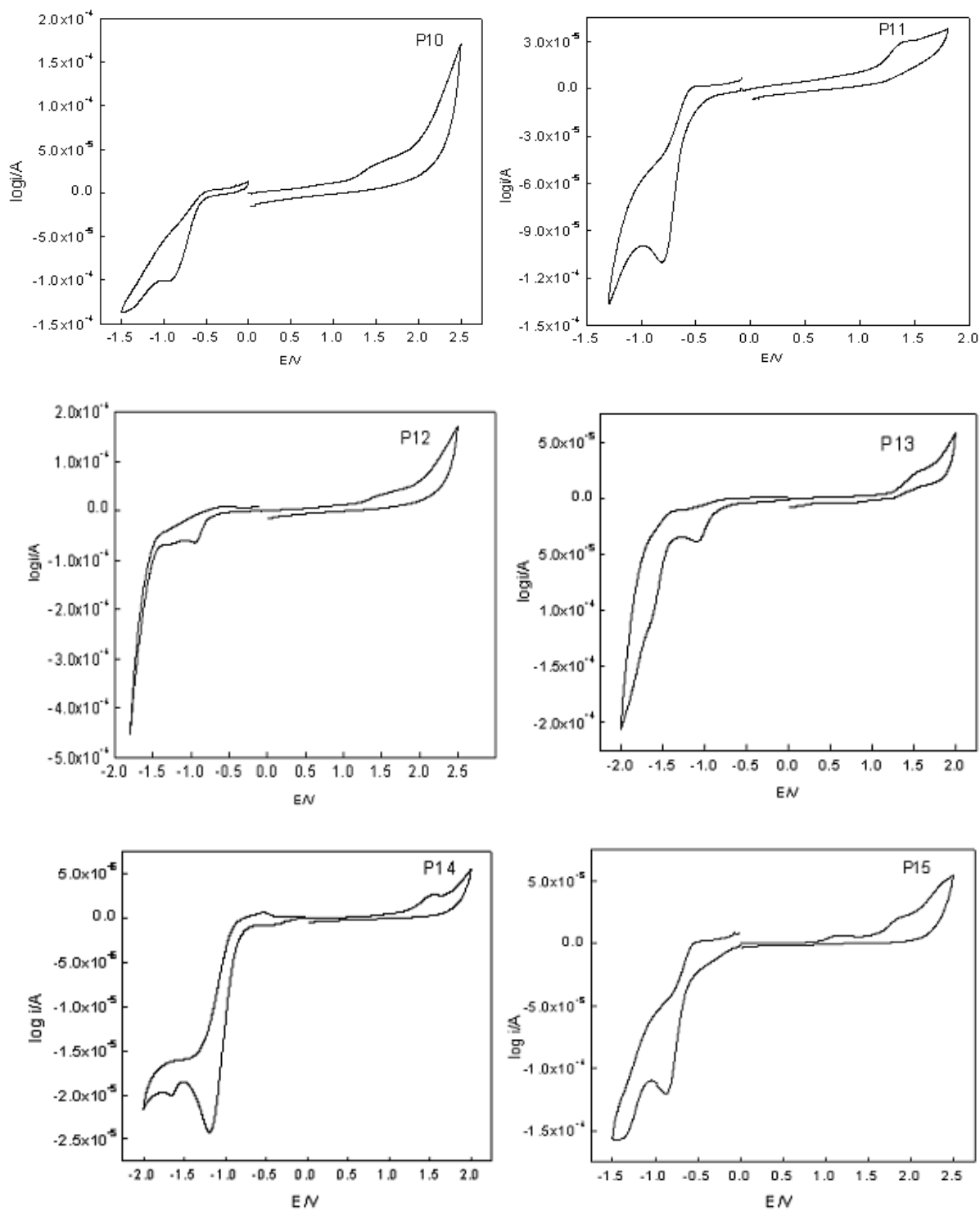
Figure 4.5 (a) Cyclic voltammetric waves of **P10-P15**
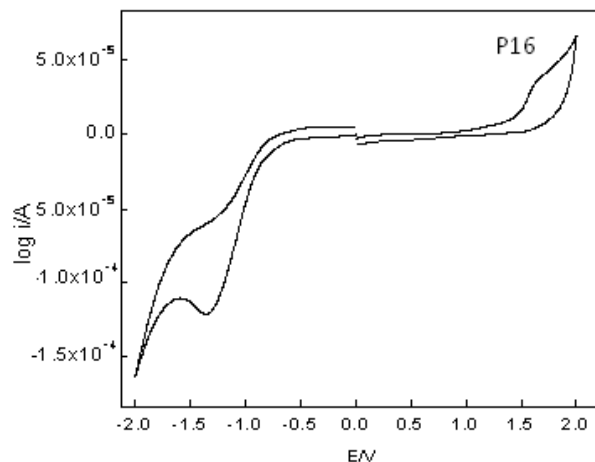
Figure 4.5 (b) Cyclic voltammetric waves of **P16**

4.3 LINEAR OPTICAL STUDIES

The investigation of linear optical properties of new polymers would make possible in understanding the changes produced in the electronic energy of molecules, due to electronic transitions of valence electrons by the absorption of light in UV-visible region. The emission of light by the molecule during the electronic transition from excited state to ground state, would give the valuable information in deciding the molecules as fluorescent light emitting materials. This study also helps in evaluating λ_{abs}, λ_{ems} bathochromic and hypochromic shifts for the samples and also to understand the effect of substituents on them. In the present work, the absorption and emission properties of new polymers were studied using UV-visible and fluorescence spectroscopy in order to assess their suitability in applications for optic devices.

4.3.1 Absorption and emission spectroscopy

UV-visible absorption and fluorescence emission spectroscopic techniques are important tools used to obtain the absorption and emission characteristics of any compound either in solution or solid state. The absorbance of light energy or electromagnetic radiation by molecule excites electrons from the ground level to the excited state of the compound. Further, it emits the light while relaxing from excited state to ground state with the loss of some energy in the form of heat. Generally, the transitions observed in the conjugated molecules are attributed to the electronic excitation from π-π^* states while transitions in emission spectroscopy is due to the relaxation from

π^*-π states. Above 200 nm only the two lower energy transitions, i.e, n-π^* and π-π^*, are achieved as a result of the energy available from the photons.

When sample molecules are exposed to light having an energy that matches a possible electronic transition within the molecule, some of the light energy will be absorbed as the electron is promoted to a higher energy orbital. As a simple rule, energetically favored electron promotion will be from the HOMO, usually the singlet ground state, S_0, to the LUMO and the resulting species is called the singlet excited state S_1. Absorption bands in the visible region of the spectrum correspond to transitions from the ground state of a molecule to an excited state that is 160-330 kJ above the ground state. Compounds that absorb in the visible region of the spectrum generally have some weakly bound or delocalized electrons. In these systems, the energy difference between the LUMO and the HOMO corresponds to the energies of quanta in the visible region.

Fluorophores, also termed as chromophores play the main role in fluorescence spectroscopy and imaging. A fluorophore is a component that causes a molecule to absorb photons of a particular wavelength and then emit energy at a different but equally specific wavelength. The amount and wavelength of the emitted energy depend on both the fluorophore and its chemical environment. Generally, the fluorescence involves allowed transitions from higher to lower excited singlet states with a nanosecond lifetime.

4.3.2 Materials, instrumentation and measurement methods

The UV-visible and fluorescence spectra of samples were recorded using GBC Cintra 101 UV-visible and Perkin Elmer LS55 fluorescence spectrophotometers, respectively. The absorption and emission measurements of polymers **P1-P16** were taken for dilute solutions (10^{-5} M) of polymers in THF.

4.3.3 Results and discussion

The linear optical characterization data of polymers evaluated using UV-visible and fluorescence spectroscopy are tabulated in **Table 4.5.** Their spectral features are discussed in the following section.

Polymers P1-P3 (Series-1)

The UV-visible and fluorescence absorption spectra of polymers **P1-P3** in THF solution are shown in **Figures 4.6** and **4.7**, respectively. Here, the absorption maxima were found to be 394, 388, 372 nm for polymers **P1-P3**, respectively. These absorption maxima were comparable to those of thiophene-1,3,4-oxadiazole copolymers (Yu et al. 1998 and Huang et al. 1999). The increase in length of alkoxy chain at 3 and 4 positions of thiophene has resulted in red-shift of absorption maxima by ~5-20 nm. It was expected that the insertion of alkoxy chain at 3 and 4 positions of thiophene would increase the absorption and emission maxima. As expected, the increase in absorption maxima was observed due to the increased electron donating tendency of lengthy alkoxy chain. The absorption maxima of polymers in film states were around 405-415 nm as shown in **Figure 4.8**. It is observed that in solid state the absorption maxima and absorption edge were red-shifted due to the interactions between conjugated polymer chains. Even red-shift around 20 nm was observed in florescence emission of polymers with increase in alkoxy chain length. Further, in case of polymers **P1-P3**, the emission maxima were found to be 489, 470, 455 nm, respectively. Also, they emit intense bluish-green fluorescence. The absorption maxima, emission maxima and optical bandgap of polymers **P1-P3** calculated from the absorption edge are tabulated in **Table 4.5**.
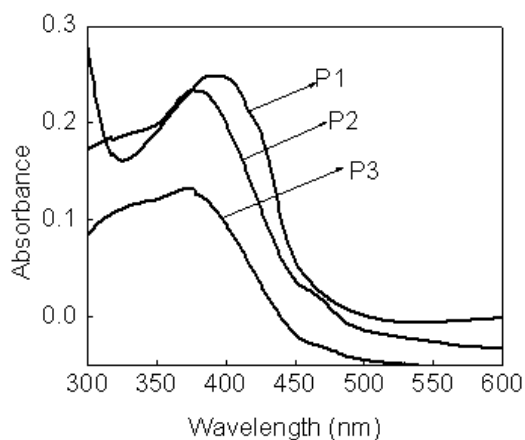
Figure 4.6 UV-vis absorption spectra of	**Figure 4.7** Fluorescence spectra of
P1-P3	**P1-P3**
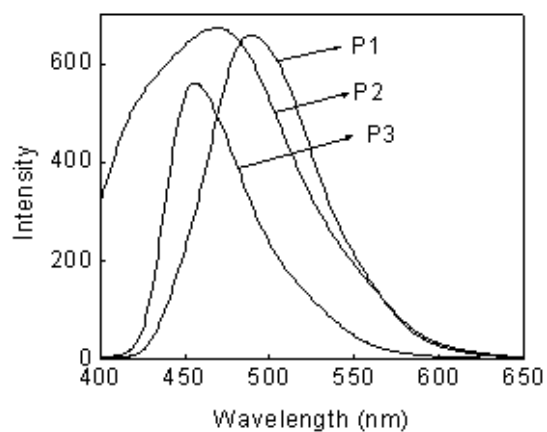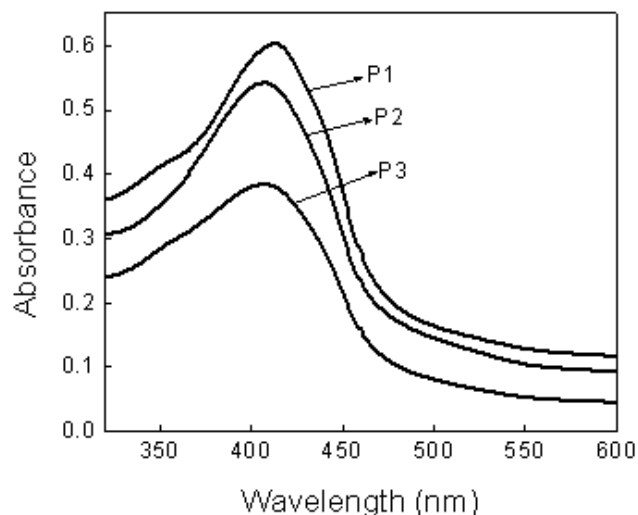
Figure 4.8 UV-vis absorption spectra of **P1-P3** in film state

Table 4.5 The absorption maxima, emission maxima and optical bandgap (^bE_g) of **P1-P3**

Sample	UV-vis absorption λ_{abs}(nm)		Emission maxima λ_{ems} (nm)	Optical bandgap (^bE_g)
	Solution	Film		
P1	394	413	489	2.44
P2	388	408	470	2.38
P3	372	406	455	2.43

Polymers P4-P6 (Series-2)

The absorption and emission spectra of polymers **P4-P6** are given in **Figure 4.9** and **Figure 4.10**, respectively. The values of absorption and emission maxima are tabulated in **Table 4.6**. The absorption maxima were determined to be 398, 391 and 385 nm for polymers **P4-P6**, respectively. As observed for Series-1, variation in alkoxy chain substitution at 3 and 4 positions of thiophene showed red-shift in both absorption and emission maxima in the present series. No significant variation was detected on increasing length of the alkoxy chain but a little red-shift around 15 nm in absorption was observed. The polymer **P4** containing tetradecyloxy chain showed higher emission maxima than that of **P5** and **P6** carrying dodecyloxy and hexyloxy chains. Their emission maxima were determined to be 492, 468 and 449 nm. In solid state absorption spectra

polymers **P7-P9** is as shown in **Figure 4.11**. A red-shift in the absorption maxima is observed due to the inter chain interactions. A red-shift around 15-20 nm was observed in fluorescense emission of polymers **P4-P6**. The emitted light was observed to be bluish-green coloration.
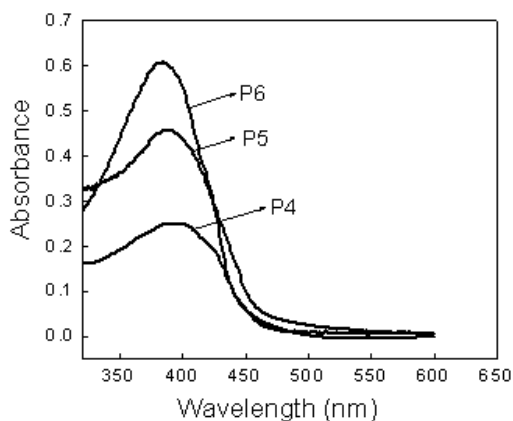
Figure 4.9 UV-vis absorption spectra of
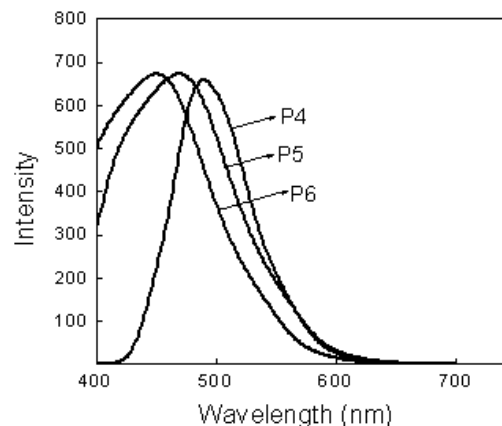
P4-P6

Figure 4.10 Fluorescence spectra of

P4-P6
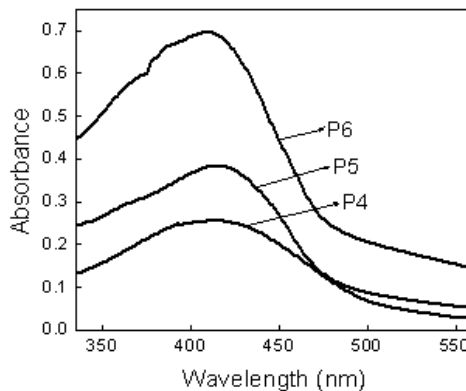
Figure 4.11 UV-vis absorption spectra of **P4-P6** in film state

Table 4.6 The absorption maxima, emission and optical bandgap (^bE_g) of polymers **P4-P6**

Sample	UV-vis absorption λ_{abs} (nm)		Emission maxima λ_{ems} (nm)	Optical band gap (^bE_g)
	Solution	Film		
P4	398	417	461	2.46
P5	391	415	492	2.47
P6	385	410	468	2. 41

Polymers P7-P9 (Series-3)

The absorption spectra of polymers **P7-P9** are given in **Figure 4.12** and their emission spectra are shown in **Figure 4.13**. The absorption maxima were determined to be 393, 388 and 385 nm for polymers **P7-P9**, respectively. In polymer **P7**, a red-shift of about 20 nm was observed when compared to λ_{max} of polymers **P8** and **P9**. This is mainly due to the presence of 4-methoxybenzyl substitution at 3 and 4 positions of thiophene in **P7.** The terminal substituents (methyl and nitro groups) on resulting polymers showed slight or moderate influence on absorption maxima. However, the terminal substituent, i.e methoxy group of benzyloxy unit attached at 3 and 4 positions of thiophene in polymer **P7** has great influence on its emission maxima. This may be due to the fact that the lone pair of electrons present on the oxygen atom of methoxy groups might have contributed to the increased delocalization of electrons in the substituted moiety. Consequently, a significant red-shift was observed in polymer **P7**. The florescence emission maxima for polymers **P7-P9** were observed at 535, 494 and 485 nm, respectively. The polymers showed green light emission for **P7** and bluish-green emission for P8 and P9, on irradiation of samples under UV-light. The absorption and emission maxima are tabulated in **Table 4.7**.
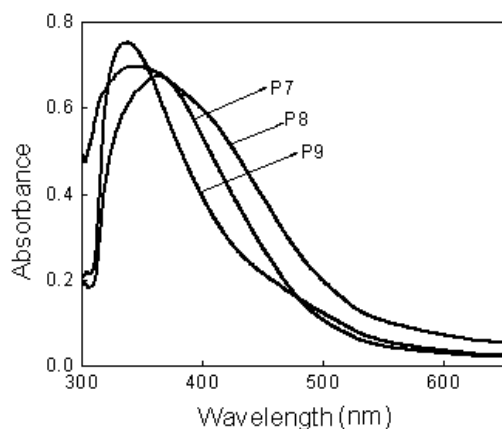
Figure 4.12 UV-vis absorption spectra of **P7-P9**
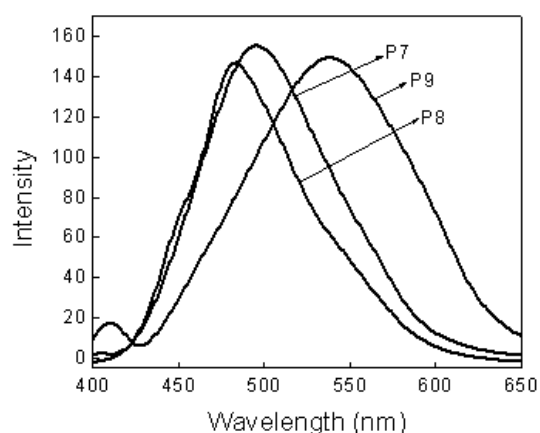
Figure 4.13 Fluorescence spectra of **P7-P9**

Table 4.7 The absorption maxima and emission maxima for **P7-P9**

Sample	UV-Vis (λ_{abs}) nm	Emission maxima(λ_{ems}) nm
P7	364	535
P8	336	494
P9	343	485

Polymers P10-P16 (Series-4)

The UV-visible spectra of polymers **P10-P16** are shown **Figure 4.14**. The absorption maxima for polymers were found to be 360, 377, 356, 381, 363, 339 and 375 nm for **P10-P16** polymers, respectively. The polymers containing thiophene (**P10**) and EDOT (**P14**) spacers showed absorption maxima 356 and 363 nm, respectively and it was observed that there is little red-shift in **P14** carrying EDOT which exerts more electron releasing behavior than thiophene ring and lowers the HOMO level. A shift in absorption maxima was observed in polymer **P13** containing phenylenevinylene spacer group, when compared to other polymers. This is mainly ascribed to the enhanced extent of conjugation along the main polymeric chain. The decrease in absorption maxima was observed for polymer **P15** containing naphthalene spacer group. The presence of this bulky aromatic naphthalene group has hindered and reduced the extension of conjugation and affects the HOMO and LUMO energy levels. As a result, a decrease in absorption maxima was observed in polymer **P15** containing naphthalene spacer group. The polymer **P11** containing pyridine spacer unit showed more absorption maxima than those of polymers **P10**, **P12**, **P13**, **P15** and **P16**. This is mainly ascribed to the electron affinitiy nature of pyridine. When it is present in the polymer chain with electron donating units it raises the LUMO energy level and thereby increases its absorption maxima. The fluorescence emission spectra of polymers **P10-P16** are given in **Figure 4.15**. The emission maxima of polymers **P10-P16** appeared at 544, 566, 552, 469, 449, 443 and 490 nm, respectively. The polymers displayed green to bluish-green emission under the irradiation of UV light. The absorption and emission maxima are listed in **Table 4.8**.
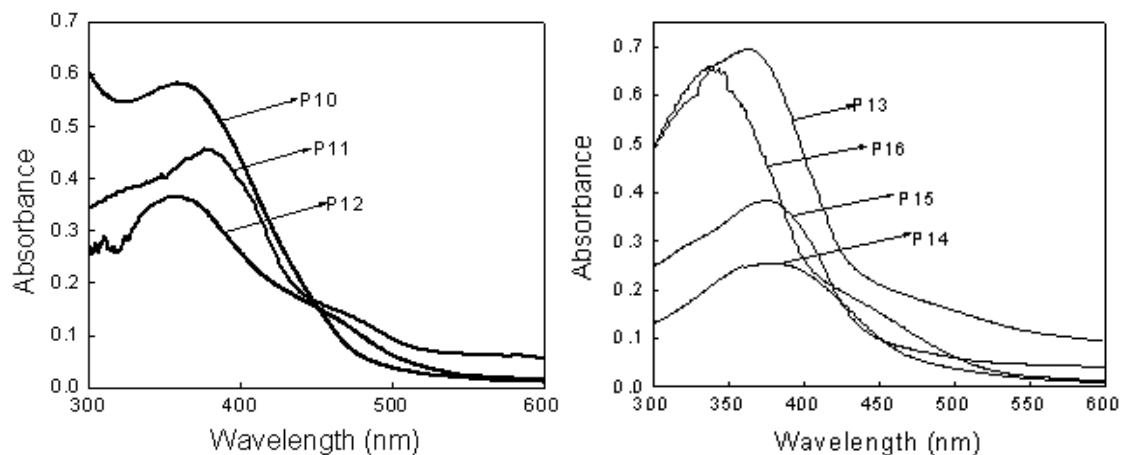
Figure 4.14 UV-vis absorbance spectra of **P10-P16**
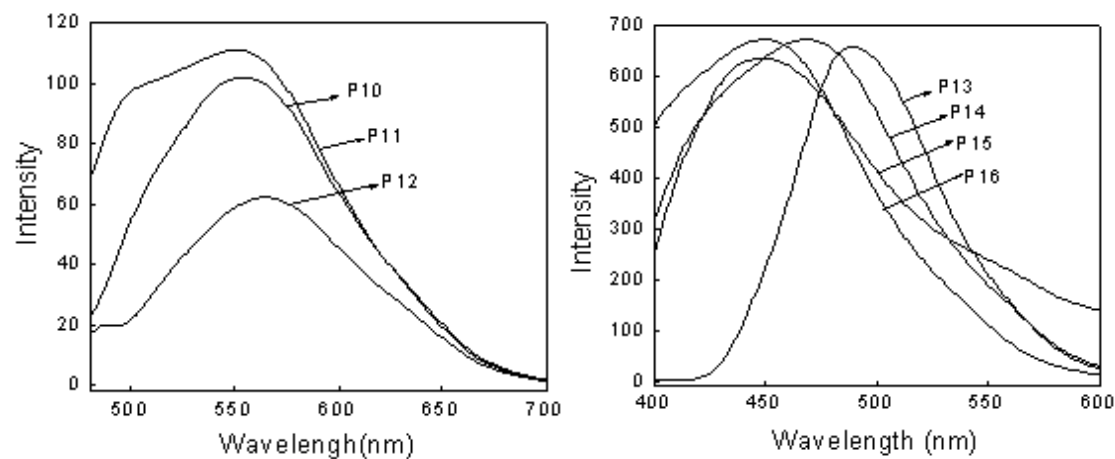
Figure 4.15 Fluorescence emission spectra of **P10-P16**

Table 4.8 The absorption maxima and emission maxima for polymers **P1-P16**

Sample	UV-Vis (λ_{abs}) nm	Emission maxima(λ_{ems}) nm
P10	360	544
P11	377	566
P12	356	552
P13	381	469
P14	363	449
P15	339	443
P16	375	490

Chapter 4

4.4 NONLINEAR OPTICAL STUDIES

The NLO studies of new polymers involve determination of certain characteristic parameters such as absorption coefficients, optical limiting behavior, two/three/multi-photon absorption processes. The evaluation of these properties is quite useful in order to find their suitability for applications in nonlinear optical devices. At present, there is a tremendous increase in the study and usage of organic NLO active polymers in various applications like frequency doublers, optical limiting devices, and electro-optic EO switches and modulators (Williams 1984, Prasad 1989, Heeger 2001). In view of this, the new polymers were subjected to NLO studies.

4.4.1 Materials, instrumentation and measurement methods

For the investigation of NLO properties Z-scan and DFWM methods were used. A detailed account of these techniques is discussed in section **1.7.4**. A complete description of measurement, apparatus set-up and experimental protocol followed for NLO studies is as follows.

4.4.1.1 Z-scan technique

In our Z-scan setup we used a stepper-motor controlled linear translation stage to move the sample through the beam in precise steps. The polymer samples (**P1-P16** in THF solution) were taken in 1 mm cuvettes. The transmission of the sample at each point was measured by means of two pyroelectric energy probes (Rj7620, Laser Probe Inc.). One energy probe monitors the input energy, while the other monitors the transmitted energy through the sample. The second harmonic output (532 nm) of a Q-switched Nd: YAG laser (Quanta Ray, Spectra Physics) was used for exciting the molecules. The laser pulse width is 7 nanoseconds. Laser pulse energy of approximately 200 microjoules was used for the experiments. The pulses were fired in the "single shot" mode, allowing sufficient time between successive pulses to avoid accumulative thermal effects in the sample.

4.4.1.2 Degenerate four wave mixing (DFWM) method

DFWM experiment (**Figure 1.8**) was conducted to evaluate NLO properties of **P1-P6** keeping carbon disulphide as reference sample. In this method, we used plane

polarized 7 ns pulses at 532 nm obtained from the second harmonic output of a **Q**-switched Nd: YAG laser. A polarizer kept in the beam path on a rotatable mount was used to change the intensity of the beam falling on the sample. The sample (THF solution) was taken in a 1 mm glass cuvette. The input energy was monitored using a pyroelectric energy probe. The generated signal beam was measured in the far field using a calibrated photodiode.

4.4.1.3 Results and discussion

The results of Z-scan and DFWM measurement methods for different series of polymers are discussed in the following sections.

Polymers P1-P3 (Series-1)

The Z-scan curves obtained from the experiments of samples **P1-P3** are given in **Figure 4.16**. It was found that numerically a 2PA type process gives the best fit to the measured Z-scan data. Samples have a linear absorption of about 40-60% at the excitation wavelength in the 1 mm cuvette and hence strong two-step excited state absorption would happen along with genuine 2PA in the present case. The net effect is then known as an "effective" 2PA process. The data obtained were fitted to the nonlinear transmission equation for a 2PA process, given by equation (1) (Karthikeyan et al. 2008).

$$T(z) = [1/\pi^{1/2}q(z)]\int_{-\infty}^{+\infty}\ln[1+q(z)\exp(-\tau^2)]d\tau \qquad \ldots\ldots\ldots\ldots\ldots (1)$$

where T(z) is the sample transmission at position z. $q(z) = \beta I_0 L/[1+(z/z_0)^2]$, where I_0 is the peak intensity at the focal point, $L = [1-\exp(-\alpha l)]/\alpha$, where l is the sample length and α is the linear absorption coefficient, and $z_0 = \pi\omega_0^2/\lambda$ is the Rayleigh range, where ω_0 is the beam waist radius at focus and λ is the light wavelength, β is the effective 2PA coefficient.

The numerically calculated values of the effective 2PA coefficient are 1.0×10^{-11} m/W for **P1**, 5.3×10^{-11} m/W for **P2** and 1.4×10^{-11} m/W for **P3**. For comparison, under similar excitation conditions, good NLO materials like Cu nanocomposite glasses offered effective 2PA coefficient values 10^{-10} to 10^{-12} (Sivaramakrishnan et al. 2007), bismuth nanorods and CdS quantum dots gave 5.3×10^{-11} m/W, 1.9×10^{-9} m/W, respectively

(Kurian et al. 2007). These values indicate that the present samples possess an optical nonlinearity comparable to good optical limiters reported in literature. Thus, new polymers **P1-P3** can find potential applications in optical limiting devices.
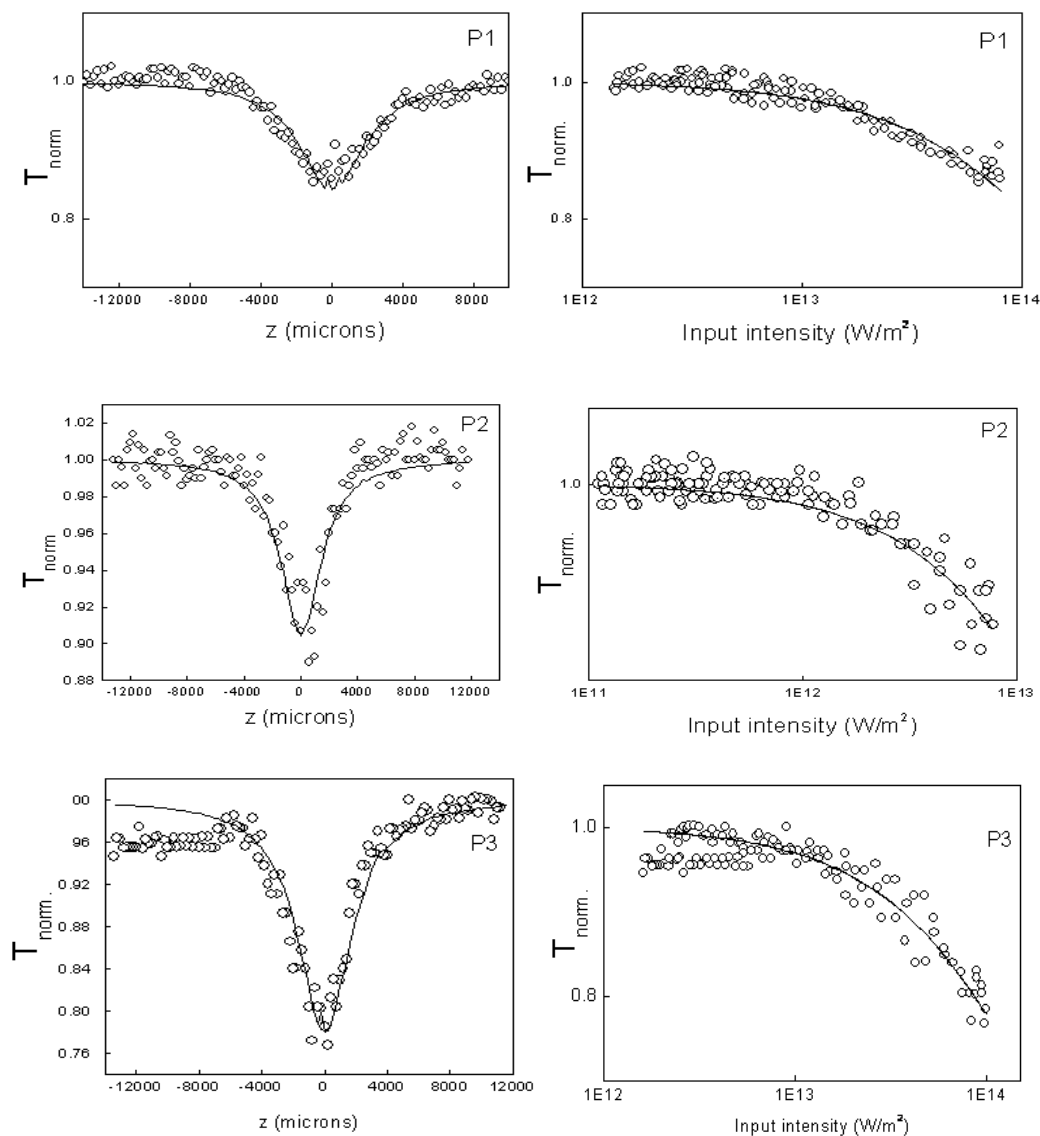
Figure 4.16 Z-scan and fluence curves of **P1-P3**

The results of DFWM experiment i.e. DFWM signal as a function of pump intensity for **CS₂**, polymers **P1-P3** are shown in **Figure 4.17**. Here CS_2 is the reference sample for measurement. The signal is proportional to the cubic power of the input intensity as given by (2),

$$I(\omega)\alpha(\frac{\omega}{2\varepsilon_o cn^2})\left|\chi^{(3)}\right|^2 l^2 I_0^3(\omega) \qquad \ldots\ldots\ldots\ldots. \quad (2)$$

where $I(\omega)$ is the DFWM signal intensity, $I_o(\omega)$ is the pump intensity, l is the length of the sample and n is the refractive index of the medium. The solid curves in the figures are the cubic fits to the experimental data and $\chi^{(3)}$ can be calculated from the equation (3)

$$\chi^{(3)} = \chi_R^{(3)} \left[\frac{\left(I/I_0^3\right)}{\left(I/I_0^3\right)_R}\right]^{1/2} \left[\frac{n}{n_R}\right]^2 \frac{l_R}{l}\left(\frac{\alpha l}{\left(1-e^{-\alpha l}\right)e^{-\alpha l/2}}\right) \qquad \ldots\ldots\ldots\ldots. \quad (3)$$

where the subscript 'R' refers to the standard reference CS_2. '$\chi^{(3)}_R$' is taken to be 4.0 x 10^{-13} esu (Shirk et al. 1992). The figure of merit F, given by $\chi^{(3)}/\alpha$, is then calculated. F is a measure of nonlinear response that can be achieved for a given absorption loss in the medium. The F value is useful for comparing the nonlinearity of materials when they are resonantly excited (as in the present case).

The $\chi^{(3)}$ values obtained by the above method for polymers **P1-P3** are 0.92 x10^{-11} 4.18 x 10^{-11} and 1.71 x 10^{-11} esu, respectively and the F values are 2.2 x 10^{-12}, 9.65 x 10^{-12} and 4.72 x 10^{-12} esu.cm, respectively. For comparison, the F values are an order of magnitude better than those reported previously in phthalocyanine compounds (Shirk et al. 1992 and Philip et al. 1999), which are materials known to have high optical nonlinearity. Their enhanced nonlinear behavior can be explained based on their structure. In the polymers **P1-P3** alkoxy and benzyloxy pendants substituted at the 3 and 4 positions of the thiophene ring behave as donor moieties whereas 1,3,4-oxadiazole behaves as strong acceptor moiety. This alternate D-A arrangement gives rise to high π-electron density along the polymeric chain and are easily polarizable which in turn results in enhanced delocalization of the electrons in the polymer backbone. Moreover, the alkoxy and benzyloxy groups act as solubilizing group thereby facilitating the solubility of the polymers. All these factors collectively favored the nonlinear absorption of the polymers as a whole. The enhancement is well perceived as the resulting third-order

nonlinear susceptibility has increased ten-fold when compared to the results of some of earlier reported the D-A type polymers (Takahashi et al. 1997).
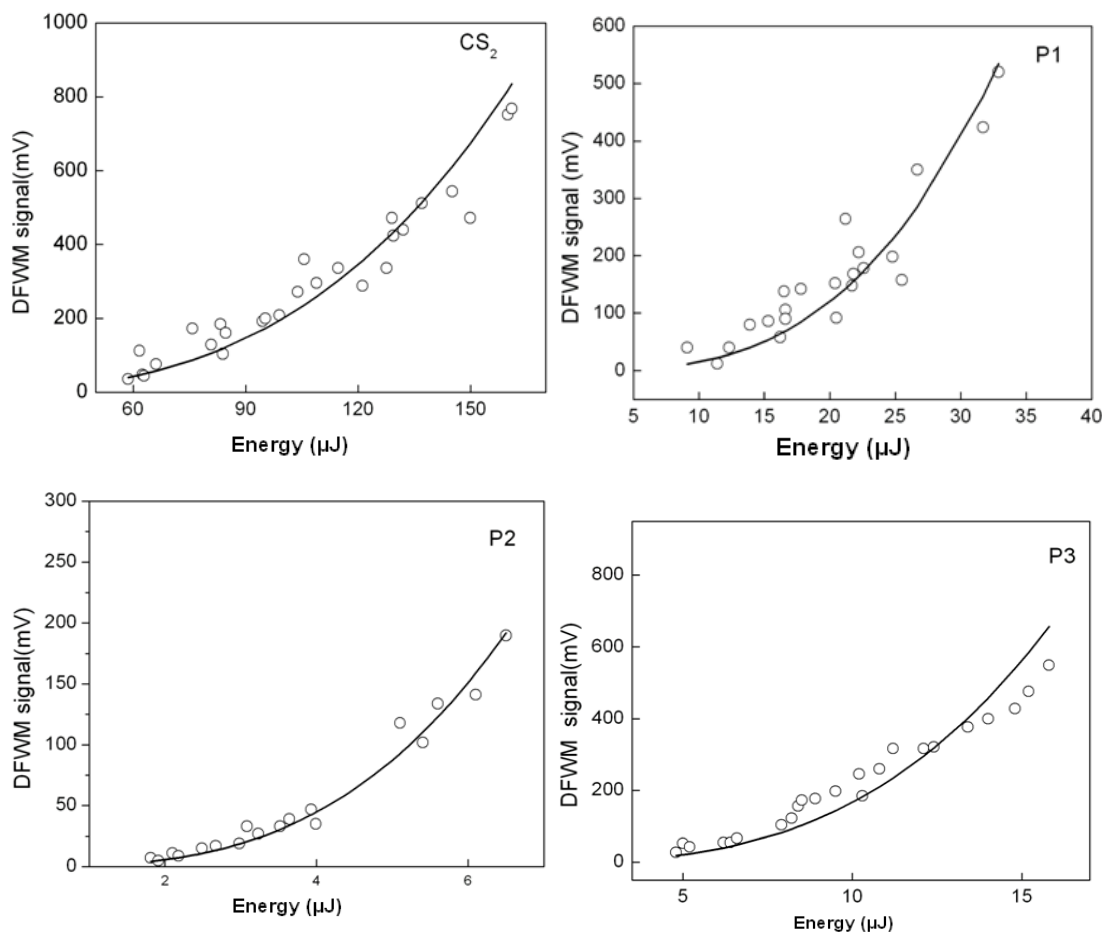
Figure 4.17 DFWM signals in CS_2 and **P1-P3**

Polymers P4-P6 (Series-2)

The open aperture Z-scan curves obtained from the samples **P4-P6** are given in **Figure 4.18**. The value of 2PA coefficient (β) was found to be of the order of 10^{-11} esu for polymers **P4-P6**, which is nearly one order of magnitude larger than the values reported for thiophene oligomers by Hein et al. (Hein et al. 1994). The observed variation of NLO responses of polymers are related to their backbone containing alternating electron donating and electron withdrawing groups in their chain. The numerically calculated values of the effective 2PA coefficient are 9.4 x 10^{-11} mW^{-1} for **P4**, 6.8 x 10^{-11} mW^{-1} for **P5** and 3.4 x 10^{-11} mW^{-1} for **P6**. These values show that the

present samples have an optical nonlinearity comparable to good optical limiters reported in literature (Sivaramakrishnan et al. 2007, Kurian et al. 2007).
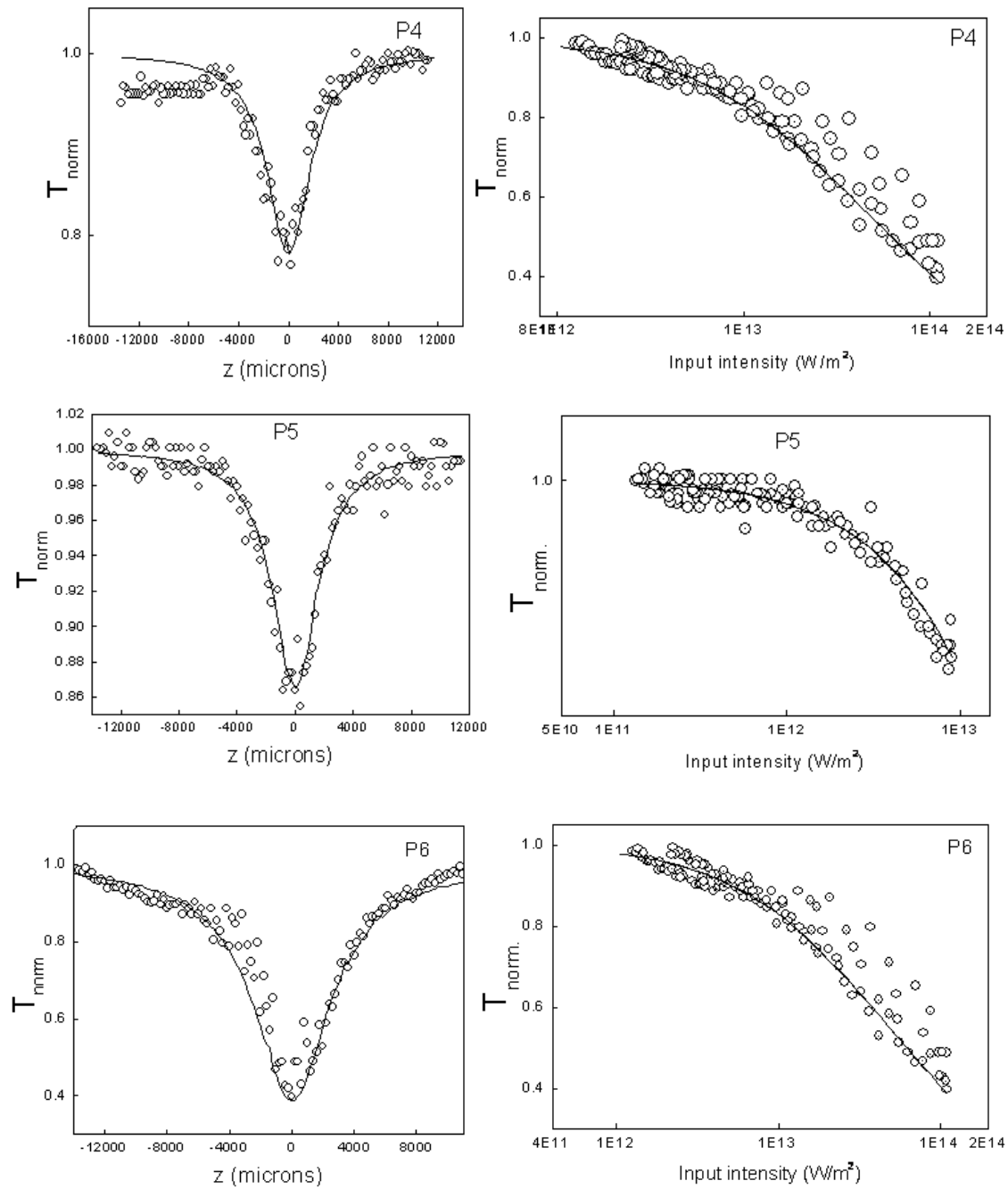
Figure 4.18 Z-scan and fluence curves of **P4-P6**

The DFWM signals measured versus pump intensity for polymers **P4-P6** are shown in **Figure 4.19**. The $\chi^{(3)}$ values obtained for **P4-P6** were 3.09 x 10^{-11}, 2.7 x 10^{-11} and 1.2 x 10^{-11} esu, respectively and the *F* values are 4.081 x 10^{-12}, 6.8 x 10^{-12} and 6.0 x 10^{-12} esu.cm, respectively. It is interesting to note that the *F* values obtained are an order of magnitude better than those of phthalocyanine compounds reported previously (Shirk et al. 1992 and Philip et al. 1999), which are materials known to have a high optical nonlinearity.

Their enhanced nonlinear behavior can be explained based on their structure. In the previously reported polymers 3,4-disubstituted thiophene pyridine, biphenyl, naphthyl, 3,4-ethylenedioxy thiophene, cyano-vinylene had been introduced in the main chain (Udaykumar et al. 2006 and Hedge et al. 2009). Whereas, in the new polymers, the reported groups were replaced by naphthalene-2-ylmethoxy pendants substituted at the 3 and 4 positions of the thiophene (electron donor). However, electron accepting 1,3,4-oxadiazole and electron donating 3,4-dialkoxythiophene units were retained in their structure. This alternate D-A arrangement gives rise to high π-electron density along the polymeric chain and are easily polarizable which in turn results in enhanced delocalization of the electrons in the polymer backbone. Moreover, the alkoxy and naphthlene-2-ylmethoxy groups act as solubilising group thereby facilitating the solubility of the polymers. The length of the alkoxy side chain also played an important role in the third order nonlinear response of the polymers. Polymer **P4** shows a little more nonlinear response than **P6**. This is due to the high electron donating ability of the tetradecyloxy groups when compared to the hexyloxy groups. Therefore, the improved third order nonlinear response is due to the enhanced π-electron delocalization in the polymers caused by the presence of electron donating alkoxy side chains and D-A arrangements. This study reveals that the nonlinear optical properties of the polymers can be tuned by the structural design with the simultaneous presence of alternating electron donor and acceptor groups along the polymer backbone.
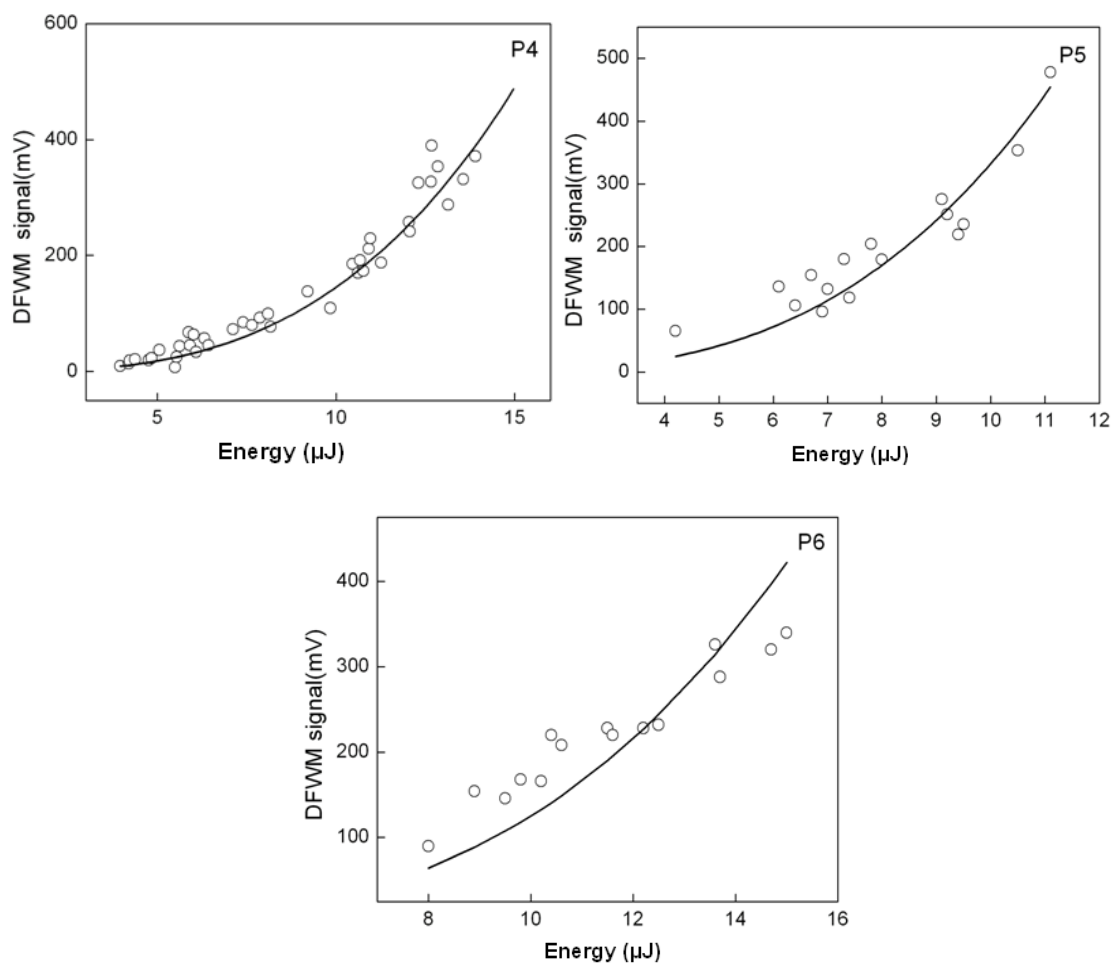
Figure 4.19 DFWM signal obtained in **P4-P6**

Polymers P7-P9 (Series 3)

The Z-scan curves for **P7-P9** are shown in **Figure 4.20**. The results indicate that polymers show good optical limiting behavior. Here the Z-scan plot shows that the transmittance decreases when pump fluence has increased. It was found that three-photon absorption (3PA) type gives the best fit to the obtained experimental data. The Z-scan curves obtained were therefore numerically fitted to the nonlinear transmission equation for a 3PA process, as given in equation (4)

$$T = \frac{(1-R)^2 \exp(-\alpha L)}{\sqrt{\pi}p_0} \times \int_{-\infty}^{+\infty} \ln[\sqrt{1 + p_0^2 \exp(-2t^2)} + p_0 \exp(-t^2)]dt \qquad \ldots \ldots (4)$$

where T is the transmission of the sample, R is the Fresnel reflection coefficient at the sample-air interface, α is the absorption coefficient, and L is the sample length. Here p_0 is given by $[2\gamma(1-R)^2 I_0^2 L_{eff}]^{1/2}$, where γ is the 3PA coefficient, and I_0 is the incident intensity. L_{eff} is given by $[1-\exp(-2\alpha L)]/2\alpha$. The values of 3PA coefficient (γ) obtained for **P7-P9** from the curve fitting are 2.5×10^{-24}, 1.6×10^{-24} and 1.0×10^{-24} m^3W^2, respectively.
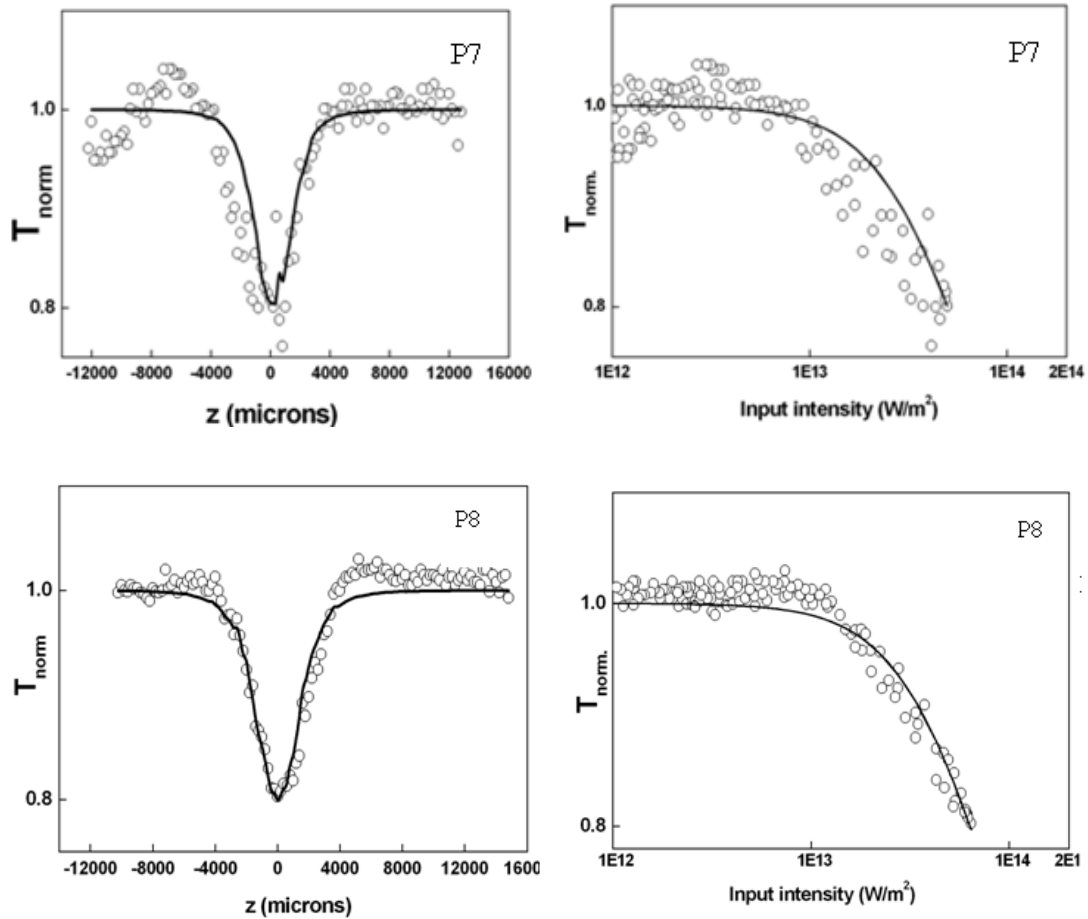
Figure 4.20 (a). Z-scan and fluence curves of **P7** and **P8**
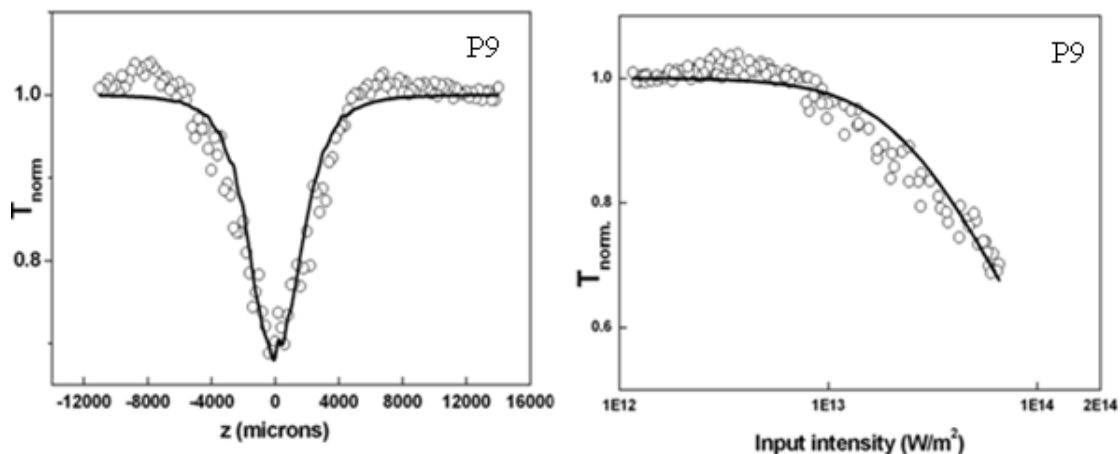
Figure 4.20 (b) Z-scan and fluence curves of **P9**

Generally, 3PA cross sections are low when compared with one photon absorption process, but it becomes significant when samples are irradiated with intense laser pulses of picoseconds or shorter duration. With nanosecond pulse excitation, accumulative nonlinear effects may take place. These, however, will appear like pure 2PA or 3PA in a simple transmission measurement such as the Z-scan. These combined nonlinearities hence are termed as "effective 2PA" and "effective 3PA" in processes to distinguish them from pure 2PA and 3PA processes. Such absorptive nonlinearities were earlier reported in fullerenes (C_{60}), metals, semiconductors, nanoclusters, fluorine derivatives (Tutt et al. 1993, Philip et al. 2000, Cohanoschi et al. 2006, Wang et al. 2001, Nair et al. 2008). In 3PA process, excitation is proportional to the cube of the incident intensity. This aspect could help to obtain higher contrast and resolution in imaging, since 3PA provides stronger spatial confinement. In the recent years significant progress in 3PA based applications has been witnessed, including three-photon pumped lasing and 3PA-based optical limiting and stabilization. Interestingly, **P7-P9** showed 3PA absorption process, as concluded from the experimental data.

The enhanced NLO absorption of **P7** and **P8** is mainly ascribed to presence of electron donating 3,4-dodecyloxythiophene and 3,4-bis[(3-methyl/4-methoxybenzyl)oxy] thiophene moieties placed alternatively with electron withdrawing 1,3,4-oxadaizole ring. The electron releasing nature of methyl and methoxy groups attached to benzyl group in polymers **P7** and **P8**, respectively contributed significantly to the observed effect. In

polymer **P9**, the extent of D-A type of arrangement has weakened due to decreased donor nature of nitro group attached to benzyloxy group at 3,4-positions of thiophene. Consequently, the observed 3PA coefficient for **P9** is less than that of polymers **P7** and **P8**. The presence of terminal methoxy (**P7**) and methyl (**P8**) substituents increases the electron donating tendency and thereby facilitatiting the ease of electron acceptance by adjacent 1,3,4-oxadiazole, this may cause difference between dipole moments of ground state and excited states of molecules. In case of **P9** the terminal nitro group slightly reduced the electron donating nature of the bis 3,4-[4-nitrobenzyloxy thiophene] and also 3PA value. The enhanced D-A type arrangement in conjugated polymers **P7-P8** gives rise to high π-electron density along the polymeric chain and so these molecules are easily polarizable, which has reflected in their nonlinear absorption.

4.2.3.4 Polymers P10-16 (Series-4)

Fluence open aperture and Z-scan curves obtained from the samples **P10-P16** are given in **Figure 4.21**. The nonlinear transmission behavior of the present samples can be modeled by defining an effective nonlinear absorption coefficient α(I), given by the equation:

$$\alpha(I) = \frac{\alpha_0}{1 + (I/I_s)} + \beta I \qquad \dots \dots \dots \dots \dots \dots \dots (5)$$

where α_0 is the unsaturated linear absorption coefficient at the wavelength of excitation, I is the input laser intensity and is the saturation intensity (intensity at which the linear absorption drops to half its original value), $\beta I = \sigma N$ is the excited state absorption (ESA) coefficient, where σ is the ESA cross section and N(I) is the intensity-dependent excited state population density. For calculating the transmitted intensity for a given input intensity, the propagation equation,

$$\frac{dI}{dz'} = -\left[\left(\alpha_0 / 1 + I/I_s\right) + \beta I\right]I \qquad \dots \dots \dots \dots \dots \dots \dots (6)$$

was numerically solved. Here 'z' indicates the propagation distance within the sample.
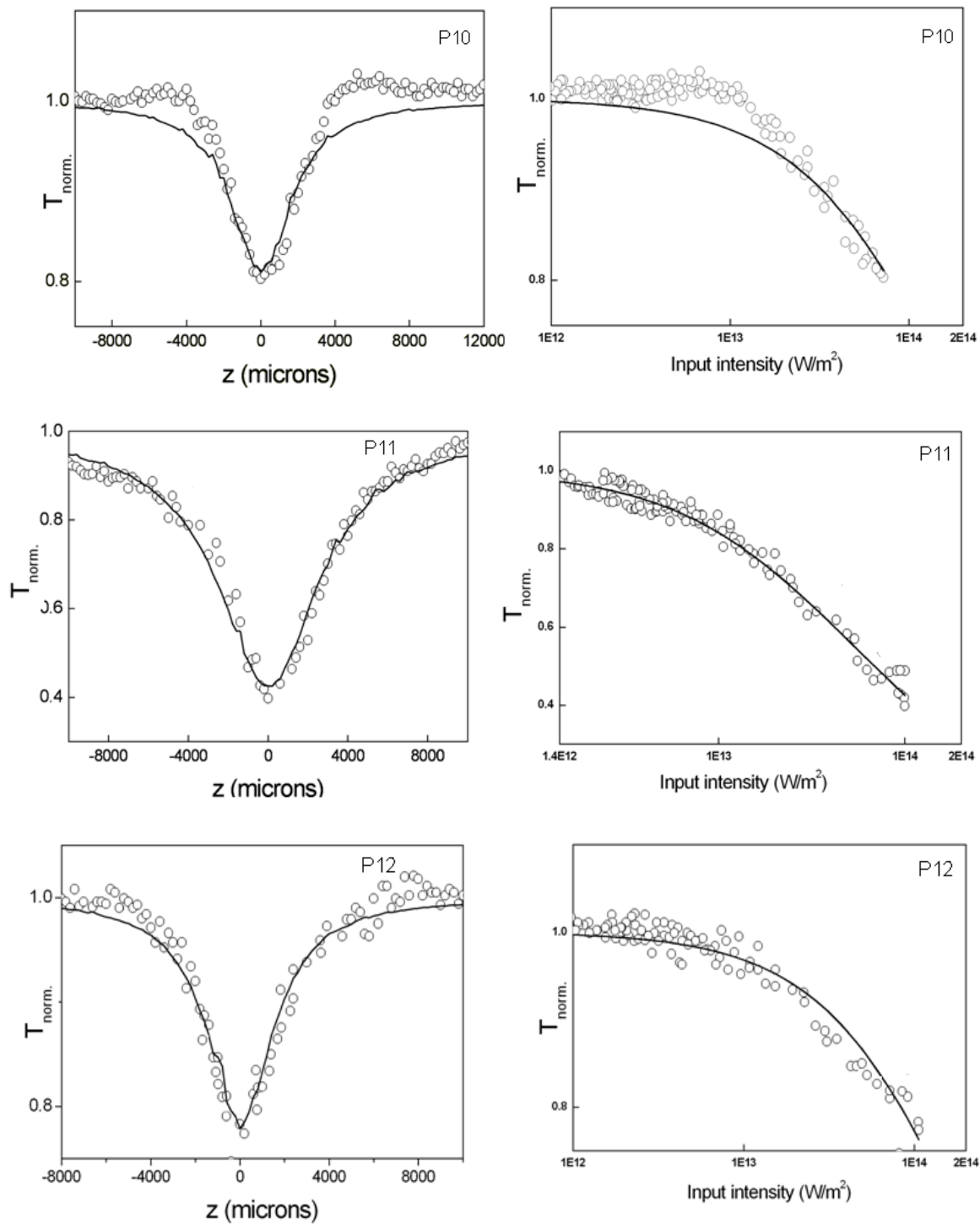
Figure 4.21 (a) Z-Scan and fluence curves of **P10-P12**
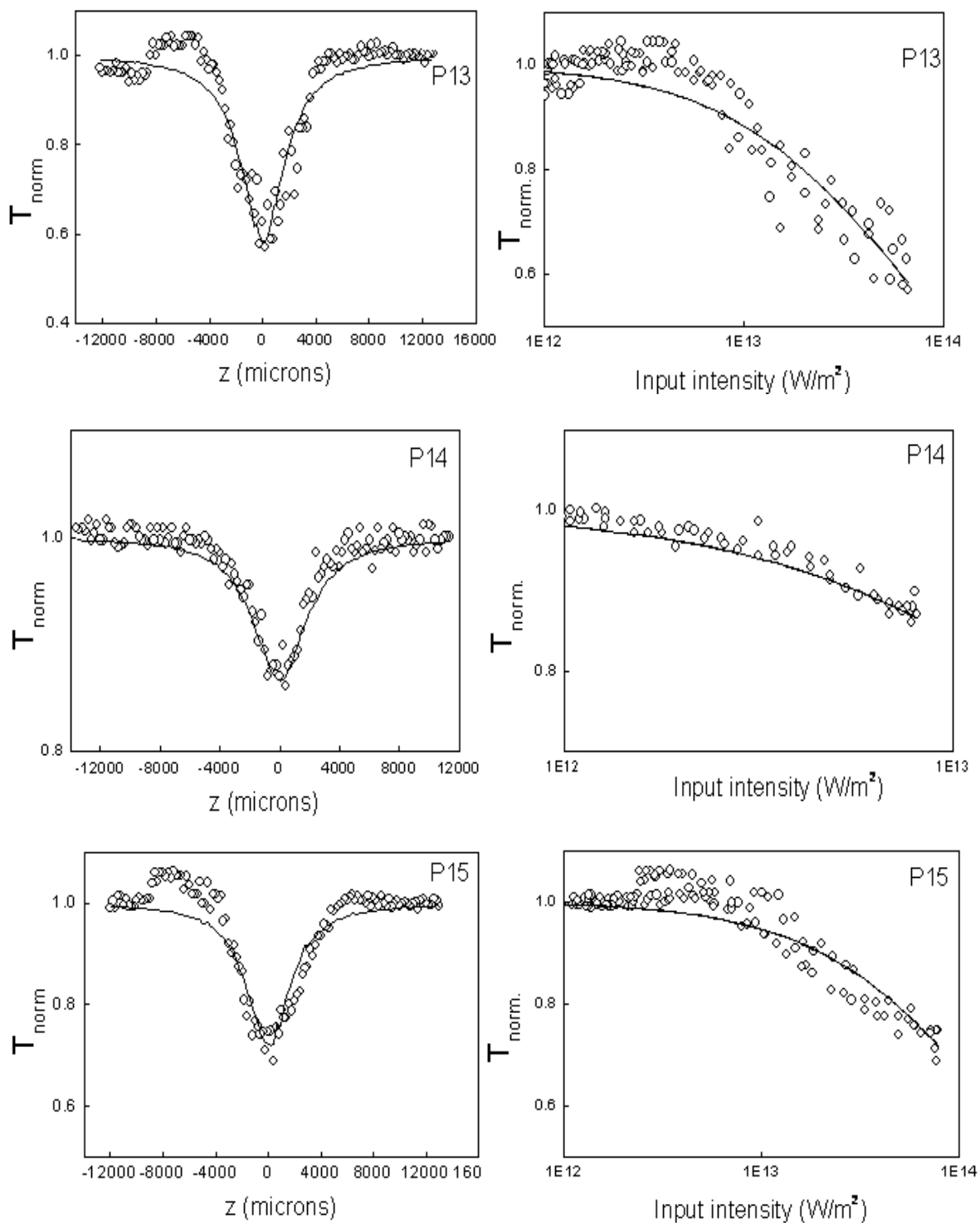
Figure 4.21 (b) Z-Scan and fluence curves of **P13-P15**
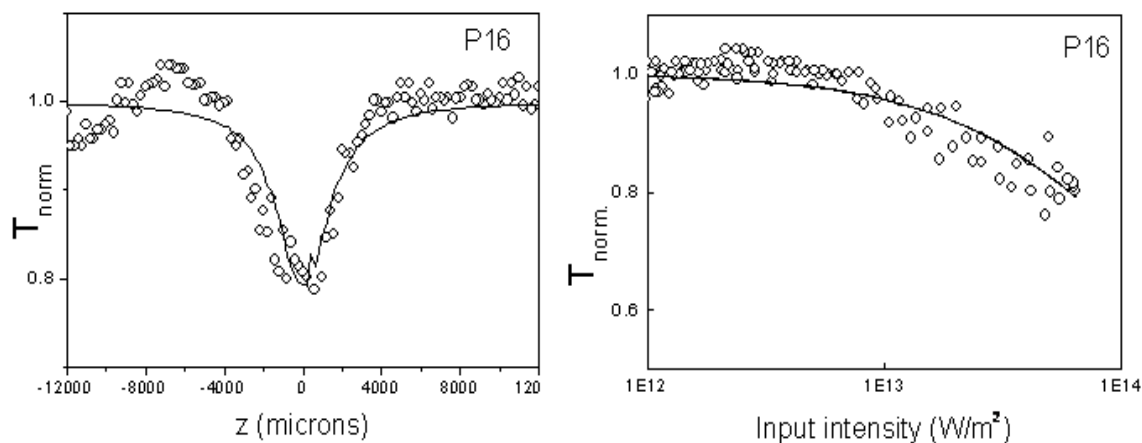
Figure 4.21 (c) Z-Scan and fluence curves of **P16**

The experimental data obtained from Z-scan measurements were used to find the type of absorption process. Numerically, a 2PA type process was found to give the best fit to the nonlinear transmission equation (1). Samples **P10-P16** have a linear absorption of about 50-70% at the excitation wavelength when taken in the 1 mm cuvette. Therefore, strong two-step excited state absorption would happen along with genuine 2PA in the present case. The net effect is then known as an "effective" 2PA process.

The observed nonlinear behavior of the polymers **P10-P16** can be explained based on their structural features. The alternate D-A arrangement in these polymers gives rise to high π-electron density along the polymeric chain and are easily polarizable which in turn results in enhanced delocalization of the electrons in the polymer backbone. In the new polymers 3,4-bis(4-(decyloxy)-3-methoxybenzyloxy)thiophene acts as electron donor moiety whereas 1,3,4-oxadiazole behaves as electron acceptor group. The numerically calculated values of the effective 2PA coefficient were found to be 2.9×10^{-11}, 8.0×10^{-11}, 1.4×10^{-11}, 5.5×10^{-11}, 8.1×10^{-11}, 6.2×10^{-11} and 1.8×10^{-11} m/W for **P10-P16**, respectively. As expected, polymers containing thiophene (**P11**) and thiophene derivative i.e EDOT (**P14**) exhibited more absorption coefficient. It is attributed to the presence of five membered heterocyclic thiophene and EDOT as spacer groups in the main polymeric chain and also its incorporation in the system could lead to enhanced molecular hyperpolarizability. They increase the electron delocalization in the main chain

and also offer more effective π-conjugation between donor and acceptor groups, in turn resulting in larger nonlinearities. Polymers containing naphthalene (**P15**) and phenylvinylene (**P13**) as spacers showed more absorption coefficient values. Comparatively less β value was observed for polymer consisting pyridine (**P12**) and biphenyl (**P16**) and benzene (**P10**). However, in polymer **P12** the **2**PA coefficient value is quite less, which is mainly due to the presence of pyridine ring next to the electron withdrawing 1,3,4-oxadiazole moiety. These observed values are comparable with those of good NLO materials. Under similar excitation conditions, Cu nanocomposite glasses were shown to possess effective 2PA coefficient values of the order 10^{-10} to 10^{-12} m/W (Sivaramakrishnan et al. 2007), while bismuth nanorods and CdS quantum dots were shown to have 5.3 x 10^{-11} m/W (Kurian et al. 2007). From the results, it is evident that polymers **P10-P16** are potential candidates for optical limiting devices.

4.5 CONCLUSIONS

The studies of electrochemical properties as determined by the cyclic voltammetry reveal that new polymers possess HOMO energy level in the range of -5.3 to -6.0 eV and LUMO energy level in the range of -3.2 to -3.8 eV due to the presence of good conjugation and enhanced D-A arrangement along the polymeric chain. The new polymers showed the bandgap in the range of 1.8 to 2.5 eV. The reduction potentials of new polymers are lower than that of PBD (one of the good charge carrier). The studies reveal that by varying the substitution in the polymer backbone or side chain it is possible to alter the HOMO and LUMO energy levels. Such tuning of energy levels is important for the fabrication of polymers in opto-electronic devices. Further, the results of linear optical studies were accounted for the substitution effects of different groups in the polymer chain. The polymers exhibited bluish-green and green fluorescence under the irradiation of UV-light. This suggests that, polymers can also be used as good fluorescent materials.

NLO studies of newly synthesized D-A type polymers using Z-scan technique and DFWM measurement method indicate that they are good optical limiting materials. The results reveal that new polymers belonging to Series 1, 2 and 4 showed 2PA. Whereas,

polymers of Series-3 exhibited 3PA process. The good NLO response of polymers may be attributed to the presence of polarizable donor and acceptors in the polymer main chain with enhanced D‑A nature and also due to the extended conjugation in the polymer. The observed nonlinearity of polymers is comparable with earlier reported good NLO materials C_{60}, semiconductors, metal nanoclusters and pthalocyanines. From the results, it is clear that polymers **P1-P16** can have potential applications in optical limiting devices.

Chapter 5

Abstract

This chapter includes the summary of the entire research work carried out along with the conclusions drawn from the present studies. Scope for further work has also been incorporated.

5.1 SUMMARY

Amongst many classes of materials polymeric structures containing π-electron conjugated chains showed continuing interest in various fields. They are potential candidates for their applications in important areas like LEDs, PV cells, TFTs, frequency doublers, optical limiters, optical storage devices, and electro-optic switches and modulators. The key advantage of organic conjugated polymers is their ease of processing different techniques. They possess good optical and electronic properties of semiconductors with the processing advantages and mechanical properties of polymers. Also, these polymers offer added advantages like good environmental stability and low cost of manufacturing. In addition, polymeric systems with delocalized π-electrons with D-A arrangement were shown to possess very high molecular polarisability and optical nonlinearities.

Based on the thorough literature survey, four new series of polymers based on 3,4-disubstituted thiophene and 1,3,4-oxadiazole were designed. In our new design various conjugated spacer groups were introduced into the polymer chain in order to study their effect on electrochemical and optical properties. It was hoped that the new polymers would show low bandgap, good solvent processability and NLO properties.

In the present research work, we focused on the design, synthesis, electrochemical, linear and nonlinear optical studies of four new series of D-A type conjugated polymers. The following four new series of polymers were synthesized starting from simple organic compounds.

a. Polymers carrying 3,4-dialkoxythiophene, 1,3,4-oxadiazole and 3,4-dibenzyloxythiophene (**P1-P3, Scheme 3.1**)

b. Polymers carrying 3,4-dialkoxythiophene, 1,3,4-oxadiazole and 3,4-dinaphthyloxythiophene (**P4-P6, Scheme 3.2**)

c. Polymers carrying 3,4-bis(methoxy/methyl/nitrobenzyloxy)thiophene, 1,3,4-oxadiazole and 3,4-dialkyloxythiophene (**P7-P9, Scheme 3.3**)

d. Polymers carrying 3,4-bis(alkoxybenzyloxy)thiophene, 1,3,4-oxadiazole and different aromatic spacers (**P10-16, Scheme 3.5**)

To synthesize above series of polymers through polyhydrazide route, new monomers, viz. 4-bis(benzyloxy)thiophene-2,5-dicarboxylic acid chloride (**4a**), 3,4-bis(naphthalen-2-ylmethoxy)thiophene-2,5-dicarboxylic acid chloride (**4b**), 4-bis[(4-methoxybenzyl)oxy] thiophene-2,5-dicarboxylic acid chloride (**4c**), 3,4-bis[(3-methylbenzyl)oxy] thiophene-2,5-dicarboxylic acid chloride (**4d**), 3,4-bis[(4-nitrobenzyl)oxy] thiophene-2,5-dicarboxylic acid chloride (**4e**), 3,4-bis(4-(decyloxy)-3-methoxybenzyloxy)thiophene-2,5-dicarbohydrazide (**12**) were synthesized starting from diethyl 3,4-dihydroxythiophene-2,5-dicarboxylate through multistep reactions. Synthetic methods used for their preparations were established with respect to reaction parameters. All the newly synthesized intermediates and monomers were well characterized by FTIR, ^{1}H NMR, and ^{13}C NMR spectroscopy followed by elemental analysis.

The target polymers were synthesized from newly synthesized monomers using appropriate synthetic routes. Their synthetic methods were established. The polymers were purified by soxhlet extraction and solvent washings followed by centrifugation. The structures of newly synthesized polymers were confirmed by FTIR, ^{1}H NMR spectral and GPC techniques. Also, the polymers were studied for their thermal stability using thermogravimetric analysis.

Further, polymers were subjected to electrochemical and optical studies. The cyclic voltammetric technique was employed to investigate the electrochemical properties of the new polymers. The optical properties of the polymers were studied by UV-visible and fluorescence spectral analyses. Furthermore, their NLO properties were investigated by Z-scan and DFWM techniques.

5.2 CONCLUSIONS

From the studies, the following important conclusions were drawn.

➤ The four new series of D-A type conjugated polymers (**P1-P16**) comprising of 16 polymers were designed based on the thorough literature survey.

➤ The synthetic and purification methods for new intermediates, monomers and polymers were developed and established.

➤ The new polymers show moderate solubility in common organic solvents, owing to the presence of alkoxy side chain in all the polymers.

➤ The molecular structures of new intermediates, monomers and polymers were established by different spectral techniques.

➤ The weight average molecular weights of the polymers are in the range of 3000-27000 g/mol and the polydispersity in the range of 1.3-2.8 showing good film forming ability. Also, they possess good solvent processability.

➤ TGA analysis reveals that the polymers are thermally stable up to about 300 °C.

➤ The electrochemical studies reveal that the new polymers possess HOMO energy levels in the range of -5.3 to -6.0 eV and LUMO energy levels in the range of -3.2 to -3.8 eV, due to the presence of good conjugation and enhanced D-A strength along the polymeric chain.

➤ The new polymers show the bandgap in the range of 1.8 to 2.5 eV. Among all the polymers, **P14** shows least bandgap of 1.86 eV and polymer **P15** displays the highest bandgap of 2.48 eV.

➤ The reduction potentials of new polymers are lower than that of PBD (one of the good charge carriers). Hence, the polymers may be used in opto-electronic devices as electron transporters.

➢ The polymers in dilute solution show bluish‑green to green florescence under the irradiation of long UV‑radiations indicating that they are good fluorescent materials.

➢ Results of NLO studies by Z‑scan and DFWM methods using 5 ns laser pulses at 532 nm indicate that all the polymers behave as good optical limiters. The NLO absorption involves both 2PA and 3PA processes.

➢ Polymers belonging to Series‑3 (**P7-P9**) exhibit 3PA whereas polymers of Series 1, 2 and 4 show 2PA processes. This discrepancy observed in polymers **P7-P9** is due to presence of favorable structural features for NLO absorption.

➢ Amongst polymers exhibited 2PA, polymer **P14** containing EDOT as conjugated spacer shows the maximum absorption coefficient. Amongst polymers involved 3PA process, polymer **P7** displays the highest absorption coefficient. This is mainly attributed to high donor-acceptor strength produced by good electron donating systems.

➢ NLO absorption coefficient increases with increase in alkyl chain length. It is clear from the literature that when the alkyl chain length increased to 1-hexadecyl the NLO absorption coefficient decreased. This is due to the more flexibility of 1-hexadecyl chain. As a result degree of orientation of the molecule is more dominant. Keeping this in reference we have studied the effect of alkyl chain length till dodecyl alkyl chain in combination with different acceptor and spacer groups

➢ The good optical limiting behavior of new polymers **P1-P16** suggests that they are promising candidates for their applications in photonics as optical limiters.

5.3 FUTURE SCOPE

The increasing demand of more and more cost effective materials for opto‑electronic applications has led to a tremendous growth of conjugated polymers. Among them, D‑A type conjugated polymers are potential candidates for photonic applications. The art of engineering the conjugated polymers by introducing different donor and acceptor groups is rapidly being taken up by many material scientists around the globe as

they have received significant scientific and technological interest due to their broad range of applications in many fields. As per the requirement, donors and acceptors can be chosen and tailored into a D-A type conjugated polymer with exciting novel properties and functionalities. Keeping these factors in view, the scope of the present work can be extended but not limited to the following experiments.

- ➢ Studies on photovoltaic properties and fabrication of photovoltaic devices
- ➢ Studies on light emitting and electroluminescent efficiency in PLEDs and their fabrication
- ➢ Studies on optical switching properties of polymers and development of optical limiting devices

The field of conjugated polymers is incredibly large and since the quest for new novel materials is never ending, scope for the future work is bright.

REFERENCES

Acierno, D., Amendola, E., Bellone, S., Concilio, S., Iannelli, P. and Neitzert, H. C. (2003). "Synthesis and characterization of a new class of nematic photoluminescent oxadiazole-containing polyethers." *Macromolecules,* 36(17), 6410-6415.

Agarwal, A.K. and Jenekhe, S.A. (1993). "Synthesis and processing of heterocyclic polymers as electronic, optoelectronic, and nonlinear optical materials. 2. New series of conjugated rigid-rod polyquinolines and polyanthrazolines." *Macromolecules*, 26(5), 895-905.

Ahn, T., Lee, S.G. and Shim, H.K. (2002). "Systematic approach of blue-light-emitting copolymers by introducing various naphthalene linkages into fluorene containing PPV derivatives," *Opt. Mat.,* 21(1-3), 191-197.

Ak, M., Cirpan, A., Yilmaz, F., Yagci, Y. and Toppare, L. (2005). "Synthesis, characterization of hexamethylene diamine bis-(3-thiophen acetic acid) (HDTA) and electrochromic properties of its copolymers with thiophene." *Eur. Polym. J.*, 41(5), 967-973.

Akcelrud, L. (2003). "Electroluminescent polymers." *Prog. Polym. Sci.,* 28(6), 875-962.

Audebert, P., Kamada, K., Matsunaga, K. and Ohta, K. (2003). "The third-order NLO properties of D-π-A molecules with changing a primary amino group into pyrrole." *Chem. Phys. Lett*., 367(1-2), 62-71.

Babel, A., Wind J.D. and Jenekhe, S.A. (2004). "Ambipolar charge transport in air-stable polymer bled thin-film transistors." *Adv. Funct. Mater*., 14(9), 891-898.

Babudri, F., Farinola, G.M., Lopez, L.C., Martinelli, M.G. and Naso, F. (2001). "A synthetic strategy leading to monodisperse PPV oligomers by coupling reactions of vinyltrimethylsilanes." *J. Org. Chem.,* 66(11), 3878-3885.

References

Beaujuge, P.M., Pisula, W., Tsao, H.N., Ellinger, S., Mullen K. and Reynolds, J.R. (2009). "Tailoring structure-property relationships in dithienosilole-benzothiadiazole donor-acceptor copolymers." *J. Am. Chem. Soc.*, 131(22), 7514-7515.

Blumstengel, S., Sokolik, I., Dorsinville, R., Voloschenko, D., He, M., Lavrentovich, O. and Chien, L.C. (1999) "Photo and electroluminescence studies of 2,5-bis-[20-(400-(6-hexoxybenzyl)-10-ethenyl]-3,4-dibutyl thiophenes." *Synth Met*., 99(1), 85-90.

Borbone, F., Carella, A., Roviello, A., Casalboni, M., Matteis, F.D., Stracci, G., Rovere, F.D., Evangelisti, A. and Dispenza, M. (2011). "Outstanding poling stability of a new cross-linked nonlinear optical (NLO) material from a low molecular weight chromophore." *J. Phys. Chem. B.,*115(42), 11993-12000.

Bottino, F.A. Pasquale, G.D. and Pollicino, A. (1999). "Synthesis and characterization of novel poly(arylene ether)s containing 1,3,4-oxadiazole units. *Macromol. Rapid. Commun*., 20(8), 405-409.

Boyd, R. (1992) Nonlinear optics Academic Press, San Diego.

Breitung, E.M., Shu, C.F. and McMahon, R.J. (2000). "Thiazole and thiophene analogues of donor-acceptor stilbenes: Molecular hyperpolarizabilities and structure-property relationships." *J. Am. Chem. Soc.,* 122(6), 1154-1160.

Brown, A.R., Bradley D.D.D., Burn, P.L., Holmes A.B. and Kraft, A. (1992). "Poly(p-phenylenevinylene) light-emitting diodes: Enhanced electroluminescent efficiency through charge carrier confinement." *App. Phy. Lett*., 61(23), 2793-2795.

Bugatti, V., Concilio, S., Iannelli, P., Piotto, S.P., Bellone, S. Ferrara, M. Neitzert, H.C. Rubino, A. Sala, D.D. and Vacca, P. (2006). "Synthesis and characterization of new electroluminescent molecules containing carbazole and oxadiazole units." *Synth. Met.*, 156(1), 13-20.

References

Burroughes, J.H., Bradley, D.D.C., Brown, A.R., Marks, R.N., Mackay, K., Friend, R.H., Burn, P.L. and Holmes, A.B. (1990). "Light-emitting diodes based on conjugated polymers." *Nature,* 347, 539-541.

Caruso, U., Casalboni, M., Fort, A., Fusco, M., Panunzi, B., Quatela, A., Roviello, A. and Sarcinelli, F. (2005). "New side-chain polyurethanes with highly conjugated push-pull chromophores for second order NLO applications." *Opt. Mat.*, 27(12), 1800-1810.

Cheng, L.T., Tam, W., Marder, S.R., Steigman, A.E., Rikken, G. and Spangler, C.W. (1991). "Experimental investigations of organic molecular nonlinear optical polarizabilities. 1. Methods and results on benzene and stilbene derivatives." *J. Phys. Chem.*, 95(26), 10631-10643.

Chihaya, A., Tetsuo, T. and Shogo, S. (2006). "Blue light-emitting organic electroluminescent devices." *Appl. Phys. Lett*., 56(9), 799-801.

Cho, M.J., Choi, D.H., Sullivan, P.A., Akelaitis, A.J.P. and Dalton, L.R. (2008). "Recent progress in second-order nonlinear optical polymers and dendrimers." *Prog. in Polym. Science*, 33(11), 1013-1058.

Chung, S.J., Kwon, K.Y., Lee, S.W., Jin, J.I., Lee, C.H., Lee, C.E. and Park, Y. (1998). "Highly efficient light-emitting diodes based on an organic-soluble poly(*p*-phenylenevinylene) derivative carrying the electron-transporting PBD moiety." *Adv. Mat.,* 10(14), 1112-1116.

Cohanoschi, I. Garcia, M. Toro, C. Belfield, K.D. and Hernandez, F.E. (2006). "Three-photon absorption of a new series of halogenated fluorene derivatives." *Chem. Phys. Lett.,* 430(1-3), 133-138.

Colladet, K., Fourier, S., Cleij, T.J., Lutsen, L., Gelan J., Vanderzande, D., Nguyen, L.H., Neugebauer, H., Sariciftci, S., Aguirre, A., Janssen, G. and Goovaerts, E. (2007). "Low band gap donor-acceptor conjugated polymers toward organic solar cells applications." *Macromolecules*, 40(1), 65-72.

References

Dalton, L.R., Harper, A.W., Ghosn, R., Steier, W.H., Ziari, M., Fetterman, H., Shi, Y., Mustacich, R.V., Jen, A. K. Y. and Shea, K. J. (1995). "Synthesis and processing of improved organic second-order nonlinear optical materials for applications in photonics." *Chem. Mater*., 7(6), 1060-1081.

de Leeuw, D.M., Simenon, M.M.J., Brown, A.R. and Einerhand, R.E.F. (1997). "Stability of n-type doped conducting polymers and consequences for polymeric microelectronic devices." *Synth. Met.*, 87(1), 53-59.

Delgado, M.C.R., Casado, J., Hernández, V., Navarrete, J.T.L., Orduna, J., Villacampa, B., Alicante, R., Raimundo, J.M., Blanchard, P. and Roncali, J. (2008). "Electronic, optical, and vibrational properties of bridged dithienylethylene-based NLO chromophores."*J. Phys. Chem. C.*, 112(8), 3109-3120.

Della-Casa, C., Fraleoni-Morgera, A., Lanzi, M., Costa-Bizzarri, P., Paganin, L., Bertinelli, F., Schenetti, L., Mucci, A., Casalboni, M., Sarcinelli, F. and Quatela A. (2005). "Preparation and characterization of non-linear optical properties." *Eur. Polym. J.*, 41(10), 2360-2369.

Diaz, A.F Kanazawa, K.K. and Gardini, G.P. (1979). "Electrochemical polymerization of pyrrole." *J. Chem. Soc. Chem. Commun*., 14, 635-636.

Domenico, A., Simona, C., Angela, D., Pio, I. L., Stefano. P. P. and Paola, S. (2002). "Synthesis and liquid crystalline properties of low molecular mass compounds containing the 1,4-bis(5-phenyl-1,3,4-oxadiazolyl) benzene unit." *Liq. Cryst.*, 29(11), 1383-1392.

Eckhardt, H. Shacklette, L. W., Jen, K. Y. and Elsenbaumer, R. L. (1989). *J. Chem. Phys*., 91(2), 1303-1316.

Elsenbaumer, R.L., Jen, K.Y. and Oboodi, R. (1986). "Processible and environmentally stable conducting polymers." *Synth. Met.,* 15(2-3), 169-174.

Faccinetto, A., Mazzucato, S., Pedron, D., Bozio, R., Destri, S., and Porzio, W. (2008). "Non-resonant z-scan characterization of the third-order nonlinear optical

properties of conjugated poly(thiophene azines)." *Chem. Phys.Chem.*, 9(14), 2028-2034.

Faid, K., Cloutier, R. and Leclerc. M. (1993). "Design of novel electroactive polybithiophene derivatives." *Macromolecules, 26*(10), 2501-2507.

Feng, L.X. and Wang, Z. C. (2008). "Synthesis, characterization, and photophysics of a novel conjugated polymer with 1,3,4-oxadiazole, carbazole, and naphthalene units." *J. App. Polym. Sci*., 108(3), 1995-2000.

Fink J.K. (2008). "High performance polymers." William Andrew Inc.Norwich

Grazulevicius, J.V., Strohriegl, P., Pielichowski, J. and Pielichowski, K. (2003). "Carbazole-containing polymers: synthesis, properties and applications." *Prog. Polym. Sci*., 28(9), 1297-1353.

Groenendaal, L., Bruining, M.J., Hendrickx, E.H.J., Persoons, A., Vekemans, J.A.J.M., Havinga, E.E. and Meijer, E.W. (1998). "Synthesis and (non)linear optical properties of a series of donor-oligopyrrole-acceptor molecules." *Chem. Mater.*, 10(1), 226-234.

Groenendaal, L., Jonas, F., Freitag, D., Pielartzik, H. and Reynolds, J. R. (2000). "Poly (3,4-Ethylenedioxythiophene) and its derivatives: past, present and future." *Adv. Mater.,* 12(7), 481-494.

Guan, M., Chen, Z.Q. Bian, Z.Q. Liu, Z.W. Gong, Z.L. Baik, W. Lee, H.J. and Huang, C.H. (2006). "The host materials containing carbazole and oxadiazole fragment for red triplet emitter in organic light-emitting diodes." *Org. Electron.*, 7(5), 330-336.

Gubler, U. Concilio, S. Bosshard, Ch. Biaggio, I. Gunter, P. Martin, R.E. Edelmann, M.J. Wytko, J.A. and Diederich. F. (2002). "Third-order nonlinear optical properties of in-backbone substituted conjugated polymers." *App. Phy. Lett*., 81(13), 2322-2324.

Gunes, S. Neugebauer, H. and Sariciftci, N.S. (2007). "Conjugated polymer-based organic solar cells." *Chem. Rev*., 107(4), 1324-1338.

Halls, J. J. M., Walsh, C. A., Greenham, N. C., Marseglia, E. A., Friend, R. H., Moratti, S. C. and Homles, A. B. (1995). "Efficient photodiodes from interpenetrating polymer networks." *Nature*, *376*, 498-500.

Haung, W., Meng, H., Yu, W.L., Pei, J., Chen, Z.K. and Lai, Y.H. (1999). "A novel series of p-n diblock light-emitting copolymers based on oligothiophenes and 1,4-bis(oxadiazolyl)-2,5-dialkyloxybenzene." *Macromolecules,* 32(1), 118-126.

Havinga, E.E., Hoeve W.T. and Wynberg. H. (1993). "Alternate donor-acceptor small band-gap semiconducting polymers; Polysquaraines and polycroconaines." *Synth. Met.*, 55(1), 299-306.

Hegde, P. K, Adhikari, A. V., Manjunatha, M.G., Poornesh, P. and Umesh, G. (2009). "Third-order nonlinear optical susceptibilities of new copolymers containing alternate 3,4-dialkoxythiophene and (1,3,4-oxadiazolyl)pyridine moieties." *Opt. Mat.*, 31(6), 1000-1006.

Henckens, A., Colladet, K., Fourier, S., Cleij, T. J. Lutsen, L. Gelan, J. and Vanderzande, D. (2005). "Synthesis of 3,4-Diphenyl-substituted poly(Thienylene Vinylene), low-band-gap polymers via the dithiocarbamate route." *Macromolecules,* 38(1)*,* 19-26.

Horiguchi, E., Kitaguchi, T. and Matsui, M., (2006). "Substituent effects of 2,3-dicyano-5-[4-(diethylamino) styryl]-7 methyl-6H-1,4-diazepines on their use as red dopants in single-layer organic electroluminescence devices." *Dyes Pigm.*, 70(1), 43-47.

Huang, W,. Meng, H., Yu, W.L., Pei, J., Chen, Z.K. and Lai, Y.H. (1999). "A novel series of p-n diblock light-emitting copolymers based on oligothiophenes and 1,4-Bis(oxadiazolyl)-2,5-dialkyloxybenzene." *Macromolecules*, 32(1) 118-126.

Huang, W. S., Humphrey, B. D. and MacDiarmid, A. G. (1986). "Polyaniline, a novel conducting polymer. Morphology and chemistry of its oxidation and reduction in aqueous electrolytes." *J. Chem. Soc., Faraday Trans. 1* 82(8), 2385-2390.

Huang, W., Yu, W. L., Meng, H., Pei, J. and Li, S. Y. (1998). "New series of blue-light-emitting polymers constituted of 3-alkylthiophenes and 1,4-di(1,3,4-oxadiazolyl)phenylene." *Chem. Mater.*, 10(11), 3340-3345.

Janietz, S. and Wedel, A. (1997). "Electrochemical redox behavior and electroluminescence in the mixed energy-sufficient system thianthrene and 2-(4-biphenyl)-5-(4-*tert*-butylphenyl)-1,3,4-oxadiazole." *Adv. Mater.* 9(5), 403-407.

Jenekhe, S.A., Lu, L. and Alam, M.M. (2001). "New conjugated polymers with donor-acceptor architectures: Synthesis and photophysics of carbazole-quinoline and Phenothiazine-quinoline copolymers and oligomers exhibiting large intramolecular charge transfer." *Macromolecules*, 34(21), 7315-7324.

Kaloian, K., Bahtiar, A., Bubeck, C., Mühling, B. and Meier, H. (2005). "Third-order nonlinear optical figure of merits for conjugated TTF-quinone molecules."*J. Phys. Chem. B,* 109(2), 10184-10188.

Kanis, D.R., Ratner, M.A. and Marks, T.J. (1994). "Design and construction of molecular assemblies with large second-order optical nonlinearities. Quantum chemical aspects." *Chem. Rev.*, 94(1), 195-242.

Karikomi, M., Kitamura, C., Tanaka, S. and Yamashita, Y.(1995). "New narrow-bandgap polymer composed of benzobis(1,2,5-thiadiazole) and thiophenes." *J. Am. Chem. Soc.*, 117(25), 6791-6792.

Karthikeyan, B., Anija, M., Suchand S.C.S., Muhammad Nadeer T.M. and Philip, R. (2008). "Optical and nonlinear optical properties of copper nanocomposite glasses annealed near the glass softening temperature." *Opt. Commun.*, 281(10), 2933-2937.

Kerr, T. A., Wu H. and Nazar L. F. (1996). "Concurrent Polymerization and Insertion of Aniline in Molybdenum Trioxide: Formation and Properties of a [Poly(aniline)]$_{0.24}$MoO$_3$ Nanocomposite."*Chem. Mater.*, 8(8), 2005-2015.

Kim, S.O., Chung, D.S., Cha, H., Hwang, M.C., Park, J.W., Kim, Y.H., Park, C.E. and Kwon, S.K. (2011). "Efficient polymer solar cells based on dialkoxynaphthalene

and benzo[c][1,2,5]thiadiazole: A new approach for simple donor-acceptor pair." *Sol. Enrgy. Mater. Sol. Cells,* 95(7), 1678-1685.

Koynov, K., Bahtiar, A., Bubeck, C., Mühling, B. and Meier, H. (2005). "Effect of donor-acceptor substitution on the nonlinear optical properties of oligo(1,4-phenyleneethynylene)s studied by third harmonic generation spectroscopy." *J. Phys. Chem. B.*, 109(20), 10184-10188.

Krishnamoorthy, K, Kanungo, M., contracter, A,Q. and Anil Kumar. (2001). "Electrochromic polymer based on a rigid cyanobiphenyl substituted 3,4-ethylenedioxythiophene." *Synth.met.*, 124(2-3), 471-475.

Kurian, P.A., Vijayan, C., Sandeep, C.S.S., Philip, R. and Sathiyamoorthy, K. (2007). "Excitonic transitions and off-resonant optical limiting in CdS quantum dots stabilized in a synthetic glue matrix." *Nano. Res. Lett*., 2(11), 561-568.

Lee, B.L. and Yamamoto, T. (1999). "Syntheses of new alternating CT-type copolymers of thiophene and pyrido[3,4-*b*]pyrazine units: Their optical and electrochemical properties in comparison with similar CT copolymers of thiophene with pyridine and quinoxaline." *Macromolecules*, 32(5), 1375-1382.

Levesque, I., and Leclerc, M. (1995). "Ionochromic effects in regioregular ether-substituted polythiophenes." *J. Chem. Soc. Chem. Commun*., 22, 2293-2294.

Li, Q., Zhong, C., Huang, J., Huang, Z., Pei, Z., Liu, J., Qin, J. and Li, Z. (2011). "Conjugated polymers with pyrrole as the conjugated bridge: Synthesis, characterization, and two-photon absorption properties." *J. Phys. Chem. B.*, 115(27), 8679-8685.

Li, X. and He. D. (2012). "Synthesis and optical properties of novel anthracene-based stilbene derivatives containing an 1,3,4-oxadiazole unit." *Dyes Pigm.*, 93 (1-3), 1422-1427.

Li, X.C. Spencer, G.C.W. Holmes, A.B. Moratti, S.C. Cacialli, F. and Friend. R.H. (1996). "The synthesis, optical and charge transport properties of poly(aromatic oxadiazole)s." *Synt.Met*., 76(1-3),153-156.

Li, Z., Wang, L., Xiong, B., Ye, C., Qin, J. and Li, Z. (2010). "Novel, side-on, PVK-based nonlinear optical polymers synthesis and NLO properties." *Dyes Pigm.,* 84(1), 134-139.

Li, Z., Wang, L., Xiong, B., Ye, C., Qin, J. and Li, Z. (2010). "Novel, side-on, PVK-

Li, Z., Yu, G., Li, Z., Liu, Y., Ye, C. and Qin J. (2008). "New second-order nonlinear optical polymers containing the same isolation groups: Optimized syntheses and nonlinear optical properties." *Polymer,* 49(4), 901-913.

Li, Z., Zeng, Q., Yu, G., Li, Z., Ye, C., Liu, Y. and Qin, J. (2008). "New azo chromophore-containing conjugated polymers: Facile synthesis by using ''Click'' chemistry and enhanced nonlinear optical properties through the introduction of suitable isolation groups." *Macrmol. Rapid. Comm*., 29(2), 136-141.

Lima, A., Scotland, P., Sadki, S. and Chevrot, C. (1998). "Electropolymerization of 3,4-ethylenedioxythiophene and 3,4-ethylenedioxythiophene methanol in the presence of dodecylbenzenesulfonate." *Synth. Met*., 93(1), 33-41.

Liou, G,S., Huang, N.K. and Yang, Y.I.L. (2006). "Blue-light-emitting and anodically electrochromic materials of new wholly aromatic polyamides derived from the high-efficiency chromophore 4,4′-dicarboxy-4′-methyltriphenylamine." *J. Polym. Sci. Part. A:Polym. Chem*., 44(13), 4095-4107.

Liou, G.S., Hsiao, S.H., Huang, N.K. and Yang, Y.L. (2006) "Synthesis, photophysical, and electrochromic characterization of wholly aromatic polyamide blue-light-emitting materials." *Macromolecules*, 39(16), 5337-5346.

Meng, H. and Huang, W. (2000). "Novel photoluminiscent polymers containing oligothiophene and m-phenylene-1,3,4-oxadiazole moieties." *J.Org. Chem*., 65(13), 3894-3901.

References

Mikroyannidis, J.A., Barberis, V.P., Ding, L. and Karasz, F.E. (2004). "Synthesis, optical properties, and electroluminescence of conjugated poly(p-phenylenevinylene) derivatives containing 1,3,4-oxadiazole and pyridine rings in the main chain." *J. Poly. Sci. Part A Poly. Chem.*, 42(13), 3212-3223.

Miyaura, N and Suzuki, A. (1995). "Palladium-catalyzed cross-coupling reactions of organoboron compounds." *Chem.Rev.*, 95(7), 2457-2483.

Neitzert, H. C., Ferrara, M., Rubino, A., Concilio, S., Iannelli, P. and Vacca, P. (2006). "Monitoring of the initial degradation of oxadiazole based blue OLED's." *J. Non-Cryst Solids.,* 352(9-20), 1695-1699.

Ng, S.C., Ding, M., Chan, H.S.O. and Yu, W.L. (2001). "The synthesis and characterization of fluorescent poly(heteroaromatic oxadiazole)s." *Macromol. Chem. Phys.*, 202(1), 8-13.

Ng, S.C., Ding, M., Chan, H.S.O. and Yu, W.L. (2001). "The synthesis and characterisation of fluorescent poly(heteroaromatic oxadiazole)s." *Macromol. Chem. Phys.*, 202(1), 8-13.

Ohsedo, Y., Imae, I. and Shirota, Y. (2000). "Electrochromic properties of new methacrylate copolymers containing pendant oligothiophene and oligo(ethyleneoxide) moieties in the presence of a polymer-gel electrolyte." *Electrochimica Acta*, 45, 1543-1547.

Ojha, U.P., Krishnamoorthy, K. and Anil Kumar. (2003). "Synthesis and characterization of aromatic polyoxadiazoles containing 3,4-alkylenedioxythiophenes." *Synth. Met.*, 132(3), 279-283.

Paik, K.L., Baek, N.S., Kim, H.K., Lee, J.H. and Lee, Y. (2002). "White light-emitting diodes from novel silicon-based copolymers containing both electron-transport oxadiazole and hole-transport carbazole moieties in the main chain." *Macromolecules, 35*(18)*,* 6782-6791.

References

Pal, B., Yen, W.C. Yang, J.S. and Su, W.F. (2007). "Substituent effect on the optoelectronic properties of alternating fluorene‑thiophene copolymers." *Macromolecules,* 40(23), 8189‑8194.

Peng, Z. and Zhang J. (1999). "Novel oxadiazole-containing conjugated polymers as efficient single-layer light-emitting diodes." *Synth.Met*., 105(1),73‑78.

Peng, Z., Bao, Z., and Galvin, M.E. (1998). "Oxadiazole‑containing conjugated polymers for light‑emitting diodes." *Adv. Mat.,* 10(9), 680‑684.

Philip, R. Ravikanth, M. and Ravindra Kumar, G. (1999). "Studies of third order optical nonlinearity in iron (III) phthalocyanine μ-oxo dimers using picosecond four‑wave mixing." *Opt. Commun*., 165(1‑3) 91‑97.

Pinar, C., Simge, T., Ertugrul, S., Idris M. A., Cihangir, T., Levent T. (2008). "Multichromic conducting copolymer of 1-benzyl-2,5-di(thiophen-2-yl)-1H-pyrrole with EDOT." *Sol. Enrgy. Mater. Sol. Cells,* 92(2), 154‑159.

Pomerantz, M. (2002). "Advances in polymer science 158. Polymers for photonics applications I: Nonlinear optical and electroluminescence polymers." *J. Am. Chem. Soc.*, 124(50), 15143‑15143.

Pommerehne, J., Vestweber, H., Guss, W., Mahrt, R.F., Bassler, H., Porsch, M. and Daub, J. (1995). "Efficient two layer leds on polymer blends." *Adv. Mater*., 7(6), 551‑554.

Prasad, P.N., Williams, D.J. (1990). "Introduction to nonlinear optical effects in molecules and polymers." John Wiley & Sons. Inc. New York.

Ramos-Ortíz, G., Maldonado, J.L., Hernández, M.C.G., Zolotukhin, M.G., Fomine, S., Fröhlich, N., Scherf, U., Galbrecht, F., Preis, E., Salmon, M., Cárdenas, J. and Chávez, M.I. (2010). "Synthesis, characterization and third‑order non‑linear optical properties of novel fluorene monomers and their cross‑conjugated polymers." *Polymer,* 51(11), 2351‑2359.

Reppert, J. Rao, A.M. Anija, M. Philip, R. and Kuthirummal, N. (2007). "Nonlinear optical scattering and absorption in bismuth nanorod suspensions." *Appl. Phys. Lett.,* 91(9), 093104.

Roncali, J. (1992). "Conjugated poly(thiophenes): synthesis, functionalization, and applications."*Chem. Rev*., 92(4), 711-738.

Ronchi, A., Cassano, T., Tommasi, R., Babudri, F., Cardone, A., Farinola, G.M. and Naso, F. (2003). "$\chi^{(3)}$ measurements in novel poly(2′,5′-dioctyloxy-4,4′,4″-terphenylenevinylene) using the Z-scan technique." *Synth. Met.,* 139(3), 831-834.

Samoc, M. Samoc, A. and Barry, L.D. (2000). "Two-photon and one-photon resonant third-order nonlinear optical properties of π-conjugated polymers." *Synth.Met*., 109(1-3), 79-83.

Samoc, M., Gauthier, N., Cifuentes, M. P., Paul, F., Lapinte, C. and Humphrey, M. G. (2006). "Electrochemical switching of the cubic nonlinear optical properties of an aryldiethynyl-linked heterobimetallic complex between three distinct stages." *Angew. Chem. Int. Ed.,* 45(44), 7376-7379.

Samoc, M., Samoc, A. and Luther-davies, B. (2000). "Two-photon and one-photon resonant third-order nonlinear optical properties of π-conjugated polymers." *Synth. Met*., 109(1-3), 79-83.

Sariciftci, N.S., Braun, D., Zhang, C., Srdanov, V., Heeger, A.J., Stucky, G and Wudl, F. (1993). "Semiconducting polymer-buckminsterfullerene heterojunctions: Diodes, photodiodes, and photovoltaic cells." *App. Phys. Lett.,* 62(6), 585-591.

Sheik-Bahae, M., Said, A.A., Wei, T.H., Hagan, D.J. and Stryland, E.W. (1990). "Sensitive measurement of optical nonlinearities using a single beam." *IEEE J. Quantum. Electron.*, 26(4), 760-769.

Shi, Y., Zhang, Y.Q.C., Zhang, H., Bechtel, J.H., Dalton, L.R., Robinson, B.H. and Steier, W.H. (2000). "Low (Sub-1-Volt) Halfwave Voltage Polymeric Electro-optic

Modulators Achieved by Controlling Chromophore Shape." *Science,* 288(5463), 119-122.

Shirk, J.S., Lindle, J.R., Bartoli, F.J. and Boyle, M.E. (1992.) "Third-order optical nonlinearities of bis(phthalocyanines)." *J. Phys. Chem*., 96(14) 5847-5852.

Sivaramakrishnan, S. Muthukumar, V.S. Sivasankara Sai, S. Venkataramanaiah, K. Sivaramakrishnan, S., Muthukumar, V.S., Sai, S.S., Venkataramanaiah, K. Reppert, J., Rao, A.M., Anija, M., Philip, R. and Kuthirummal, N. (2007). "Nonlinear optical scattering and absorption in bismuth nanorod suspensions.*"Appl. Phys. Lett*., 91(9), 093104.

Skotheim, T.A., Elsenbaumer, R.N. and Reynolds, J.R. (1998). "Handbook of conducting polymers, 2nd edition." Marcel Dekker, New York.

Strukelj, M., Papadimitrakopoulos, F., Miller, T.M. and Rotheberg, L.J. (1995). "Design and application of electron-transporting organic materials." *Science,* 267, 1969-1972.

Sung, H.H. and Lin. H.C. (2004). "Novel alternating fluorene-based conjugated polymers containing oxadiazole pendants with various terminal groups." *Macromolecules,* 37(21), 7945-7954.

Sutherland, R.L. (1996). *Handbook of nonlinear optics,* Marcel Dekker Inc. New York.

Takahashi, M., Tsuchida, E., Nishide, H., Takahashi, M., Yamada, S., Matsuda H. and Nakanishi, H. (1997). "Optical nonlinearity of an open-shell and degenerate π-conjugated polymer: poly(4-oxyphenyl-1,2-phenylenevinylene) radical." *Chem. Commun*., 19,1853-1854.

Thomas, C.A., Zong, K., Abboud, K.A., Steel, P.J. and Reynolds, J.R. (2004). "Donor-mediated band gap reduction in a homologous series of conjugated polymers." *J. Am. Chem. Soc*., 126(50), 16440-16450.

References

Torre, G.D.L., Vazquez, P., Agullo-Lopez, F. and Torres, T. (2004). "Role of structural factors in the nonlinear optical properties of phthalocyanines and related compounds." *Chem. Rev*., 104(9), 3723-3750.

Tutt, L.W. and Boggess, T.F. (1993). "A review of optical limiting mechanisms and devices using organics, fullerenes, semiconductors and other materials." *Prog. in Quant. Electr.,* 17(4), 299-338.

Udayakumar, D. and Adhikari, A.V. (2006). "Synthesis and characterization of new light-emitting copolymers containing 3,4-dialkoxythiophenes." *Synth. Met.,* 156(18-20), 1168-1173.

Van Mullekom, H., Vekemans, J.A.J.M., Havinga, E. and Meijer, E.W. (2001). "Developments in the chemistry and band gap engineering of donor-acceptor substituted conjugated polymers." *Mater. Sci. Eng. R*, *32*(1), 1-40.

Varanasi, P.R., Jen, A.K.Y., Chandrasekhar, J., Namboothiri, I.N.N. and Rathna, A. (1996). "The important role of heteroaromatics in the design of efficient second-order nonlinear optical molecules:Theoretical investigation on push-pull heteroaromatic stilbenes." *J. Am. Chem. Soc.,* 118(49), 12443-12488.

Verbiest, T., Houbrechts, S., Kauranen, M., Clays, K. and Persoons, A. (1997). "Second-order nonlinear optical materials: Recent advances in chromophore design." *J. Mater. Chem.,* 7, 2175-2189.

Vidal, J.C. Esperanza, G.R. and Castillo, J.R. (2003). "Recent advances in electropolymerized conducting polymers in amperometric biosensors." *Microchim. Acta,* 143(2-3), 93-111.

Wang, P., Ming, H. Xie, J. Zhang, W. Gao, X., Xu, Z. and Wei, X. (2001). "Substituents effect on the nonlinear optical properties of C_{60} derivatives." *Opt. Commun*., 192(3-6), 387-391.

References

Wang, Y.Z., Gebler, D.D., Spry, D.J., Fu, D.K., Swager, T.M., MacDiamid, A.G. and Epstein, A.J. (1997). "Novel light‑emitting devices based on pyridine‑containing conjugated polymers." *Electron. Devices,* 44(8), 1263‑1268.

Wu, C.G., Lin, Y. C. Wu, C. E. and Huang, P. H. (2005). "Synthesis and photo‑physics of new highly luminescent poly(alkylthiophene) derivatives with pyridine in the backbone." *Polymer*, 46(11), 3748‑3757.

Wu, T.Y., Lee, N. C. and Chen, Y. (2003). "Synthesis and characterization of new poly(*p*-phenylenevinylene) derivative containing 5,5′-diphenyl-2,2′-*p*-(2,5-bis-hexyloxyphenylene)‑bis‑1,3,4‑oxadiazole and distyrylbenzene moieties." *Synth. Met.,* 139(2), 263‑269.

Yasuda, T., Namekawa, K., Iijima, T. and Yamamoto, T. (2007). "New luminescent 1,2,4‑triazole/thiophene alternating copolymers: Synthesis, characterization, and optical properties." *Polymer*, 48(15), 4375‑4384.

Yu, W.L., Meng, H., Pei, J. and Haung, W. (1998). "Tuning redox behavior and emissive wavelength of conjugated polymers by p‑n diblock structures." *J. Am. Chem. Soc.,* 120(45), 11808‑11809.

Yu, W.L., Meng, H., Pei, J., Huang, W., Li, Y. and Heeger, A.J. (1998). "Synthesis and characterization of a new p‑n diblock light‑emitting copolymer." *Macromolecules*, 31(15), 4838‑4844.

Yuen, J. D., Fan, J., Seifter, J., Lim, B., Hufschmid, R., Heeger, A. J. and Wudl, F. (2011). "High performance weak donor-acceptor polymers in thin film transistors: Effect of the acceptor on electronic properties, ambipolar conductivity, mobility, and thermal stability." *J. Am. Chem. Soc.*, 133(51), 20799-20807.

Zhan, X., Liu, Y., Zhu, D., Huang, W. and Gong, Q. (2001). "Large femtosecond third‑order nonlinear optical response in a novel donor‑acceptor copolymer consisting of ethynylfluorene and tetraphenyldiaminobiphenyl units." *Chem. Mater.*, 13(5), 1540‑1544.

References

Zhang, K., Tieke, B., Forgie, J.C., Vilela, F. and Skabara, P.J. (2012). "Donor-acceptor conjugated polymers based on *p*- and *o*-benzodifuranone and thiophene derivatives: Electrochemical preparation and optical and electronic properties." *Macromolecules*, 45(2), 743-750.

Zhang, Y., Hau, S.K., Yip, H.L., Sun, Y., Acton, O. and Jen, A.K.Y. (2010). "Efficient polymer solar cells based on the copolymers of benzodithiophene and thienopyrroledione." *Chem. Mater*., 22(9), 2696-2698.

Zhou, G., Liu, Y. and Ye C. (2004). "Optical-Limiting Properties of Poly(arylene ethynylenes) containing thiophene ring."*J.App. Polym. Sci*., 93(1), 131-135.

Zhu, W., Yao, R. and Tian, H. (2002). "Synthesis of novel electro-transporting emitting compounds." *Dyes Pigm.*, 54(2), 147-154.

Zhu,Y., Chmpion, R.D. and Jenekhe, S.A. (2006). "Conjugated donor-acceptor copolymer semiconductors with large intramolecular charge transfer: Synthesis, optical properties, electrochemistry, and field effect carrier mobility of thienopyrazine-based copolymers."*Macromolecules,* 39(25), 8712-8719.

Zhu,Y., Yen, C.T., Jenekhe, S.A. and Chen, W.C. (2004). "Poly(pyrazinoquinoxaline)s: New *n*-type conjugated polymers that exhibit highly reversible reduction and high electron a`ffinity." *Macromol. Rapid. Commun., 25(21)*, 1829-1834.

Zyss, J. (1994). Molecular Nonlinear Optics: Materials, Physics, and Devices. Academic Press, Boston, MA.